STUDIES OF THICKNESS DEPENDENCE OF INTERNAL FIELDS IN M-I-M STRUCTURES USING LANGMUIR FILMS OF SOME LONG-CHAIN COMPOUNDS

Thesis

Submitted to the University of Roorkee
for the award of the degree of
DOCTOR OF PHILOSOPHY
in
PHYSICS

By
SHRI KRISHNA GUPTA

DEPARTMENT OF PHYSICS
UNIVERSITY OF ROORKEE
ROORKEE (INDIA)
September, 1977

To,

My wife Usha

and

daughter Shilpi

C E R T I F I C A T E

This is to certify that the thesis entitled ' STUDIES OF THICKNESS DEPENDENCE OF INTERNAL FIELDS IN M-I-M STRUCTURES USING LANGMUIR FILMS OF SOME LONG CHAIN COMPOUNDS' which is being submitted by Mr. Shri Krishna Gupta in fulfilment for the award of the degree of Doctor of Philosophy in Physics from the University of Roorkee, is a record of his own work carried out by him under my supervision and guidance. The matter embodied in this thesis has not been submitted for the award of any other degree.

This is further to certify that he has worked for a period equivalent to 24 months full time research for preparing this thesis for Ph.D. Degree at this University.

Dated: Sept. 6th, 1977

(V.K.Srivastava)
Physics Department
University of Roorkee
Roorkee-247672
(INDIA)

ACKNOWLEDGEMENT

It is a privilege and a matter of great pleasure to express my deep sense of gratitude to my teacher and supervisor Dr. V.K.Srivastava, Reader, Physics Department, University of Roorkee, who has been a source of inspiration for me. His constant encouragement and valuable guidance, specially during the less productive periods, were of great help for me for the completion of this work. In fact it is not possible to thank him suitably for all the help he rendered.

I am also grateful to Dr. C.M.Singal for his interest in the problem and for the cooperation he rendered so freely. He really obliged me in numerous ways particularly during his stay in this department.

I would like to express my indebtedness to Prof. S.K.Joshi, Head of Physics Department, University of Roorkee, for his interest in the process of this work and for providing the laboratory and other facilities.

I also take this opportunity to express my sincere thanks to all my colleagues in particular M/S B.K.Jain, A.K.Singh,and A.K.Kapil for the cooperation received from them so generally.

The Ph.D.thesis and the Review article (Physics of Thin Films, 7, 311, 1973) of Dr. V.K.Srivastava are highly acknowledged for providing handful information on Langmuir film systems from time to time.

It will be unjust if I forget the encouragement,

I received from my parents, to pursue this work.

Finally the financial support from the council of Scientific and Industrial Research, India is gratefully acknowledged.

ABSTRACT

Intrinsic Field in an M-I-M (metal-insulator-metal) structure is an important consideration† in the design of some thin film devices as proposed by Mead††. Simmons' demonstrated the existence of intrinsic field inside the M-I-M-structures with dissimilar electrodes. The naturally grown aluminium oxide in dry oxugen was used as insulator in his work. However in this work the dependence of the internal field on insulator thickness was not studied. Present investigations consitute a systematic thickness dependence studies of internal field in metal-insulator-metal structures with Langmuir films of barium palmitate, barium margarate, barium stearate and stearic acid as insulating films. The different electrodes deposited at the two faces of the dielectric are aluminium as the base electrode and tin, silver, bismuth, lead and tellurium as the top electrodes.

The Langmuir films which have been chosen for the present investigations are almost ideally suited for such thickness dependence studies. The striking features of these films are that their thickness are closely controllable (down to one monolayer of ~ 25 Å), extremely uniform and accurately known. An optical device namely ' Thin Film Thickness Step Gauge' has been developed using Langmuir films (Chapter IV). The observance of homogeneity of

† J.G.Simmons, Phys. Rev. Letters, 10, 10 (1963)

†† C.A. Mead, J.Appl. Phys. 32, 646 (1961) and Phys. Rev. Letters, 6, 545 (1961).

colours, in white fluorescent light, on this step gauge provides sufficient evidence for the uniformity of thicknessos of these films. It is also possible to obtain them almost free from holes and conducting imperfections. Even with the evaporated film systems, for example, it is difficult to carry out such a thickness dependent studies because the very small and uniform thicknesses of such films are notoriously difficult to obtain. Furthermore, their thicknesses will have to be measured and they will not be closely controllable.

The sandwich structures of the type Al-Film-Metal were obtained using ' built-up' Langmuir films of metallic salts of some long-chain fatty acids | $CH_3(CH_2)_{n-2}COOH$| with different number of carbon atoms in the chain length, as the insulating media, between two vacuum evaporated metal electrodes. Insulating films were 'built-up' by a delicate but established technique of Blodgett and Langmuir (Chapter IV). These films are crystalline in nature forming hexagonal crystals with the symmetry axis (optic axis) perpendicular to the plane of the film. A great care is, however, needed at all stages during films deposition to minimise accidental vibrations and dust contamination for obtaining films free from gross defects. It is to be emphasized that a film with odd number of layers has one unpaired dipolar layer whereas a film with even number of layers does not have any unpaired layer (chapter IV).

The measurement of internal voltage has been carried

out by using the current-voltage characteristics in the two polarities i.e. by evaluating the difference in breakdown voltages in the two polarities. Another method, known as the direct voltage measurement method, has also been used in which the internal voltage of the sample can be measured directly using a high impedance electrometer amplifier as a voltage measuring device and the voltage has been found to be ~~constituent~~ consistent with that derived from the study of I-V charactiristic

It has been found that in the M_1-O-M_2 structure (where M_1 and M_2 refer to different electrodes and 'O' refers to organic films), the internal voltage decreases linearly with increasing thickness of the dielectric film. This decrease in the internal voltage has been explained in terms of trapped charges present in the Langmuir film. Also the films with odd and even number of layer behave in interestingly different manner. For even number of layer films, i.e., when the dielectric has no net dipole moment, the internal voltage is related to the difference of the work function of the two metals. For the case when the insulator has a net dipole moment i.e. for the case of film with odd number of monolayers, the internal voltage is found to increase (Chapter VII and VIII).

By plotting the current voltage characteristics in two polarities on a linear scale, it has been found that the sandwich behaves like a diode structure. The working inverse voltage of such a diode has been found comparable with the internal voltage. The maximum forward current is

of the order of nanoamperes (Chapter VII).

It has been shown theoretically (Chapter II) that the internal voltage is equal to the work-function difference of the two metal electrodes. Therefore by measuring the value of internal voltage for different metal combinations, the difference in work function for the respective combination has been determined. As mentioned earlier, in all the structures Al was used as the base electrode, therefore, taking aluminium as standard, the work functions of other metals have been determined. The study of work function for various thicknesses of the metal film has also been carried out. The work function was found to be almost independent of the thickness as expected. Discharging of the internal voltage in closed circuit and its subsequent recovery in open circuit has also been studied, thereby calculating the life time and time constant of the structure (Chapter VII).

The above interesting study of internal voltage has also been extended to the 'built-up' films with similar electrodes. The sandwich with even number of layers showed no voltage as expected. However, with the odd number of monolayers, the sandwich (Al-O-Al) showed a voltage which is also expected. But it must be emphasized that this voltage has nothing to do with the Simmons' effect arising because of the difference in the electrode work-functions. This internal voltage developed in odd number of layers

with symmetric electrodes has been attributed to the polarization existing in the unpaired layer. A theoretical formulation has also been developed and the analysis has led to an interesting and new method of determining the dipole moment of the molecules which can be suitably oriented in the form of Langmuir films. The method has been applied for determining the dipole moment of barium stearate and stearic acid molecules.

The study of dynamic dielectric characteristics (dielectric loss) also becomes important in the context of the dielectric diode device mentioned above. Therefore the dielectric loss of Langmuir films and its thickness dependence in the range of ultrathin films has also been studied in detail. The dielectric loss has been found to decrease rapidly as one goes from 1 to 2 monolayers but as the thickness of the dielectric increases the decrease in ' tan δ ' values becomes slow and subsequently the loss values tend to the bulk values. These results have been interpreted in terms of voids present in the dielectric film. The loss due to series electrode resistance has also been taken into account.

The following is the subject matter of the thesis which has been arranged in nine chapters.

Chapter I - This chapter deals with the theoretical justification of existence of intrinsic

fields in metal-insulator-metal junctions. A brief description about the behaviour of conduction mechanism in insulating thin films has been given. The nature of metal-insulator and metal-insulator-metal contacts has also been described in detail.

Chapter II - Past studies on intrinsic fields in other thin film systems have been reviewed. The nature of present investigations and the suitability of Langmuir films for intrinsic field studies has also been described.

Chapter III - In this chapter discussion of the surface tension phenomena, formulation of monolayer on water-air interface, mechanism of monomolecular spreading on water, non-occurrance of polymolecular film and some fundamental information about the individual molecules is made very explicitly.

Chapter IV - The 'building up' process of depositing the films (particularly Y-type films) has been described in detail. A brief discussion about the so called X and Z type of films has also been given.

Chapter V - This chapter describes the various thickness

determination studies of Langmuir films. Some electrical properties of these 'built-up' films have also been reviewed briefly.

Chapter VI - The experimental details of sandwich fabrication, selection and cleaning of the substrate and measurement set-up have been given in this chapter. The methods of measurement of internal voltage have also been described.

Chapter VII - Results and discussion of a detailed and systematic study of internal voltage in metal-insulator-metal structure with asymmetric electrodes on 'built-up' films have been carried out. The development of a dielectric diode, method of measurement of work function of metal electrodes and its determination has also been described. Decay and recovery of internal voltage with time has also been studied and discussed.

Chapter VIII - In this chapter, results and discussion of internal voltage in metal-insulator-metal structure with similar electrodes have been described. A new method of

determining the dipole moment of orientable molecules has also been developed.

Chapter IX - This chapter deals with the studies of thickness dependence of dielectric loss in ultrathin Langmuir films. The results and discussion have also been described.

LIST OF PUBLICATIONS

1. Thickness Influence On Dielectric Loss.
   (with V.K.Srivastava)
   J.Phys. Chem. Solids, 37, 975 (1976).

2. Thickness Dependence of Internal Voltage in Metal-Insulator Metal Structure with dissimilar electrodes.
   (with V.K.Srivastava and C.M.Singal)
   J.Appl. Physics, 48, 2583 (1977).

3. Thin Film Thickness Step Gauge
   (with V.K.Srivastava, A.K.Kapil and C.M.Singal)
   Pramana 7, 397 (1976).

4. Diode Characteristics of a Metal-Insulator-Metal Structure
   (with V.K.Srivastava and C.M.Singal)
   J.Electrocom. Sci. and Technol (U.K.) Vol.3, No.2,p.119 (1976).

5. Further Evidence For Thickness Influence on Dielectric Loss.
   (with V.K.Srivastava)
   J. Phys. Chem. Solids 38, 1111 (1977).

6. Intrinsic Voltage In Insulating Films In Al - Barium Stearate - Al Structures.
   (with V.K.Srivastava, A.K.Kapil and C.M.Singal)
   J. Appl. Phys. (Accepted for Publication).

7. Thickness Influence on Dielectric loss in Ultrathin Films.
   (with V.K.Srivastava)
   Proceedings of Nuclear Physics and Solid State Physics Symposium Calcutta (India), Vol. 18C, p.587 (1975).

8. Internal Voltage Studies in Langmuir Films.
   (with V.K.Srivastava and C.M.Singal)
   Proceedings of Nuclear Physics and Solid State Physics Symposium Ahmedabad (India), Vol. 19C,p.88 (1976).

9. Determination of Dipole Moment of Barium Stearate Molecule in Monomolecular Films Sandwiched between Metal Electrodes.
   (with V.K.Srivastava, A.K.Kapil and C.M.Singal)
   Proceedings of Nuclear Physics and Solid State Physics Symposium Ahmedabad (India, Vol. 19C, p. 94 (1976).

10. Thickness Dependence of the Work Function of Metal Films.
    (with V.K.Srivastava and C.M.Singal)
    (To be Communicated).

Contd...

11. Determination of the Dipole Moment of Stearic Acid Molecule by the Study of the Internal Voltage. (with V.K.Srivastava and C.M.Singal)
(To be Communicated).

Note: In the above papers the contribution of other authors is only in the form of marginal discussion.

C O N T E N T S

CHAPTER I

INTRINSIC FIELD IN METAL-INSULATOR-METAL JUNCTIONS

1.1 INTRODUCTION

(a) Conductivity of Thin Insulating Films.

An insulator is a material which contains very few volume-generated carriers, in many instances considerably less than one per cm^3, and thus has virtually no conductivity. The conductivity of the insulating thin film materials does not necessarily fall into this category; that is, although these materials have energy gaps greater than about 2 eV or so, the electrical properties may bear no resemblance to what is intrinsically expected of such a material. This is because it is becoming increasingly clear that the electrical properties of thin film insulators are determined not by the intrinsic properties of the insulator but by other properties such as the nature of the electrode-insulator contact. A suitable (ohmic) contact (sec. 1.2 a) is capable of injecting additional carriers into the insulator far in excess of the bulk-generated carriers (1-3).

There are also several reasons for believing that the observed conductivity in thin film insulators is due often to extrinsically rather than intrinsically bulk generated carriers. Consider the intrinsic current density carried by an insulator

$$I = e \mu N_c F \exp\left(-\frac{E_g}{2kT}\right) \qquad ..(1.1)$$

where e is the electronic charge, μ is the mobility, F is the field in the insulator, N_c is the effective density of states in the insulator, E_g is the insulator energy gap, k is the Boltzmann's constant, and T is the absolute temperature. At room temperature, $N_c = 2.5 \times 10^{19}$ cm^{-3}, and assuming E_g = 3 eV and μ = 100 cm^2 V^{-1} S^{-1}, then even for F = 10^6 V cm^{-1} the current density is only of the order of 10^{-18} A cm^{-2}. This is many orders of magnitude smaller than the current densities observed for thin film materials which have energy gaps greater than 3 eV. Secondly, the observed thermal - activation energy associated with the conductivity of the film is much smaller than would be expected ($\simeq E_g/2$) if the conductivity were intrinsic in nature.

One of the sources of the extrinsic conductivity in evaporated films is thought to be the inherent defect nature of the chemical compound. Stoichiometric films of compound insulators are notoriously difficult to prepare by evaporation, because the decomposition and preferential evaporation of the lower-vapour-pressure constituent atom. For example, using the compound as starting material, elemental Cd tends to evaporate more rapidly from CdS; as a result CdS films contain donor centers of free cadmium (4). SiO yields a film containing a mixture of compounds varying from SiO to SiO_2, as well as free Si (5-8), the free Si per se may act as donor centers in these films or alternatively vacancies existing

in the insulator may be the source. A further problem that arises is the contamination of the films by deposits arising from the sublimation of the crucible, or by residual gas.

Another important fact to be considered in thin film insulators is traps. Insulating films deposited onto amorphous (e.g., glass) substrates are usually, at best, polycrystalline, and in many cases are amorphous. For crystalline size of 100 $\mathring{A}$, trapping levels as high as 10^{18} cm^{-3} are possible because of grain boundary defects alone; in vacuum deposited CdS, trapping densities as high as 10^{21} cm^{-3} have been reported (9). Furthermore, vacuum deposited films contain large stresses which induce further trapping centers.

It follows that vacuum - deposited thin - film insulator can contain large density of both impurity and trapping centers. A judicious study of electrical conduction in vacuum - deposited thin films can not be accomplished without consideration of these possibilities.

(b) Band Structure

A well-defined energy gap is a property of a crystalline solid, and in thin films in general one is not dealing with such materials, one is mostly concerned with polycrystalline, or even amorphous, insulators. However, it can be shown that the essential features of the band structure of a solid are determined by the short-range ord-

er within the solid; thus the general properties of the band structure of the crystalline state are carried over to polycrystalline state. The lack of the long-range order in a non crystalline solid causes smearing of the conduction and valence-band edges, among other things, so that the energy gap is no longer well defined. What is normally done in the study of thin insulating films is to assume that this smeared-out energy gap, to a first order approximation can be represented by a well-defined energy gap which is representative of perhaps an average value of the actual nondiscrete energy gap.

1.2 METAL-INSULATOR CONTACTS

In order to measure the conductivity of an insulator, it is of course, necessary to connect electrodes to its surfaces in order to facilitate injection of electrons into and their withdrawal from the bulk of the insulator. Clearly, the conductivity of the insulator per se will determine the conductivity of the system, since it is much lower than that of the electrodes. In terms of the energy band picture, the action of the insulator is to erect between the electrodes a potential barrier, extending from the electrode Fermi level to the bottom of the insulator conduction band. This barrier impedes the flow of electrons from one electrode to the other, which would normally flow virtually unimpeded if the insulator were not there (i.e. metal-metal contact). Clearly, then

the height of the potential barrier is an important parameter and is determined by the relative alignment of the electrode and insulator energy bands. The relative alignment of the bands is determined by the rule that in thermal equilibrium the vacuum and Fermi levels must be continuous throughout the system. (The vacuum level represents the energy of an electron at rest just outside the surface of the material, and the energy difference between the vacuum and Fermi levels is called the work function of the material). The equilibrium conditions can be satisfied only when the work function of the metal say ψ_m and that of the insulator say ψ_i are equal. However, the equilibrium condition is also satisfied when $\psi_m \neq \psi_i$, because of the charge transfer from the electrode to the insulator or vice versa.

The shape of the potential barrier just within the surface of the insulator depends on whether or not the insulator is intrinsic or extrinsic, and on the relative magnitudes of the work functions of the metal and insulator, among other things.

At reasonable applied fields there will normally be a sufficient supply of carriers available to enter the insulator from the cathode (negatively biased electrode) to replenish the carriers drawn out of the bulk of the insulator. Under these conditions the current-voltage (I-V) characteristics of the sample will be determined by the bulk properties of the insulator. This conduction process is referred as bulk-limited. At high fields, or

if the contact is blocking, the current capable of being supplied by the cathode to the insulator will be less than that capable of being carried in the bulk of the insulator. Under these conditions the I - V characteristics of the sample will be controlled primarily by conditions existing at the cathode - insulator interface; this conduction process is referred to as being emission - limited or contact - limited.

The types of contact that can exist at a metal-insulator interface fall into three categories; (a) Ohmic contact, (b) neutral contact, and (c) blocking contact. These contacts are discussed in some detail below.

(a) Ohmic Contact - Mott -Gurney Contact.

To achieve an ohmic contact at a metal-insulator interface (1), the electrode work function ψ_m should be smaller than the insulator work function ψ_i, as shown in Fig.1.1a. Under these conditions, in order to satisfy thermal equilibrium requirements, electrons are injected from the electrode into the conduction band of the insulator, thus giving rise to a space-charge region in the insulator. This space-charge region is shown in Fig.1.1b to extend a distance λ_o into the insulator, and is termed the accumulation region. In order to satisfy charge- neutrality requirements an equal amount of positive charge, say, Q_o, accumulates on the electrode surface. The electrostatic interaction between the positive and negative

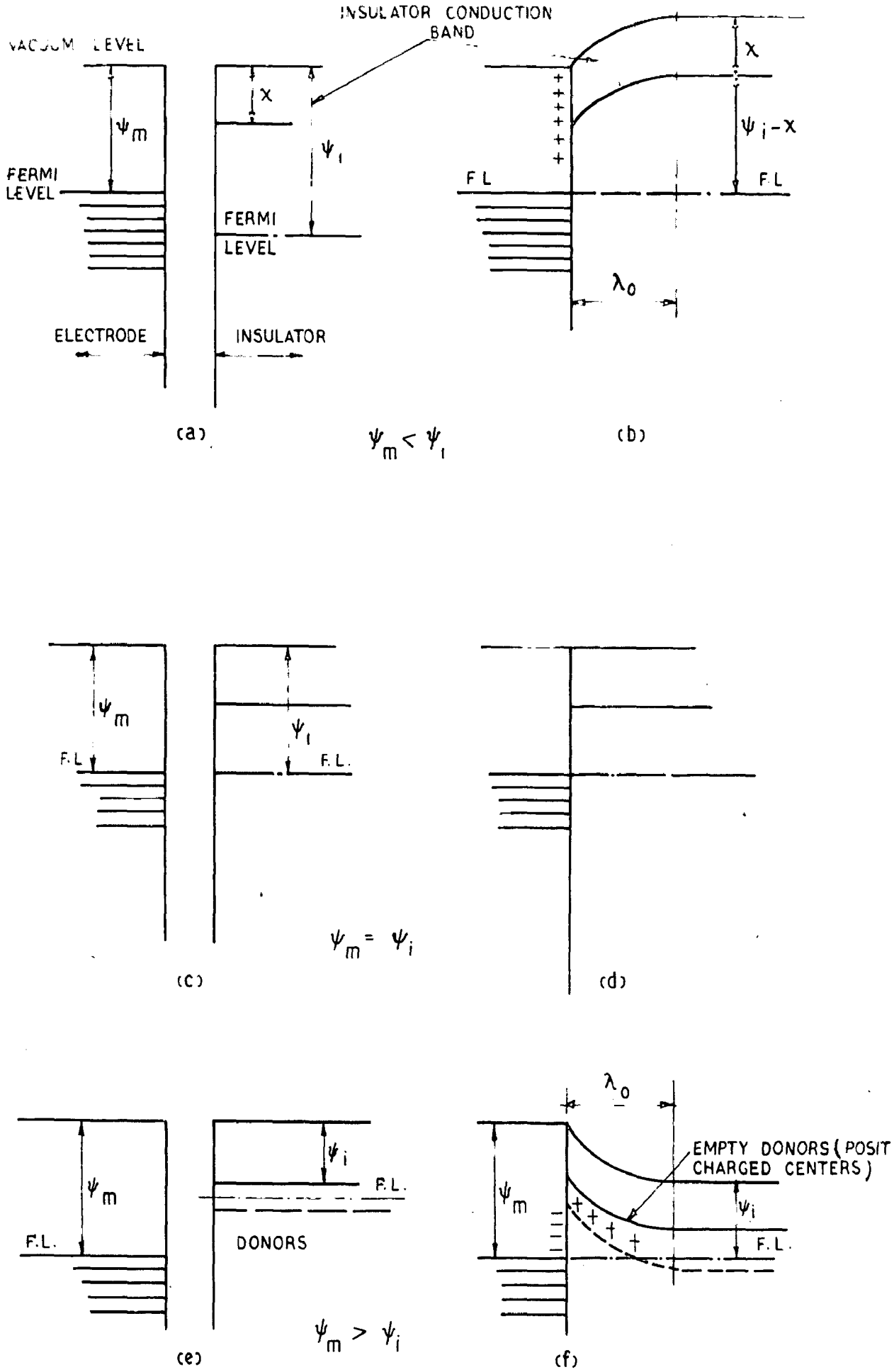

FIG.1·1 ENERGY DIAGRAMS SHOWING THE REQUIREMENTS AND TYPE OF CONTACT
(a, b) OHMIC CONTACT (c, d) NEUTRAL CONTACT
(e, f) BLOCKING CONTACT

charge induces a local electric field within the surface of the insulator, the strength of which falls off with distance from the interface and is zero at the edge of the space-charge region (i.e. at λ_o from the interface). This field causes the bottom of the conduction band to rise with distance of penetration into the insulator until it reaches the equilibrium value $\psi_i - X$, where X is the insulator affinity (distance between conduction band and vacuum level).

The field F within the accumulation region is related to the space-charge density $\rho(x)$ within the accumulation region by Poisson's equation:

$$\frac{dF}{dx} = \frac{\rho(x)}{K\epsilon_o} \qquad .(1.2)$$

where K and ϵ_o are, respectively, the dielectric constant of insulator and permittivity of free space. The information regarding conditions in the space-charge region can be obtained by substituting $\rho(x) = eN_c \exp(-\psi/kT)$ in equation (1.2) where ψ is the potential energy of the insulator conduction-band edge with respect to the electrode Fermi level:

$$\frac{dF}{dx} = \frac{1}{e}\frac{d^2\psi}{dx^2} = -\frac{eN_c}{K\epsilon_o}\exp\left(-\frac{\psi}{kT}\right) \qquad (1.3)$$

on integration and using $\frac{d\psi}{dx} = 0$ at $\psi = \psi_i - X$, equation (1.3) yields

$$\frac{d\psi}{dx} = \left(\frac{2e^2kTN_c}{K\epsilon_o}\right)^{1/2}\left[\exp\left(-\frac{\psi}{kT}\right) - \exp\left(-\frac{\psi_i - X}{kT}\right)\right]^{1/2} \qquad .(1.4)$$

Integrating(1.4) using the boundary conditions $\psi = \psi_m - X$ and $(\psi_i - X)$ at $X = 0$ and λ_o, respectively, the depth of accumulation region is obtained as

$$\lambda_o = \left(\frac{2kT\, K\epsilon_o}{e^2 N_c} \right)^{1/2} \left\{ \frac{\pi}{2} - \mathrm{Sin}^{-1} \left[\exp\left(-\frac{\psi_i - \psi_m}{2kT} \right) \right] \right\}$$

$$\exp\left(\frac{\psi_i - X}{2kT} \right) \qquad .(1.5)$$

For $\psi_i - \psi_m > 4kT$, it reduces to

$$\lambda_o \simeq \frac{\pi}{2} \left(\frac{2kT\, K\epsilon_o}{e^2 N_c} \right)^{1/2} \exp\left(\frac{\psi_i - X}{2kT} \right) \qquad ..(1.6)$$

The total amount of charge injected into the insulator to form the ohmic contact is determined as follows: From equation(1.2),using boundary conditions that $F = F_o$ and 0 at $x=0$ and λ_o, respectively, we have

$$\int_{F_o}^{0} dF = -\frac{1}{K\epsilon_o} \int_{0}^{\lambda_o} \rho(x)\, dx$$

$$\text{or} \quad F_o = \frac{Q_o}{K\epsilon_o} \qquad .(1.7)$$

where $Q_o = \int_0^{\lambda_o} \rho(x)\, dx$ is the total space charge per unit area in the accumulation region. Since $\psi = \psi_m - X$ at $x = 0$, we have from equation(1.4),assuming $\psi_m < \psi_i - 2kT$, which is the normal case,,

$$F_o = \left(\frac{2kT\, N_c}{K\epsilon_o} \right)^{1/2} \exp\left(-\frac{\psi_m - X}{kT} \right) \qquad .(1.8)$$

Comparing equations(1.7)and (1.8)

$$Q_o = (2K\epsilon_o kT N_c)^{1/2} \exp\left(-\frac{\psi_m - X}{kT}\right) \qquad ..(1.9)$$

(b) Neutral Contact

When there is no reservior of charge at the contact (Q_o=0), this type of contact is known as the neutral contact. The condition $Q_o = 0$ implies that $\psi_m = \psi_i$ which means that the conduction band is flat right upto the interface, as shown in Fig. 1.1d.

For initial voltage bias the cathode is capable of supplying sufficient current to balance that flowing in the insulator, so that the conduction process is ohmic. There is no theoretical limit to the maximum current an insulator per se may carry, provided a high enough voltage supply is available. (There are, in fact, practical limitations such as Joule heating and dielectric breakdown, which determine the maximum voltage that an insulator can withstand before catastrophic breakdown occurs.) There is, however, a limit to the current that the cathode can supply and this is the saturated thermionic (Richardson) current over the barrier. When this limit is reached, the conduction process is no longer ohmic in nature. The maximum field that may be applied to the insulator before the current supplied by the cathode saturates is obtained by equating the saturated thermionic current $\frac{n_o ev}{4}$ to the current flowing in the insulator $n_o e\mu F$, where n_o is the density

of electrons in the cathode with energies greater than the interfacial potential barrier and v is the thermal velocity of the carriers:

$$\frac{n_o e v}{4} = n_o e \mu F$$

or $$F = \frac{v}{4\mu} \qquad (1.10)$$

(c) Blocking Contact - Schottky Barrier

The condition for a blocking contact is $\psi_m > \psi_i$, and in this case electrons flow from the insulator into the metal to establish thermal equilibrium conditions. A space-charge region of positive charge, the depletion region, is thus created in the insulator and an equal negative charge resides on the metal electrode. As a result of the electrostatic interaction between the oppositely charged regions, a local field exists within the surface of the insulator. This causes the bottom of the conduction band to band downward until the Fermi level within the bulk of the insulator lies ψ_i below the vacuum level. An intrinsic insulator, however, contains such a low density of electrons that it would have to be inordinately thick to provide the required positive space-charge region to satisfy the above condition. Thus the conduction band of an intrinsic insulator at a blocking contact does in fact slope only imperceptibly downward; that is we have

what is essentially a neutral contact.

If the insulator contains a large density N_d of donors, Fig.1.1f, and assuming that the donors are fully ionized and uniformly distributed (N_d cm^{-3}) in the region extending from the interface to a depth λ_o, the depletion region, the Poisson's equation(1.2)for this system is given by

$$\frac{d^2\Psi}{dx^2} = \frac{e^2 N_d}{K\epsilon_o} \qquad (1.11)$$

and the depth of depletion region λ_o is given by

$$\lambda_o = \left[\frac{2(\Psi_m - \Psi_i)\, K\epsilon_o}{e^2\, N_d} \right]^{1/2} \qquad (1.12)$$

The depletion region has a much lower electron density than the bulk of the insulator; hence its conductivity is much lower. Thus any voltage applied to the system can, to a good approximation, be assumed to be absorbed entirely across the depletion region. Under these conditions, when the metal is negatively biased, the boundary condition leading to equation(1.12) is modified to read $\Psi = \Psi_i - X - eV$ at $x = \lambda$. The depth of the depletion region λ now becomes

$$\lambda = \left[\frac{2\,(\Psi_m - \Psi_i + eV)\, K\epsilon_o}{N_d\, e^2} \right]^{1/2} \qquad (1.13)$$

which increases with increasing voltage bias. The field at

the interface $F_o = e^{-1} \frac{d\psi}{dx}$ is

$$F_o = -\left[\frac{2 N_d(\psi_m - \psi_i + eV)}{K \epsilon_o}\right]^{1/2} \quad ..(1.14)$$

1.3 Metal-insulator -metal Systems

(a) Two Ohmic Contacts

Figure 1.2a and b illustrates two ohmic contacts on an insulator when the electrodes are at the same potential. In the case of fig.1.2 a it is seen that the accumulation regions extend right into the bulk of the insulator. As a result, the bottom of the conduction band is curved throughout its length (i.e., an electric field exists at all points within the insulator), the highest point of which is less than the equilibrium position $\psi_i - X$ above the Fermi level. This condition is due to insulator's being too thin or the interfacial potential barriers' being too high, with the result that insufficient charge is contained within the insulator to screen the interior effectively from the surface. Fig.1.2b is an illustration of good ohmic contacts on an insulator. In this case the accumulation regions effectively screen the interior of the insulator from conditions at the surfaees. The bottom of the conduction band is thus flat within the interior of the insulator (field -free interior) and the height of the conduction band within the interior, reaching its equilibrium

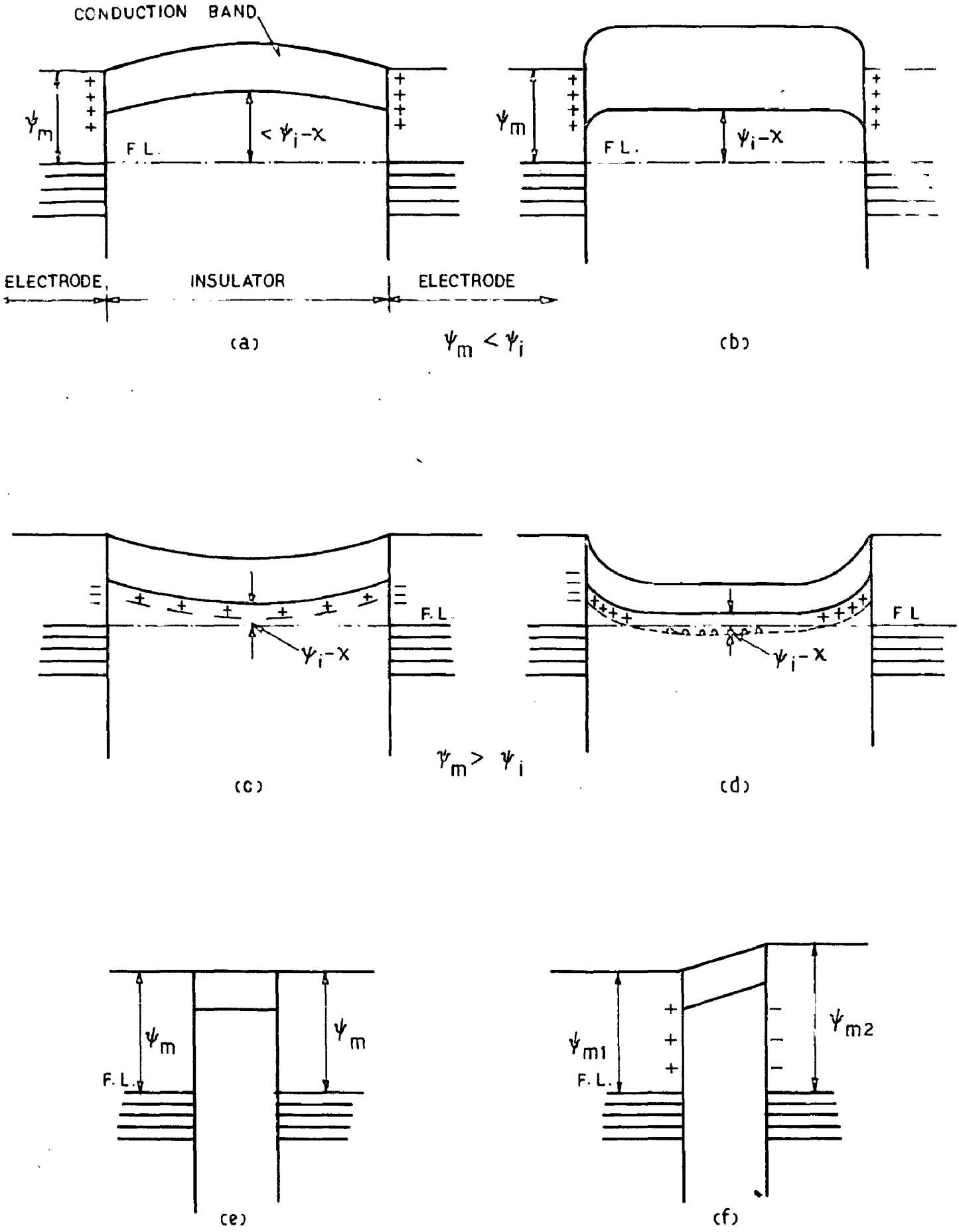

FIG. 1·2 ENERGY DIAGRAMS OF METAL INSULATOR METAL SYSTEMS
(a, b) IMPERFECT AND GOOD OHMIC CONTACTS
(c, d) IMPERFECT AND GOOD BLOCKING CONTACTS
(e, f) SIMILAR AND DISSIMILAR NEUTRAL CONTACTS

level $\psi_i - X$ above the Fermi level.

(b) Two Blocking Contacts

Figure(1.2c)and d illustrates two blocking contacts on an insulator. In fig.(1.2c)the depletion regions extend right into the interior of the insulator, as a result of the insulator's being too thin or of the doping concentrations being too low. The conduction band is curved throughout its length, with a concave upward, indicating that an electric field exists at all points throughout the length of the insulator. Because the depletion regions do not effectively screen the interior from the surfaces, the lowest point of the bottom of the conduction band is greater than $\psi_i - X$ above the Fermi level. In contrast to Fig.(1.2c) the depletion regions in Fig.(1.2d)effectively screen the interior from the surfaces, which means that the insulator is thick or the doping density is high. Under these conditions, as in the case of good ohmic contacts, the interior of the insulator is field-free, and the bottom of the conduction band attains its equilibrium position $\psi_i - X$ above the Fermi level, within the interior.

(c) Other Contacts

Figure(1.2e) and f illustrates the case of blocking electrodes on an intrinsic or very thin doped insulator. In this case the insulator is incapable of transferring sufficient charge from its interior to the electrodes to

give rise to any effective band bending. In the case of similar electrodes (Fig.1.2e), the result is that the bottom of the insulator conduction band is flat throughout its entire length.

When the insulator has dissimilar electrodes connected to its surfaces, it is clear that the interfacial potential barriers differ in energy by an amount

$$(\psi_{m_2} - X) - (\psi_{m_1} - X) = \psi_{m_2} - \psi_{m_1} \qquad \ldots (1.15)$$

as shown in fig. 1.2f. This means that a uniform intrinsic field F_{in} of strength $(\psi_{m_2} - \psi_{m_1})/es$ exists within the insulator and the conduction band must slope upward from the lower barrier with a gradient $\psi_{m_2} - \psi_{m_1}/s$. The origin of this zero-bias intrinsic field is a consequence of charge transfer between the electrodes. The electrode of lower work function, electrode 1, transfers electrons to electrode 2, so that a positive surface charge appears on electrode 1 and a negative surface charge on electrode 2. The amount of charge transferred is given by

$$Q = \frac{C(\psi_{m_2} - \psi_{m_1})}{e} = \frac{(\psi_{m_2} - \psi_{m_1})\, K\epsilon_o A}{e\, s} \qquad \ldots (1.16)$$

where C and A are capacitance of the system and area of electrodes respectively. If the insulator is very thin, the intrinsic field within the insulator can be very large;

for example, suppose s = 20 Å, and $(\psi_{m_2} - \psi_{m_1})/e = 1V$, $F_{in} = 5 \times 10^6$ V cm^{-1}. When electrode 1 is positively biased, the intrinsic field augments the applied field; that is, the field in the insulator F is given by $F = F_{in} + V/s$. When it is negatively biased, the intrinsic field acts to reduce the effect of the applied field; that is $F = \frac{V}{s} - F_{in}$. In the latter case the initial effect of the applied voltage $V < (\psi_{m_2} - \psi_{m_1})/e$ is to reduce the field in the insulator, which is zero when $V = \frac{\psi_{m_2} - \psi_{m_1}}{e}$. Increasing the applied voltage further i.e. $V > (\psi_{m_2} - \psi_{m_1})/e$, results in a reversal of the field in the insulator, which increases with increasing voltage bias. It will be apparent that, when the electrode of lower work function is negatively biased, the insulator will withstand greater voltage application before it breaks down. By investigating the breakdown voltage of very thin metal-insulator-metal junctions as a function of voltage bias (polarity), the effect of the intrinsic field can be detected(10) and measured. The difference in the breakdown voltages in the two polarities, ΔV, should obviously be equal to twice the difference of work functions of the metal electrodes when expressed in electron volts. (A further discussion follows in the chapter II.) This interesting phenomenon also has been studied in detail in the present investigations by using different metal electrodes on the two faces of dielectric films (here Langmuir films) of

different thickness.

The next chapter describes the past investigations on the intrinsic fields and the nature of present investigations.

CHAPTER II

PAST STUDIES OF INTRINSIC FIELDS

2.1 Potential Barriers Between Dissimilar Electrodes.

(a) Zero Bias

As explained in the last chapter, a high intrinsic field exists in an asymmetric tunnel junction, i.e., in a thin insulating film with dissimilar electrodes on its faces. The magnitude of this intrinsic field F_{in} is

$$F_{in} = \frac{(\psi_{m_2} - \psi_{m_1})}{e\ s} \qquad ..(2.1)$$

where s is the thickness of the insulating layer, ψ_{m_1} and ψ_{m_2} are the work functions of the metal electrodes and e is the electronic charge.

Fig.2.1 is the energy diagram for two dissimilar electrodes separated by an insulating film. The height of the barrier between the electrodes is no longer constant, but is a trapezoidal, according to Simmons'. As a result, the barrier heights at the metal insulator interfaces are no longer equal, but are related as follows:

$$\phi_2 = \phi_1 + F_{in}\ s$$

$$= \phi_1 + \frac{\psi_{m_2} - \psi_{m_1}}{e}$$

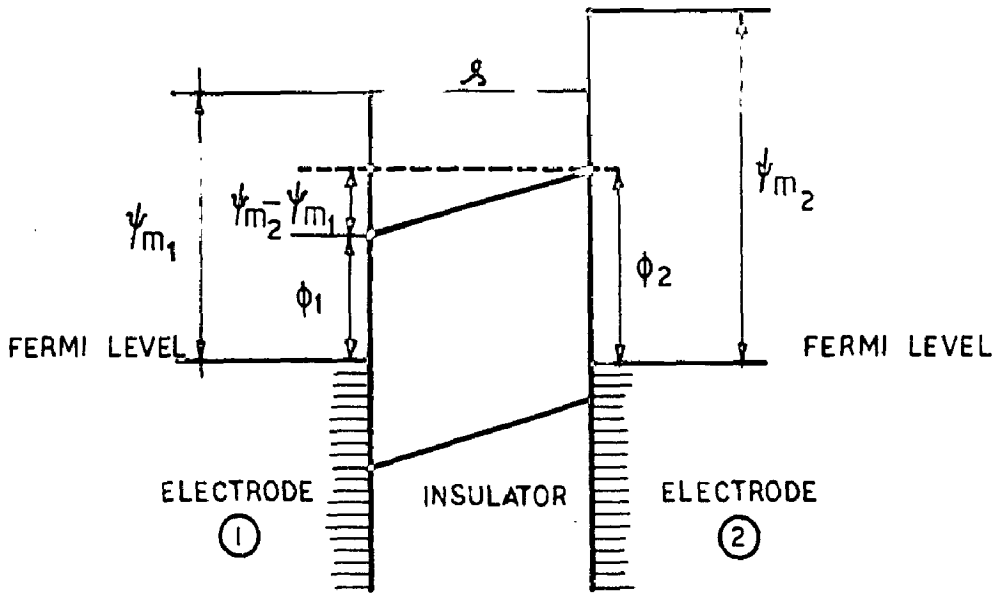

(a)

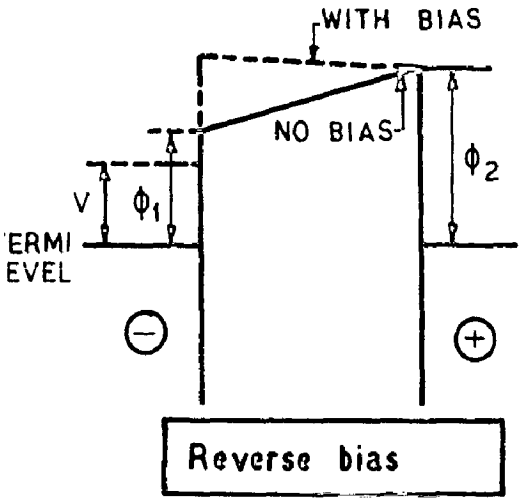

(b)

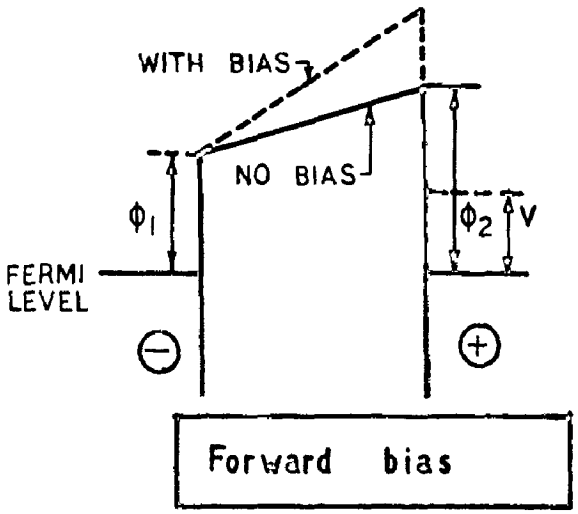

(c)

FIG. 2·1 ENERGY DIAGRAM OF AN IDEAL TRAPEZOIDAL BARRIER IN A METAL ① INSULATOR-METAL ② STRUCTURE WITH BIAS

(a) No bias
(b) Reverse bias
(c) Forward bias

$$= \phi_1 + \frac{\Delta\psi}{e} \qquad .. (2.2)$$

where $\Delta\psi = \psi_{m_2} - \psi_{m_1}$. The height of the barrier $\phi(x)$ between the electrodes is readily deduced as

$$\phi(x) = \phi_1 + \frac{\Delta\psi}{e}\ \frac{x}{s} \qquad .. (2.3)$$

As a result of (2.3), a knowledge of either of the interfacial barriers permits a complete determination of the potential barrier.

(b) With bias.

When a voltage bias is applied to an asymmetric junction the field in the insulator is augmented by the intrinsic field when the electrode of greater work function is negatively biased, and decreased when the electrode of lower work function is negatively biased. Thus the relevant equations for the potential barrier when the electrode of lower work function is negatively biased becomes

$$\phi = \phi_1 - \left(V - \frac{\Delta\psi}{e}\right)\frac{x}{s} \qquad .. (2.4)$$

and when the electrode of lower work function is positively biased, it becomes

$$\phi = \phi_1 + \left(V + \frac{\Delta\psi}{e}\right)\left(\frac{x}{s}\right) \qquad .. (2.5)$$

In the above equations the distance x is measured from the

surface of the electrode of lower work function. This field should also be manifested under voltage breakdown conditions; that is, the junction should exhibit polarity dependent dielectric strength characteristics. If a gradually increasing voltage is applied, with the electrode of lower work function negatively biased, then initial increase in voltage decreases the intrinsic field F_{in} to zero. Further increase of potential gradually increases the field in the insulator until a critical field F_d in the opposite direction is attained causing the junction to break down. The breakdown voltage V_1 under these conditions is given by

$$V_1 = (F_d + F_{in})s \qquad \ldots (2.6)$$

If V_2 is the breakdown voltage for opposite polarity then

$$V_2 = (F_d - F_{in})s \qquad \ldots (2.7)$$

The difference $\Delta V (= V_1 - V_2)$ in the breakdown voltages can be expressed in terms of the work functions of the electrodes as follows:

$$\Delta V = V_1 - V_2 = 2F_{in}s = 2\frac{(\psi_{m_2} - \psi_{m_1})}{e} \qquad \ldots (2.8)$$

$$\text{or} \quad \frac{\Delta V}{2} = \frac{V_1 - V_2}{2} = \frac{\psi_{m_2} - \psi_{m_1}}{e} \qquad \ldots (2.9)$$

The quantity $\frac{\Delta V}{2}$ is termed as internal voltage and

is the difference of work functions of two metal electrodes when expressed in electron volts. It is also to be noted that this internal voltage is independent of the thickness of the insulating layer.

2.2 Previous Studies on Intrinsic Fields in Naturally Grown Films of Al_2O_3.

The fact that a large intrinsic field can exist in a thin insulating film sandwiched between electrodes having different work functions appears to have been neglected by some workers (11-13). Simmons (10) for the first time demonstrated the existence of these intrinsic fields in the thin insulating films sandwiched between dissimilar electrodes. He fabricated various tunnel structures using Al - Al_2O_3 as the basic structure with counter - electrodes of Al, Au, Sn and Be. The junctions, in his studies, were fabricated as follows. Aluminium strips were evaporated onto carefully cleaned glass substrates in vacuum. The surface of these strips were then oxidized by exposure to dry oxygen at atmospheric pressure for a period of four hours. Finally, counter electrodes of different materials were evaporated.

The tunnel current-voltage characteristics exhibited by the symmetric structures (Al - Al_2O_3 - Al) were almost independent of polarity. These essentially nonpolar characteristics were to be expected from the symmetry of

potential barrier (as shown in Fig.(1-2e). The asymmetric structures (Al - Al_2O_3 - Au, Al - Al_2O_3 - Sn and Al - Al_2O_3 - Be) exhibited polar characteristics, with the greatest value of current occuring when the aluminium electrode was positively biased. These results suggested that the barrier was asymmetric, thus indicating that a field existed in the insulator.

The junctions were tested to destruction with the oxidized aluminium electrode of successive junctions biased alternately, first positively, then negatively. The breakdown voltage for a given type of junction and polarity was extremely consistent. The experimental mean values of ΔV for the various junctions were compared with the theoretical values of ΔV (twice the difference of work functions of the two metal electrodes expressed in electron volts) and these values were found in good agreement.

The reproducibility of the above results suggested this technique to be a good method of determining the work function of thin films, with respect to some standard. Simmons suggested that the technique could facilitate work function comparison measurements at low temperatures, where work function measurements were difficult to make using more standard techniques. Assuming Al as standard and using value of its work function, Simmons was able to calculate the work function of Sn and Be.

The intrinsic field is an important consideration(10) in

the designing of the thin film devices as proposed by Mead (12,16). The maximum energy E_m with which an electron can be injected from the emitter to the base is given by

$$E_m \simeq e\,(F_d + F_{in})\,s$$

$$= e\,F_d s + \psi_b - \psi_e \qquad (2.10)$$

where ψ_b is the work function of base material, and ψ_e is the work function of emitter material. Thus, using an emitter of lower work function than the base (that is, where $\psi_b - \psi_e > 0$) permits higher maximum electron injection energies than if the electrodes are of the same work function (where $\psi_b - \psi_e = 0$). The advantage of this principle has been neglected in the device proposed by Spratt et al (11), who injected electrons from an emitter of high work function into a base of lower work function. Ghosh and Feng (169) have drawn somewhat similar conclusions while studying photovoltaic and photoconductive properties of Al/tetracene/Au sandwich cells. They have attributed larger photovoltages partly to change in work function of the two metal electrodes. Mead and Lewicki (14) in their photoemissive measurements of the barrier heights in thin films Al-AlN-Mg tunnel junctions have shown that the barrier heights increase with increasing thickness in the range 40-100 Å of insulator thickness. An explanation of these observations was given by Simmons (15) in terms of the effect of deep traps on the barrier heights of the MIM tunnel junctions. Horiuchi et al (114) have also observed different barrier heights at the two interfaces of an MIM structure with dissimilar electrodes. They explained their results in terms of the trapezoidal energy barrier model of Simmons. In these

studies intrinsic field is involved only indirectly. However, these authors have not attempted to carry out systematic studies of the intrinsic fields in the above structures.

All the above studies by Simmons (10) were carried out for nearly fixed value of insulator film thickness. In the present investigations a detailed and systematic study of the thickness dependence of the internal field and the internal voltage, because of this field, have been carried out by using the well known Langmuir films (17,18). As will be explained below these films have been found to be almost ideally suitable for the above studies.

As far as the author is aware, no other work on internal fields of the above type has been reported after Simmons' (10) work.

Suitability of Langmuir Films for Studies of Intrinsic Fields.

The electrical behaviour of thin films obtained by a variety of processes, e.g., thermal evaporation in vacuum, have been extensively studied. But the study of mono and multilayer films obtained by the Blodgett-Langmuir technique (17,18) (Commonly referred to as Langmuir Films) has gained considerable importance only during the past decades. Unlike the evaporated films, the striking features of these organic films are their accurately controllable thicknesses down to one monolayer ($\sim$ 25 Å)

and the possibility of obtaining them almost free from holes and conducting imperfactions. These films are most suitable for thickness dependent studies because of their easy deposition, accurately known, closely controllable thicknesses which are also extremely uniform (19). These films also have the advantage that they have high dielectric strength (19).

2.3 Nature of the Present Work

(a) The present work constitutes a systematic and detailed study of intrinsic fields in the Langmuir films with asymmetric electrode structure. It has been found from the breakdown studies that a high intrinsic field exists in these films.

(b) The emphasis has been given to the studies of internal voltage because of this field. This internal voltage has been directly measured by electrometer amplifier used as a high input impedence voltage measuring device. The study has been performed on Al - O - M structures where O refers to organic films of different thicknesses and M refers to different metal electrodes namely, Ag, Sn, Pb, Bi, Te. Films of Ba palmitate, Ba margarate, Ba stearate and stearic acid were studied because the thicknesses of these Langmuir films are very accurately known. The three acids palmitic, margaric and stearic are the consecutive members of the same homologous series. Some

investigations have also been made with Sn as the bottom electrode and Al the top electrode. It has been observed that this combination does not alter the results except that it changes the polarity of current and voltage.

(c) Careful experiments were also done on symmetric Al - O - Al structures and it was very interesting to find that in the case of even number of monolayers there was no internal voltage but in the case of odd number of layers the internal voltage existed.

(d) By utilizing the phenomenon of internal fields the work function of one of the metal electrodes was determined knowing that of the other.

(e) The influence of thickness of electrode material on its work function was also studied.

(f) A new method has been developed to determine the dipole moment of suitably orientable molecules by studying the internal voltage, e.g. in the Al -Barium stearate - Al structure.

(g) Utilizing the phenomenon of internal fields a thin film dielectric diode system with the asymmetric structure Al - O - M has also been developed. Since in the context of this device the dynamic dielectric characteristics of the Langmuir films become important, a detailed and systematic study of the latter dielectric phenomenon in

Langmuir films has also been carried out.

The details of all the above investigations i.e., results, interpretation and discussion have been given in the later chapters (chapters VII,VIII and IX).

Since Langmuir films have been used as the insulating barrier in all the present investigations the next few chapters III, IV and V describe in detail the nature of these films, their deposition characteristics and their properties.

CHAPTER III

MONOMOLECULAR FILMS

3.1 Introduction

Since Langmuir films utilized in the present studies are 'built-up' from insoluble monomolecular films on water surface, first the essential details of these films are described below.

Insoluble monomolecular films on liquid-gas interface have been a subject of investigation for the last many years because of their possible application for technological and scientific purposes. For example, films which reduce evaporation losses at water surfaces, are of particular interest. In these processes, the ultimate film, which is only one molecule thick, plays the most important role. Such a film is referred to as monomolecular film or monolayer.

The existence of monomolecular film on liquid surfaces was first inferred by Lord Rayleigh (20) while interpreting Pockel's (21) observations on the reduction of surface tension of water by the contamination of its surface with olive oil. This monomolecular spreading has remained one of the most fundamental phenomenon in the study of the physics and chemistry of surfaces (22). Wide occurrence of insoluble monolayers of many organic substances is now well known (22) and Rayleigh's hypothesis of monomolecular spreading is well established. Monolayers at a liquid gas interface can be controlled, manipulated and examined under far better conditions. That is why the monolayer at the water-air interface has been extensively studied in the pioneering work of Rayleigh, Langmuir, Adam, Rideal, Harkins and others, providing

much basic information on such monolayers. Here, particular stress has been given to the understanding of monolayer properties because the 'built-up' films which have been studied extensively in the present work, have been deposited simply by transferring these monolayers on to solid surfaces.

Since the subject of monomolecular films originated with the experimental study of the surface tension of water the present chapter discusses about the surface tension phenomenon and spreading of organic substances on water surface. The Pockel's observations on monolayer spreading of olive oil on clean water surface and the effect of oily contamination on surface tension of water have been discussed in detail. Lord Rayleigh's interpretation on Pockel's observations has also been given. A brief discussion has been given on the existence of short range forces and the mechanism of monolayer spreading on water surface. Some fundamental information about individual molecules, such as the length of the molecule obtained by these experiments are also described.

3.2 SURFACE TENSION OBSERVATIONS AND MONOMOLECULAR SPREADING

a. Surface Tension of Water

Some amount of work has to be done in bringing the molecules from the interior of the liquid to its surface due to the intermolecular cohesion. This work done is stored as free energy of thus created new liquid surface. The free energy, thus stored per unit area of this newly formed liquid surface is termed as the 'surface tension' of the

liquid. It was supposed for a long time that a liquid surface resembles a 'stretched skin under tension' but it is not so and thus the term 'surface tension' is a misnomer. However, the two definitions of the surface tension that it is the force (dynes/cm) acting normal to a unit length in the liquid surface and the other stated as the free energy per unit area of the liquid surface are equivalent.

It has long been known that the surface tension of water is lowered due to oily contamination of its surface. In fact, accidental contamination of the surface had previously complicated and confused nearly all observations on surface tension phenomena. Lord Rayleigh (23,24) was the first to measure accurately the amount of this lowering of the surface tension of water resulting from olive oil contamination. He also estimated the average thickness of the oil film on water to 16 Å, by the simple area-density method.

Pockels (21) made a detailed and systematic experimental study of the effect of oily contamination on the surface tension of water. The apparatus used by her was consisting of a long narrow trough filled to the barium with water and two rectangular metal strips called 'barriers', which rested across the long edges of the trough. These movable barriers were used to sweep-off the impurities of the surface and a desired area of the surface could be selected by drawing out or drawing in these barriers across the long edges of the trough. The desired area of water surface, thus enclosed between the barriers, could now be contaminated by placing

a small drop of olive oil on the water surface. This olive oil can not leak through the barriers because they touch the water surface all along. The contaminating oil remains confined on the large or small area of the water surface by pulling-out or pulling-in the barriers along the long edges of the trough.

Pockels (21) observed that if a fairly large area of the water surface is contaminated with a very small amount of olive oil so that no excess oil in the form of small drops remains on the surface permanently, the surface tension of water remains unchanged. When the area of this contaminated water surface was reduced by gradually drawing in the ''barriers'', the surface tension was found to remain practically constant (equal to that of a clean water surface) upto a certain critical area, below which it fell rapidly. The value of this critical area depended on the amount of oil placed on the water surface. It was shown that if a given area of the water surface is contaminated with any amount of oil less than that which gives a critical thickness of about 10 $\mathring{A}$ the surface tension remains unaltered, but above this limit it falls rapidly as the amount of oil is increased. This critical amount of oil, enough to give the thickness of 10 $\mathring{A}$, can be easily estimated from the area-density method.

b. Monomolecular Spreading of Olive Oil on Water Surface.

Rayleigh (20) repeated many of Pockels' experiments to confirm her interesting observations outlined above. He

suggested that when olive oil is placed on the water surface it spreads out as a monomolecular layer on the surface and the oil molecules in the critical area observed by Pockels remain closely packed, just touching each other. These ingenious suggestions of Rayleigh were thus the origin of the fascinating subject of monomolecular films. It has been said that the molecular theory arose through Rayleigh noticing that the thickness of the films turns out to be almost the same as the known molecular length. But his detailed explanation of Pockels' observations, as given below, clearly show that the monomolecular theory rests not merely on a numerical coincidence but is based on the far firmer foundation of the idea of ''tangible' floating molecules''.

All the Pockels' observations can be beautifully explained (20,22) in the light of Rayleigh's suggestions, as follows. When a drop of olive oil is placed on the water surface the oil molecules quickly spread out as a monomolecular layer on the surface; the cause and mechanism of spreading will be discussed in a later section (3.4a). Obviously, the area of the water surface available for the spreading molecules can accomodate as many of them as can be closely packed in a completed monolayer on the area. This number 'n' of the spread molecules on the water surface is clearly given by the area of the water surface divided by the molecular cross-sectional area. If the number of molecules in the amount of oil placed on the area is less than 'n', all the molecules will spread out on the area without any

excess oil in the form of drops being left permanently on the water surface; if the available number of oil molecules is greater than n, the n molecules will spread out to form a close packed monolayer, with the excess oil remaining permanently on the water surface as lenses of considerable thickness. In the former case the spread monolayer will be incomplete in the sense that the molecules in the layer do not touch each other over the whole water surface and can move about on the surface relatively independently, while in the later case the molecules in the completed layer will be closely packed, touching each other over the whole surface.

From above it is clear that in Pockels' experiment the spreading oil molecules do not form a completed close-packed molecular layer in areas greater than the critical area. In such stages of compression of the monolayer the oil molecules do not touch each other and move about on the surface because of the excess space available. The molecules remain too far apart for the intermolecular repulsive forces to come into play. Thus, upto the critical area no work will have to be done in the process of compressing the monolayer by barriers. The free energy of the underlying water surface will therefore remain intact and the surface tension of the water will remain unchanged up to the critical area. As soon as the area of the contaminated water surface equals the critical area, the molecules in the compressed monolayer become closely packed and just touch each other. At this stage the mutual intermolecular repulsion comes into

play rather abruptly and the first resistance to compression arises. The molecules in the monolayer start experiencing an outward force tending to spread them out due to the mutual repulsion. This outward force exerted on an element of unit length in the monolayer is the ''surface pressure'' (dyn/cm) of the monolayer film. At the critical stage when the intermolecular repulsion just comes into play some work will have to be done to further compress the monolayer, even slightly. Since this required energy naturally comes from the free energy of the underlying water surface the surface tension of the water falls suddenly and rapidly, below the critical area. From energy considerations Adam (22) has shown that the reduction in surface tension is equal to the surface pressure of the film. Obviously, the value of the critical area will depend on the amount of oil placed on the water surface. Hence, the critical area having closely packed molecules just touching each other will be greater if the amount of the oil or the number of available molecules is greater.

In the above experiments of Rayleigh, the amount of the contaminating oil was kept constant and the area of the contaminating water surface was varied while in the Pockels' experiments on surface tension, she kept area of the water surface constant and contaminated it with increasing amount of olive oil. Here, so long as the area of the water surface is contaminated with an amount of oil less than one which contain 'n' molecules, the molecules in the spread monolayer will not be closely packed. The surface

tension does not change as the intermolecular repulsion at this stage does not come into play. The spread monolayer becomes closely packed when this area of water surface is contaminated with just 'n' molecules of olive oil. When the amount of oil is slightly increased to this critical limit, the intermolecular cohesion just comes into play and therefore the surface tension falls rapidly. The average thickness of the monolayer in the critical stage, as observed by Pockels in her experiments was nearly 10 Å. In this way all the Pockels' observations can be explained using Rayleigh's suggestions.

A simple interpretation of the fall in the surface tension due to the oily contamination of its surface can also be given as follows. The surface tension of water with a clean surface is determined by the cohesion or attraction between its surface molecules and those lying underneath. Because of this attraction, the surface molecules experience an inward pull in a direction perpendicular to the surface because of the attraction. When oil drop is poured on the surface, cohesion or attraction between the surface water molecules and those lying underneath is opposed by the adhesion or attraction between the oil molecules and the water molecules in the surface, as a result of this, the inward pull on the surface water molecules is bit reduced and consequently the surface tension of water with contaminated surface is less than that of the clean surface. The reduction in surface tension will obviously depend on the

adhesion or attraction between the contaminating molecules. The greater is the adhesion, more will be the reduction in the surface tension and vice-versa. But, in case, adhesion equals the intermolecular cohesion (between the water molecules itself), the interfacial surface tension would vanish and the contaminating molecules would become completely miscible with water molecules and all of them slowly go into the solution with each other.

Rayleigh's molecular theory (20) thus explains all the experimental observations in a most remarkable way. His ideas now seem to be absolutely indispensable for interpreting the basic phenomenon of surfaces. This phenomenon of monomolecular spreading has come to stay as one of the most fundamental one in the field of Physics and Chemistry of surfaces (22).

(c) Spreading of other Organic Substances on Water: Further evidence for monomolecular spreading.

As has been shown above Rayleigh's monomolecular theory provided a powerful tool for interpreting the basic surface phenomenon which could be studied experimentally by using an extremely simple apparatus, which was first used by Pockels. In fact Pockel's application of movable barriers to confine films to compress them or to remove any undesirable surface contamination laid the foundation for nearly all the work with films or liquids (22,25,26).

It was reallized from the Rayleigh's successful explana-

tion of Pockels' observations that a close study of monomolecular layers would yield the fundamental information about individual molecules e.g. length of the molecule, their cross-sectional area, the strength of intermolecular cohesion and of the polar group etc. The promise of glimpse into the fundamental aspects of individual molecules with the use of very simple apparatus has constantly inspired the extensive experimental investigations on the monomolecular films. As the monomolecular films can be regarded as a two dimensional matter existing in all the three states, solid, liquid and gaseous (22), a theoretical study of these monomolecular layers has also been very attractive. Thus, investigations in the field of monomolecular films are most interesting and fascinating ones.

The mechanical,electrical, optical and chemical properties of molecules in an oriented array had already been revealed by a large number of experimental methods which characterize monolayers and have contributed much information about the shape and size of the molecules. All,of course depend on the formation of a suitable film for study. The successful organic substances known for spreading as monomolecular layers on water surface are fatty acids,alcohols, esters, ketones, sterols, dyes, chlorophyll, proteins etc. (22,25,26,27,28). Among these substances most thoroughly investigated are the long straight chain fatty acids e.g. palmitic acid, margeric acid, stearic acid etc. (22).

Layers of these acids have a molecular structure consisting of a long hydrocarbon chain with a nonpolar (hydrophobic) methyl (CH_3) group at one end and a polar (hydrophilic) functional carboxyl (COOH) group at the other one. The parent hydrocarbons do not spread to form monolayers but the presence of this polar group at the end of long hydrocarbon chain causes the spreading of these fatty acids. The mechanism of spreading is described in sec. 3.4(a).

Devaux (29) studied a number of materials with simple but elegant experimental method and noted that the behaviour of the films is sometimes as solid and sometimes as liquid. Hardy (30) found that oils which do not contain polar functional group do not spread in the same way as the animal and vegetable oils.

The first studies on the fatty acids were made to confirm the monomolecular spreading of these acids on water surface. Langmuir (31) justified the monomolecular spreading and the formation of monolayer on water surface by estimating the thickness of the spread film using simple area-density method. If a spread film occupied an area 'A' of the water surface and 't' is the average thickness of the film, Axt = V is, obviously, the volume occupied by it. This volume V multiplied by the density d of the film material, gives the mass m of the material of the acid spread. From a knowledge of A, d and m, the average thickness of the film t can easily be estimated. When the area A is reduced down to the critical areas, the corresponding value of 't' now

obtained will be equal to the length of the molecule. This is so because the molecules stand perpendicularly on the water surface due to close packing of the molecules. Thus, the length of the molecule in monolayer could be estimated from experimentally determined critical area and the corresponding amount of acid spread. A check of the basic assumption of monomolecular spreading of the fatty acid could now become possible by tallying the length of the molecules thus measured with the values of the chain length obtained by other method e.g. X-ray diffraction measurement of the chain length in bulk crystals of the fatty acids. Thus the estimated thickness of fatty acid monolayer on the water surface by the above discussed area density method, are in agreement (32,33) with their corresponding chain lengths in bulk, studied by X-ray diffraction (34). This work thus supports the Rayleigh's hypothesis (20) of monomolecular spreading and has established that the spreading of fatty acid on water is monomolecular in nature. Many other substances e.g. alcohols, esters, ketones, sterols, dyes, chlorophyle, proteins etc. have also been found to spread monomolecularly. Thus, Rayleigh's hypothesis of monomolecular spreading originally put forward for the case of olive oil only, now seem to be applicable in general for all the substances stated above.

The study of the nature of spreading of the fatty acid on water surface by estimating the thickness of the spread layer by the area density method, however, is open

to objection. One of the objections against the area density method, discussed above, is that the density of the layer has invariably been assumed to be equal to that of the substances in bulk. This assumption is justified only when the substance in bulk has closed packed layered structure similar to that in the monomolecular film which in general is not true. Therefore, the area density method can not be expected to yield accurate value of the thickness. However, Langmuir and Adam had great confidence in the area-density method in studying the nature of spreading of fatty acids on water and conclussions drawn by them for the monomolecular spreading are essentially correct, because the density of the monolayers of the fatty acid happens to be very close to that of the acid in bulk.

3.3 SHORT RANGE FORCES AND ADSORPTION: NON OCCURRENCE OF POLYMOLECULAR FILMS.

To provide strong support for the idea of molecular orientation of surfaces and the short range of molecular forces which was developed by Langmuir (35) and Harkins (36) separately. Langmuir performed some classic experiments on adsorption of hydrogen and oxygen in highly evacuated bulbs containing heated tungsten filaments. He also believed that the short range forces are responsible for nearly all types of adsorption. Thus, if the surface of a solid or liquid is covered by a similar layer of foreign atoms or molecules, its adsorption properties completely change since the molecule

in the consecutive layers can be in contact with those in the preceding one only and not in contact with the substrate.

The concept of short range forces, therefore, leads directly to the monomolecular spreading of the insoluble fatty acids, having hydrophilic (water loving) carboxylic groups in contact with the water surface and the hydrophobic (water hating) methyl group away from the water surface in a vertical position. The attachment and orientation of polymolecular chain will not take place in the absence of long range surface forces because the hydrophillic group in the second layer could not come into contact with water. Thus, Langmuir's postulate of short range forces, which is responsible for adsorption on liquid surfaces also can be regarded as the theoretical justification for Rayleigh's idea of monomolecular spreading. The occurrence of monomolecular layers of a large number of insoluble substances on water, also give strong support to Langmuir postulate.

Hardy (37) while working on monomolecular orientation in surface, believed the cohesive forces between the molecules to be of long range in nature, often acting through distances of several thousand Ansgstrom units and thus thought that the orientation extended through many layers of molecules. The observation of Rothen (38) on adsorption involving large molecules, provide definite evidence for the existence of long range molecular forces. Therefore, now it seems that Langmuir's postulate of short-range forces being involved in adsorption phenomena may not

be generally applicable and that Hardy's long range molecular forces do exist in the case of some large molecules.

3.4 FUNDAMENTAL CHARACTERISTICS OF MONOLAYERS.

(a) Mechanism of Spreading of Monolayers on Liquids.

A nonvolatile substance, insoluble in a liquid, spreads on its surface if the adhesion between the molecule of the substance and that of the liquid is greater than the cohesion between molecules of the substance itself (22). A quantitative condition for the spreading of liquid B on liquid A can be given in terms of Harkins (25) ''spreading coefficient'' defined as

$$S_{B/A} = Y_A - (Y_B \cdot Y_{AB}) \qquad (3.1)$$

where $S_{B/A}$ is the spreading coefficient of liquid B on liquid A, Y_A and Y_B are the surface tensions of the liquids, and Y_{AB} the interfacial tension between the two. If $S_{B/A}$ is positive, the spreading will take place spontaneously and if it is negative liquid B will rest on liquid A as a lens. In practice, however, this criterion has to be applied with caution (26,p.16). The mechanism of the spreading of the substance on liquid surfaces is explained here taking the case of olive oil on water. Water molecules are in constant motion along the surface diffusing long distances and the motion of these surface water molecules cause the expanding movement of the oil drop. Oil molecules adhere to the water molecules and are carried outwards along the surface because of the surface diffusing motions. The surface

diffusion motions of water molecules go on continuously underneath the oil drop and the oil molecules which spread first are continuously pushed out farther by the outward surface pressure of those just leaving the oil drop. Obviously, the spreading of a liquid on solid surface can not take place by the above mechanism since the (surface) atoms or molecules of solids remain practically fixed up in their positions.

The spreading and the stability of a foreign monolayer at the liquid gas interface under given conditions is dependent on a delicate balance among the properties of the substances involved. The substances like long-chain fatty acids and alcohols have a molecular structure composed of a large nonpolar or hydrophobic portion 'the hydrocarbon chain' and at the other extremely a polar or hydrophilic carboxylic or hydroxylic (-COOH or -OH) functional group. The polar groups tend to confer water solubility, while the nonpolar part prevents it and the formation of an insoluble monolayer is determined by the balance between them. Short chain fatty acids and alcohols such as acetic acid and methyl or ethyl alcohols, are of course, completely miscible with water but the solubility of these substances in water decreases as the length of the hydrocarbon is increased. Thus in the case of the spreading of stearic acid on water, the adhesion (or affinity) of the stearic acid molecule, containing a polar carboxylic group to the polar water molecule is greater than the cohesion (or affinity) between stearic acid molecules themselves. Therefore, the stearic acid molecules thus spread

out due to the surface diffusing motions of water molecules will attach themselves to the water molecules by their hydrophilic (water loving) carboxylic group (heads) and since the nonpolar hydrocarbon chains with hydrophobic methyl groups are very weakly attached by water molecules, they remain more or less vertically oriented with the methyl groups (tails) on top. The presence of polar groups in the chain may result in its slight tilting. If the polar or hydrophilic group is not present in the substance, its spreading on water is not possible as is the case with long chain hydrocarbons such as decane ($C_{10}H_{22}$) or cetane ($C_{16}H_{36}$) and liquid petrolatum. These substances do not spread at all on water. A drop of such oils remain on the water surface ~~as a lens of considerable thickness without spreading.~~ Further, the interactions between and within the molecules forming monolayers are also important. If the intermolecular interactions are strong enough, its spreading as monolayers is difficult even when a suitable polar group is present.

The factors as mentioned above affecting the spreading depend, not only on the nature of the film forming material but also on the nature of both the liquid and gaseous phases. These various factors are also important in governing the structure and stability of an insoluble monomolecular film. To study a certain compound which does not form an insoluble monolayer on pure water, it may be possible to spread it on some other subphase. While the

concept of opposing insolubility of a hydrocarbon chain and solubility of a polar functional group is adequate for understanding the formation on air-water interface whereas on the other liquid subphases, other kinds of attraction than the strong dipole-water interaction can be effective. It appears, for example, that n-octacosane, the 28 - carbon saturated hydrocarbon, will spread to form a stable monolayer on mercury (39). Presumably, in this case where the liquid subphase has a very high surface tension, dispersion forces are adequate to provi attraction between the organic compund and the surface, and a film is formed in which the molecules are spread out flat on mercury. There are also some fluorinated organic compounds which can spread to form insoluble monolayers on organic liquids. In these cases, parts of the molecules are attracted to the subphase while other parts prevent complete solution.

3.4 (b) The Formation of Spread Monolayers

There are two ways in which a monolayer can spread if a volatile solvent is used for the purpose. In some systems for example fatty acids dissolved in hexane or petroleum ether on water, the droplets of the spreading solution spontaneously thin out into a layer - the monolayer - forming molecules positioning themselves at the solvent - water interface. On subsequent evaporation of the solvent the spread monolayer remains on the water surface. With some other systems, e.g., spreading solutions

in dilute benzene, the solution droplets shed from their edges a dilute mixed film of the monolayer - forming substance and solvent, which spreads over the available water surface. With subsequent evaporation of the solvent from the mixed film, the reservoir of the solution droplets shed more film for spreading. The relative interfacial surface tensions involved determine which kind of spreading will occur in a particular situation. In both the processes, however, the monolayer left is, in general, not in a state of absolute stable equilibrium (26) and the free energy of the system is not minimum.

Sometimes spreading can also be achieved without the use of a solvent e.g. oleic acid, cetyl alcohol. In these cases the diffusion processes govern the mechanism of spontaneous spreading, and the film-forming molecules leave the bulk phase and diffuse over the underlying liquid surface. The process of spreading may be hastened by convective flow in the liquid and, in some cases, by vapour phase transport(26). With sufficient material, the spreading will continue until the surface pressure has risen the 'equilibrium spreading pressure'. This equilibrium value depends on the relative magnitude of the forces tending to hold the molecules in a monolayer at the air-water interface and those favouring their retention in the bulk droplet or crystal. If the surface available is large enough, the material applied to the surface spread out completely, the observed surface pressure will be less than

the ''equilibrium spreading pressure''.

3.4 (c) The Monolayer States

Henri Devaux (29) pointed out that the molecules in the monomolecular films may exist in many different forms corresponding to the three states of matter viz, solid, liquid and gaseous. He showed that the fluidity of a monolayer can be qualitatively estimated from the mobility of talc particles dusted into the film. Various monolayer states represent different degrees of molecular freedom or order resulting from the intermolecular forces in the film and between film and subphase. The state and stability of monolayer depend on the amount and distribution of the lateral intermolecular adhesive forces and the strength of anchorage of the molecules to the surface respectively. If the anchorage or the perpendicular attraction between the film molecules and the liquid is weak, the film may not be formed at all or it will tend to crumple up under small lateral compression but if the anchorage or the attraction between the molecules in the monolayer and that of the liquid is sufficiently strong and the lateral adhesion is small the film molecules move about independently on the surface partaking in the translatory motion of the underlying liquid molecules. Such a film resembles a gas on the surface and is called a gaseous or vapour film. A strong lateral adhesion makes the molecules adhere together into large coherent islands of films and restrains their

free thermal motions on the surface. The existence of the states of monolayer depends on a delicate balance of intermolecular attractive or repulsive forces. The film is liquid or solid depends on whether the molecular movement is less or more restricted, determined by the amount and small details of distribution of the intermolecular adhesive forces (22).

3.4 (d) Fundamental information about individual molecules from Monolayer States.

Langmuir's film balance (22) whose range has recently been considerably extended by the use of an electron microscope and radio isotopes (40), remains the principle instrument for basic studies on monomolecular films. With the use of this classically simple device, the primary measurements of the size of the molecules, the estimation of their shape, their cohesion and the location and strength of their charged active groups can be obtained.

The film balance essentially consists of a small shallow waxed trough filled with water on which the monolayer of substance dissolved in a volatile solvent is spread. A barrier in the form of waxed rectangular bar is laid across the long edges of the trough behind the monolayer. The film is made to push against a delicately suspended floating barrier which measures the surface pressure exerted by the film as the film is compressed. The pressure of the film against the float is balanced by twisting torsion-wire to which the float is attached. The degree of twisting

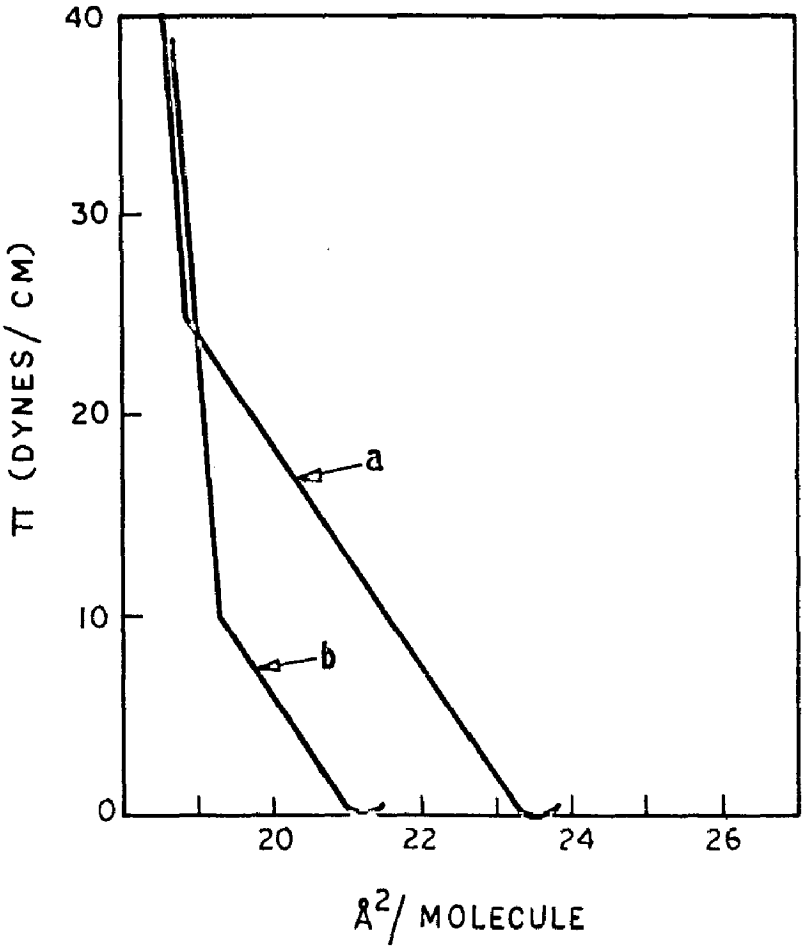

FIG. 3·1 Π-A DIAGRAMS OF SOME TYPICAL CONDENSED MONOLAYERS OF LONG-CHAIN COMPOUNDS.

(a) UN IONIZED FATTY ACIDS AND (b) FATTY ALCOHOLS HAVE BOTH MOLECULAR AREAS OF ABOUT 20 Å² AT HIGH SURFACE PRESSURE. FROM G.L.GAINES, JR, Insoluble monolayers at liquid qas interfaces © 1966 BY JOHN WILEY AND SONS, INC., NEW YORK.

required to keep the float stationary is a measure of the surface pressure. Greatest care has to be taken to minimize the temperature variation, accidental contamination, vibrations and dust particles, which may cause major errors in the experiment.

A simple curve Fig3.1 plotted between surface pressure and area (pressure-area curve of the monolayer) yields, among other things, the cross section and length of the molecule, and the approximate location and strengths of its polar groups. The approximate strength of the intermolecular cohesion or the compressibility of the monolayer can also be obtained from the slope of the pressure-area curve showing decrease in surface area with the increase in surface pressure. Experimentally it is found that many monolayers can be compressed to pressures considerably higher than their equilibrium spreading pressures. Eventually, however, it is found impossible to increase the surface pressure further, and the area of the film decreases if the pressure is maintained constant or the pressure falls if the film is held at constant area. This condition is referred to as the collapse point of the monolayer. The molecules in the monolayer near the collapse pressure are tightly packed together and the film collapses on slightly increasing the pressure. The cross-sectional area of the molecules can be determined with a prior knowledge of the number of molecules in the monolayer i.e. the number of molecules in the amount of the substance spread.

The length of the molecule or the thickness of the monolayer can be found by the area-density method. The collapse pressure gives both the strength of anchorage of the film to the surface i.e. the strength of the polar group and the strength of cohesion. Stearic acid, for example, has been found to have a cross-sectional area of 20 Sq. angstroms and a chain length of 25 angstroms. The monolayers of stearic acid have a high collapse pressure of 42 dynes/cm and low compressibility (or high molecular cohesion).

3.5 INHOMOGENEITY OF MONOLAYERS

It was long ago that the investigators assumed the monolayers to be homogeneous at all stages of compression. Zocher and Stiebel (41) first examined the monomolecular films to show them to be inhomogeneous at low surface pressure and sometimes even in the region of collapse pressures. His apparatus consisted of a powerful dark field illuminator mounted in the bottom of a trough and focused on the surface of the liquid bearing monolayer. A microscope was used above this surface to detect inhomogeneity of the film. This technique was later improved by Adam (42), who suggested that varying the liquid level in the trough provided a simple means for accurate focussing. The ultramicroscope has also been used by Bruum (43) in an interesting study of collapsed films. The method, however, was capable of detaching only gross impressions of the size and shape of these aggregates.

Later, Feachem, Bouchet, Tronstad and others (44,45,46) have used the elliptically polarized light reflected from surfaces covered by the monolayers, for studying the structure of the films. However, this method could not contribute much regarding the structure of monolayer because of the difficulties in the interpretation of the optical effect of the films in terms of the individual molecules but is capable of indicating the inhomogeneities in the film (47).

Measurement of the surface potential, which depends on molecular concentration or packing in a monolayer, also showed the films to be inhomogeneous (except gaseous) (47). Because of the dimensions of the electrodes used in this method it cannot, of course, resolve the detailed fine structure of the monomolecular film.

Beautiful and extensive study of the monolayer structure at various stages of compression has been made by direct electron microscopy by Epstein (48). He showed that it was possible to detect fatty acid monolayer films, after depositing them on glass slides and shadowing with an evaporated metal film. Ries (40) and his coworkers refined this technique to study the monolayer structure at various stages of compression. The electron micrographs taken by them clearly show that at low pressure the film is inhomogeneous and with increasing compression or pressure large homogeneous areas of continuous monolayers appear. These micrographs also suggested the collapse mechanism and has also been used to determine the thickness of monomolecular

films by the shadow casting technique (40). More information about mixed films or monolayers with two or more components was obtained using combined film balance and electron microscope technique in conjunction with radio-active tracer technique (40). The results obtained are of biological importance.

The next chapter describes the technique of the building up of the multilayer Langmuir films by transferring monolayers on solids (glass slides).

CHAPTER IV

BUILT-UP MOLECULAR LANGMUIR FILMS

INTRODUCTION

The monomolecular films are of great interest because of their formation at surfaces or interfaces. The transferring of these monolayers on solid surfaces is also equally interesting. The present chapter deals with the experimental method of 'building-up' of multilayer films. The nature of these built-up films has also been described. Particular emphasis has been given for the 'building-up' process of the so called Y-type films because these films have been used for investigations in the present work. A brief discussion about the so called X and Z type of films has also been given.

4.1 'BUILDING-UP' OF MULTILAYERS ON SOLIDS

Experimental: Blodgett-Langmuir Technique

Langmuir (49) was the first to realize the fascinating possibility of building up multilayer films by the successive deposition of monolayers, one on the top of the other, on the same solid substrate. The highly interesting technique was subsequently developed and perfected by Blodgett and is now well known as the Langmuir-Blodgett technique (17,18,50). This is probably the only technique by which one can deposit a film with a known and controllable number of molecular layers. This technique has been described here in detail for depositing films of metal-organic compounds, specially for barium stearate. However, the same method is valid

for the other similar substances like barium palmitate, and margarate which have also been studied in the present work.

The technique for 'building-up' of these films requires a very simple apparatus consisting of a long narrow trough T (Fig.4.1) usually made of inert materials such as teflon, perspex etc. Metals such as copper or aluminium are not used because they may stop the deposition. The trough used in the present work is of specific design. It is much less deep throughout (about 0.75 inches) and deeper at one end where the slide is to be dipped. With this relatively small amounts of deionized water is needed. The inside of the trough is heavily waxed. Waxing of the trough is necessary in order to obtain a higher water level at the edges, which ensures that there is no leakage of the monolayer past the barriers. The barriers, rectangular in shape, such as glass strips, must also be waxed all around to render them hydrophobic. The trough is first levelled and then filled to the brim with deionized and doubly distilled water (specific resistance $\simeq 6 \times 10^5$ Ohm cm) having a low concentration of barium by adding 3×10^{-5}M barium chloride. For obtaining good deionized water the ion exchange resin columns together with double distillation plants were used. For easier deposition, the pH of the solution is adjusted to greater than 6 by adding a specific quantity of an alkaline substance. For example, $KHCO_3$ (potasium bicarbonate) at a concentration of 4×10^{-4}M holds the pH at about 7.2 . This results in easier deposition of Y-type films. (The type of these films is discussed later.) The surface of the liquid

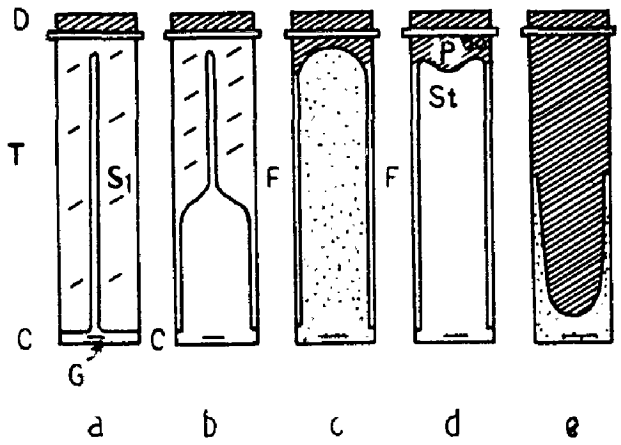

AFTER LANGMUIR PROC ROY SOC. A, 170, 1 (1939)

FIG. 4·1 DIAGRAMMATIC REPRESENTATION OF THE APPARATUS FOR BUILDING UP THE FILMS

is now thoroughly cleaned by sweeping the waxed barrier across the long edges of the trough and finally leaving it resting on the trough end (Fig.4.1a). Another barrier rests at the other end of the trough which is used to hold the waxed silk thread S_1 placed upon the water surface as shown in the Fig.4,1 . The thread is waxed so that it does not wet and sink into the water and it is carefully made to touch the water surface at every point to avoid any possibility of leakage of the spread monolayer.

Stearic acid (or other material to be deposited) dissolved in benzene (concentration $\simeq 3\times10^{-4}$ by weight) is now placed on the water surface near D in the form of a small droplet which spreads spontaneously and pushes the thread outwards to take the shape as shown in Fig. 4.1b. (If the first drop does not spread quickly, it is an indication that the surface is not perfectly clean). As soon as the spreading is complete, the thread is fastened to the trough edges by two small clips F . At this stage the divalent barium ions present in the solution undergo surface reaction with the stearic acid molecules to form the barium stearate soap and the solvent (benzene) slowly evaporates leaving behind a monolayer of barium stearate on the surface, its boundary being confined by the thread. If a second drop is put near G after the spread is complete, it would not spread and remain as residue which is an indication that the available surface has been covered with the monolayer. The stearate molecules at this stage remain standing upright

with their reactive carboxyl groups touching the water surface but some of them also tend to bend over the water surface due to relatively large space available for them. It is shown in Fig. 4.2 a). A small droplet of oleic acid called ''piston oil'' is now placed on the surface at P which thus exerts a constant lateral compression of about 30 dynes/cm on the spread monolayer. It has been found that this much surface pressure ($\simeq$ 30 dynes/cm) is sufficient to compress a monolayer of stearic acid into the condensed solid phase and the molecules remain relatively closely packed Fig.4.2b). The thread boundary now separates the whole surface area between the barriers into two regions with a stearate monolayer on one side of the thread and oleic acid on the other, which press each other to give an equilibrium shape to the thread (shown in Fig.4.1d). The transfer of monolayer onto the ''conditioned'' slide may now be accomplished by moving the dipper near G up and down repeatedly across the monolayer covered surface. ''Conditioning'' of the slide here means to render it hydrophobic initially. This can be achieved simply by rubbing the slide surface with a waxy solid, e.g. ferric stearate. It has been found that a pure aluminium or silver film deposited on the cleaned slide by thermal evaporation also behaves as a hydrophobic surface for good multilayer deposition. The ambient temperature during the'building-up' process should be maintained at about 22^{o}C.

The monolayer is thus transferred on the conditioned

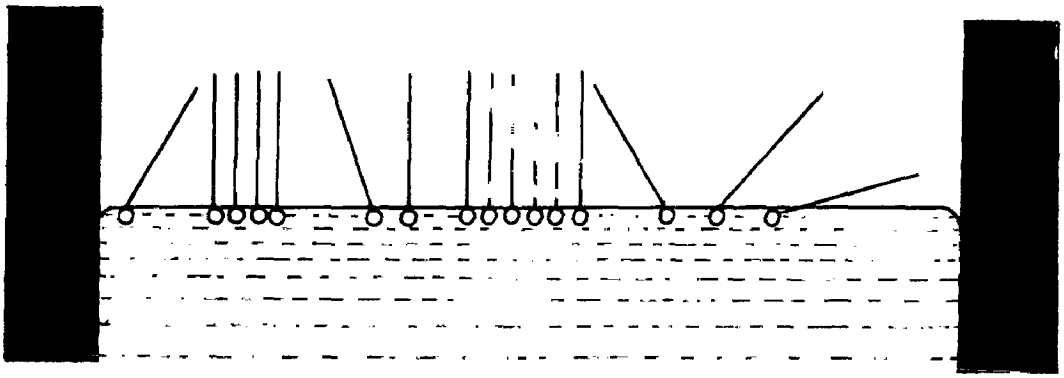

(a)

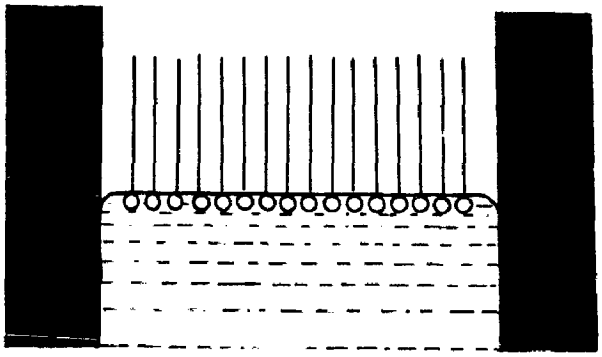

(b)

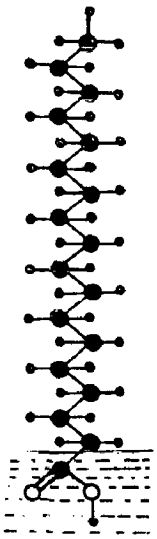

(c)

AFTER RIES SCIENTIFIC AMERICAN, 204, 152 (1961)

FIG. 4·2 DIAGRAMS SHOWING STEARIC ACID MOLECULES ON WATER SURFACE

a MOLECULE BENDING
b MOLECULES STANDING CLOSE PACKED
c STEARIC ACID MOLECULE STANDING ON WATER

(Small spheres represent hydrogen atoms and the bigger ones represent carbon atoms)

●-Carbon atom •-Hydroqen atom ○-Oxyqen atom

slide on both its downward and upward journey, and the process may be continued till the thread S moved forward through an area to attain the shape shown in Fig.4.1d. Every time the thread moves forward through an area equal to that of the slide on which the film is being deposited and the thread motion takes place because of the constant compression provided by the ''piston oil''. This visible motion of the thread is a very clear cut indication that layers are being transferred on the slide every time on dipping or withdrawal of the latter. The film thus built-up is termed Y-type and contains an even number of layers outside water. Film thickness can be calculated accurately by counting repeatedly the number of monolayers and multiplying it with the known monolayer thickness. To obtain an odd number of monolayers outside the water surface, it is necessary first to dip the slide in the solution and then to spread the stearic acid. In this case, the first layer will be transferred when the slide is moved upward and finally an odd number of layers will be obtained. This process has been found quite satisfactory even to obtain single monolayer. To obtain X-type of films, it is necessary to make the solution more alkaline (pH = 9) and then the transfer would follow only during the down trips of the slide.

For the deposition of stearic acid films only deionized and doubly distilled water is filled in the trough without adding barium chloride or similar salts. It is also not necessary to control the pH of the water by adding

$KHCO_3$ (51). Fig.4.2cgives a pictorial representation of the orientation of a stearic acid molecule on the water surface with their polar carboxylic groups touching water surface. The above set up for film deposition has been made completely automatic by a slow speed motor control with a counter for counting the number of layers transferred. The whole assembly was designed and fabricated in the laboratory.

4.2 TYPES OF'BUILT-UP'FILMS: X,Y,Z TYPES OF DEPOSITION

As the basic mechanism and process of deposition throws light on the interesting molecular orientation and structure in the various built-up films and also clarifies the apparently obscure phenomenon of monolayer deposition it is discussed in detail below.

From aquous substrates, the experimental possibility of transferring the monolayers onto solid surfaces was first realized by Langmuir (49). Miss Blodgett and other subsequent workers (17,18,48,50,52,53) have since carried out detailed investigations of this phenomenon, the basic points of which are now well established (Sec 4.1).

Only condensed monolayers, which do not tend to spread indefinitely as the surface pressure is reduced to zero i.e. no compression, and thus act as two dimensional solids or liquids rather than gases (50) are found to exhibit the phenomenon of deposition on glass or metal surfaces. Initially fatty acids condensed by means of calcium, or barium ions in the substrate were used for investigation (17,18)

but subsequently many other types of organic compounds have been employed, e.g. esters, ketones, phenols, proteins etc.

Bikerman (53,54) hypothesized that the nature of the deposition of monolayers on a solid depends on the contact angle between the solid and the film-covered water surface. The monolayer is, of course,supposed to be kept under constant compression for facilitating the transfer process. When the solid plate is being dipped across a fatty acid monolayer on water, for example, the curve of contact between the water and the solid surface advances relative to the slide. This gives the ''advancing'' contact angle. When the slide is withdrawn one similarly gets the ''receding'' contact angle. Obviously,when the slide is entering the water and the advancing angle is obtuse the water surface will fold down naturally onto the solid surface, thus turning the uppermost groups of the monolayer, i.e. methyl groups, toward the solid surface for deposition of the molecule. The molecules will be deposited with their methyl groups in contact with the slide and the surface of the deposited monolayer will be composed of carboxylic groups. (Fig.4.3b). This orientation of the monolayer with the methyl groups toward the solid surface and the carboxyl groups away from it is termed '' exotropic''. As the adhesion of the methyl groups to the solid surface is relatively low, the slide should obviously be lowered into the water at a slow speed for deposition of the monolayer. It is observed that if the advancing angle is acute the methyl groups of the molecules in

the monolayer remain turned away from the solid surface and there will be no deposition when the solid is entering the water surface. Thus, a monolayer can be deposited on a slide at its first entry into the water only if the slide surface has been rendered fairly hydrophobic (as mentioned earlier in sec. 4.1), giving a large contact angle. Therefore, no deposition will take place on the first immersion of an ordinary glass slide which is wettable by water (low contact angle).

When the slide is being extracted from water solution and the receding angle is acute the water surface folds up on to the slide, thus turning the lowermost group of the monolayer, i.e. the polar carboxylic groups, toward the solid surface for deposition of the molecules. The water molecules which are sandwiched between the carboxyl groups of the monolayer and the solid surface are slowly squeezed out because of the strong affinity between the polar carboxylic groups and the solid surface. The molecules this time are thus deposited with their carboxyl groups in contact with the solid surface and the surface of the deposited monolayer will be composed of methyl groups. This orientation of the monolayer with the carboxyl group towards the solid surface and the methyl group away from it is termed '' endotropic''. Evidently, when the receding angle is obtuse the carboxyl groups of the molecule remain turned away from the solid surface and there will be no deposition when the solid leaves the water surface. Thus a monolayer can be deposited on a hydrophilic

solid surface, i.e. wettable by water and therefore having a low contact angle, like that of an ordinary glass slide, on its withdrawal across the water surface. In practice it can easily be seen that if the speed of withdrawing the slide is high, the sandwiched molecules will not be effectively squeezed out and there will be no deposition. The squeezed out water molecules are forced to come down on the surface not due to gravity but because of their replacement by the fatty acid molecules in the monolayer whose polar carboxylic groups have a strong adhesion to the solid surface.

Thus, from above it is clear that if both the advancing and receding angles are obtuse deposition will take place only on the lowering of the slide. Such a deposition or film thus built-up is termed X-type which is therefore made up of a series of exotropic layers oriented in such a way that the methyl groups are toward the solid surface and the carboxyl groups away from it. As such the surface of the X-films will be composed of carboxyl groups. Since here the molecules in the layers are oriented in the same direction, the distance between any two successive planes containing carboxyl groups (or methyl groups) should be clearly equal to the chain length of the molecule, assuming a perpendicular orientation of the molecules on the solid surface (Fig.4.3a)

When the advancing angle is obtuse and the receding angle is acute the deposition will obviously take place on both lowering and withdrawing the slide across the water surface. This deposition or film thus built-up is called

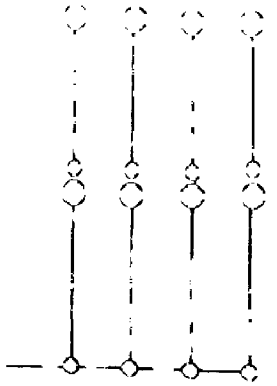

FIG. 4·3 : DIAGRAMMATIC REPRESENTATION SHOWING THE MOLECULAR ORIENTATION IN A X-TYPE FILM

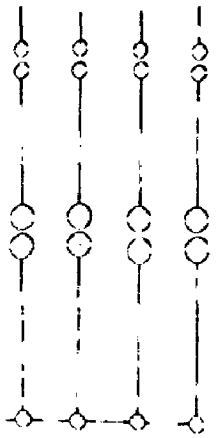

FIG 4·3 : DIAGRAMMATIC REPRESENTATION SHOWING THE MOLECULAR ORIENTATION IN A Y-TYPE FILM

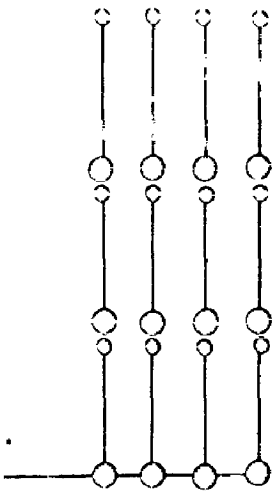

FIG. 4·3 : DIAGRAMMATIC REPRESENTATION SHOWING THE MOLECULAR ORIENTATION IN A Z-TYPE FILM

(In the above diagrams the small spheres represent methyl groups and the bigger ones represent carboxyl groups)

Y-type. This is the type of film which has been most commonly studied. Evidently, a Y-type of film will be made up of a series of alternating exotropic and endotropic layers. Thus, the surface of a Y-film will be composed of methyl groups. Since here the molecules in adjacent layers are oppositely oriented, the distance between two successive planes containing carboxyl groups (or methyl groups) will clearly be equal to twice the molecular chain length, assuming a perpendicular orientation of the molecules on the solid surface. (Fig.4.3b).

When both the advancing and receding angles are acute the deposition will clearly take place on withdrawal of the slide across the monolayer. Such a deposition or film thus built-up has been termed Z-type. The deposition is rather uncommon and there does not seem to be any well documented report on such films. Obviously, a Z-type film will be made up of a series of unidirectionally oriented endotropic layers. As such the surface of a Z film will also be composed of methyl groups. The distance between two successive planes containing carboxyl groups (or methyl groups) should be equal to the molecular chain length, in the case of perpendicular orientation of the molecules on the solid surface (See Fig.4.3c).

The only other combination of contact angles remains the one in which the advancing angle is acute and the receding angle obtuse. Obviously, there must be no deposition at all in this case either on lowering or withdrawing the

slide across the monolayer.

As the contact angle between the film-covered water surface and the solid being dipped is well known to depend on the nature of the film forming substance, the rate of dipping or withdrawal, the surface pressure of the film (55), and the pH of the solution, etc, clear-cut and specific experimental conditions have to be laid down for the deposition of any given type of film, i.e., X,Y or Z. As desired above, this has been done, by Blodgett and Langmuir for the case of Y films of metal stearates. It is also important to note that the contact angle between a liquid and a solid is considerably modified (22, p.185) by any contamination, greasy or otherwise, of the solid surface and also by its roughness. Therefore great care has to be taken regarding these factors also while following the experimental conditions for depositing a particular type of film.

4.3 THE BUILDING-UP PROCESS OF Y-FILMS

Mono and multilayer films of long-chain organo metallic compounds can be 'built-up' by the technique described by the above technique of Blodgett and Langmuir (17,18). The process for 'building-up' of Y-films by depositing successive monolayers as have been used in the present work is illustrated in Fig.4.4. In this case the slide has suitably been rendered hydrophobic by depositing a thin aluminium layer in a high vacuum by thermal evaporation. If the deposition is to be done on glass slide, it is made hydrophobic by placing some molten ferric-stearate on the surface and rubbing it vigorously

with a clean piece of muslin leaving just an invisible layer of ferric stearate molecules. Fig.4.4a shows the lowering of the slide across the monolayer on the water surface with polar carboxyl groups (as shown by circles) touching the water molecules. Under the conditions, the first layer is transferred on to the slide on the first down trip (Fig.4.4b). The following up-trip causes the deposition of the second layer (Fig.4.4c), the next down journey (Fig.4.4d) gives third layer and so on. The film thus formed on the slide will contain only even number of layers. For getting a film having odd number of layers outside water, the slide is first dipped into the solution and then the spreading of the monolayer is done on the surface of water. In this case when the slide is taken out, first layer will be deposited on it. Subsequent deposition made by dipping and withdrawing the slide will give the second, third layers and so on. Thus in the deposited Y-films containing even number of layers, both,the upper and lower surface of the film are made up of hydrophobic methyl groups and in those having odd number of layers, the upper surface consists of methyl group while the lower one is composed of hydrophilic carboxyl groups.

4.4 EXPERIMENTAL DETAILS

a. List of Precautions

i) In the present investigations extremely pure samples (Price's Bromborough's) of palmitic, margaric and stearic acids were

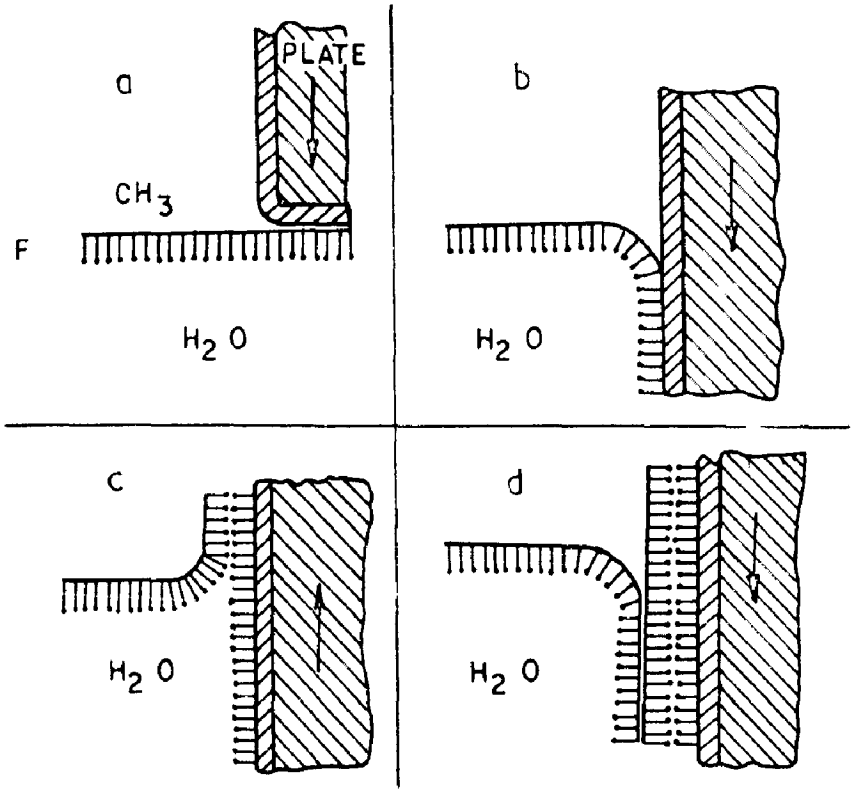

AFTER LANGMUIR PROC ROY SOC. A, 170, (1939)

FIG 4·4 DIAGRAMS SHOWING THE BUILDING UP PROCESS OF Y TYPE FILMS.

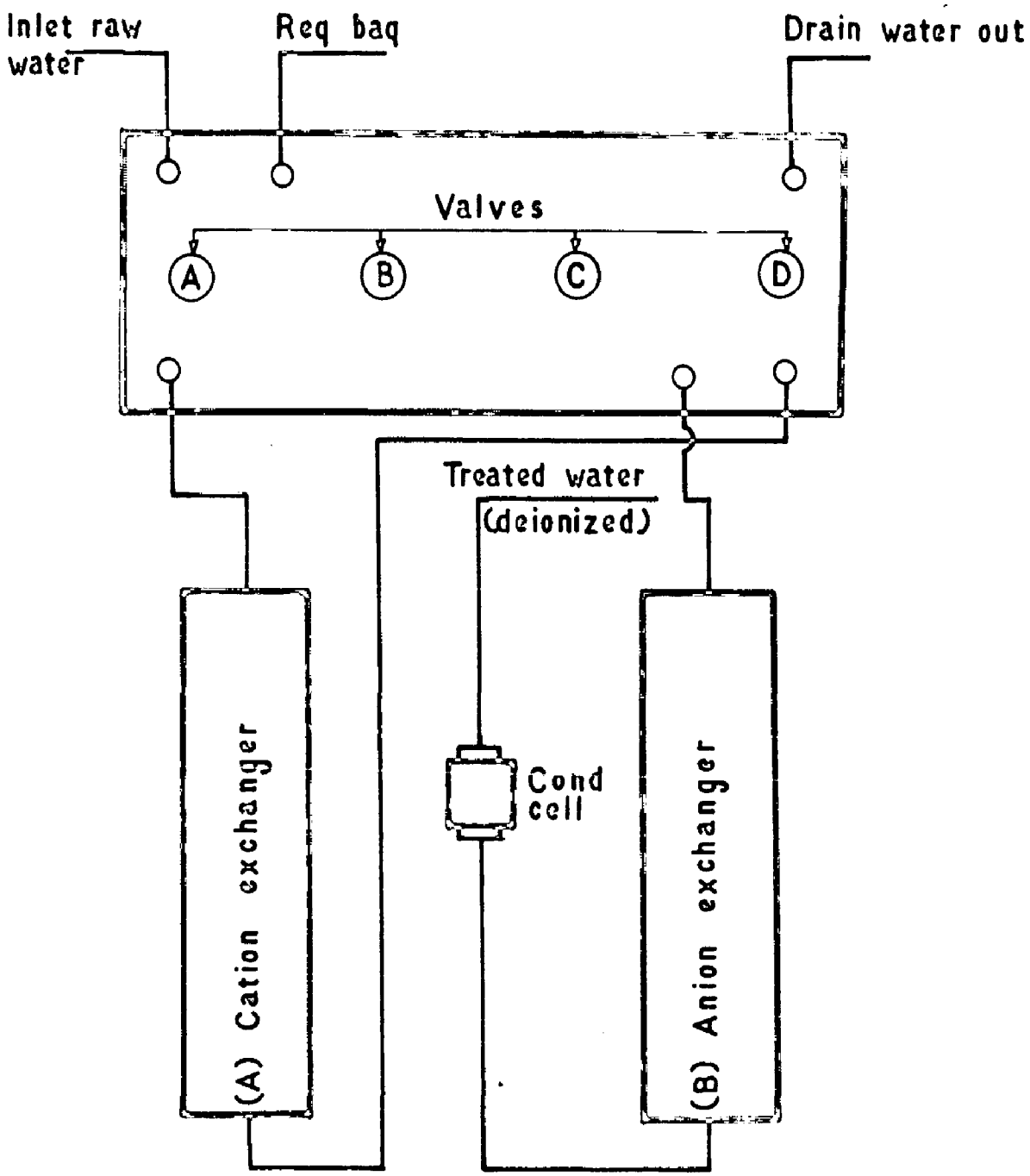

FIG. 4·5 BLOCK DIAGRAM OF PERMUTIT PORTABLE DE-IONISER

used. Oleic acid, benzene and wax used were of E merk's grade. Barium chloride and potassium bi-carbonate were of analar grade.

ii) The water used for solution preparation was deionized and then doubly distilled. Deionized water was produced by passing ordinary water through the columns of a 'deionizer'. A block diagram of this deionizer is shown in Fig.4.5. It must be remarked here that deionized water, if used directly, may contain some organic impurities. For greater details reference is made to the recent work of Nathoo (51).

iii) The whole experimental set-up was covered up with transparent shield box in order to avoid dust contamination or the introduction of any foreign material. Departure from this precaution may cause disruption of the film structure. All the operations needed during experimentation were done from out side (see Fig.4.6).

iv) Great care was taken against mechanical vibrations or other disturbances during deposition. Any mechanical vibration may result in major cracks in the deposited film giving rise to voids and inhomogeneities in the film. For this, the Langmuir trough was kept on a rigid foundation and an automatic slow speed motor driven arrangement was used for the upward and downward journey of dipper mounted with 'conditioned'' slide.

v) The small deposition cabin was equipped with an air conditioner (with humidity control) in order to bring the temperature to the required value (about $22^{o}C$). The air

conditioner also helped in making the cabin dust free.

vi) The pH of the solution was always maintained to about 7.2 by adding specific quantity of $KHCO_3$. Any departure from its pH may markedly affect the nature of the deposited film.

vii) Since the hands of the worker are themselves the most likely source of greasy contamination, cleaned surgical gloves were used during the entire process of deposition.

b. Automatic slow speed motor driven arrangement

This is a modification over the previous arrangement in which the dipper was manually operated up and down for the successive depositions. There was a chance of possible mechanical cracking of the deposited films. It is an experience of the author that a considerable percentage of films shorted when sandwiched between metal electrodes. After making the modification over the previous arrangement the percentage of such conducting films reduced considerably.

The arrangement is shown in photograph 4.6. Fig.4.7 is a self explanatory sketch of the above arrangement. There is a slow speed motor which can be attached with dipper by a rubber pully. The motor is fixed on a rigid surface and its motion is apparently vibration free. Any vibration if exist is absorbed by rubber pulley and the motion of the dipper is quite free and smooth. A low voltage power supply has been used for input to motor as it operates at 6 volts. The stand carrying the motor arrangement was completely separate

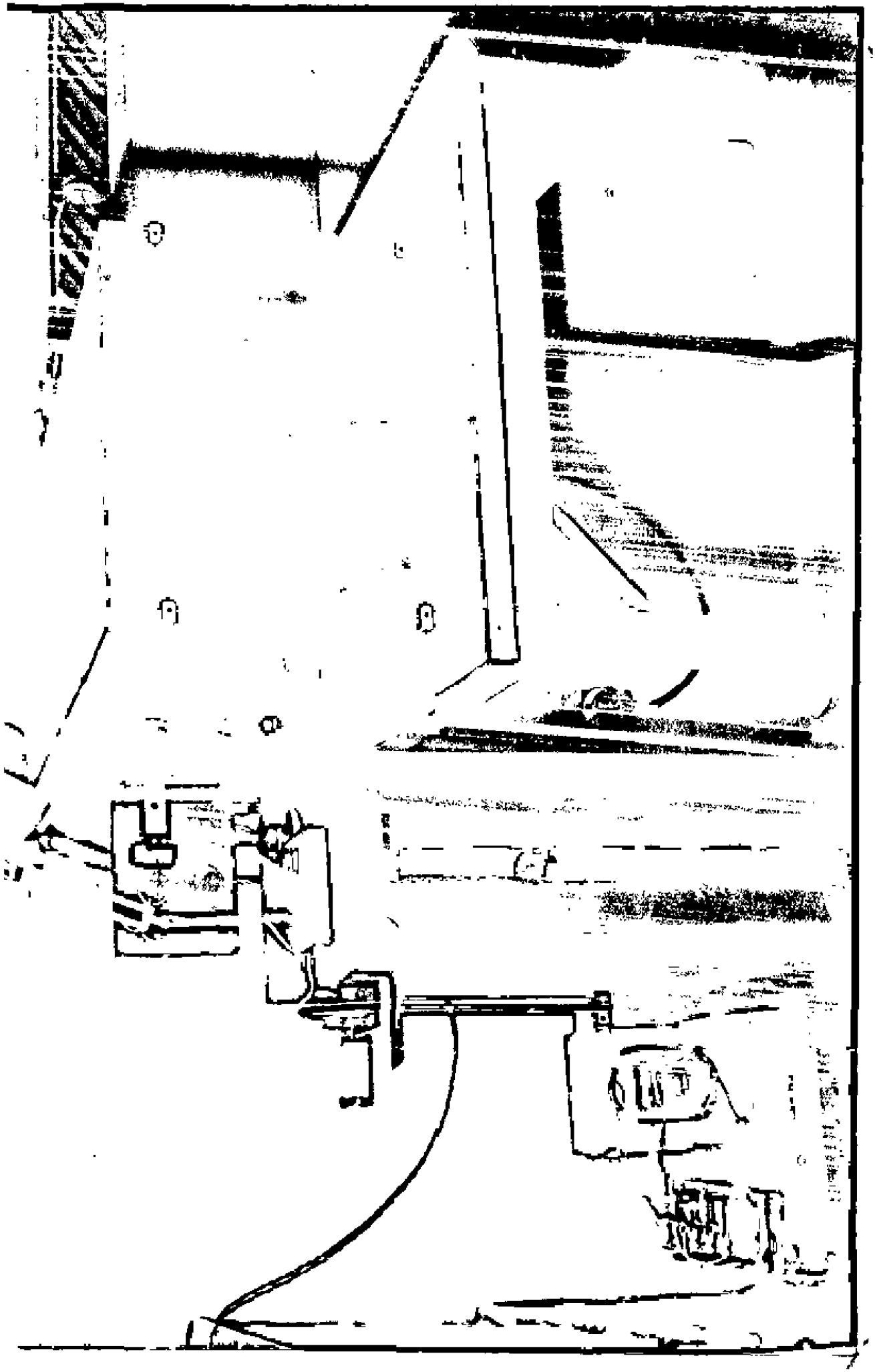

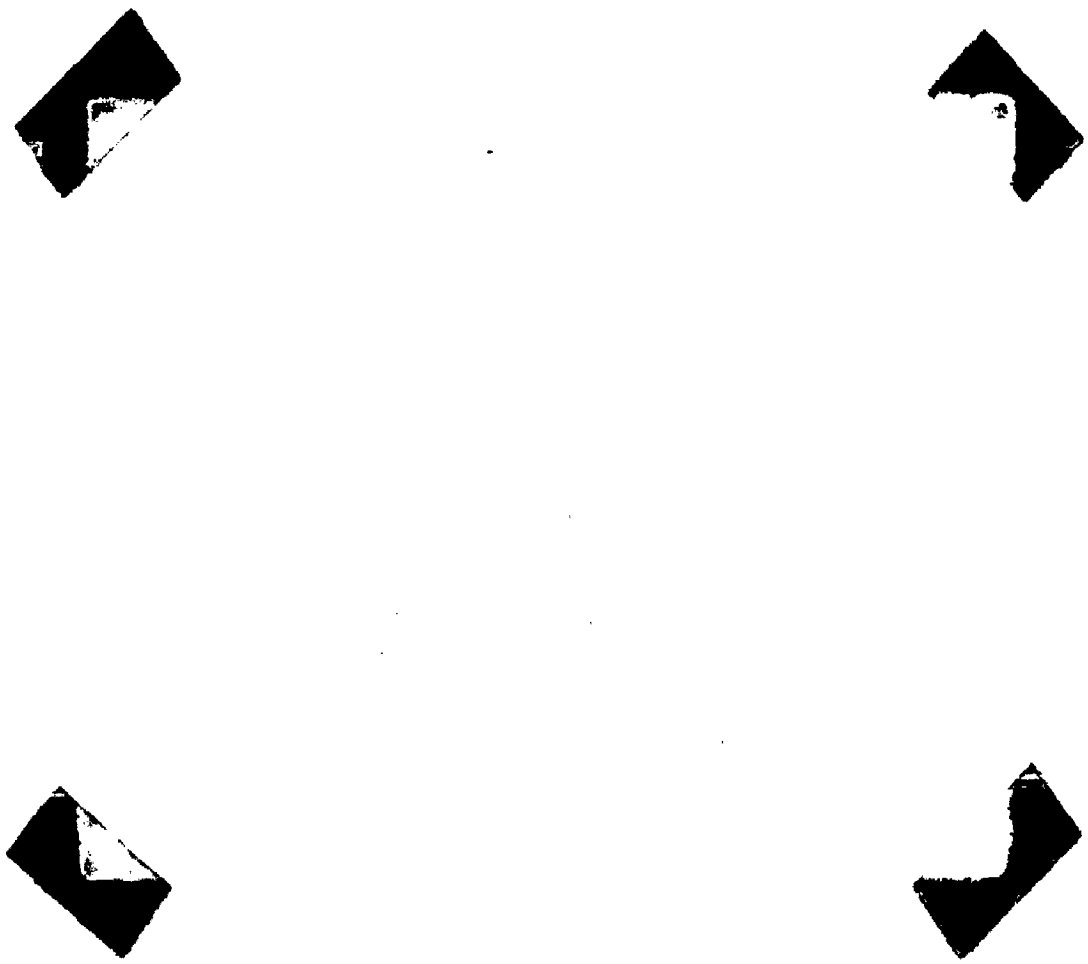

FIG.4.6 PHOTOGRAPH OF FILM DEPOSITION APPARATUS

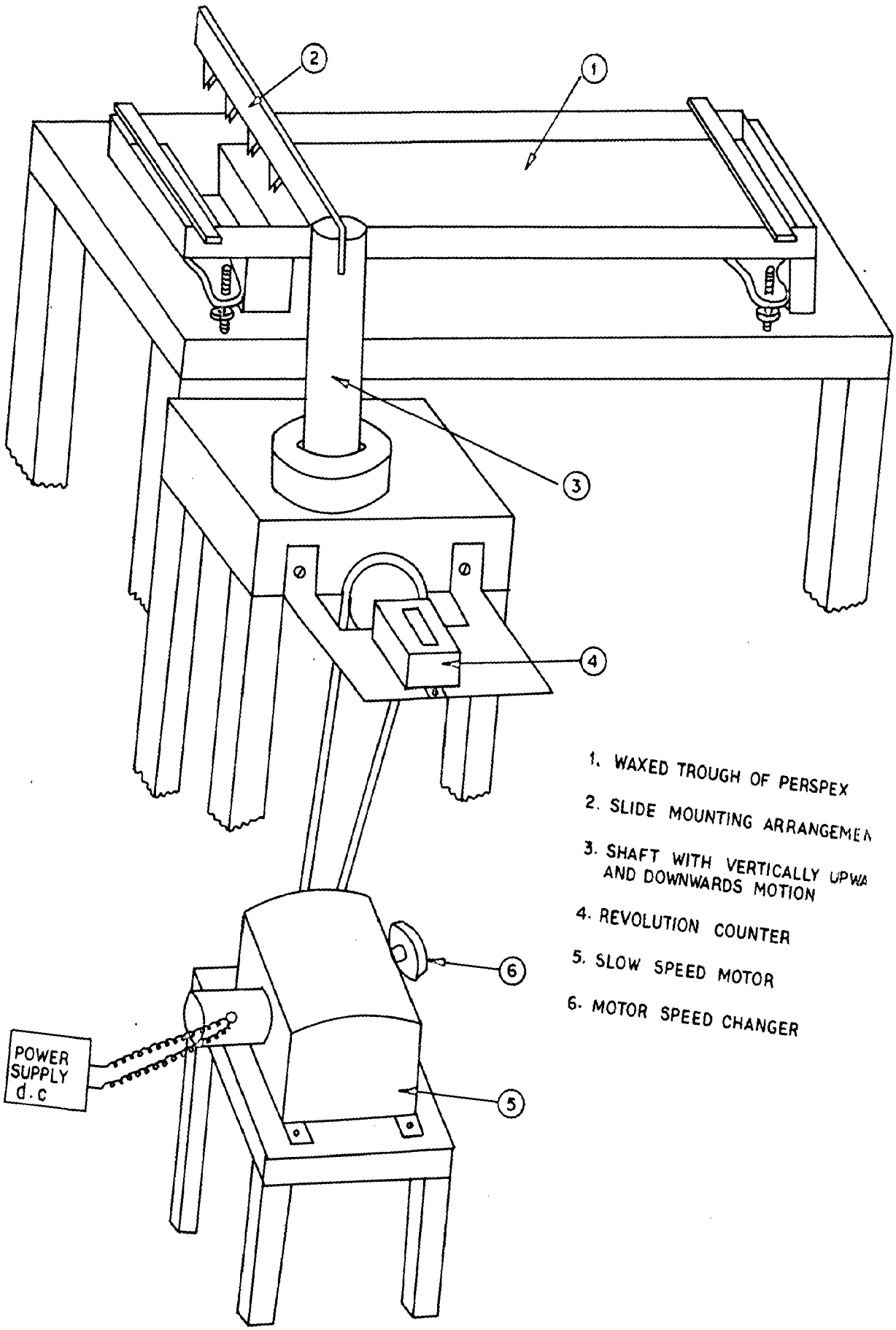

FIG. 4·7 DEPOSITION APPARATUS FOR LONG CHAIN FATTY ACID THINFILMS BY BLODGE LANGMUIR TECHNIQUE

from the table on which the trough was placed.

It has been found that the films deposited by this arrangement are uniform. An indirect proof of this is the thin film step gauge device fabricated by the author (56) using barium stearate films. A brief description of the optical device is as follows:

Langmuir films (refractive index n_1 1.43) in tens of steps have been deposited onto an E.D.F. (extra dense flint) glass slide (refractive index n_2 1.65). The condition of destructive interference in reflected light $n_o n_2 = n_1^2$ is nearly satisfied for the three media MgF_2 (n_o=1.35), barium stearate (n_1 = 1.43) and E.D.F. glass (n_2= 1.65). Distinct interference colours are observed when seen in white flourescent light. The step gauge may be used for estimating the thickness of dielectric films e.g. MgF_2, ZnS, Al_2O_3 etc deposited by evaporation technique. This is done by depositing this film in a coating unit on a dummy E.D.F. slide (refractive index 1.65) and then matching the colours of this film with one of the steps on the step gauge. For other details of the device a reference is made to the paper (56). The main idea to describe the step gauge here is that the colours on the step gauge on any particular step are quite homogeneous indicating that the film deposited by the above technique is uniform.

Next chapter describes in detail about the structure and properties of 'built-up' films.

CHAPTER V

STRUCTURE AND PROPERTIES OF 'BUILT-UP' FILMS

After discussing how the Langmuir films are prepared the necessity arises obviously to know about their structure and other properties. The present chapter, therefore, constitutes a systematic discussion about structural, dielectric and electrical properties of these films.

5.1 General Properties

The built-up films of Barium-stearate deposited by the technique of Blodgett and Langmuir, have been studied in detail (17,18,50,57). The films consist of superposed sheets of oriented molecules and have been shown to form positive uniaxial birefringent crystals, with the optic axis perpendicular to the plane of the film. In the condensed layers of long-chain fatty acid soaps, the molecules stand very nearly perpendicular to the plane of the solid surface (58,59). Electron diffraction investigations (60) show that the films actually form hexagonal crystals with the symmetry axis i.e. the optic axis, perpendicular to the plane of the film. X-ray diffraction studies on the films also proved that the films are crystalline in nature forming very thin crystals having known number of molecular layers.

The built-up films of these fatty acid soaps, say barium stearate can be of X,Y or Z type depending on the molecular orientation in adjacent layers of films as has already been discussed in sec. 4.2. There it has been

shown theoretically, that the surfaces of Y and Z films should be composed of methyl groups while those of X films should be composed of carboxyl groups (in the case of barium stearate, divalent barium ion is substituted for hydrogen atoms of the carboxyl groups). Since the methyl groups are hydrophobic i.e. practically no affinity for water,the surface of Y and Z films are expected to be hydrophobic i.e. nonwettable by water having large contact angle. On the other hand the surface of X-film should be hydrophilic having very low contact angle with water as it consists of hydrophilic (wettable by water) carboxyl groups. However, Langmuir (50) experimentally found that the surfaces of both X and Y films have almost the same contact angle with water. No work seems to have been done on Z films whose deposition is rather uncommon. Also X-ray diffraction studies of the built-up X and Y films of barium stearate (61,62) have shown that the lattice spacing normal to the film is the same in both types of films and this spacing is equal to the distance between two successive planes containing barium atoms i.e. carboxyl groups (see sec. 5.2 b). It has been shown in sec. 4.2 that for X-films the distance between the two successive barium atoms should be half of that for Y-films. The contact angle and spacing anomalies regarding X-and Y-films of barium stearate as described above have been explained by Langmuir (63) in terms of the overturning of molecules in adjacent layers of the X-film just after deposition. This overturning of molecules

in the layers of the X-film which results in a molecular reorientation or a sort of recrystallisation in the film, according to Langmuir arises because of the thermal vibrations. This molecular reorientation can be possible at ordinary room temperatures because the molecules in the films are bound together with very weak Vander Waâl's forces and the films have low melting points. The molecules in the first and second layers of aY-film are strongly anchored with their polar carboxyl groups face to face (fig.4.3b) forming a stable configuration and hence the reorientation of the molecules in these films is not at all expected. This anchoring in the case of X-films is relatively weak due to the methyl (inert) and carboxyl groups being face to face (fig.4.3d),and this results in unstable configuration. This unstable structural configuration of X-film tends to attain the stable structure of Y-film by the general overturning of molecules in the layers of X-films under the influence of thermal vibrations until the molecules in the first and successive double layers of the X-film become strongly and stablyanchored with their carboxyl groups face to face. The X-film thus becomes identical to Y-film and gives the same contact angle (with water) and normal spacing as the Y-film.

5.2 Studies on Thickness Determination

Thickness is perhaps the most significant film parameter. Mainly two types of methods have been used to

determine the thickness of a monomolecular film of a long chain organic substance. Either the thickness was determined by the area-density method (already described in sec. 3.2 c) which requires the film to remain on the water surface or by using optical methods which require the films to be deposited on the solid surface. The well known optical methods of measuring film thickness will be described in detail because the thickness of these films has been used in the present work.

5.2 a. Optical Methods

(i) Interferometric Method

Blodgett and Langmuir (17,18,57) have determined the thickness of 'built-up' barium stearate films by interference of monochromatic polarized light reflected by the films. In this method the angle of incidence is varied until the reflected intensity becomes minimum. The thickness of the film is calculated from a knowledge of this angle of incidence, wavelength of the monochromatic light used and the ordinary refractive index of the film. Later, Jenkins and Norris (64) also determined the thickness by the same method. In their work, they kept the angle of incidence constant and varied the wavelength until the reflected intensity recorded by a spectrophotometer reduced down to minimum. Holley (61) made use of a Michelson Interferometer in another attempt for thickness determination.

(ii) Polarimetric Method

Rothen and Hanson (65-67) performed ellipsometric studies to measure the thickness very precisely . The sensitivity of this apparatus is quite high and it is capable of detecting even small changes in thickness. This polarimetric method is based on the measurement of the change in ellipticity of light reflected from the film. Stearic acid or Barium stearate films of known number of layers were used as optical gauge for comparison purposes. Mattuck (68,69) recently used an interference reflectometer of barium stearate itself to determine the thickness by Hartman's polarimetric method (70) utilizing white light interference fringes.

These optical methods involve the refractive index of the film and require the use of standard reference film with known optical characteristics. The refractive index of the film can not be assumed to be equal to that of the substance in bulk, an unambiguous determination of the refractive index of the film is necessary for evaluating metrical thickness of the films. Also any differential phase changes upon reflections have to be eleminated to avoid spurious effects in thickness determination.

(iii) Multiple Beam Interferometric (MBI) Method

Tolansky's (71,72) multiple beam interferometric technique was first used by Courtney-Pratt (73,74) for determining the thickness of molecular films. He applied

this method to molecular layers of fatty acids spread by the droplet retraction technique on mica cleavage surface This method making use of doubly silvered mica, forming the interference system does not directly yield the metrical thickness as it required the knowledge of the refractive index of the film. Moreover, the differential phase changes upon reflections at mica silver and monolayer silver interfaces are involved which are not unambiguously known. This method has been used (75,76) in connection with other types of studies also, involving deposited monolayers.

An accurate determination of the metrical thickness of 'built-up' films of barium stearate and other substances was first carried out by Srivastava and Verma (77,78) using multiple beam interferrometric technique (73,74). Their method is independent of the optical properties of the film and therefore directly determines the metrical thickness. Also, the differential phase changes have been eliminated by using the standard reference film of barium stearate itself.

5.2 b. Lattice Spacing 'c': X-ray Diffraction Studies

The studies of X-ray diffraction on 'built-up' films of various long-chain organic compounds have been carried out by many workers (53,61,77,79-90) making use of the conventional sealed off X-ray source. These X-ray diffraction studies have shown that the 'built-up' films are crystalline in nature and the process of building-up the

films is merely mechanically growing the crystal layer by layer. Indeed, the building up technique can sometimes be used for crystallisation of some otherwise intractable substances, for example, unsaturated acids (80). Most of the workers in their X-ray diffraction studies used relatively thick built-up films having large number of layers while Bisset and Iball (88) investigated barium stearate and palmitate films containing only few layers. These workers, from their detailed intensity work have established an analogy between optical diffraction from ruled gratings and X-ray diffraction from these layers. Clark and Leppla studied a few layers of lead stearate (83,91). The lattice spacing of built-up lead stearate films was also measured by Stephens and Turck-lee (92) using electron microscopic technique.

Holley and Bernstein (84,85) and Fankuchen (62) measured the lattice spacing of built-up barium stearate films perpendicular to the plane of the film. The lattice spacing in both X and Y types of films was found to be the same. Since the molecules in the X-films are unidirectionally oriented, their spacing normal to the film should be half to that in Y-films in which the molecules in adjacent layers are oppositely oriented. The above apparently surprising result can be interpreted in terms of Langmuir theory of overturning and anchoring of molecules discussed earlier (63). As the molecules in adjacent layers in a Y-film of barium stearate are oppositely oriented (Fig.4.3b)

the barium atoms are located close to parallel planes having a spacing twice to the molecular chain length. Since scattering of X-rays from carbon and hydrogen atoms can be assumed to be very small as compared to that from barium atoms (large atomic number), the lattice spacing normal to the film measured by X-ray diffraction must correspond to the distance between adjacent planes containing barium atoms i.e. unit cell height 'c'. Therefore, half of the lattice spacing must be equal to the metrical thickness of the monomolecular film of barium stearate.

Recently,Srivastava and Verma (78) studied the X-ray diffraction effect in built-up films of barium palmitate, margarate, stearate and behenate and measured the 'c' spacing of these films. A microfocus X-ray source described by Ehrenberg and Spear (93) was used and the diffracted spectra were recorded on a Bragg-Muller spectrograph. Films were 'built-up' on silvered microscopic slides and it was found that the silver coating of the slide,forming the supporting base for built-up films does not produce any diffraction effects to confuse or interfere with the interpretation of the pattern obtained from the film. The monomolecular spreading of film on water is also supported by the good agreement found between the measured value of thickness by interference and the chain length measured by X-ray diffraction. They also found that the lattice spacing perpendicular to the supporting surface is twice the thickness of the monomolecular films measured optically.

5.2 c. Electron Optical Studies

For investigating the detailed structure of thin film systems the obvious choice, naturally, the well-known electron diffraction technique. The technique was first used by Havinga and de Wael (58,59) and Germer and Storks (60) for the 'built-up' mono-and multilayer films of fatty acids and their soaps. In their pioneering work, Germer and Storks have carried out a detailed structural analysis of 'built-up' films of stearic acid and barium stearate. The hydrocarbon chains of the barium stearate molecule were found to form hexagonal arrays with their axes oriented normal to the substrate and separated by 4.85 Å. The stearic acid molecules form monoclinic crystals. On a clean metal surface, the molecules in the first layer are oriented with their chain axes almost normal to the substrate and the chains are laterally close-packed but irregularly arranged. Barium stearate molecules have a more precise normal alignment than stearic acid molecules. In layers on top of the first one the molecules of the acid as well as of the soap are regularly arranged in the way these molecules are arranged on Resoglaz foils. In barium stearate, the arrangement is random about the normal to the surface although often large single crystals are formed. In the case of stearic acid it was found that crystals are formed with the chain axes nearly in the plane containing the surface normal and the dipping direction and pointing upward from the surface. Stephens and Turck-lee (92)

also used electron diffraction technique for studying the structure of 'built-up' lead stearate films and suggested a monoclinic or Orthorhombic structure depending on the space group.

Optical studies of barium stearate films have also shown that the multilayers constitute uniaxial crystals with the optic axis perpendicular to the plane of the film. The birefringenee is readily demonstrated (18) by placing a 1000 layer film, 'built-up' on glass, between two crossed nicol prisms or crossed polaroids, the film being placed azimuthal angle 45^{o}. The investigation of the birefringence of a 1000 layer film of barium stearate has also been done later (18) using an ired-gypsum plate in the usual way and the results show that the film behaves as a positive uniaxial crystal. Such uniaxial crystals are characterized by two refractive indices. The refractive indices measured by Blodgett and Langmuir (18) are found to be n_1 = 1.491 and n_2= 1.535 for 'built-up'barium stearate films. The equations used describe the refraction of extraordinary ray, the intensity of the ray reflected from the upper surface and from the film solid boundary, the phase change at the boundaries, Brewster's angle and other properties of birefringent films. Lucy (94) also measured the refractive indices of barium stearate 'built-up' films and found the values n_1=1.419 and n_2=1.550.

Faucher et al. (95) have also developed a theory for determining the optical constants of 'built-up' barium

stearate films on micrograss slides coated with chromium. They have shown a good agreement between their theoretical formulae and the experimental measurements.

Recently, Tomar and Srivastava (96-99) have also measured the refractive index of the built-up barium-stearate films and other substances. Their recent measurements (99) of reflectance and transmittance on such built-up films have tested the validity of Schopper's formulae (100) and have indeed confirmed that these films are optically anisotropic. A theory of refractive index of'built-up' films has also been developed by Khanna and Srivastava (101).

5.3 ELECTRICAL PROPERTIES OF FILMS

Since the electrical properties of Langmuir films are of importance in the context of the present work a detailed discussion of these follows:

(a) Dielectric Constant Measurements.

A study of the dielectric constant of thin built-up multilayers is of importance because of the possibility of their use in the development of some thin film electronic and other devices. The dielectric constant of built-up films was measured by a number of workers in different thicknesses and frequency ranges. Early studies of the dielectric behaviour of built-up stearate multilayers were carried out by Porter and Wyman (102-104), Race and Reynolds (105-107), and Buckwald,Zahl and co-workers(108,109).

Porter and Wyman and Race and Reynolds carried out small area probe measurements using small droplet of mercury which forms the upper electrode of the capacitor. Film of organic layer was deposited on the aluminized slide forming the lower electrode of the capacitor. Porter and Wyman, who made measurements on multilayers containing 7 to 141 barium stearate monolayers, obtained the values of dielectric constant ranging from 1.9 to 3.5 with an average of ~ 2.5. Race and Reynolds made their measurements on somewhat thicker films and obtained values of 2.44 - 2.56 for barium stearate and 2.5 for calcium stearate. The dielectric constant was found to be independent of frequency between 40 and 10^6 Hz.

Buchwald , Zahl and co-workers (108,109) studied the insulating behaviour of stearate films containing 1 to 41 monolayers by immersing the multilayer-coated metal rods into conductive salt solutions. They found a decrease in capacity with an increasing number of layer. However, they found atleast two-fold variation in apparent dielectric constant which were influenced by the choice and concentration of the electrolyte.

Recently, Handy and Scala (110) investigated the electrical properties of barium stearate films using the evaporated metal electrodes rather than mercury drops to sandwich the organic films deposited on aluminium slides. They found the dielectric constant to be varying from 2.1 to 4.2 with an average value of 2.5, which is evidently the

same as reported by earlier workers on stearate films. The capacitance was also measured as a function of frequency and a slight change in the capacitance with frequency was observed.

Drexhage and Kuhn (111) who have studied the capacitance as a function of thickness of cadmium stearate films have shown the constancy of dielectric constant with thickness. Mann and Kuhn (112) calculated the dielectric constant of monolayers of cadmium salts of fatty acids of different chain lengths containing 18-22 carbon atoms. The capacitance was measured with a L-C precision bridge of Rode and Schwarz at a frequency of 1000 c.p.s. and the dielectric constant was found to be increasing with decreasing chain length. Recently Holt (113) has shown that in general the standard deviation in capacitance per unit area of each film is as low as 3% , that is, of the same order as the accuracy to which the areas of the electrodes can be measured. He has found no variation of capacitance with frequency. Horiuchi et al (114) have also carried out similar measurements on barium stearate films and shown capacitance to be frequency independent over a wide range (1KHz. - 1MHz.). The dielectric constant was calculated to be 2.5 as has been reported in earlier studies.

Srivastava and co-workers (115,116) have recently developed a theoretical formulation for the static dielectric constant of such films, e.g., barium stearate

etc. Since these crystal films are composed of long-chain molecules as entities, the conventional theory of dielectrics can not be applied here as such because of the necessity to calculate the intramolecular and intermolecular interactions. The calculated value of dielectric constant has been found to be 1.6 for a monolayer and 3.0 in the case of multilayer films of barium stearate. Khanna and Srivastava (117) have also carried out both the theoretical calculation as well as the experimental measurements of the static dielectric constant of built-up films of several other compounds and have found good agreement between the calculated and measured values. They have also studied (118) experimentally, the thickness dependence of the dielectric constant of built-up films. In these cases the dielectric constant saturates after increasing with thickness. In fact, an exactly similar thickness dependence of dielectric constant has been observed in evaporated ZnS films (119), which has been interpreted in terms of decreasing porosity or increasing continuity of films with increasing thickness.

(b) Dielectric Loss Measurements.

Dielectric loss is a macroscopic property of the substance. Very few systematic studies have been made on loss properties of built-up molecular films. The dielectric losses in anodic oxide films and evaporated film systems have been studied extensively and are reviewed in several

articles (120 - 131). Race and Reynolds (105) have made some measurements on dielectric loss (tan δ) for 'built-up' stearate films. The plot of the dielectric loss against frequency show larger deviation. However these deviations appear to be random and show no definite dependence on frequency. The order of magnitude of tan δ measured was low (less than 0.001 with a standard deviation of 17%) as compared to that obtained by Haskins and his co-workers (108). Assuming equivalent parallel resistance and capacitance of the films, their (108) data indicate a two-fold variation in dielectric constant and 15 - fold variation in tan δ as a function of thickness and the order of magnitude of tan δ in their case was 1000-10,000 times higher than the value obtained by Race and Reynolds (105). The wide difference in their values was caused by the electrolyte in which the film was immersed.

Recently, Holt (113) and Handy and Scala (110) carried out detailed studies of dielectric behaviour of Langmuir films. Holt (113) obtained some information that the tangent loss (tan δ) drops from 0.02 at 225 $\mathring{A}$ to 0.006 at 3700 $\mathring{A}$ for stearate films. However, in his work no systematic study of the thickness dependence of tan δ was carried out. The variation in loss angle with frequency followed normal thin film behaviour. Handy and Scala (110) showed the variation of dissipation factor with frequency. They observed a slight maximum near 700 H_{zs} and interpreted it as suggesting the presence of

weak polar adsoption mechanism with a characteristic relaxation time of 0.23 m sec.' At higher frequencies (>10KH$_z$), the scatter in measurement of dissipation factor become comparable with the observed values.

It is interesting to point out the recent studies on tan δ by Nathoo (51) for a 23 layer film of stearic acid at room temperature over the frequency region 10^{-4} to 100 H$_z$. Under these experimental conditions, no peaks were observed and the dielectric losses were found to decrease by an order of magnitude with increasing frequency in the range studied. However, these authors have made no attempt to study the thickness dependence of the dissipation factor in Langmuir films. In the present work a detailed and systematic thickness dependent study of the dielectric loss in Langmuir films has also been carried out (Chapt. IX).

(c) Resistivity Measurements.

Thin anodized as well as thermally oxidized films of some inorganic materials and some organic polymer films are generally good insulators with high resistivities. Zahl and co-workers (108, 109) have measured the resistivity of organic multilayer films and an increase in resistance was observed with increasing number of monolayers. However, there was several orders of magnitude variation in resistivity which was influenced by the choice and concentration of electrolyte. The variations in resistivity values were generally ascribed to inhomoge-

neties or voids in the films. Porter and Wyman (102) also measured the resistance of stearate 'built-up' films and found an increase in resistivity with increase in thickness. Recently, Handy and Scala (110) have also measured the resistivity of Langmuir films at low voltages (below 50 mV) where the conduction behaviour is ohmic. They plotted the resistivity against thickness and found that the points were approximately uniformly distributed over a certain limited area of the plot. For a given thickness, the upper limit of resistivity was corresponding to those layers which possess the smallest fraction of voids. They found that there was a wide range of variation of resistivity values for the same number of layers which supported the contention that the organic films in general possess porous structure.

(d) Dielectic Break down In Films.

The well-known phenomenon of dielectric breakdown in solids involves some fundamental processes not yet fully understood in detail. A great amount of work, particularly on evaporated film systems, has been carried out and has been well reviewed recently (132 - 134).

Langmuir films of fatty acid salts are known to have high breakdown strength of the order of 10^6 V cm^{-1}. The earliest studies of the breakdown of these films under d.c. voltage were carried out by Porter and Wyman (102). Similar attempts were made by Race and

Reynolds (105) in the early period and the data was collected on films of cadmium arachidate. These earlier measurements do not predict anything about the breakdown mechanism and no efforts were made by these workers to interpret their data in terms of any known theory at that time. Some more attempts also yielded only the order of magnitude of dielectric strength of Langmuir films. For instance, Thiessen et al (135) were able to apply electric fields upto 5×10^6 V cm^{-1} on barium and calcium stearate capacitors in the thickness range 100 Å - 1000 Å. Similarly Holt (113) reported the dielectric strength $\sim 10^6$ V cm^{-1} for varying thickness range of barium stearate.

A systematic and detailed study of dielectric breakdown in built-up barium stearate films was first carried out by Srivastava and co-workers (136 - 143). Results on the thickness dependence of d.c. breakdown field (136) have been reported in the thickness range 25 - 2000 Å. The breakdown strength has been found to be a power dependent function of thickness ($d^{-\alpha}$) as predicted by Forlani and Minnaja's electronic breakdown theory (132, 144), based on an electron ionization avalanche mechanism. The dielectric strength of barium stearate films for various thicknesses is of the order of 10^6 V/cm. Incidentally, Thiessen et al. (135) have already shown that electric fields up to 5×10^5 V/cm can be applied to barium and calcium stearate capacitors, 100 - 1000 Å (4- 40 layers) in thickness. The a.c. dielectric strength ($\sim 10^6$ V/cm)

is found to be somewhat smaller than the corresponding dc strength of the film and the breakdown field is found to be linearly increasing with frequency. By using the ultra thin Langmuir films of barium stearate (1-10 monolayers), the first experimental evidence for Schottky emission dominated dielectric breakdown was given by Srivastava (145).

The temperature dependence of the onset dc breakdown field (143) in the films has also been studied in the range 77°K to 320°K. The breakdown field has been found to decrease slightly with increasing temperature. The temperature dependence of the dc destructive breakdown field was also studied in the temperature range 77°K to 320°K. Detailed interpretation of the data was given in terms of tunneling and Schottky emission phenomenon (146).

(e) Tunneling Properties.

Considerable interest has been revived in studies of electrical conduction through thin insulating films since Mead proposed (12) the hot electron transport through thin (100 Å) insulating films by quantum mechanical tunneling. Many workers (110, 112, 114, 147, 148) have carried out detailed studies of electrical conduction, including tunneling, through Langmuir films.

Miles and McMahon (147) studied tunneling through Sn-Barium stearate-(Pb or In) structures and found the device resistance to be strongly time dependent and not

reproducible. Handy and Scala (110), in their extensive work, investigated barium and calcium stearate Langmuir films 1 to 10 monolayers in thickness, for use as ultrathin insulating barriers between evaporated metal electrodes. Their MIM structures exhibited highly nonlinear and strongly temperature dependent characteristics. Their results show the Langmuir films to be promising for studies of electron tunneling phenomenon. However, in their work, Handy and Scala did not give an explanation of the observed temperature dependence.

Horiuchi et al. (114) also studied electrical tunneling through calcium stearate monolayers and gave details of temperature and voltage dependence of current through the Langmuir monolayers. Mann and Kuhn (112), in their interesting and thorough work, have given a quantitative proof of the tunneling theory by using the monolayers of fatty acid salts of different chain lengths. Mann et al. (148) have verified the exponential decrease of conductance with increasing barrier thickness, as predicted by the tunneling theory. The results of this research have been shown by the authors to be relevant to the photographic sensitization process. By using fatty acid monolayers as ''distance keepers'' the sensitizer was fixed at a definite distance from the silver bromide surface. Since the dye molecule was still sensitized it was concluded that the sensitization in this case was due to energy transfer rather than an electron injection mechanism

(149, 150). For details and information on related work reference is made to the original paper (148).

(f) Forming Process and Differential Negative Resistance.

The application of voltage greater than a minimum V_F across a metal-thin film insulator-metal device may cause a radical and essential change in its electrical properties, such as a large permanent increase in the conductivity. This process is designated '' forming'' process and V_F is known as '' forming voltage''. This process has been found to occur most readily in many thin film insulators with reactive anions such as oxides and fluorides and was thought to be a characteristic feature of non-stoichiometric insulators. The ''formed'' samples showed a pronounced differential negative resistance (DNR) in its I-V characteristics (151 - 163). Until a few years ago, DNR behaviour was established only for amorphous or polycrystalline insulators. Recently investigations on Langmuir films by Gundlach and Kadlec (164, 165) have shown that DNR also occurs when organic monolayers are sandwiched between metal electrodes and formed.

Gundlach and Kadlec performed experiments both on diode structures (164) (metal-organic film - metal) and triode structures (165) (metal-film-metal-film-metal) using Al electrodes and organic film of cadmium arachidate.

(i) DNR on diode Structures

Once the sample is ''formed'' at 77°K with top Al

electrode positive, typical J-V characteristics are obtained. As a rule, DNR is not observed in the first voltage cycle but appears in the second one. However, it disappears in the successive two to four further cycles and finally the characteristic becomes smooth. The most pronounced DNR (peak to valley ratio of the current is maximum) is observed at about 190°K and it goes on diminishing beyond this voltage, disappearing above about 210°K. Almost similar results were obtained with Au as top electrode but the device always exhibited short circuit above about 170°K and in this case appreciable DNR occured at about 150°K.

(ii) DNR on triode devices

Gundlach and Kadlec (164) after a successful attempt to study the DNR on diode structures, extended their studies on triodes by making use of organic monolayers and following the arrangement and circuitry, etc. of Hickmott (157). However, all three electrodes used were of aluminium to avoid unnecessary asymmetry. The grid, of thickness ~ 50 Å, contained a significant number of pinholes and the other two electrodes (plate and cathode) were several thousand angstroms thick. The device was formed at 77°K; DNR was found to occur in the second voltage cycle and to disappear in the next few cycles. At about 170°K, the DNR was more pronounced.

In both the experiments on diodes and triodes, Gundlach and Kadlec have explained the observations

qualitatively in terms of the filamentary models of Dearnley et al. (166) according to which DNR occurs by filament breaking because the fractured filament does not contribute to the current. After the so-called dead time, the filament may reform, which presumably occurs at about 2.8 V in the present case.

The succeeding chapter describes the suitability and advantages of 'built-up' films which le to their extensive electrical investigations. Method of selection of substrate, cleaning procedure, details of the experimental set-up are discussed. Sandwich fabrication and measurement techniques of internal voltage have also been described.

CHAPTER VI

STUDIES ON INTERNAL VOLTAGE IN BUILT-UP MOLECULAR FILM SYSTEMS: EXPERIMENTAL

Thin film capacitor (TFC) is one of the many important components readily fabricated by vacuum deposition and other techniques. It is nothing but a sandwich of dielectric material film between two electrodes (of metal films). Apart from the vacuum deposited dielectric films, 'built-up' Langmuir films(18) of long-chain fatty acid compounds, also known as organo-metallic compounds, have also been used extensively as a dielectric film between metal electrodes. As described in the last chapter their dielectric and other electrical properties such as tunneling through thin barriers, temperature and thickness dependence of current-voltage characteristics, dielectric break down, differential negative resistance (DNR) etc. have been investigated experimentally by a number of workers. These 'built-up' molecular films have been proved very useful as thin insulating barriers of known and closely controllable thickness which are extremely uniform. Subsequent sections of this chapter will deal in detail about the suitability of these Langmuir films, fabrication technique of the test samples, experimental set-up and the method of measurement of internal-voltage.

6.1 Suitability and Advantages of Langmuir Films

As mentioned earlier studies of the intrinsic fields in built-up thin films of barium salts of long-chain fatty

acids | $CH_3 (CH_2)_{n-2}COOH$| of different chain lengths (n is the number of carbon atoms in the chain of fatty acid) such as palmitic (n = 16), margaric (n = 17) and stearic (n = 18) acids etc. and its thickness dependence have been carried out in the present work. The Langmuir films have been chosen for the present studies because the thickness of these films are accurately known (77,78) and the closely controllable(say 25 Å). The extreme uniformity of thickness of these films has also been established by a detailed quantitative studies of tunneling phenomenon in these systems (112). The films can be prepared relatively free from holes, gross defects and conducting imperfections (112). These films have been shown to have high dielectric strength ($\sim 10^7$ V/cm) (136, 138) and good thermal stability (113). It has also been established that these films can be exposed to vacuum and metal electrodes can be deposited on them without any damage (113). This is essential because electrodes have to deposited by vacuum evaporation on these films. Above all the films have easy reproducibility in preparation (167).

6.2 Selection of Substrate and Cleaning Procedure

Obviously, one of the major factors governing the degree of uniformity of deposited film in the above process, is the smoothness of the substrate used. Therefore, in the present studies, considerable attention has been paid to the selection of proper substrates with smooth

surfaces and subsequent thorough cleaning to minimize the appreciable variations in the electrical properties. Micro-glass slides having no scratches were first selected. The deposition was made onto these slides after cleaning them properly.

The selected microglass slides were first rinsed thoroughly with deionized and distilled water. The planeness and the smoothness of the selected slides was then checked by the standard method of matching their surfaces with a master optical flat (71). On proper illumination, the formation of reasonably straight, equidistant, parallel and smooth fringes show that the slide surfaces do not have much curvature and are almost plane (71).

The selected microglass slides were then treated with hot chromic acid rinsed with doubly distilled water and allowed to remain in a caustic soda solution for several hours. A thorough washing was done using a strong jet of doubly distilled water and dried by a current of warm air.

After the above cleaning procedure, these slides were then cleaned ultrasonically to remove any greasy contents. The ultrasonic cleaner used is shown in the figure (6.1). Trichloro-ethylene of the analar grade was used as the degreaser in the present work. These thoroughly cleaned glass slides are now ready for capacitor fabrication as will be discussed later (Sec. 6.3). These cleaned slides were preserved in a thoroughly cleaned

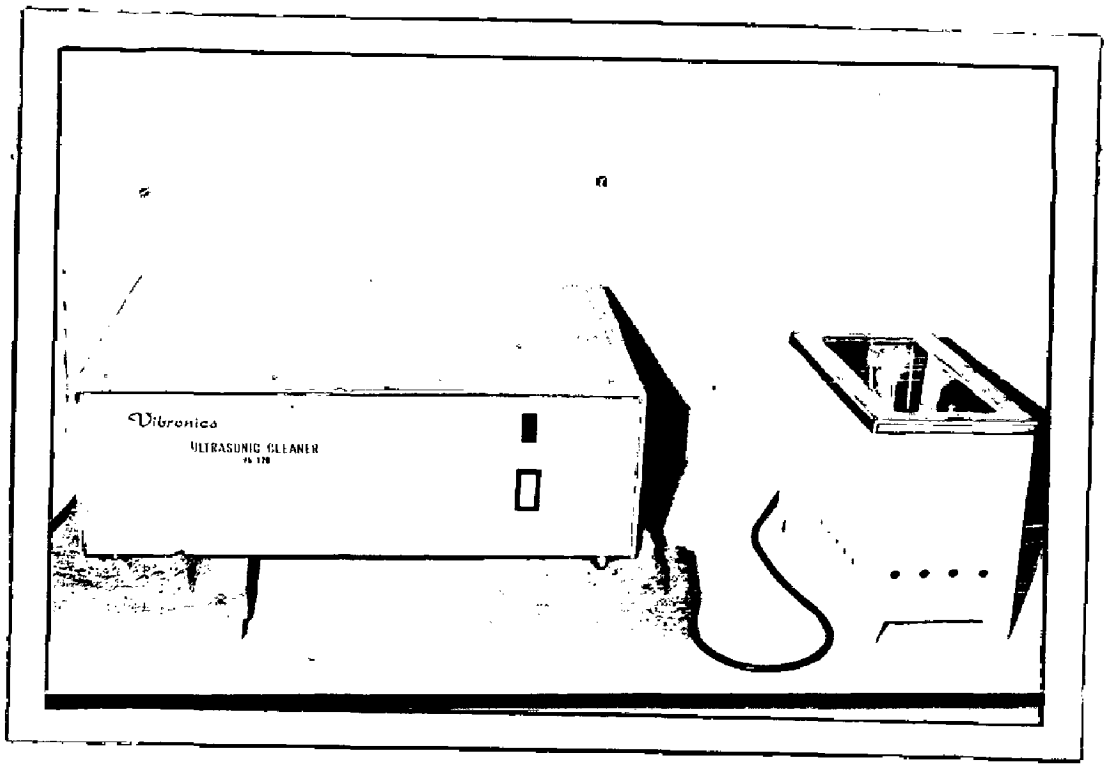

FIG.6.1 PHOTOGRAPH OF ULTRASONIC CLEANER

glass container (vacuum dessicator)till they were loaded in the vacuum chamber.

6.3 Fabrication of Test Sample

(a) Preparation of Mask.

The desired shaping of thin film system involves fabrication of masks of different shapes and using them in a variety of sequences. For the sake of simplicity physical masking technique is used in which the mask is mounted in between evaporant source and the substrate in contact with the latter. Long strips of 1mm width were made with a sharp knife on the very thin sheet of aluminium. These strips were about 2 mm apart from each other. When glass slide is placed on this mask and the metal is evaporated long narrow strips are formed on the substrate. The shape of this mask and the strip electrode system are shown in Fig.6.2 (a). This mask has been used for the first electrode (bottom electrode) deposition. The top electrode is a common strip deposited perpendicular to the bottom electrodes. Thus a comb like electrode structure is formed (Fig.6.2 b).

(b) Sample Preparation

The cleaned and carefully selected microglass slides as discussed in the preceding section (sec. 6.2) are used for the fabrication of the film sandwiches of the

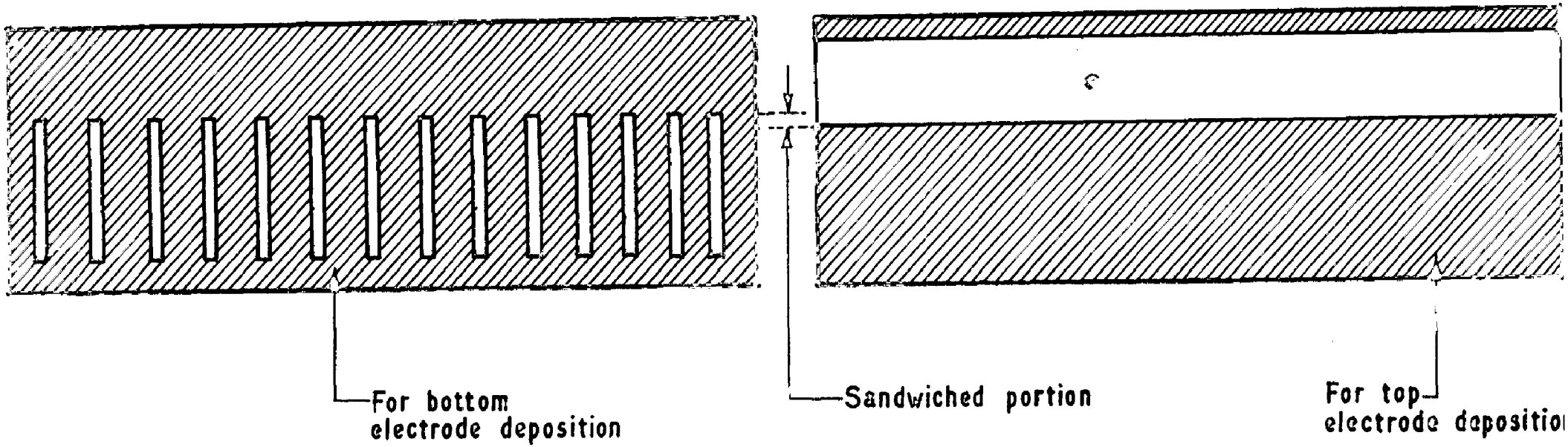

FIG. 6.2(a) MASK GEOMETRIES FOR THE ELECTRODES DEPOSITION

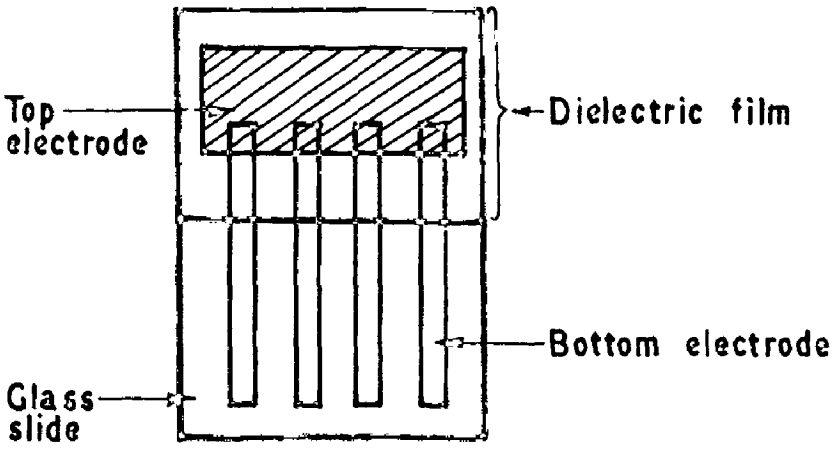

FIG. 6·2 (b) FRONT VIEW OF TEST SAMPLE

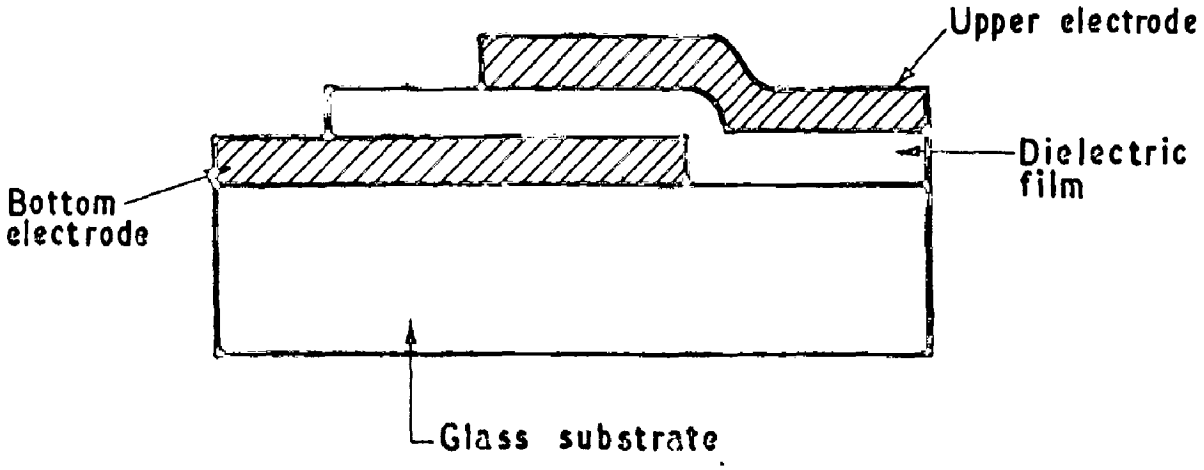

FIG. 6·2 (c) SIDE VIEW OF TEST SAMPLE

type Metal-Insulator-Metal (M-I-M). For obtaining the required structure, long narrow strips of aluminium (in general) were first deposited on the selected glass slides. The metal aluminium was deposited on the slide by thermal evaporation in vacuum ($\sim 10^{-6}$ mm of Hg) with the help of a high vacuum coating unit (Fig.6.3). Before depositing aluminium the slide was finally cleaned by ionic bombardment in vacuum. A self explanatory pipe line diagram of the evaporation unit is shown in Fig. 6.4.

High purity aluminium (99.99%) supplied by M/S Johnson and Mathey was used for evaporation and making electrodes of the sandwich structure. The thickness of the aluminium electrode was roughly kept constant every time by keeping (i) the distance between the filament and the work holder fixed (ii) placing the same amount of aluminium on the filament (iii) passing the same amount of current through filament and (iv) evaporating the metal for the same time. The thickness of the electrode used was $\sim$ 400 Å .

The 'built-up' films of barium salts of long chain fatty acids of different chain lengths are then deposited on these partly aluminized glass slides, having desired number of layers, using the Blodgett-Langmuir technique as described earlier (chapter IV sec.4.1). Y-type films have been used for the present study because their characteristics are well understood. The upper (top) common electrode of the desired metal is then evaporated on the

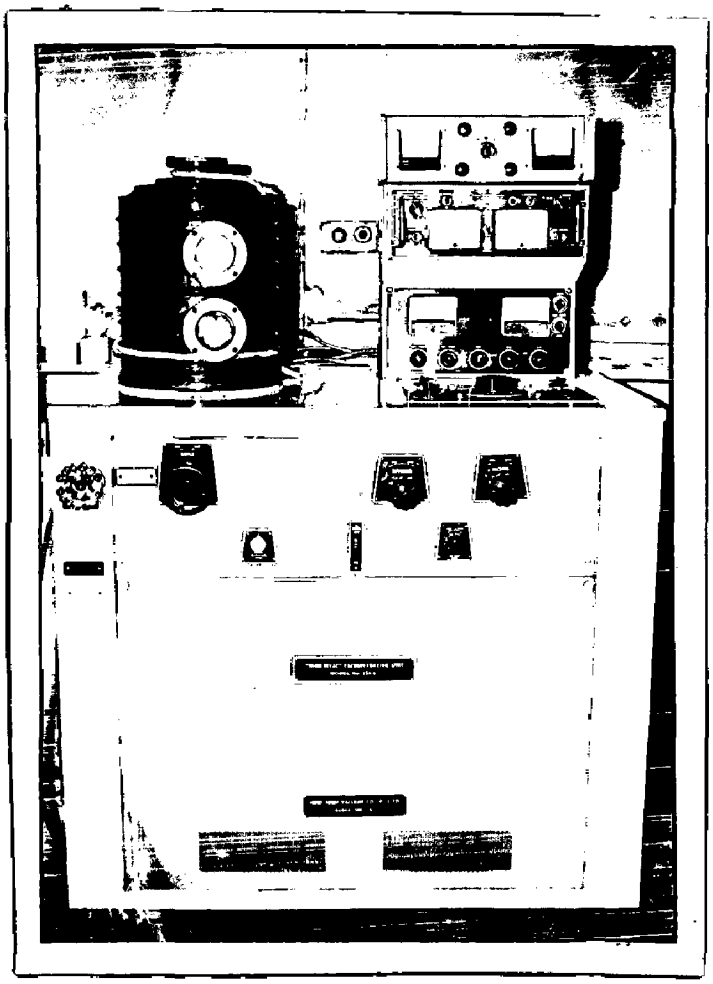

FIG.6.3 PHOTOGRAPH OF VACUUM COATING UNIT

Langmuir film by thermal evaporation in vacuum. The only precautions needed for the evaporation of second electrode are that (i) the appropriate filament or boat should be chosen (Table II) for a particular metal and (ii) Ionic bombardment cleaning should not be performed otherwise it may result in local heating of film, thereby the melting of the organic film having molecules bound together by weak Vander Wall forces. The lateral and transverse views of the sandwich structure, thus fabricated, are shown in fig.6.2 b and6.2 c. The area of each sandwich is nearly 1 mm^2.

6.4 Measurement of Internal Voltage

As discussed earlier a high intrinsic field exists in a thin insulating film sandwiched between electrodes having different work functions. Simmons (10) demonstrated the existance of this intrinsic field inside the Al_2O_3 films sandwiched between dissimilar electrodes. For thin films < 100 Å, this field is of the order of megvolts/cm. Because of its magnitude , Simmons thought that the field should be manifested under voltage breakdown conditions; that is, the junction should exhibit polar dielectric strength characteristics.

Simmons measured the breakdown voltage of M_1-I-M_2 (M_1 and M_2 are different) structure with the electrode of lower work function negatively biased and called it

as V_1. Then he reversed the polarity and measured the breakdown voltage again. He found it less than the previous one and called it as V_2. He calculated the value of $\frac{V_1-V_2}{2s}$ which is nothing but the intrinsic field (chap. II).

In the present investigation our main emphasis will be to measure the value $\frac{V_1-V_2}{2}$. We will be calling this voltage as internal voltage. The measurement techniques which have been followed in the present investigations are as follows:

(a) Breakdown-Voltage Technique

It is essentially the same as adopted by Simmons in his work. The details of the technique are as follows: The tunneling currents were measured with the top electrode based positive as well as negative. Since these built-up films are very good insulators, very small values of tunneling currents were observed (range 10^{-11} - 10^{-7} amperes). These small values of tunneling currents were measured using a sensitive electrometer amplifier. The author used a highly sensitive electrometer amplifier for the present investigations. This electrometer amplifier has current ranges from 10^{-6} - 10^{-12} amps and the voltage range 0-1 volt full scale deflection using a moving coil meter as indicator with 100 mm scale length. The input impedence of this amplifier is 10^{15} ohms. Pressure leads were used for the electrical contacts with the two electrodes. Fig.6.5 and 6.6 show the photograph and block

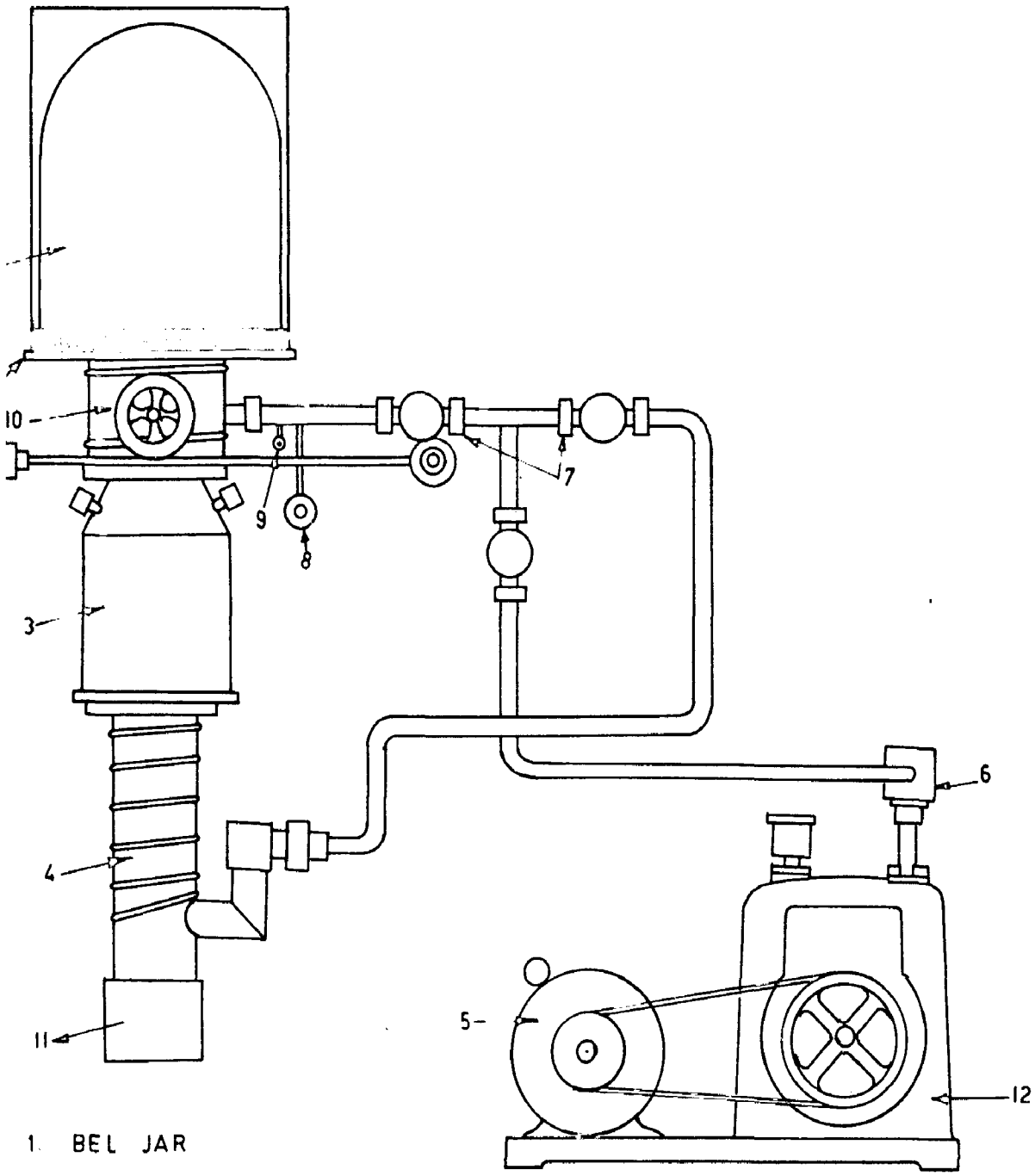

1. BEL JAR
2. BASE PLATE
3. LIQUID NITROGEN TRAP
4. DIFFUSION PUMP
5. INDUCTION MOTOR
6. MAGNETIC ISOLATION VALVE
7. COUPLING
8. AIR ADMITTANCE VALVE
9. VACUUM SWITCH
10. BAFFLE VALVE
11. HEATER
12. ROTARY PUMP

FIG. 6·4 PIPE LINE DIAGRAM OF VACUUM COATING UNIT

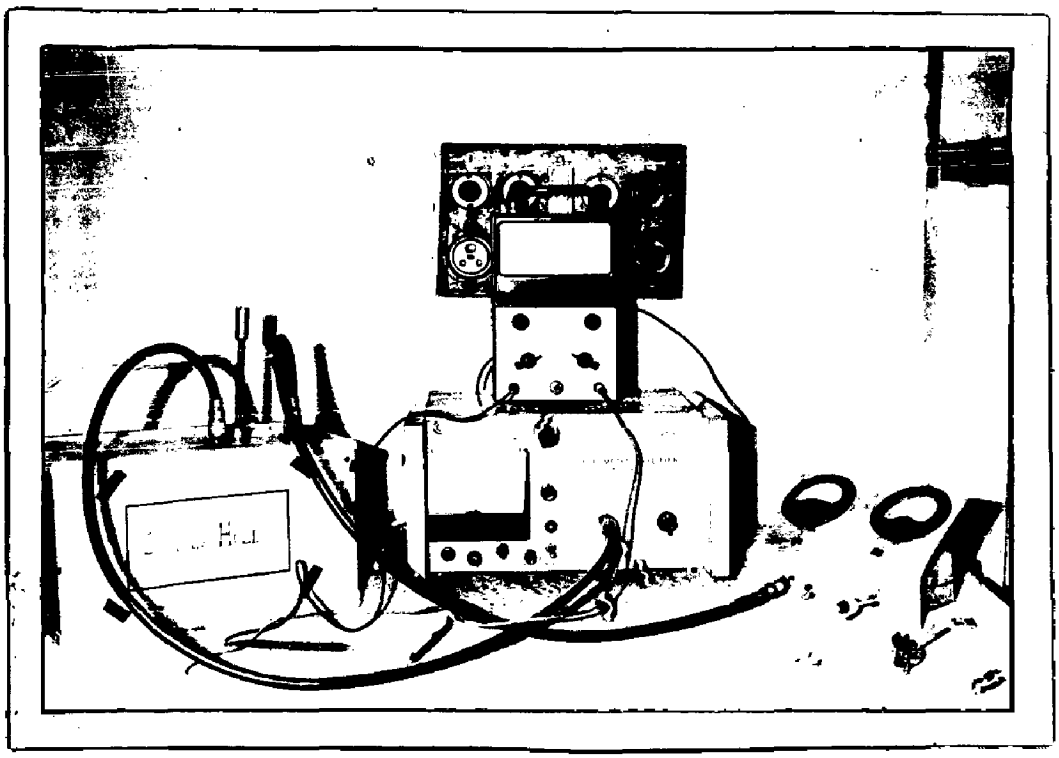

FIG.6.5 PHOTOGRAPH OF MEASUREMENT SET-UP

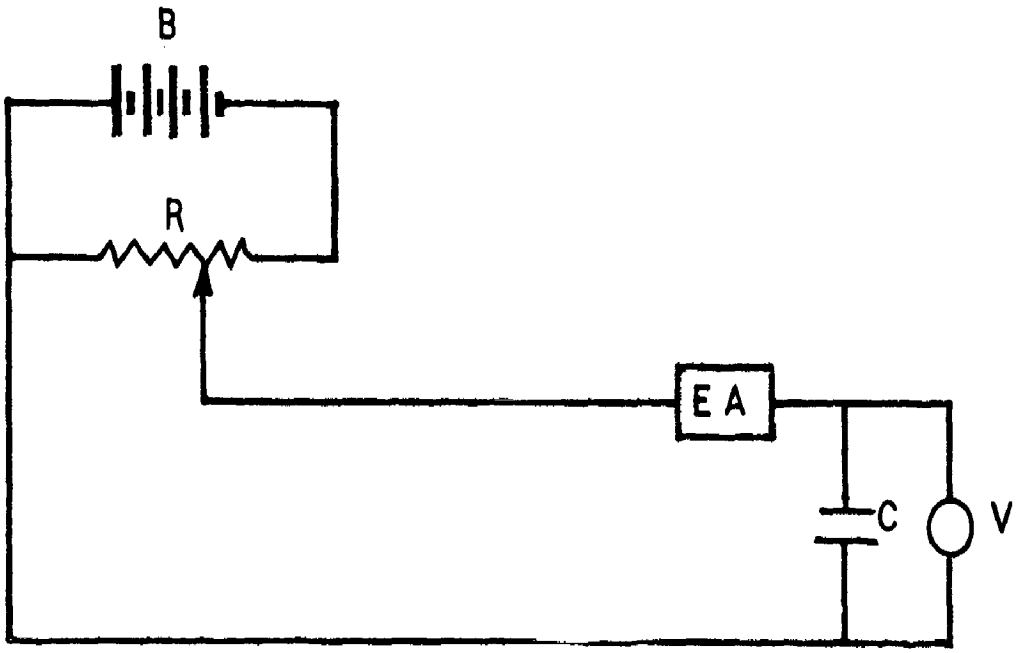

V – Voltmeter

E A – Electrometer

C – Film capacitor under test

R – Helipot

FIG. 6·6 CIRCUIT DIAGRAM FOR I-V CHARARACTERISTICS

diagram of measurement set up. The complete circuit including the low-voltage power supply, was electrically shielded to avoid any stray signal effect. This was done by using shielded cables and amphinol connectors. The possibility of any light signal falling on the test sample was avoided for the reasons which will be discussed in the chapter VIII.

A non zero current was observed even at zero applied bias indicating the existance of internal fields. If a gradually increasing voltage is applied across the electrodes of one of the junctions, with the electrode of lower work function negatively biased, then the initial increase in voltage decreases the intrinsic field F_i to zero. At this stage a zero current is observed. For Al-Ba stearate(4 layer)-Sn structure (Fig.7.4) this voltage was observed to be 0.48V with tin biased positive (170) . Further increase of potential gradually increases the field in the insulator until a critical field F_d in the opposite direction is attained and the current becomes unstable and increases as a function of time. This situation will be referred to as the onset of the breakdown. For the Al-BaSt-Sn Structure this breakdown voltage has been found to be $V_1 \simeq 1.8$ V in the present investigations. The voltage V_1 under these conditions is given by

$$V_1 = (F_d + F_i) s \qquad .(6.1)$$

where s is the thickness of the dielectric film.

A voltage bias of opposite polarity is now applied

to the second junction. Increasing the potential between the electrodes gradually increases the field in the insulator from the intrinsic field value F_i until the current again becomes unstable and increases and a function of time i.e. until the breakdown field F_d is attained. In this case there is no field reversal i.e, no zero current is observed. The breakdown voltage V_2 under these conditions is,

$$V_2 = (F_d - F_i)s \qquad (6.2)$$

For the Al-Ba stearate-Sn structure, the value of V_2 has been found to be $V_2 = 0.9V$. The difference $\Delta V = (V_1 - V_2)$ divided by a factor of two gives the value of internal voltage. Therefore the value of internal voltage for Al-Ba stearate (4 layer)- Sn structure will be 0.45 volts.

(b) Zero Current-Method

In the present investigations it was found that in the case when electrode of lower work function is negatively biased, the initial increase in voltage decreases the intrinsic field F_i to zero. At this voltage the current observed in electrometer amplifier is nearly zero. Even small increase in voltage at this stage results in change in sign of current. Since this voltage works against the intrinsic field F_i to bring it to zero, the field because of this applied voltage is equal in magnitude

to that of F_{i}. Or in other words this voltage which neutralizes the intrinsic field is nothing but equal to the internal voltage. As can be seen in the Sec. 6.4a and from fig. 7.4 the current changes sign at $V \simeq .48$ volts for the case of Al-Ba stearate (4 layer) - Sn structure. Also the internal voltage measured from difference in breakdown voltage in two polarities is 0.45 volts. The two values are very close to each other, so this method also gives quite accurate values of internal voltages and it is a good check over the previous method.

(c) Equal Magnitude of Current Method.

If we consider the linear portions on the two curves (Fig. 7.4 chap.VII)plotted as log I Vs V and look at the two values $V_{.}^{I}$ and V^{II} for the same magnitude of current it is very close to twice the internal voltage. This is expected since internal voltage tends to enhance the current in one direction and restricts it in the other direction. This is a further check over the previous two methods. These observations confirm that there exists an internal voltage and its value in the present structure lies close to 0.5 V, with the tin electrode showing positive polarity.

(d) Direct Voltage Measurement

To further verify the correctness of this internal voltage the voltage was measured directly with the high impedance ($\sim 10^{15}\ \Omega$)

meter amplifier used as voltage measuring device and it was found to be 0.49V for Al-Ba stearate (4 layer)-Sn structure, with tin showing positive polarity. The procedure is much faster and allows quite accurate determination of the internal voltage.

If one utilizes the breakdown voltage method (Simmons 10) it would give somewhat uncertain results because of the difficulty of accurately locating the breakdown point. Although all the above measurement methods (a),(b) and (c) were used for a relative study the direct voltage measurement method (d) was mainly employed because the latter method is quicker and more accurate.

The next chapter describes systematically the detailed results obtained on the measured internal voltage as a function of thickness. It also contains the detailed discussion of the results.

CHAPTER VII

RESULTS AND DISCUSSION OF INTERNAL VOLTAGE MEASUREMENTS ON LANGMUIR FILM SYSTEMS WITH DISSIMILAR ELECTRODES

This chapter describes the results and discussion of the detailed and systematic measurements on internal voltage taken on 'built-up' films of barium palmitate $| C_{15} H_{31} COO|_2 Ba$, barium margarate $| C_{16} H_{33} COO|_2 Ba$, barium stearate $| C_{17} H_{35} COO|_2 Ba$ and Stearic acid $| C_{17} H_{35} COOH|$ with aluminium as the bottom electrode and tin, silver, bismuth, tellurium and lead as the top electrodes. In one particular case tin was deposited as the base electrode and aluminium as the top electrode. The measurements have been taken on different thicknesses of the organic dielectric. The internal voltage has been extrapolated to zero thickness, for the case of even number of layers to give the actual value of difference in work functions of the two metals. Taking aluminium as reference metal and using the value of its work function, the work functions of other metals have been determined in their thin film form . Thus it was possible to study the thickness dependence of work function of these metals. The interesting difference in behaviour for the case of even and odd number of layers has also been investigated. The current versus voltage (I-V characteristics) has also been plotted on a linear scale and it was found that the sandwich structure behaves like a diode junction. These diode characteris-

tics have also been plotted for different structures.

To interpret our results more systematically it is found necessary to study the discharging and charging behaviour of M_1-O-M_2 structure with time (where M_1 and M_2 refers to different metal electrodes and O refers to organic monolayer). The discharging of these structures in closed circuit and its voltage recovery in open circuit have also been studied. All the measurements were taken at the room temperature.

7.1 Results

(a) Measurement of Internal Voltage in Asymmetric Junctions

(i) Breakdown Voltage Method: Current-Voltage characteristics.

The typical current-voltage characteristics of the substances namely, barium palmitate, barium margarate, barium stearate and stearic acid have been studied. The different structures used for investigations are aluminium-Organic layer - M, where M refers to the different metal electrodes namely, Tin, Silver, Bismuth, Tellurium and Lead which have been used for the purpose of counter electrode. In one particular case tin was used as the base electrode and aluminium as the top electrode. The tunneling currents were measured with the aluminium electrodes biased positive as well as negative and are shown in well labelled and self explanatory figures

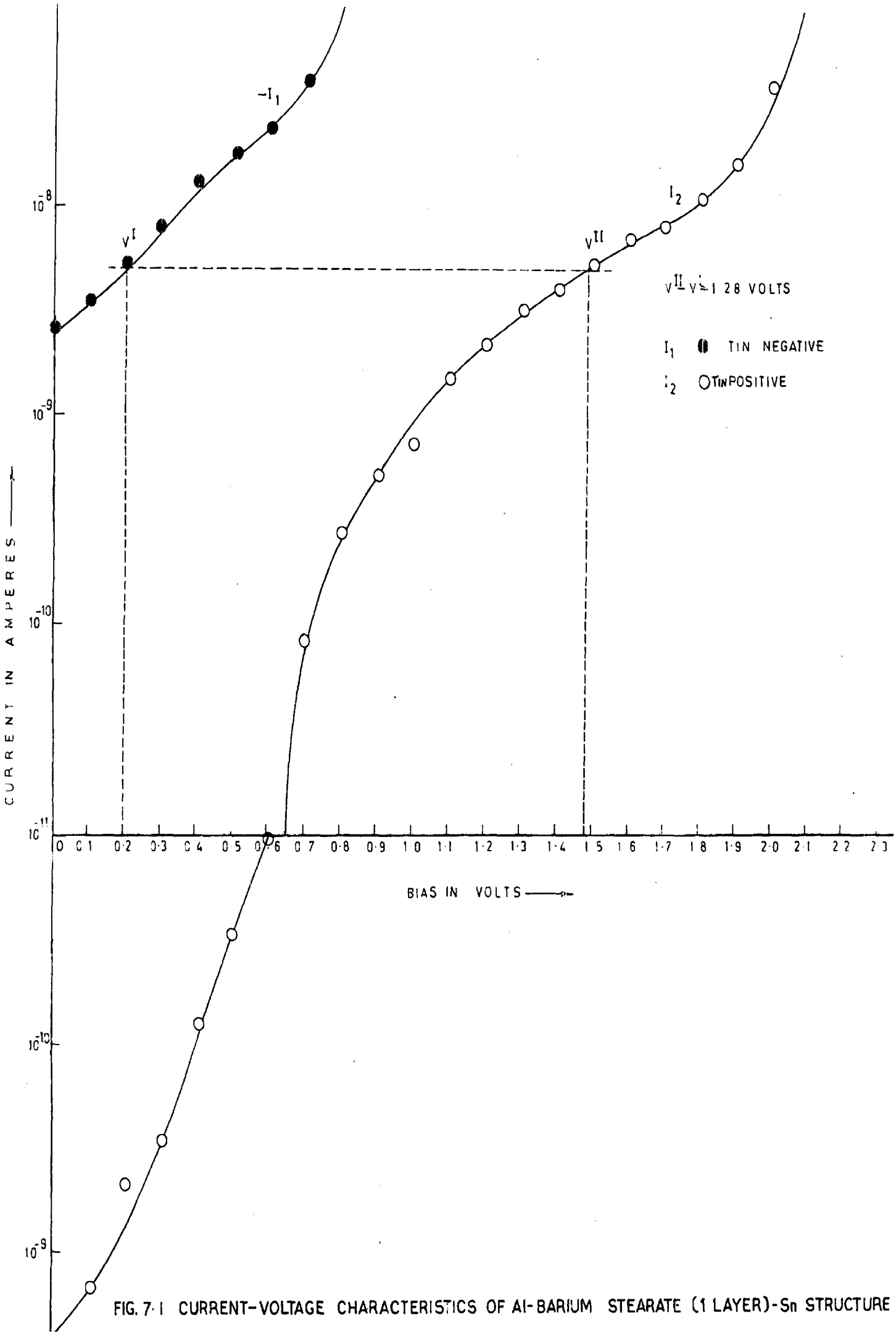

FIG. 7.1 CURRENT-VOLTAGE CHARACTERISTICS OF Al-BARIUM STEARATE (1 LAYER)-Sn STRUCTURE

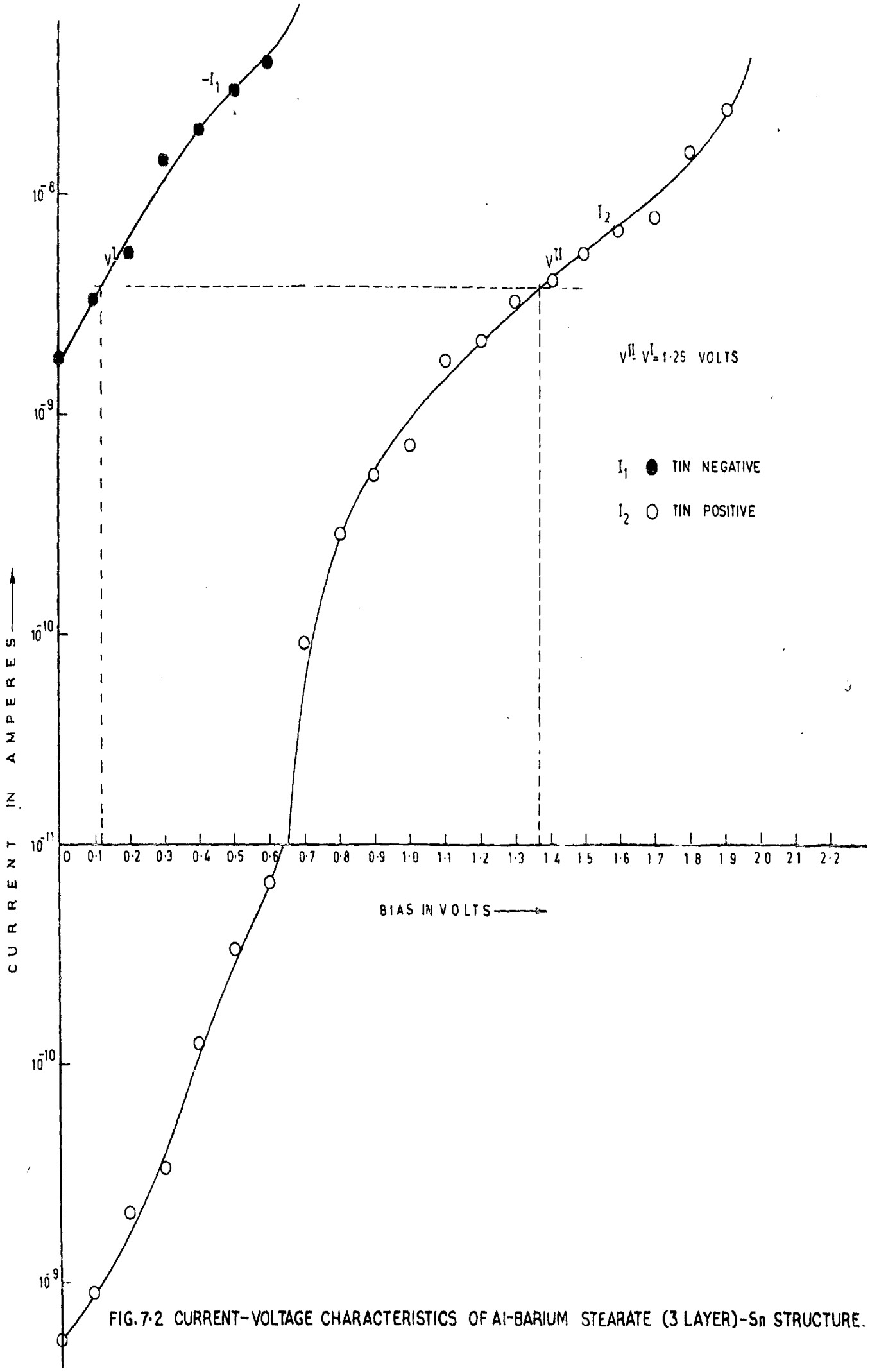

FIG. 7·2 CURRENT-VOLTAGE CHARACTERISTICS OF Al-BARIUM STEARATE (3 LAYER)-Sn STRUCTURE.

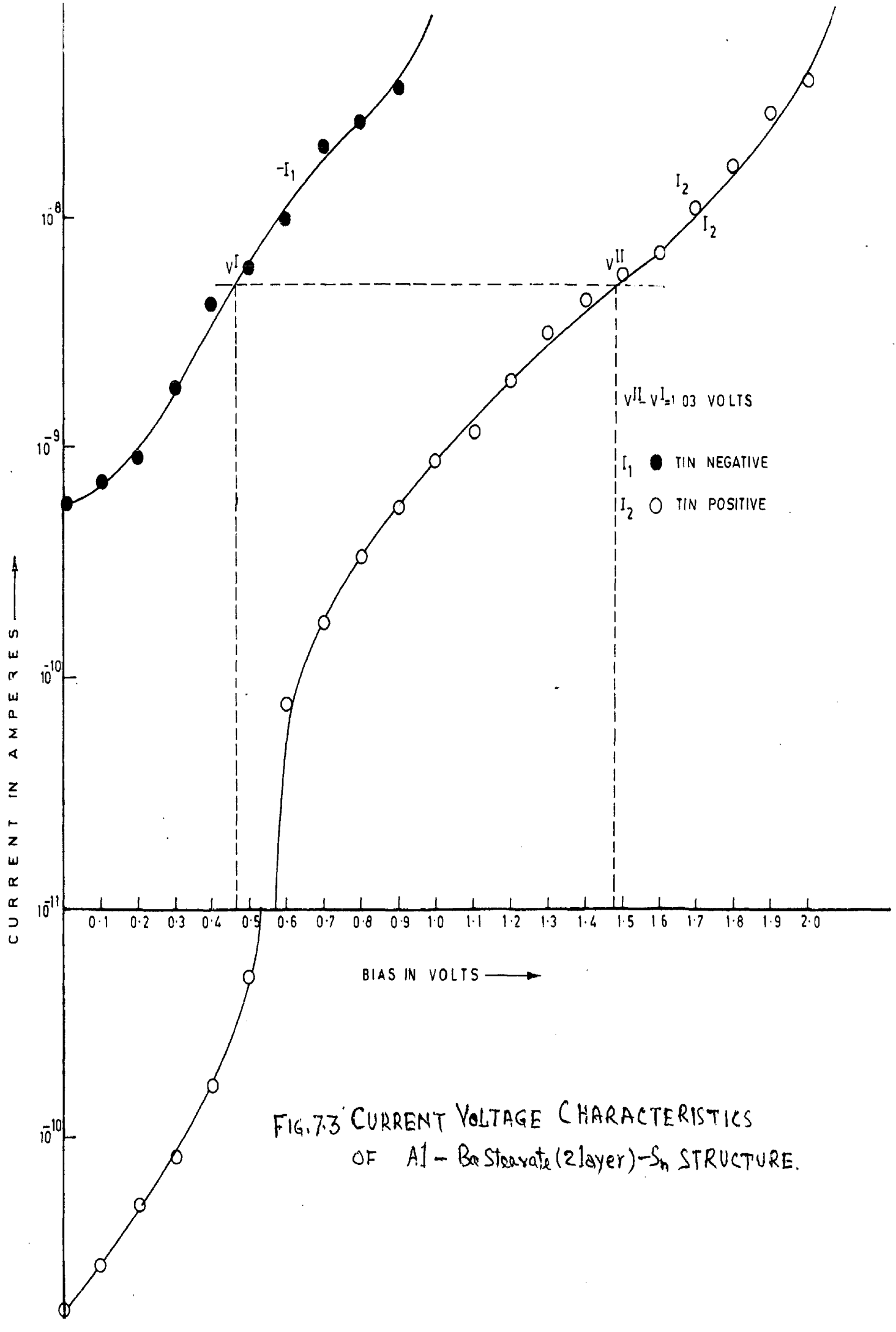

FIG. 7.3 CURRENT VOLTAGE CHARACTERISTICS OF Al – Ba Stearate (2 layer) – Sn STRUCTURE.

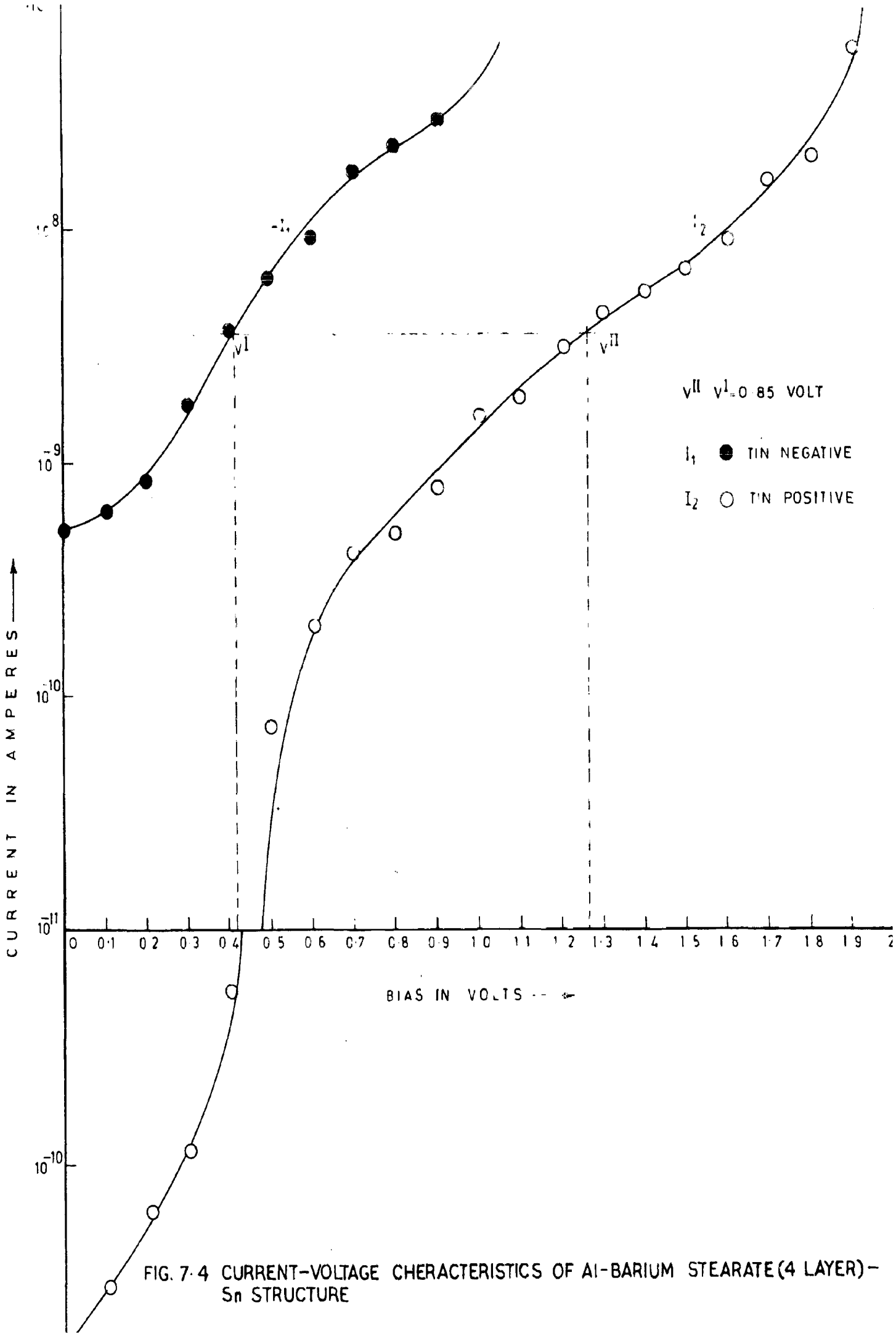

FIG. 7·4 CURRENT–VOLTAGE CHERACTERISTICS OF Al-BARIUM STEARATE (4 LAYER)–Sn STRUCTURE

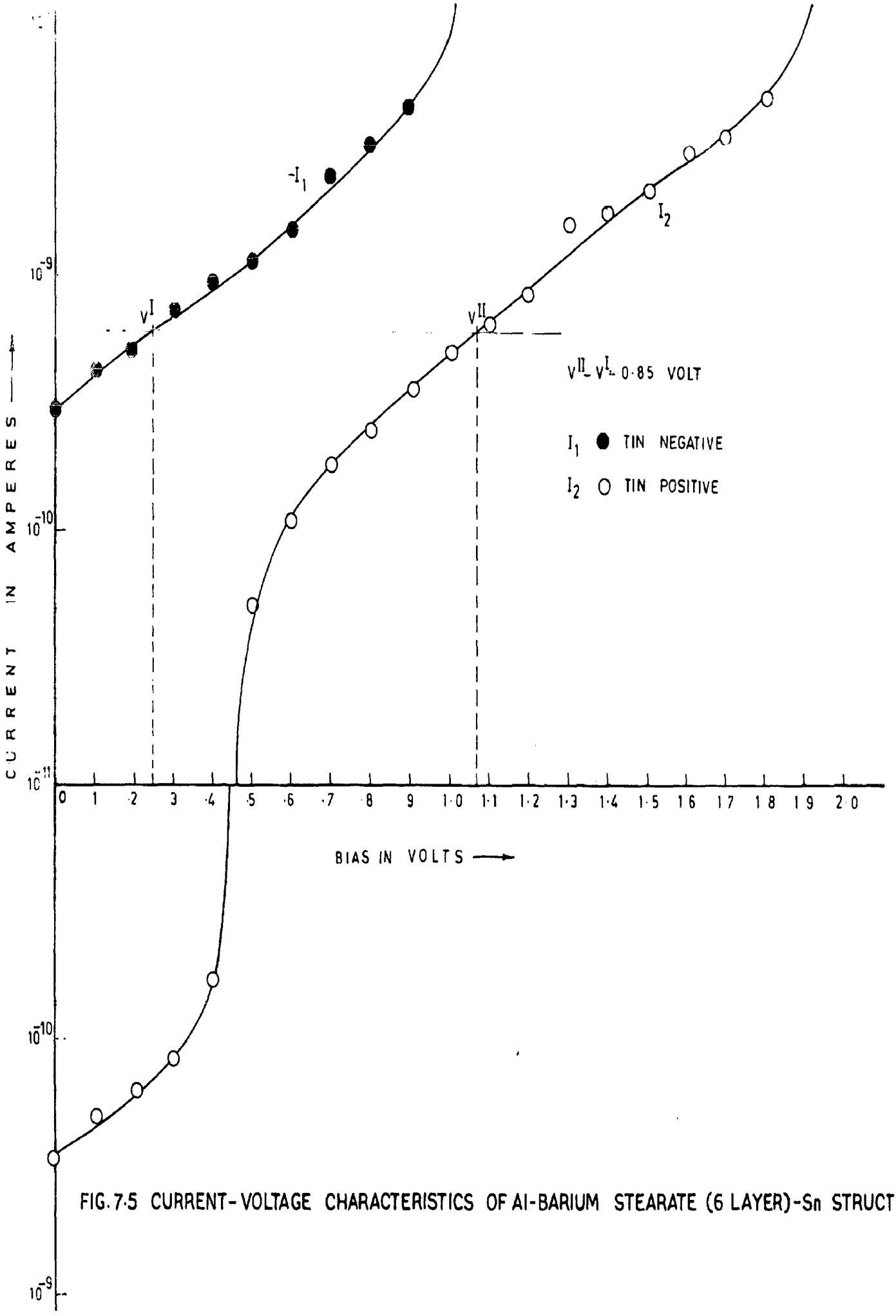

FIG. 7·5 CURRENT-VOLTAGE CHARACTERISTICS OF Al-BARIUM STEARATE (6 LAYER)-Sn STRUCTURE

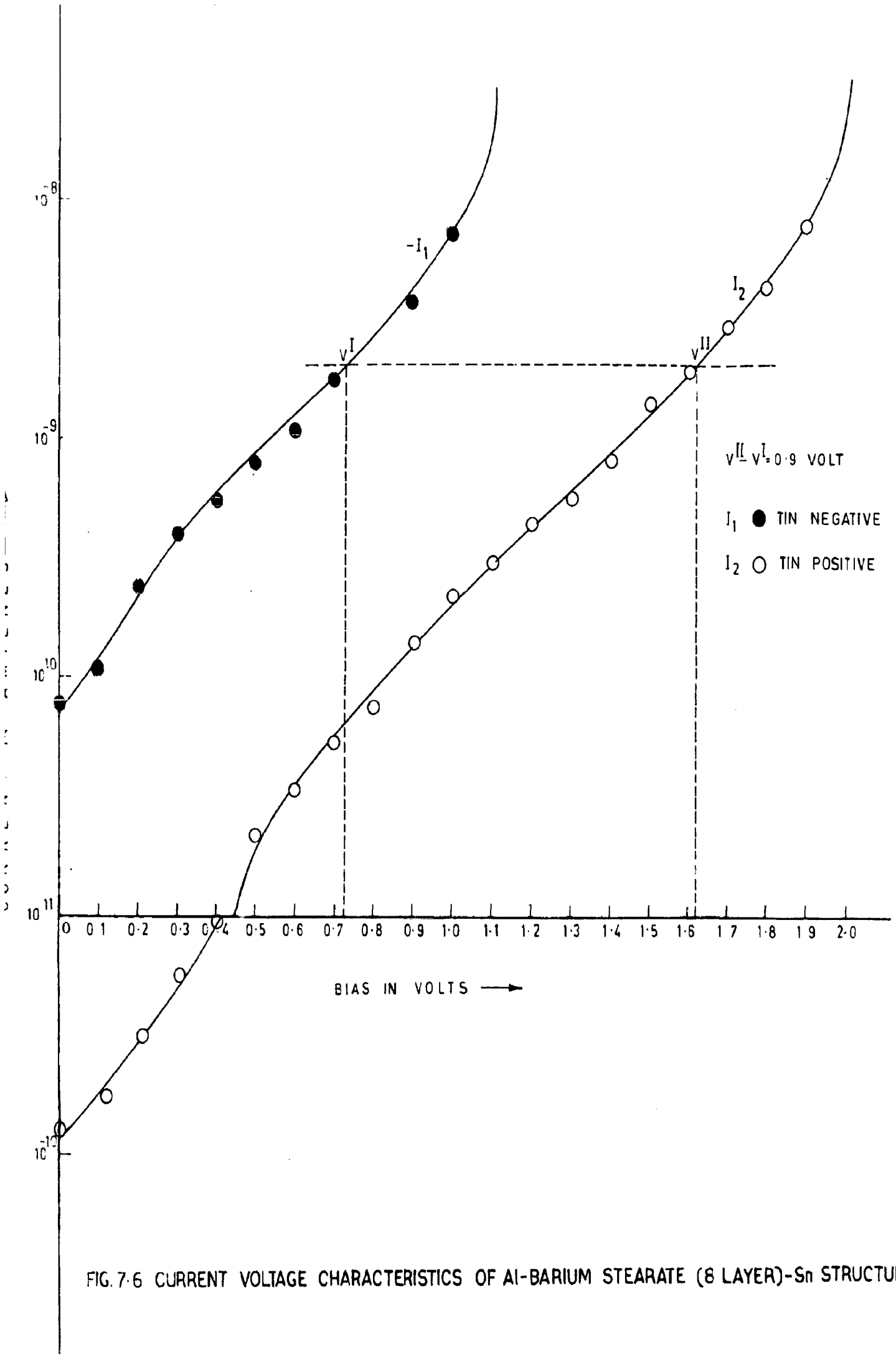

FIG. 7.6 CURRENT VOLTAGE CHARACTERISTICS OF Al-BARIUM STEARATE (8 LAYER)-Sn STRUCTURE

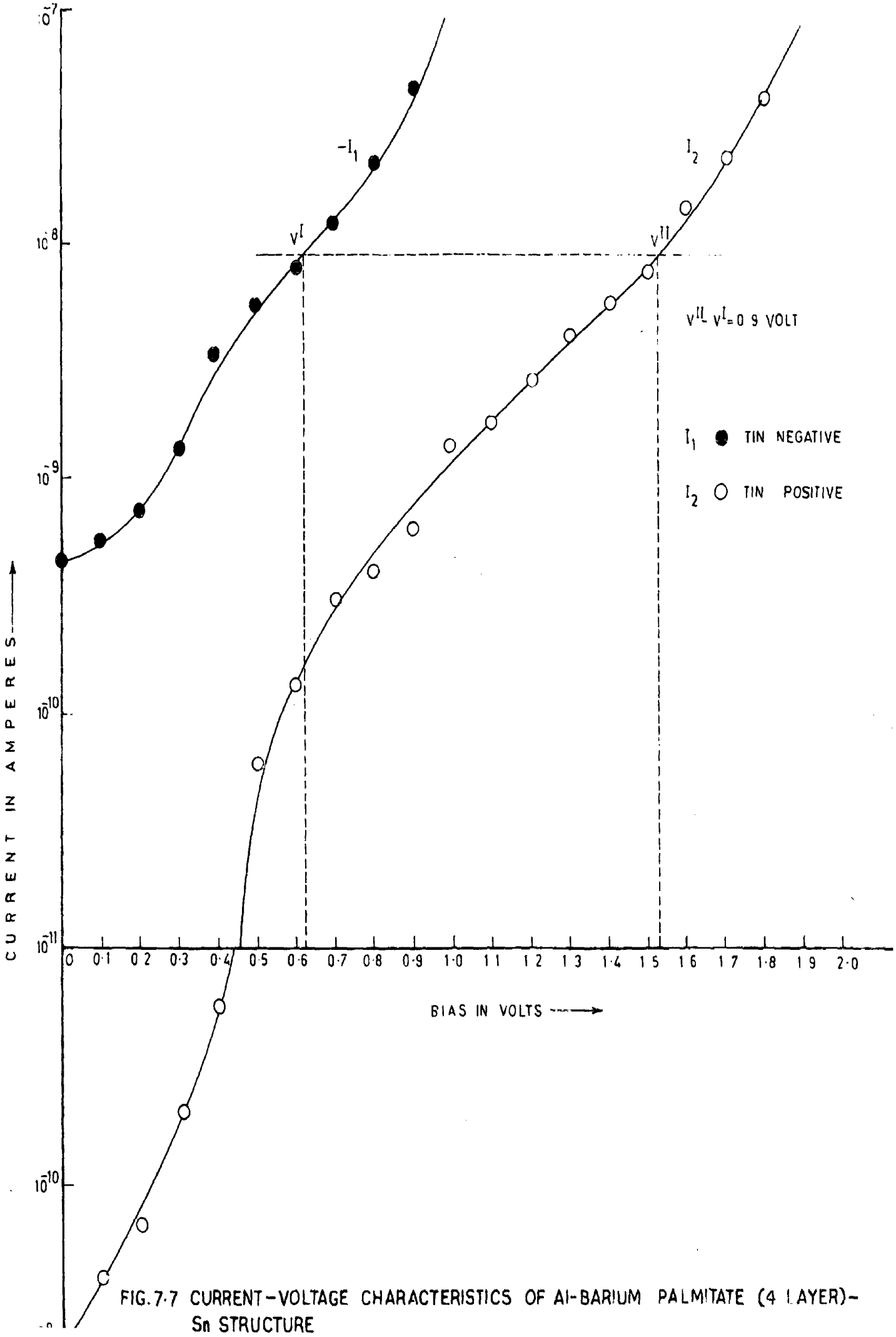

FIG. 7·7 CURRENT–VOLTAGE CHARACTERISTICS OF Al-BARIUM PALMITATE (4 LAYER)–Sn STRUCTURE

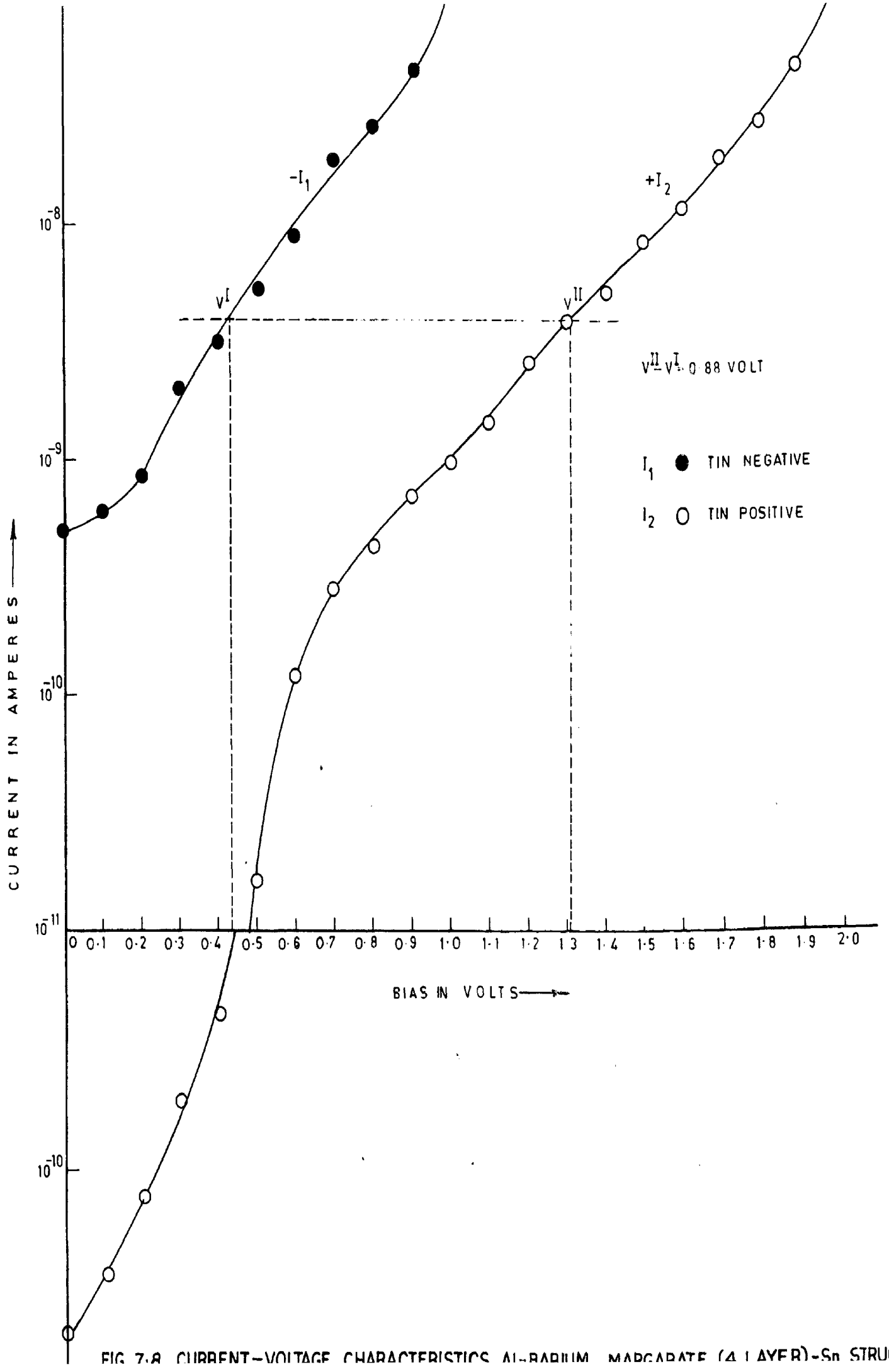

FIG 7.8 CURRENT–VOLTAGE CHARACTERISTICS AL-BARIUM MARGARATE (4 LAYER)-Sn STRUCTURE

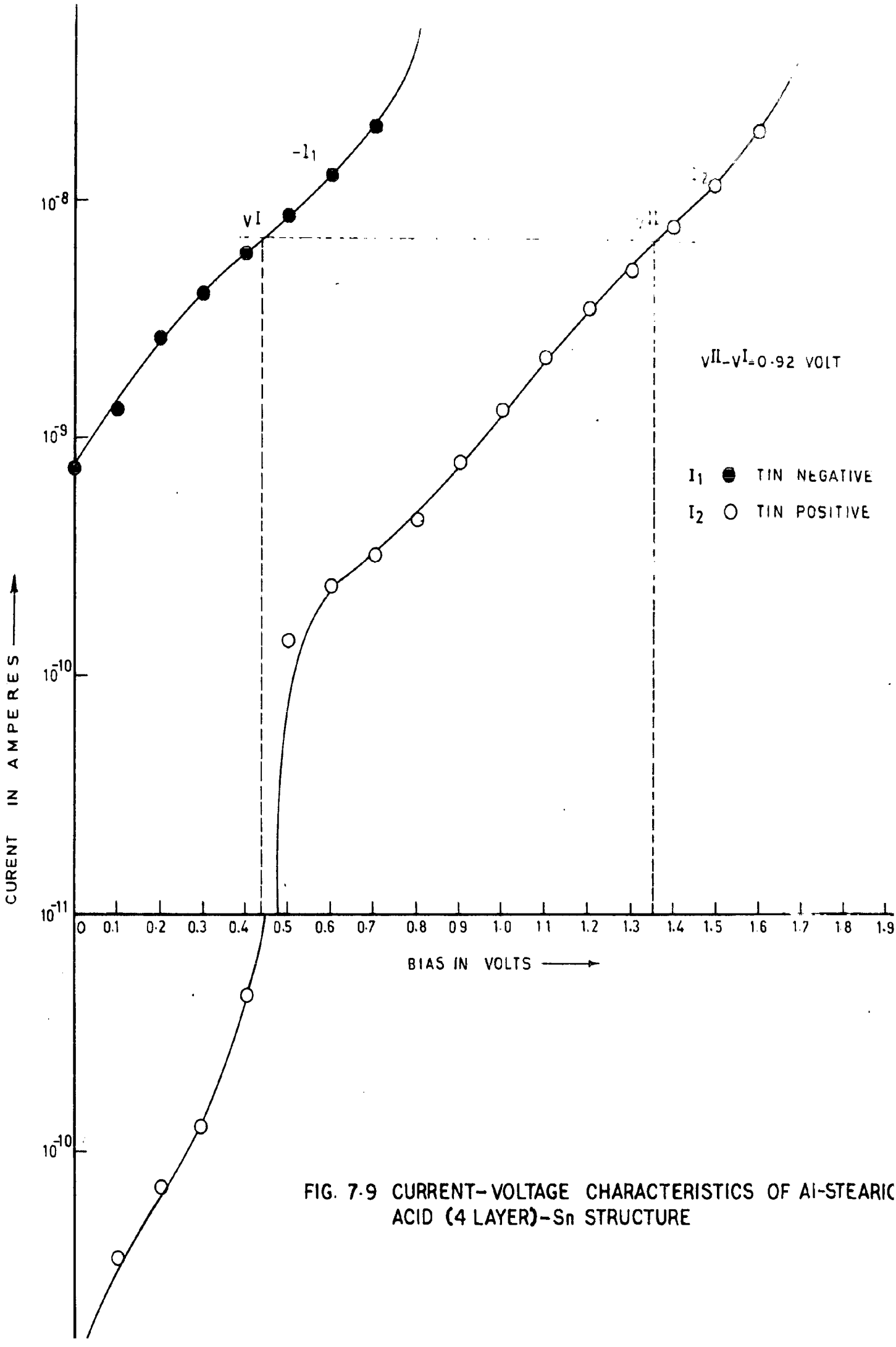

FIG. 7·9 CURRENT–VOLTAGE CHARACTERISTICS OF Al-STEARIC ACID (4 LAYER)–Sn STRUCTURE

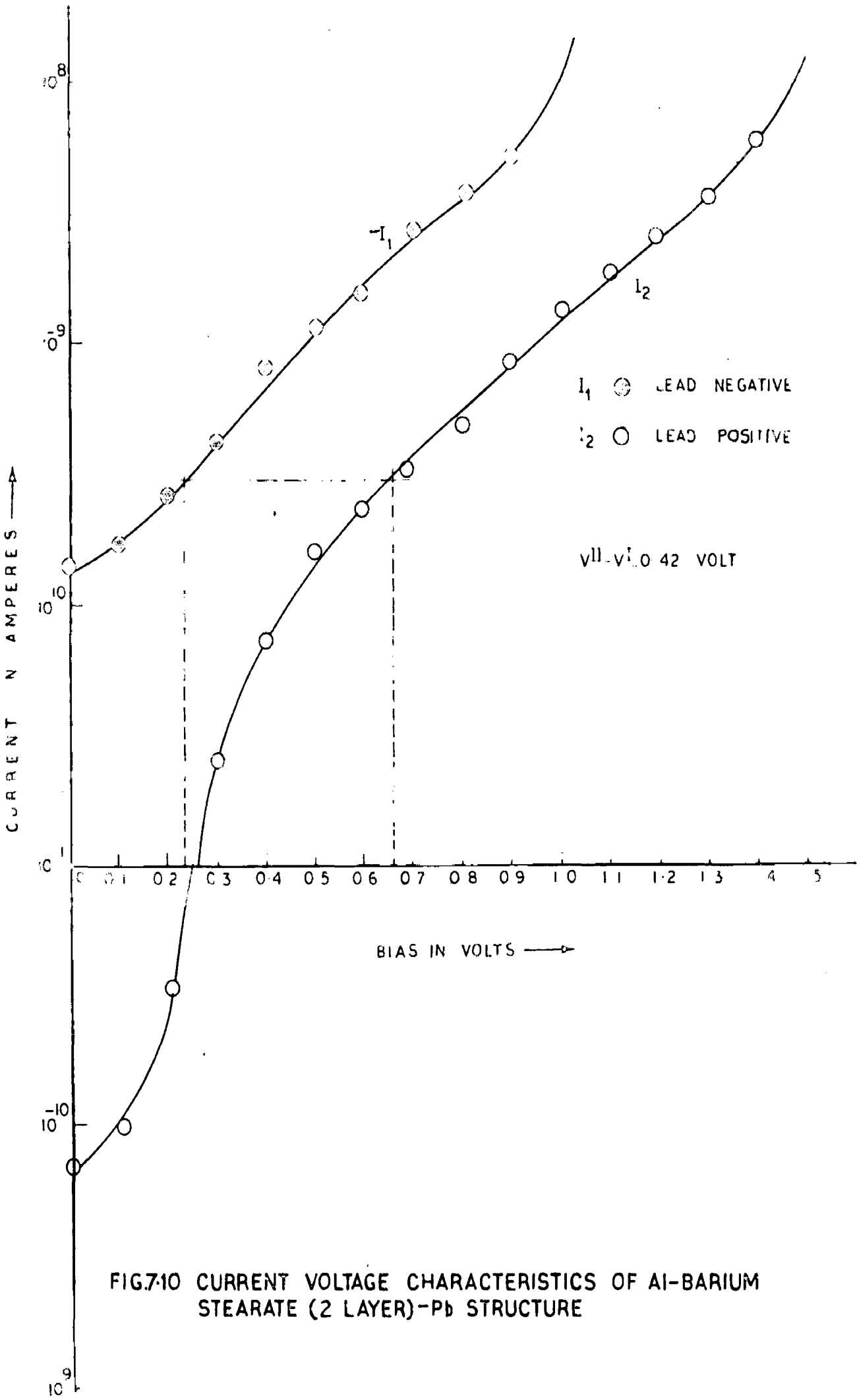

FIG.7.10 CURRENT VOLTAGE CHARACTERISTICS OF Al-BARIUM STEARATE (2 LAYER)-Pb STRUCTURE

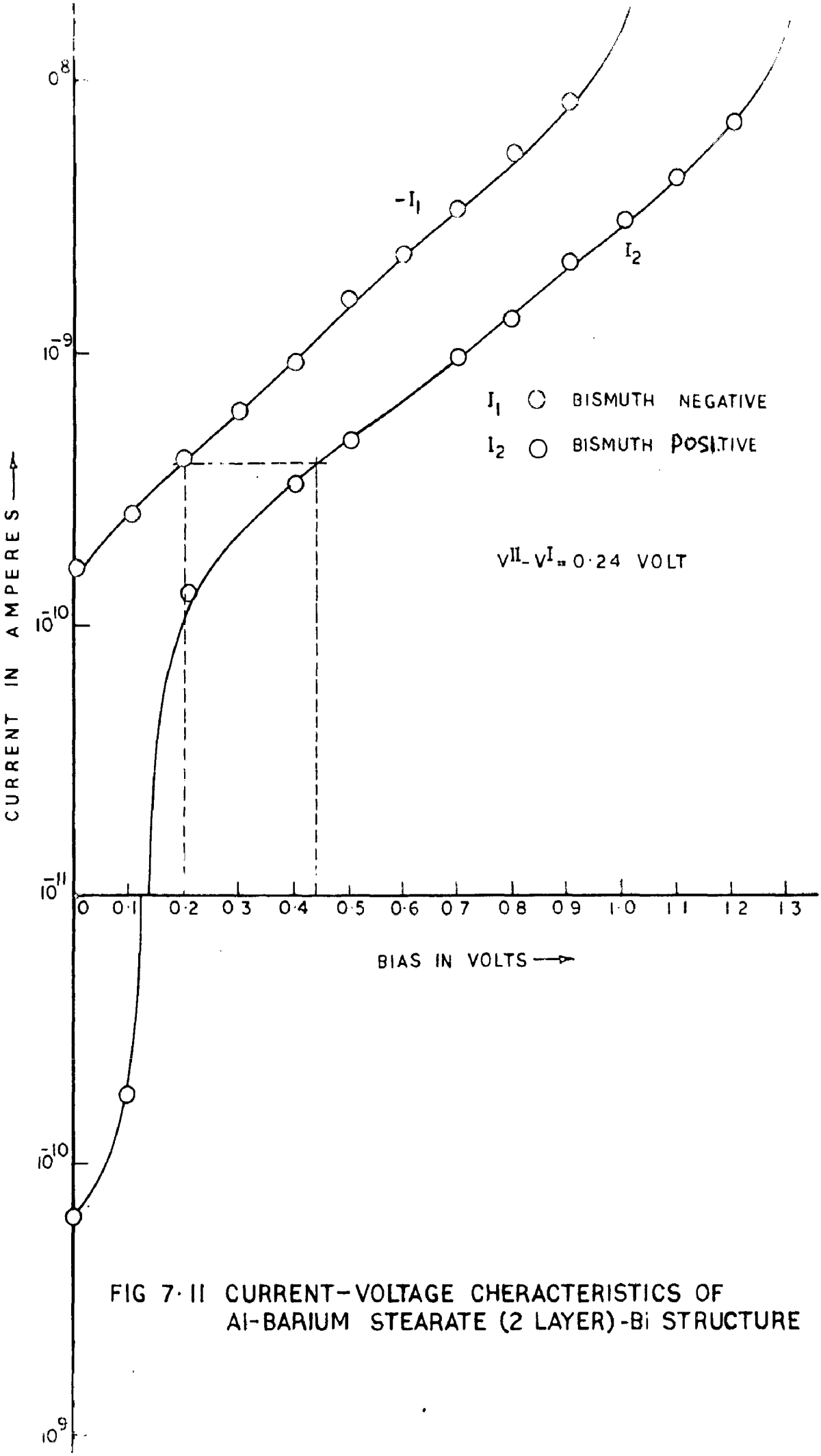

FIG 7·11 CURRENT–VOLTAGE CHERACTERISTICS OF Al-BARIUM STEARATE (2 LAYER)-Bi STRUCTURE

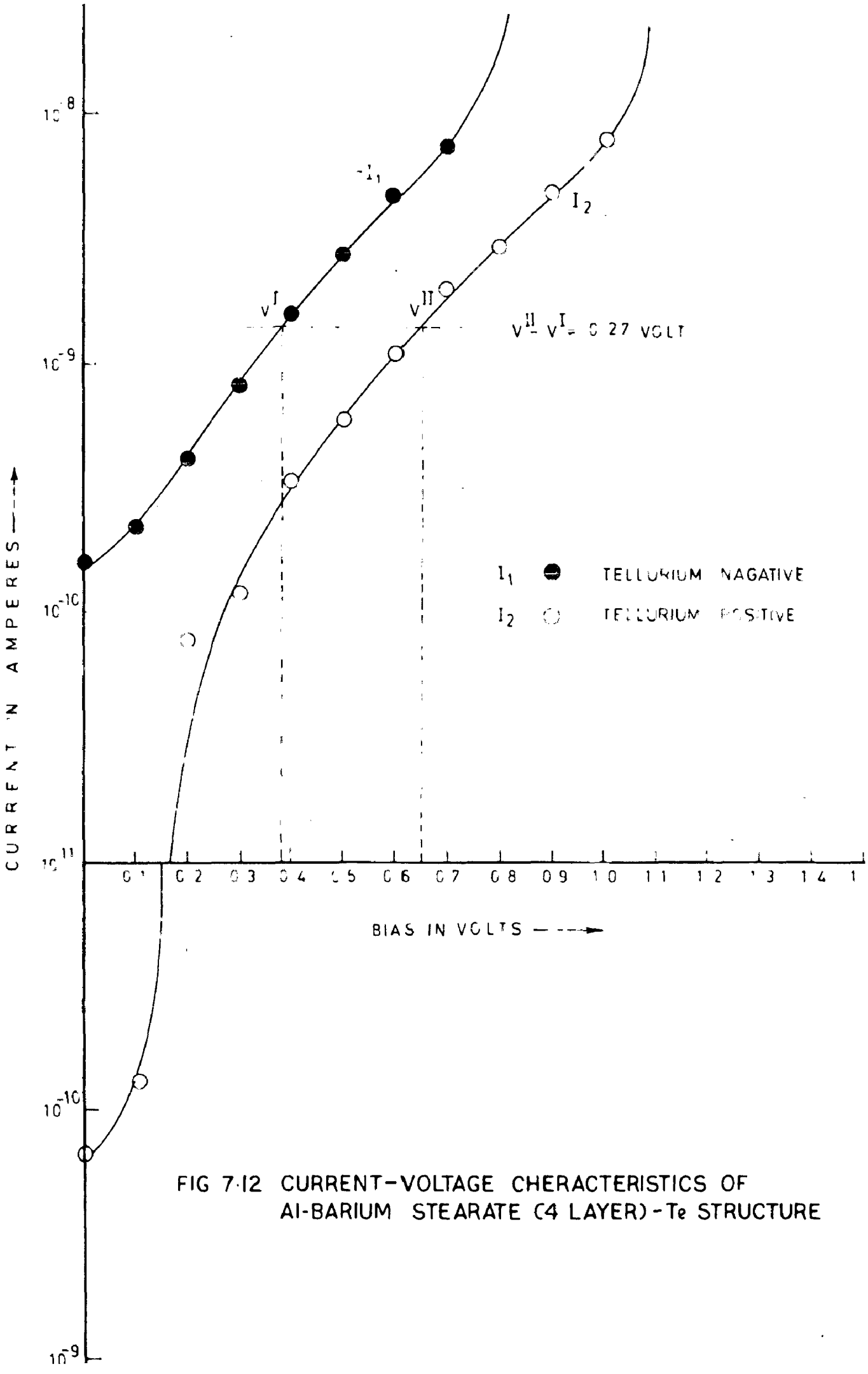

FIG 7.12 CURRENT-VOLTAGE CHERACTERISTICS OF AI-BARIUM STEARATE (4 LAYER)-Te STRUCTURE

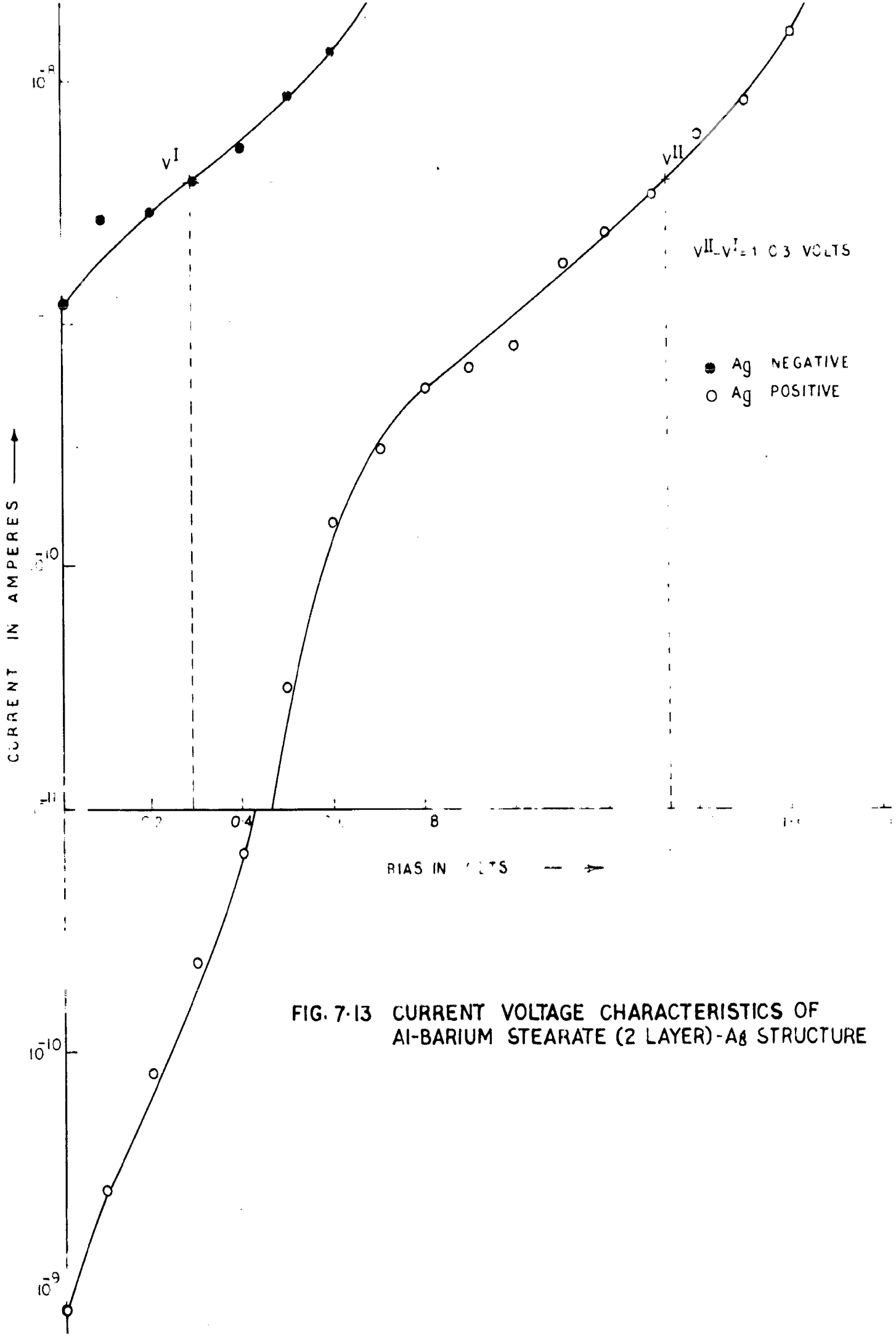

FIG. 7·13 CURRENT VOLTAGE CHARACTERISTICS OF AI-BARIUM STEARATE (2 LAYER)-Ag STRUCTURE

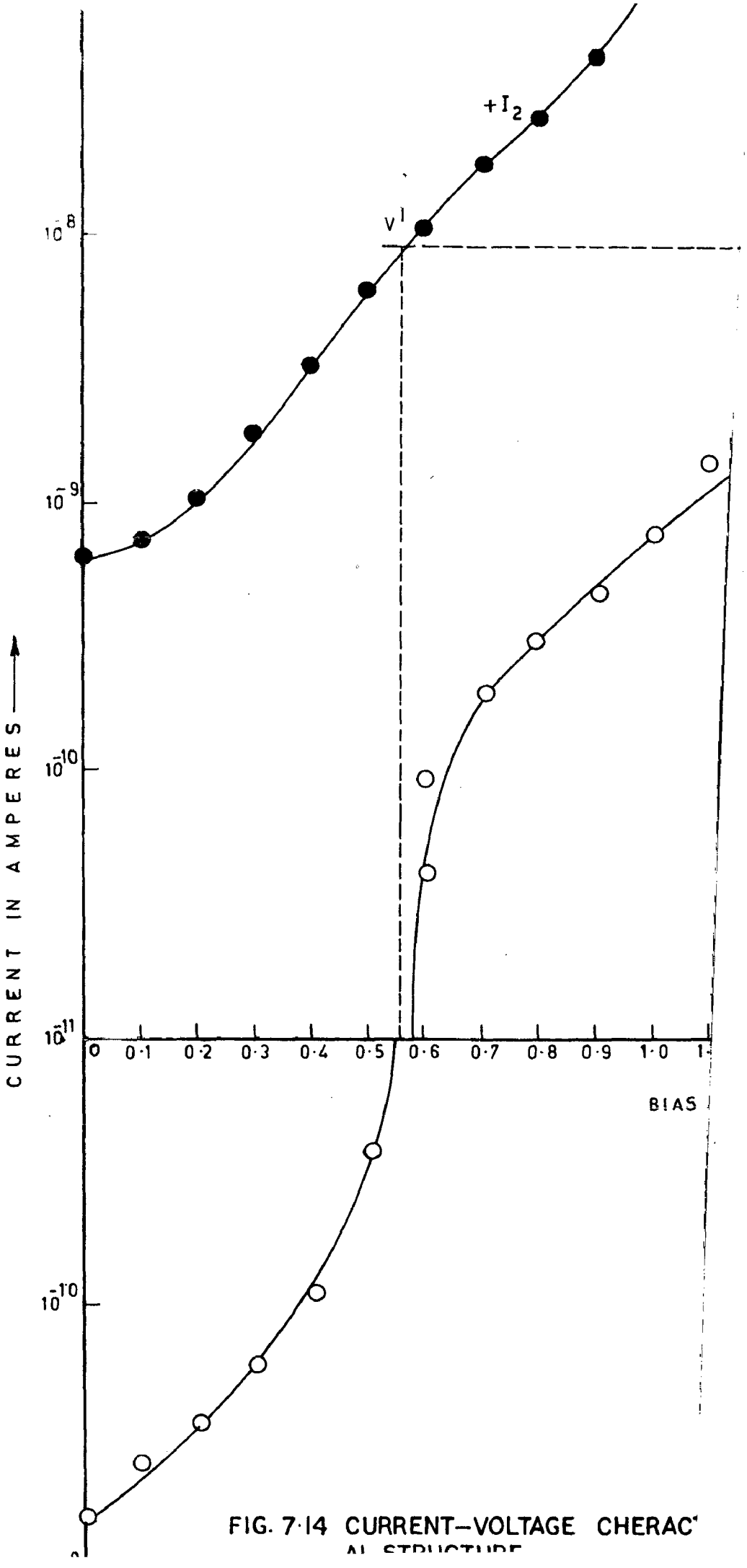

FIG. 7·14 CURRENT–VOLTAGE CHERAC'

(7.1 - 7.14) for both the polarities. As is evident from the curves the tunneling currents were in the range of 10^{-11} - 10^{-7} amperes. When aluminium is positively biased, the current in each curve increases with increasing voltage. At a certain value of voltage (which is different for different structures) the current becomes unstable and starts increasing as a function of time. For the case when the aluminium is negatively biased the current changes sign at a certain value of voltage. (This voltage is different for different structures). At higher voltages the current again becomes unstable and increases as a function of time. The point at which the current becomes unstable and increases as a function of time has been taken to be the breakdown point which characterizes the breakdown voltage. The point of instability of current, in each curve, differs for the two polarities and this indicates an internal voltage. The value of internal voltage is half of the difference of those voltages at which the currents become unstable.

(ii) Zero Current Method.

By an inspection of each curve (Fig.7.1 - 7.14) it is evident that the value of this internal voltage agrees quite well with the voltage at which the current changes its sign. Therefore the voltage at which the

current changes its sign is equal to the internal voltage.

(iii) Equal Magnitude Current Method

By inspecting at two voltages V^{I} and V^{II} in each curve (Fig. 7.1 - 7.14) for the same magnitude of current it is observed that the difference $V^{II}-V^{I}$ is very close to twice the internal voltage. This is expected since the internal voltage tends to enhance the current in one direction and restricts it in the other direction. From the above observations (i), (ii) and (iii) we are convinced that an internal voltage exists in each structure.

(iv) Direct Voltage Measurement

The internal voltage for the above samples was also measured directly with a high impedence ($\sim 10^{15}\Omega$) electrometer amplifier used as a voltage measuring device and its value was found to be in good agreement with those measured by other procedures (i), (ii) and (iii). A comparision of the values of internal voltage for different structures obtained by the above procedures is shown in Table 3. This procedure is much faster and more accurate as described in the chapter VI, Sec.6 d. Therefore, for the study of internal voltage this direct measurement method has been utilized.

7.1 b. Thickness dependence of Internal Voltage.

The values of Internal voltage have been measured

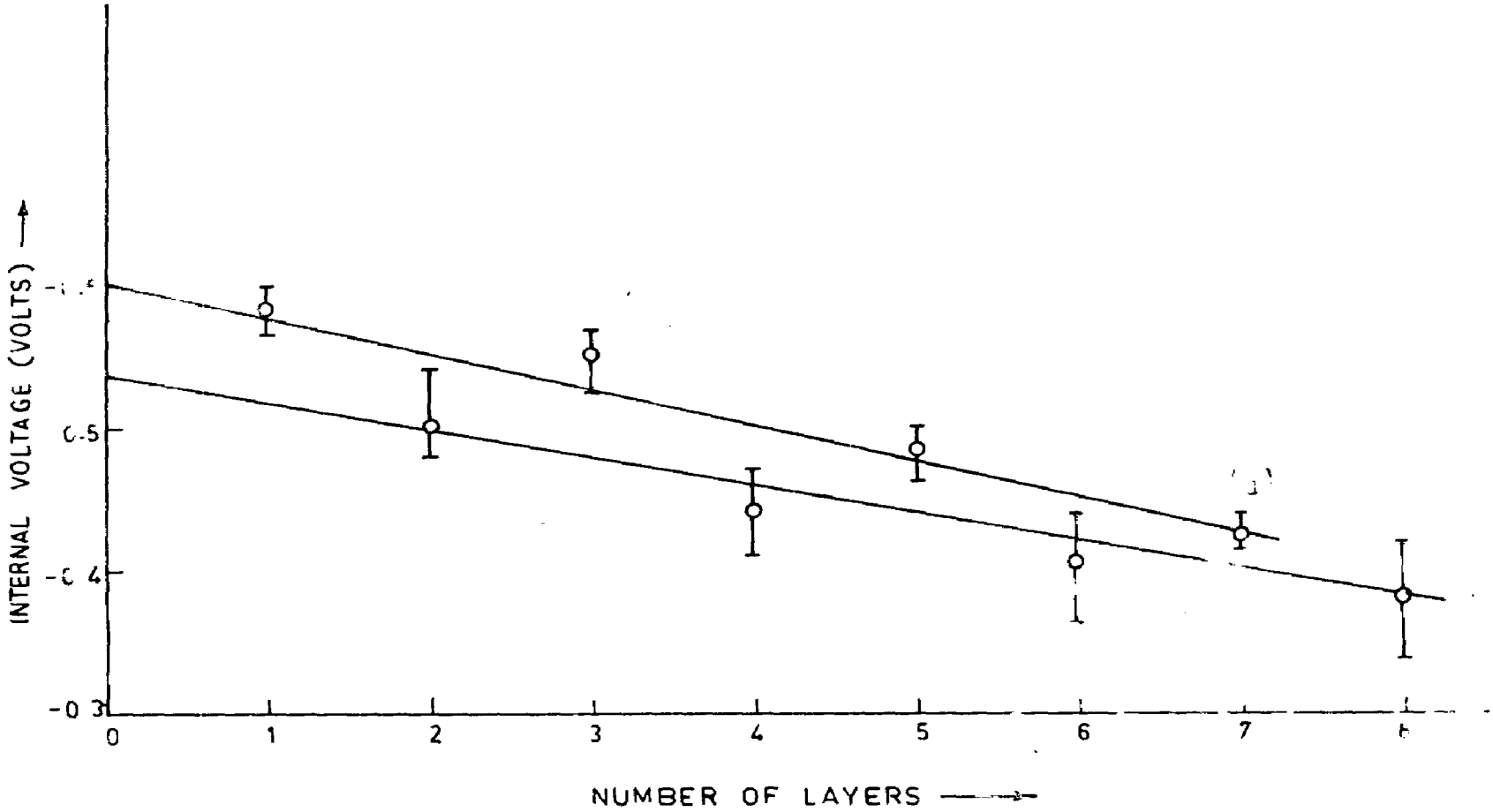

FIG 7·15 INTERNAL-VOLTAGE V_s NUMBER OF MONOLAYERS FOR Al-BARIUM STEARATE-Ag STRUCTURE

(a) FOR ODD NUMBER OF LAYER
(b) FOR EVEN NUMBER OF LAYER

(Polarity of Ag: positive)

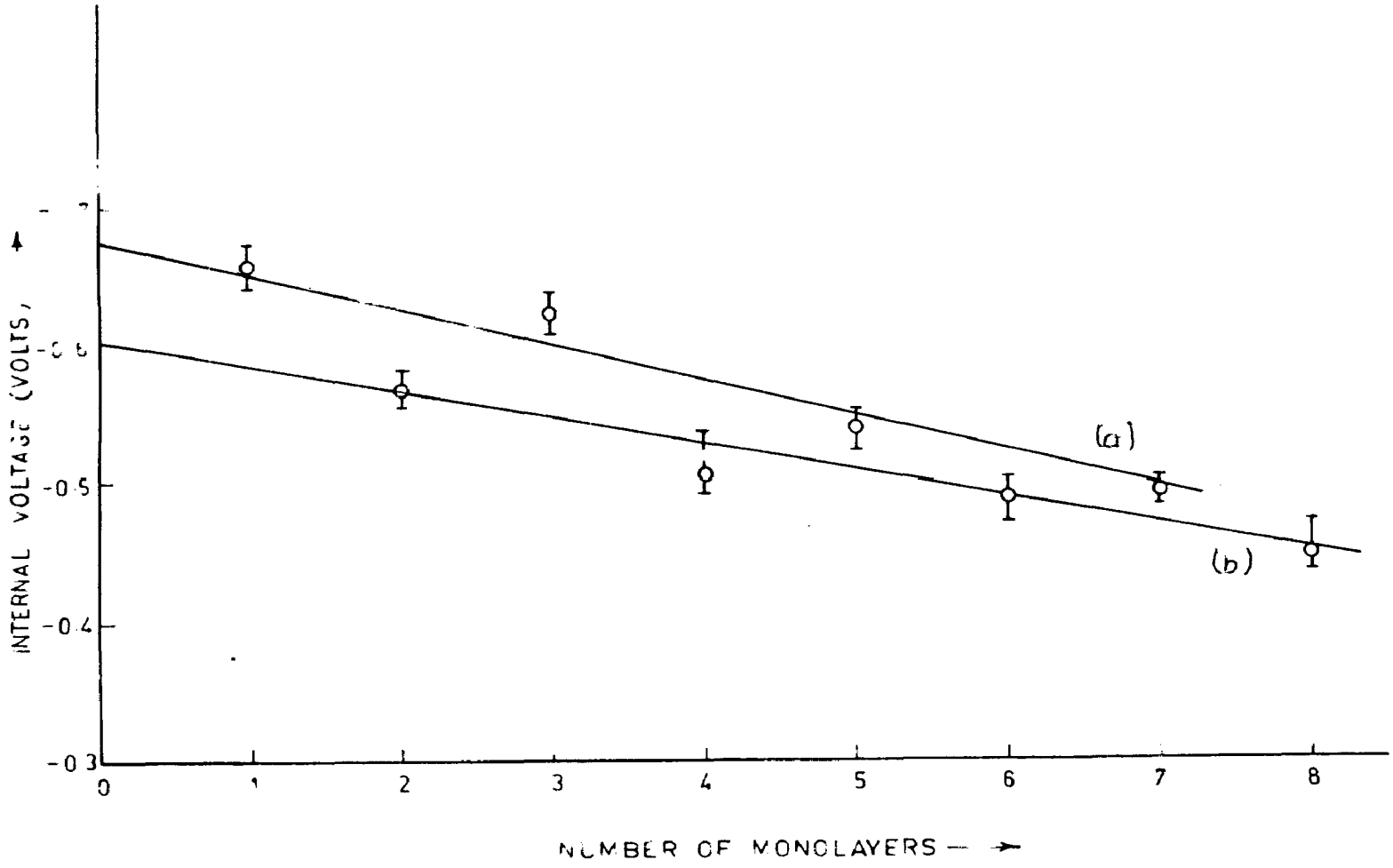

FIG. 7·16 INTERNAL VOLTAGE Vs NUMBER OF MONOLAYERS FOR Al–BARIUM STEARATE–Sn STRUCTURE
(a) FOR ODD NUMBER OF LAYERS
(b) FOR EVEN NUMBER OF LAYERS
(Polarity of Sn: positive)

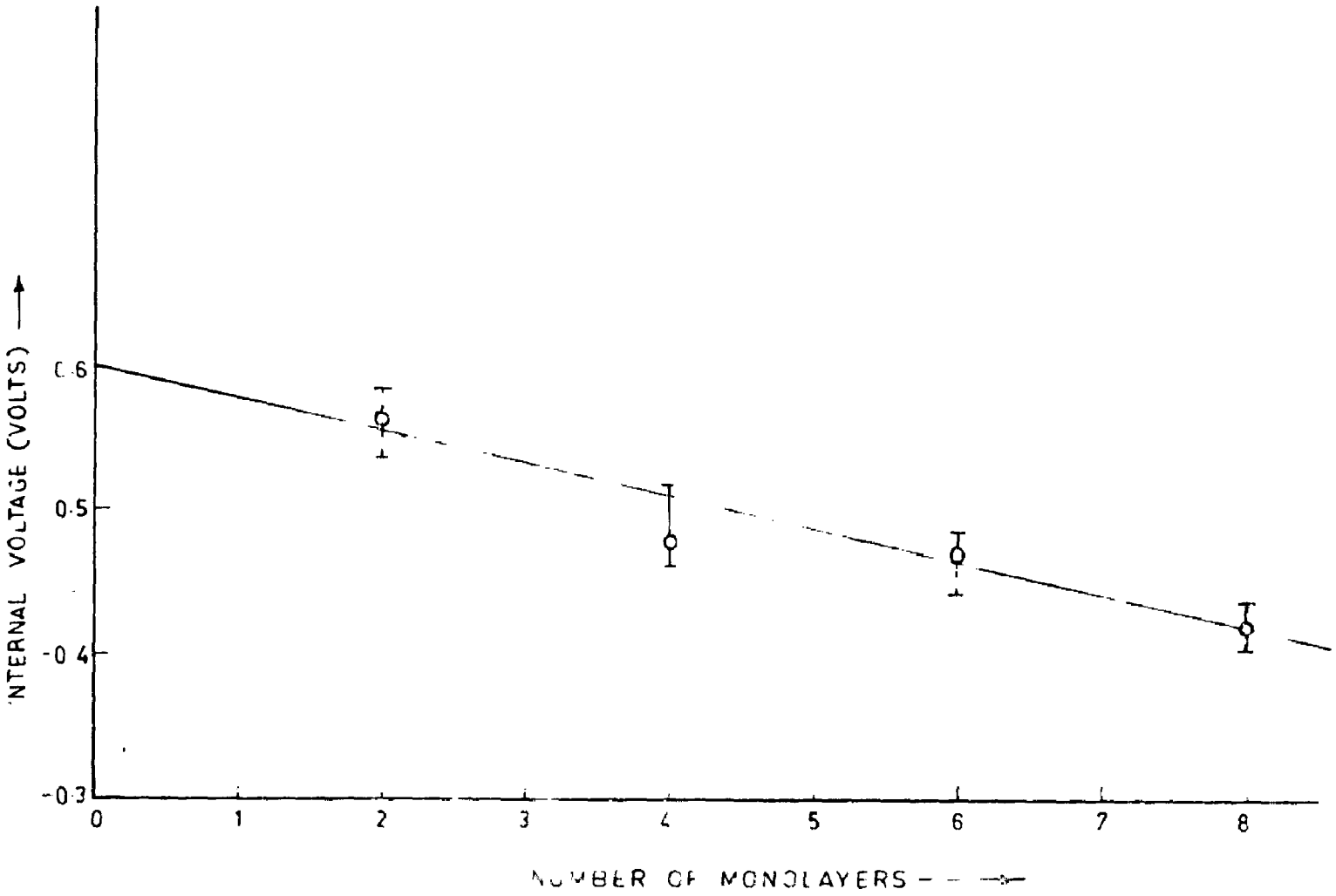

FIG. 7·17 INTERNAL-VOLTAGE Vs NUMBER OF MONOLAYERS FOR Al-BARIUM PALMITATE-Sn STRUCTURE

(Polarity of Sn: positive)

directly for different thicknesses of the various structures Al - O - M, where O refers to the organic film and M represents different metal electrodes used. The thickness of the organic film varies from 1 to 8 monolayers ($\sim$25 Å to $\sim$200 Å). Figures 7.15 to 7.23 show the plots of internal voltage versus thickness for the various structures. Figures 7.15 and 7.16 drawn for the various structures Al - Ba stearate - Ag and Al - Ba stearate-Sn show two curves each, the curve 'a' for odd number of monolayers and the curve 'b' for even number of layers. These curves demonstrate the difference in the behaviour of odd and even number of layers. The other figures 7.17 - 7.23 have been drawn for even number of organic layers. The scatter of the experimental data about the mean values of a number of observations has been shown in all the graphs by vertical bars. To determine the scatter, a number of observations have been taken for the same thickness of different test samples of the same substance. The dots in the experimental plots correspond to the mean values of a number of observations under similar conditions. The curves shown are the best fit curves about these points.

As is clear from these figures, the internal voltage decreases linearly with increasing thickness of the organic film. Each curve has been extrapolated to zero thickness for the purpose which will be discussed in a later section (Sec. 7.2). The intrinsic fields in the Langmuir films have been calculated for each thickness

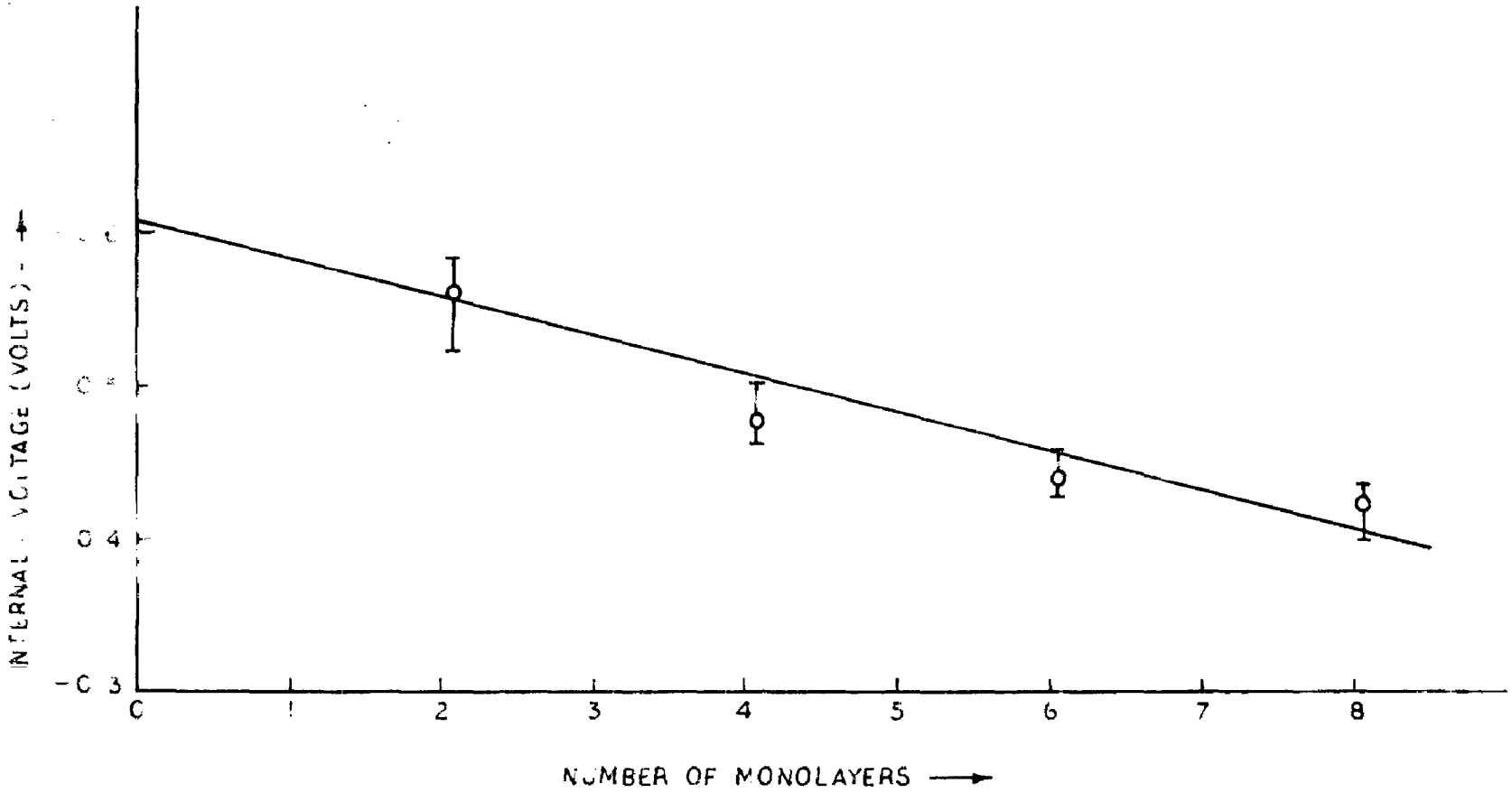

FIG 7·18 INTERNAL VOLTAGE Vs NUMBER OF MONOLAYERS FOR Al-BARIUM MARGARATE-Sn STRUCTURE

(Polarity of Sn: positive)

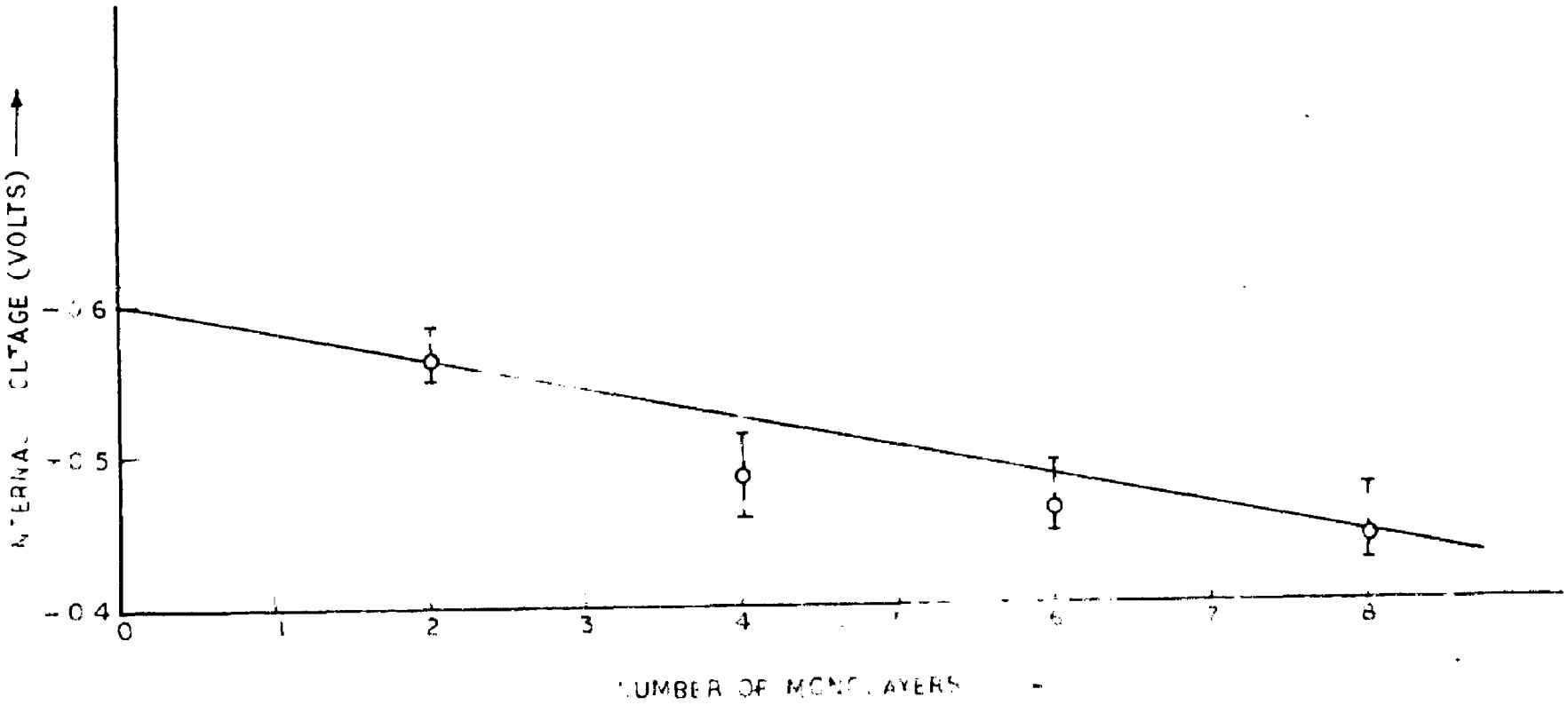

FIG. 7.19 INTERNAL VOLTAGE Vs NUMBER OF MONOLAYERS FOR Al-STEARIC ACID-Sn STRUCTURE

(Polarity of Sn: positive)

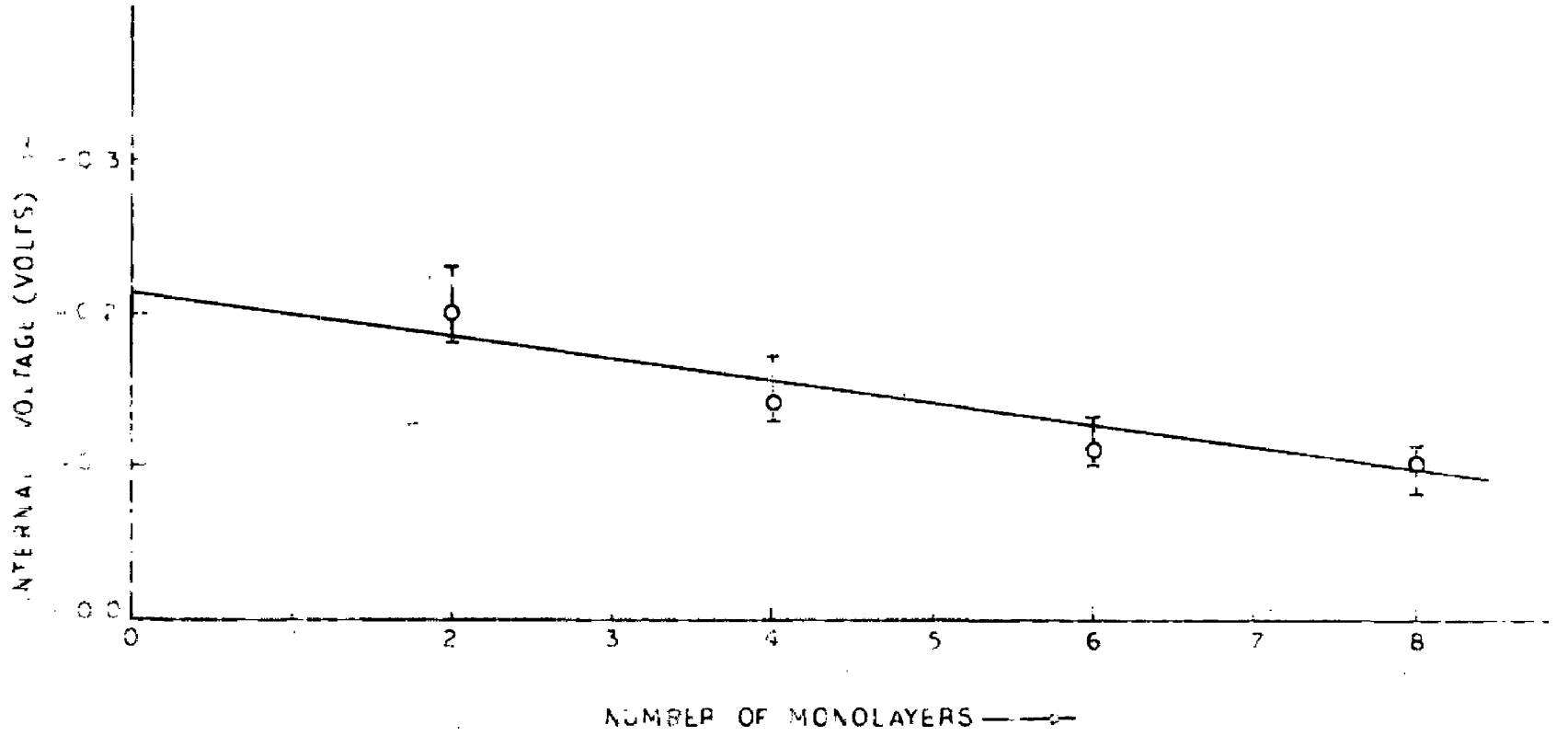

FIG. 7·20 INTERNAL VOLTAGE Vs NUMBER OF MONOLAYERS FOR Al-BARIUM STEARATE-Pb STRUCTURE

(Polarity of Pb: positive)

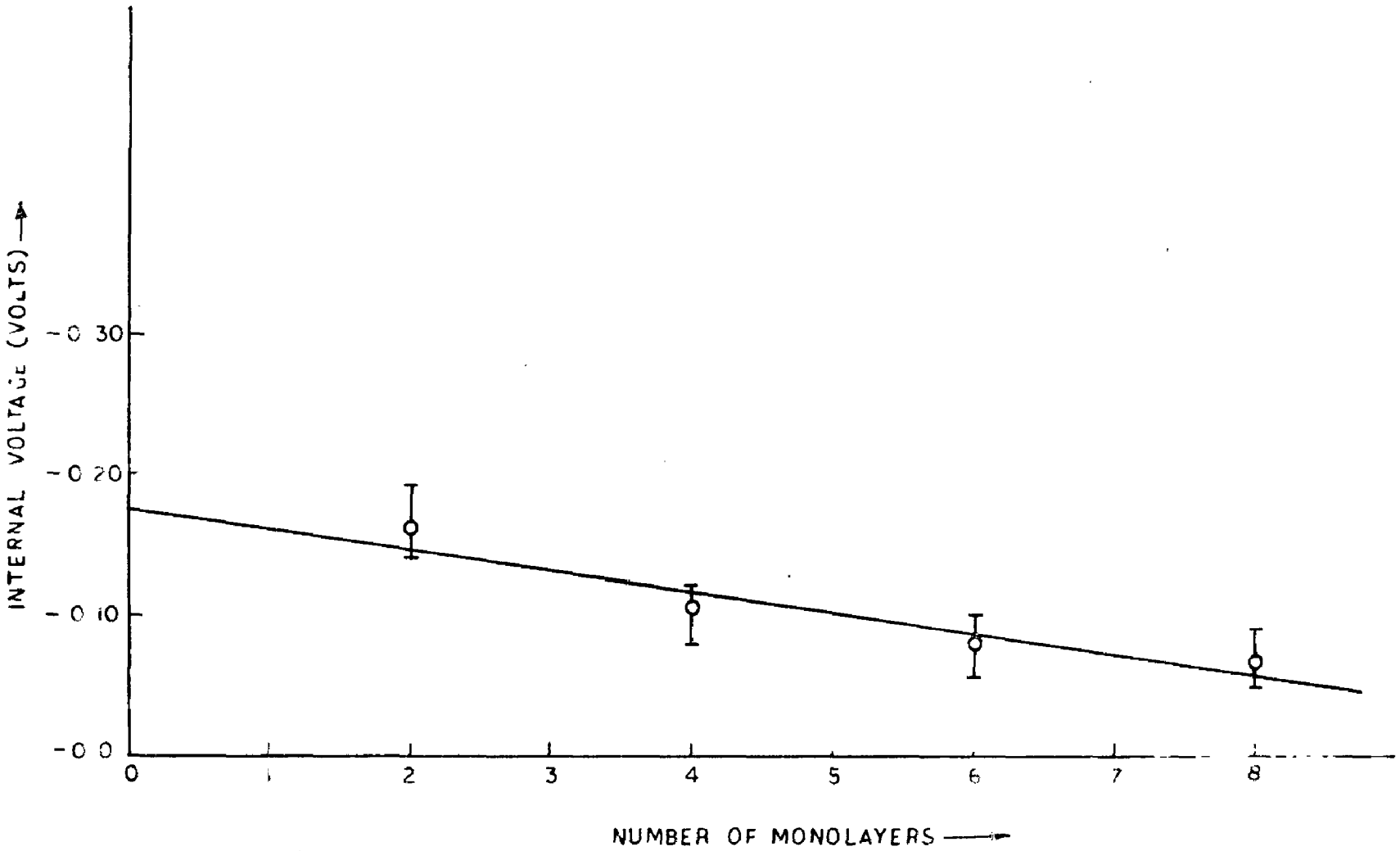

FIG. 7 21 INTERNAL VOLTAGE Vs NUMBER OF MONOLAYERS FOR Al-BARIUM STEARATE-Bi STRUCTURE

(Polarity of Bi: positive)

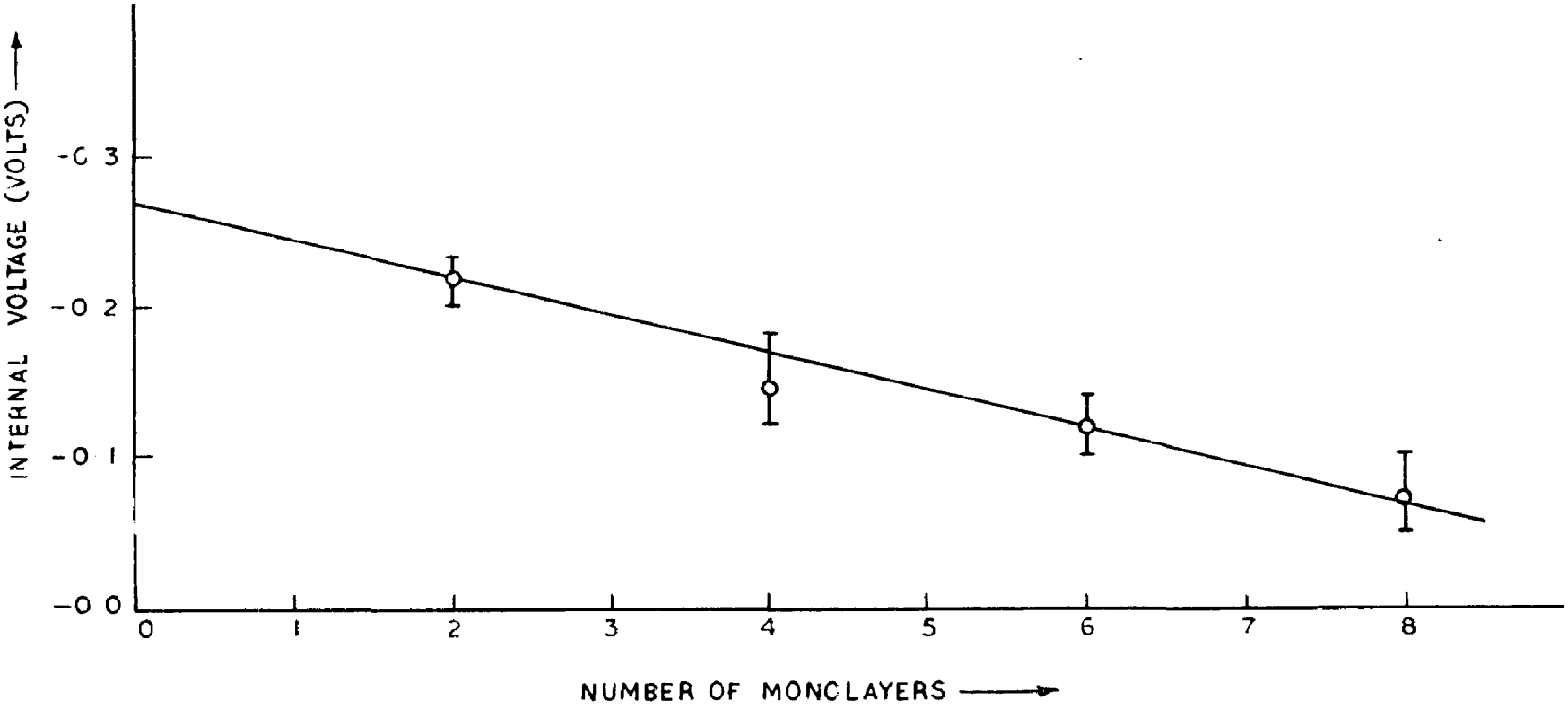

FIG. 7·22 INTERNAL VOLTAGE Vs NUMBER OF MONOLAYERS FOR Al-BARIUM STEARATE-Te STRUCTURE

(Polarity of Te: positive)

by dividing the mean value of internal voltage by thick-ness. Attempts were made to study the capacitors with Au, Cu and Be as one of the electrodes. However, these electrodes shorted presumably because the gold, copper and berryleum slowly diffuse into the insulating film. The results have been summarized in Table 4. The discussion of the results will be given in section 7.2.

7.1 c. Diode Characteristics of Metal-Insulator-Metal Structure.

Figures 7.24 - 7.37 show the current voltage characteristics for various Al - O - M structures on a linear scale. It is evident from all these figures that the different sandwich structures, composed of dissimilar metal electrodes on the two sides of Langmuir film behave like a diode. The working inverse voltage (WIV) is different for different combinations of electrode materials. For a particular thickness of the dielectric, the working inverse voltage is maximum for Al - O - Sn structure. Also it is evident that for a particular structure the working inverse volgage is maximum for a monolayer. The maximum dc forward current is of the order of nano-amperes. Table 5 summarizes the results found on different diode structures. The discussion of these diode characteristics will be given in sec. 7.2.

7.1 d. Measurement of Work Function of Different Metals and Study of Their Thickness Dependence.

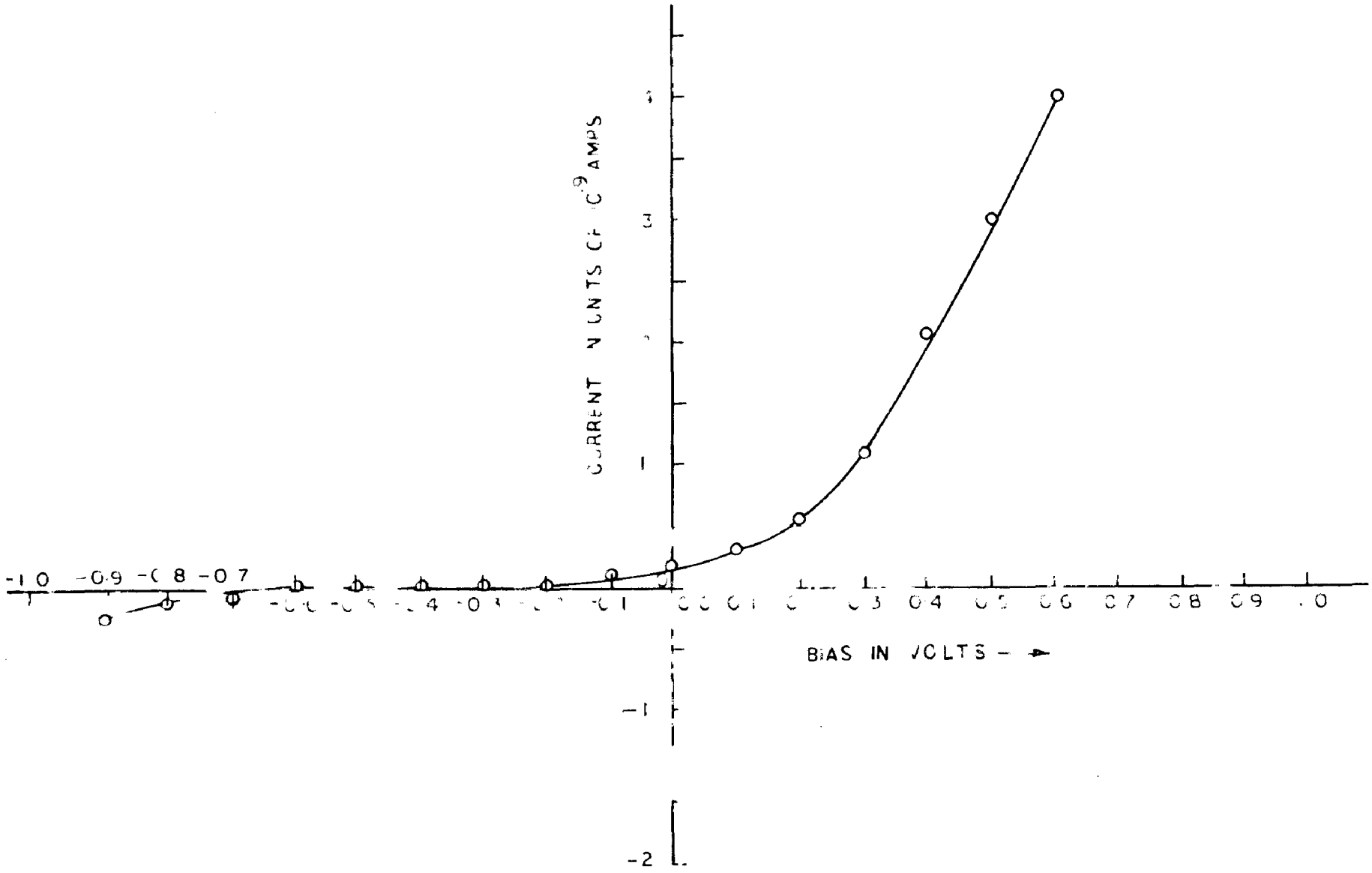

FIG. 7·24 DIODE CHARACTERISTICS OF Al-BARIUM STEARATE (1 LAYER)-Sn STRUCTURE

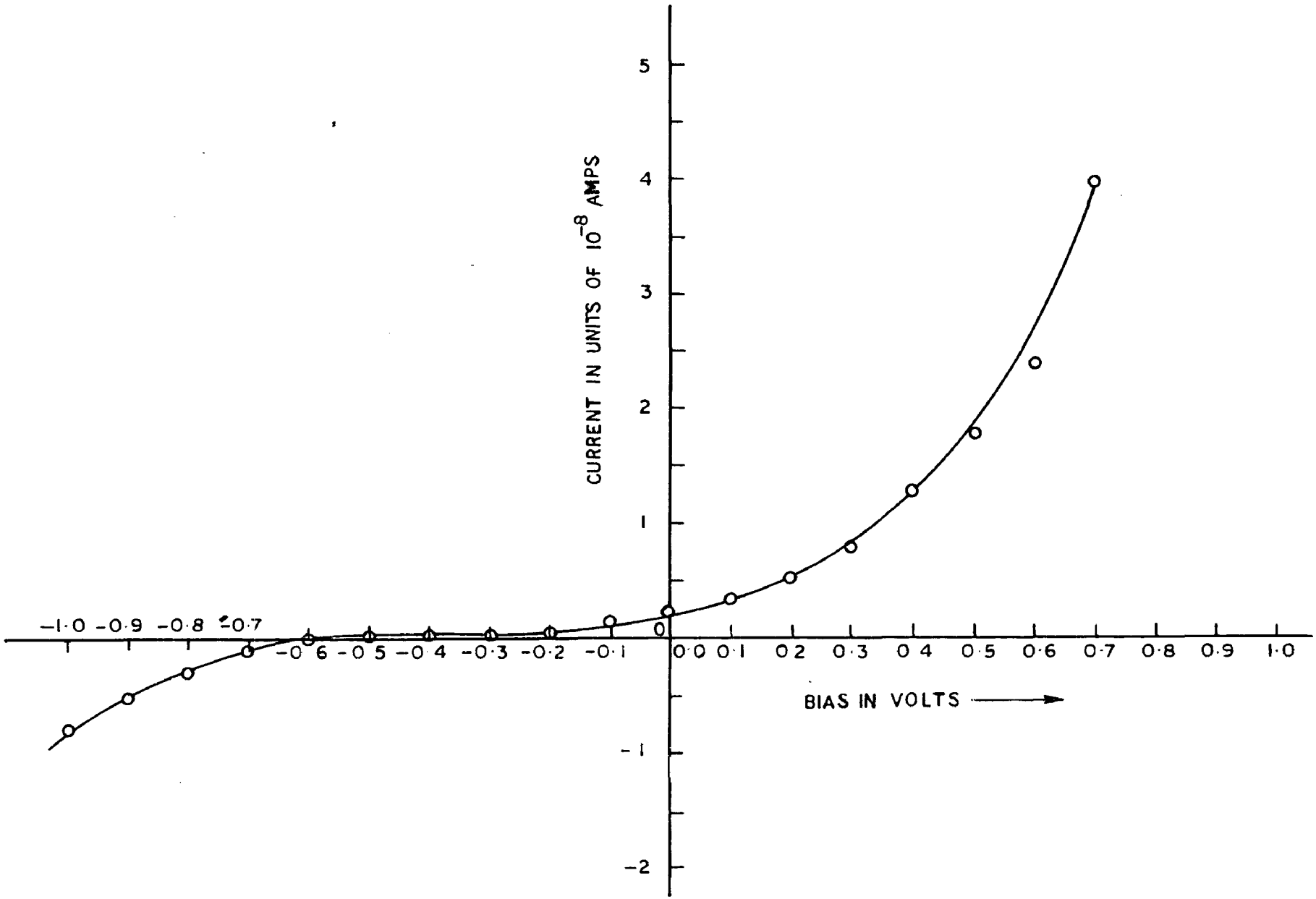

FIG. 7·25 DIODE CHARACTERISTICS OF Al–BARIUM STEARATE (3 LAYER)–Sn STRUCTURE

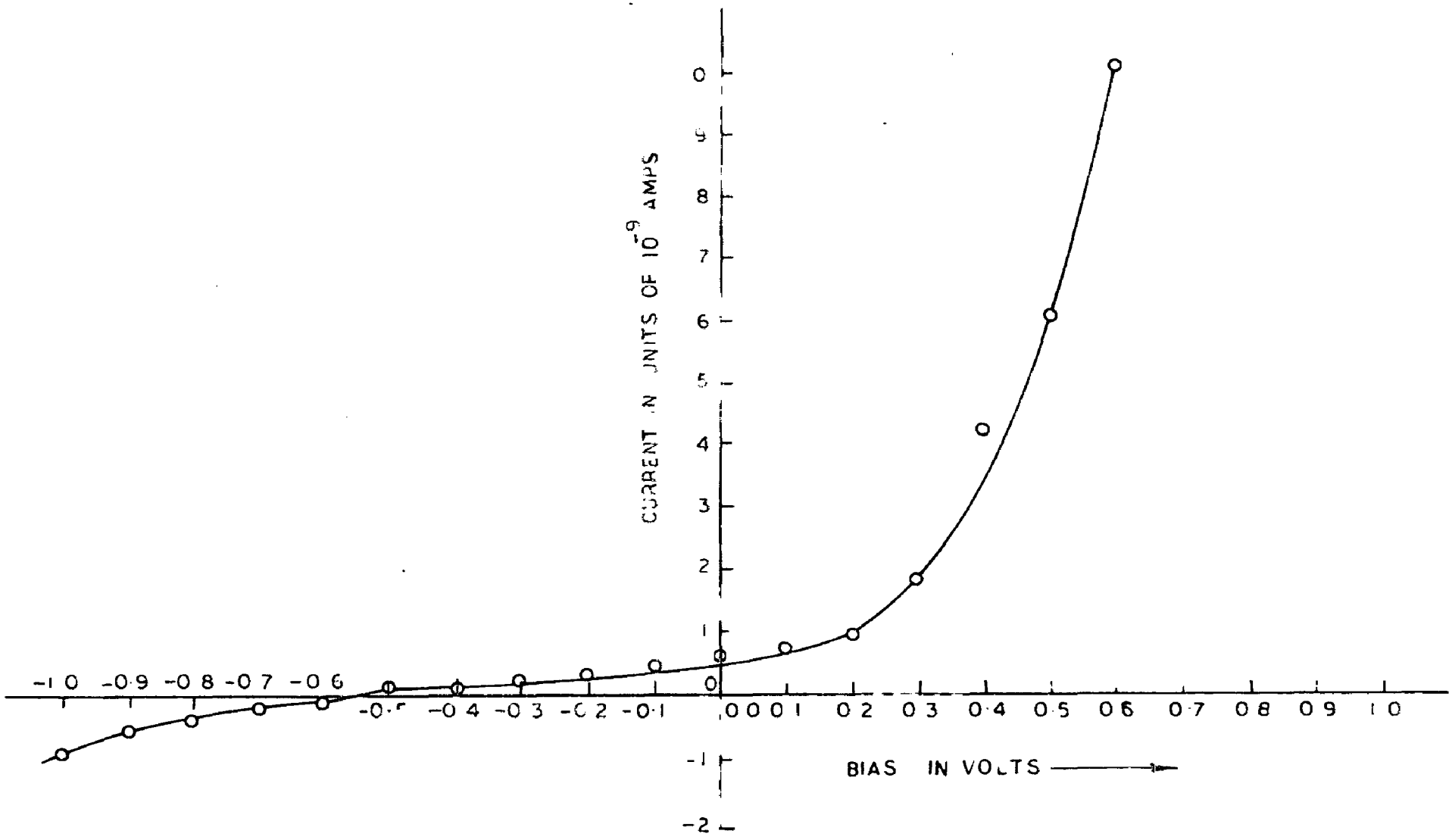

FIG. 7·26 DIODE CHARACTERISTICS OF Al-BARIUM STEARATE (2 LAYER)-Sn STRUCTURE

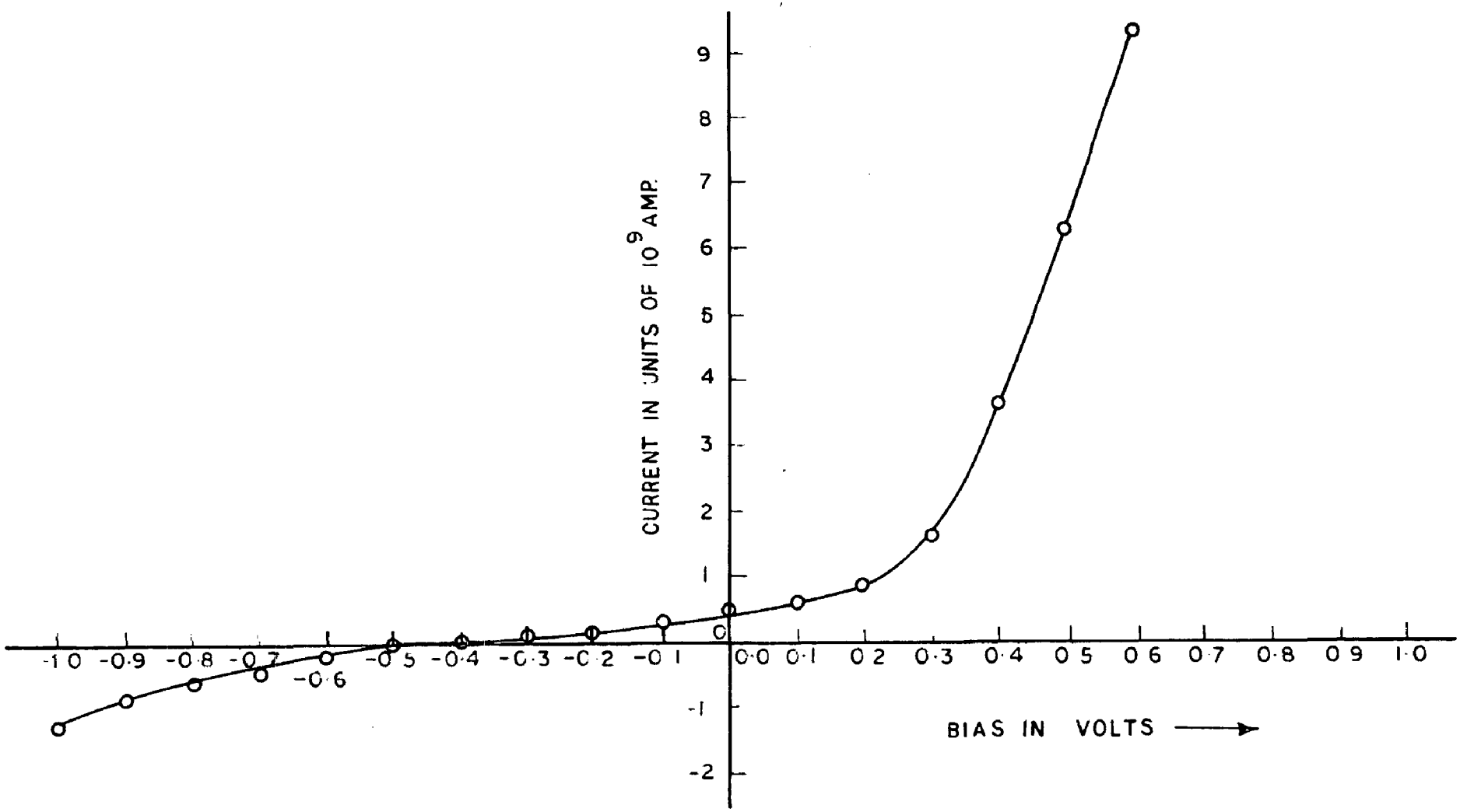

FIG. 7·27 DIODE CHARACTERISTICS OF Al–BARIUM STEARATE (4 LAYER)-Sn STRUCTURE

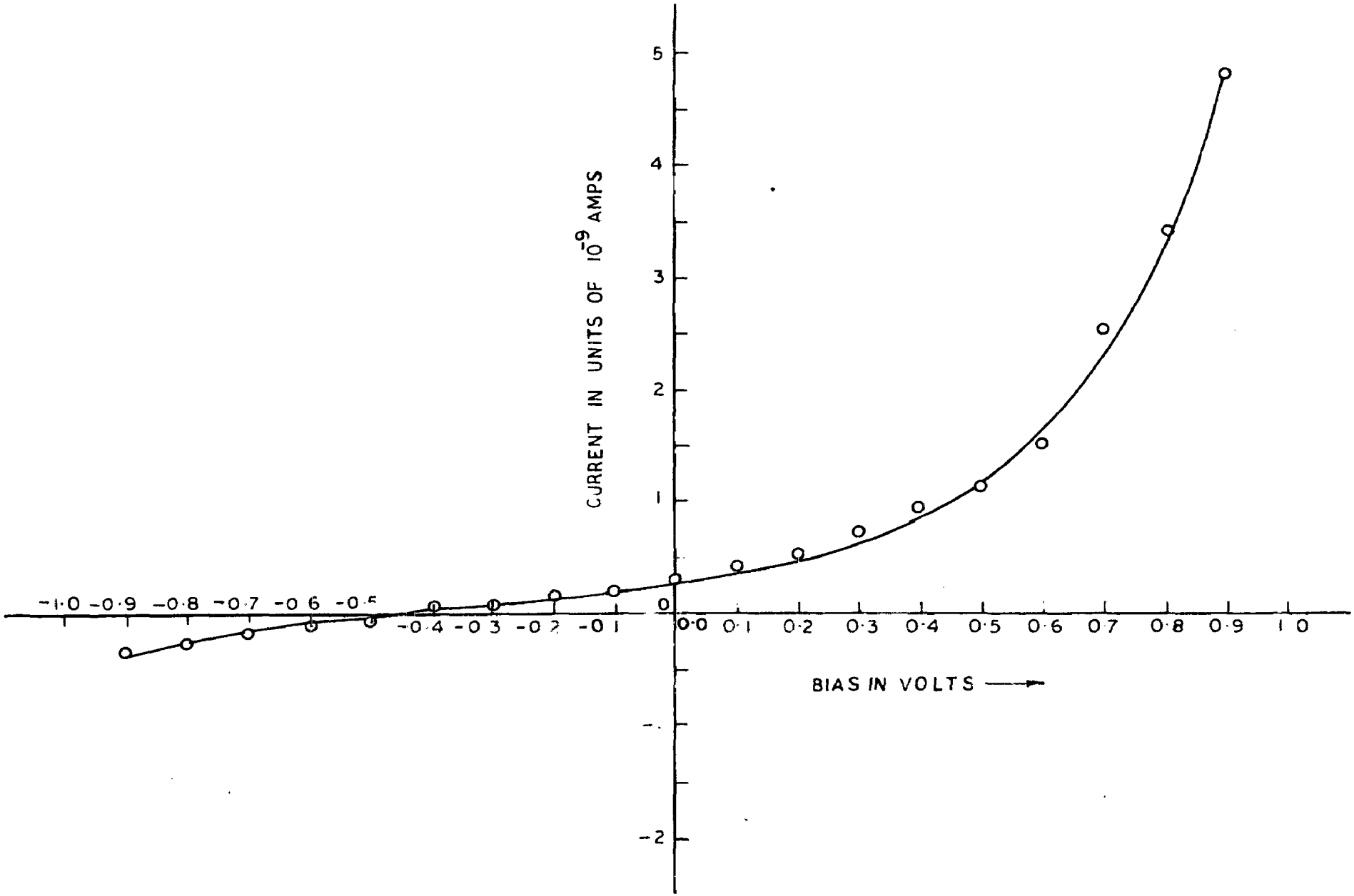

FIG. 7·28 DIODE CHARACTERISTICS OF Al-BARIUM STEARATE (6 LAYER)-Sn STRUCTURE

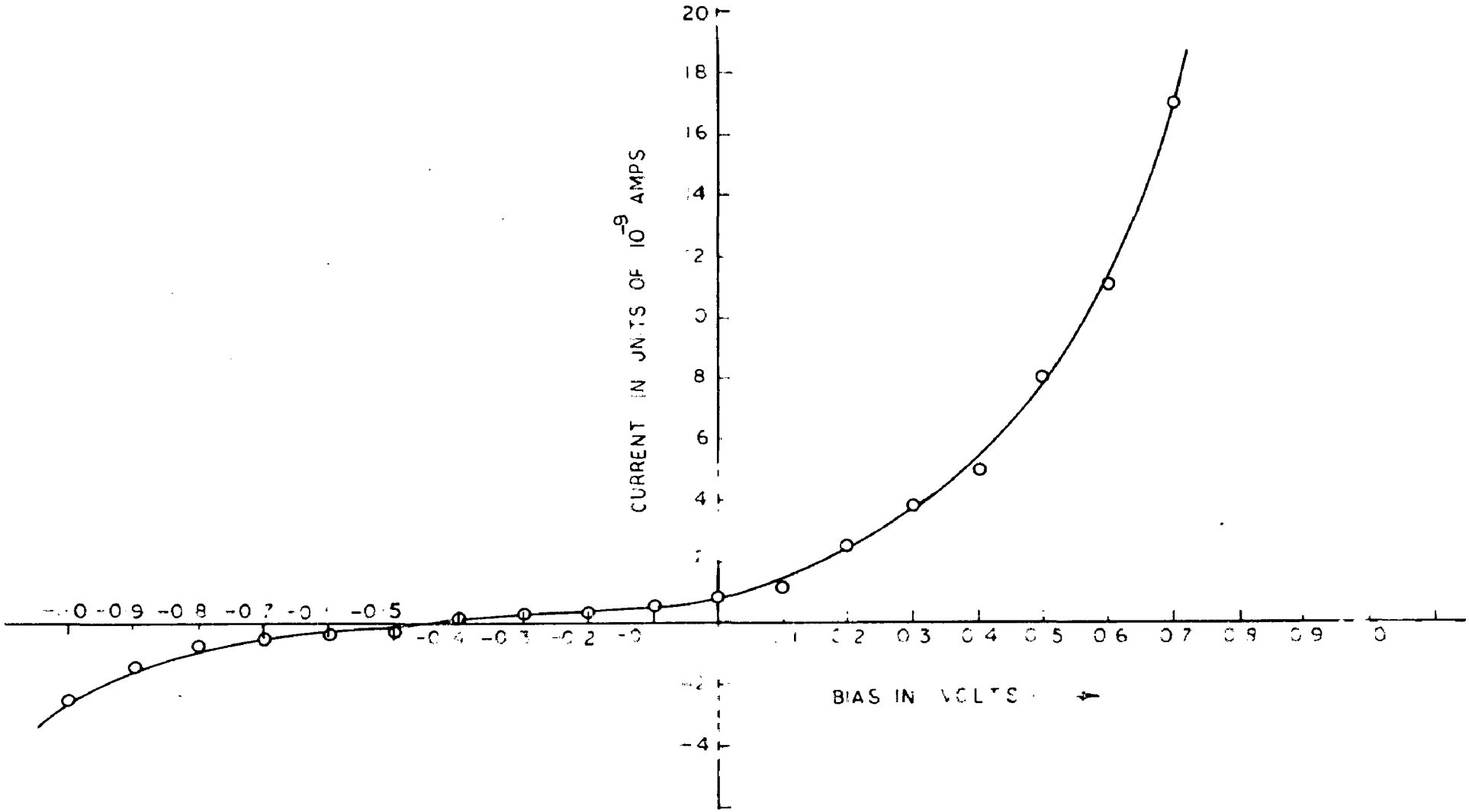

FIG. 7·29 DIODE CHARACTERISTICS OF Al-BARIUM STEARATE (8 LAYER)-Sn STRUCTURE

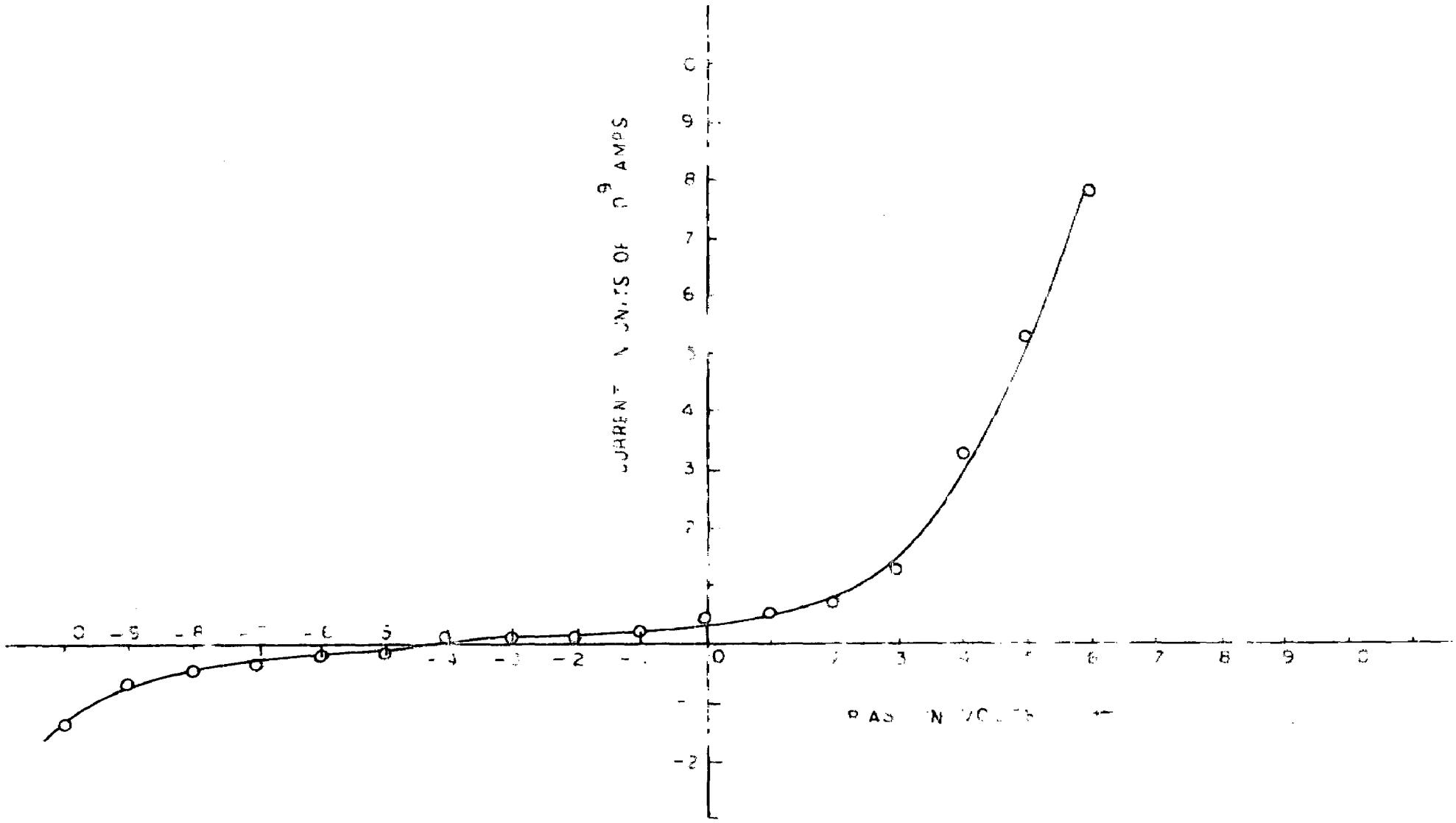

FIG. 7.30 DIODE CHARACTERISTICS OF Al-BARIUM PALMITATE (4 LAYER)-Sn STRUCTURE

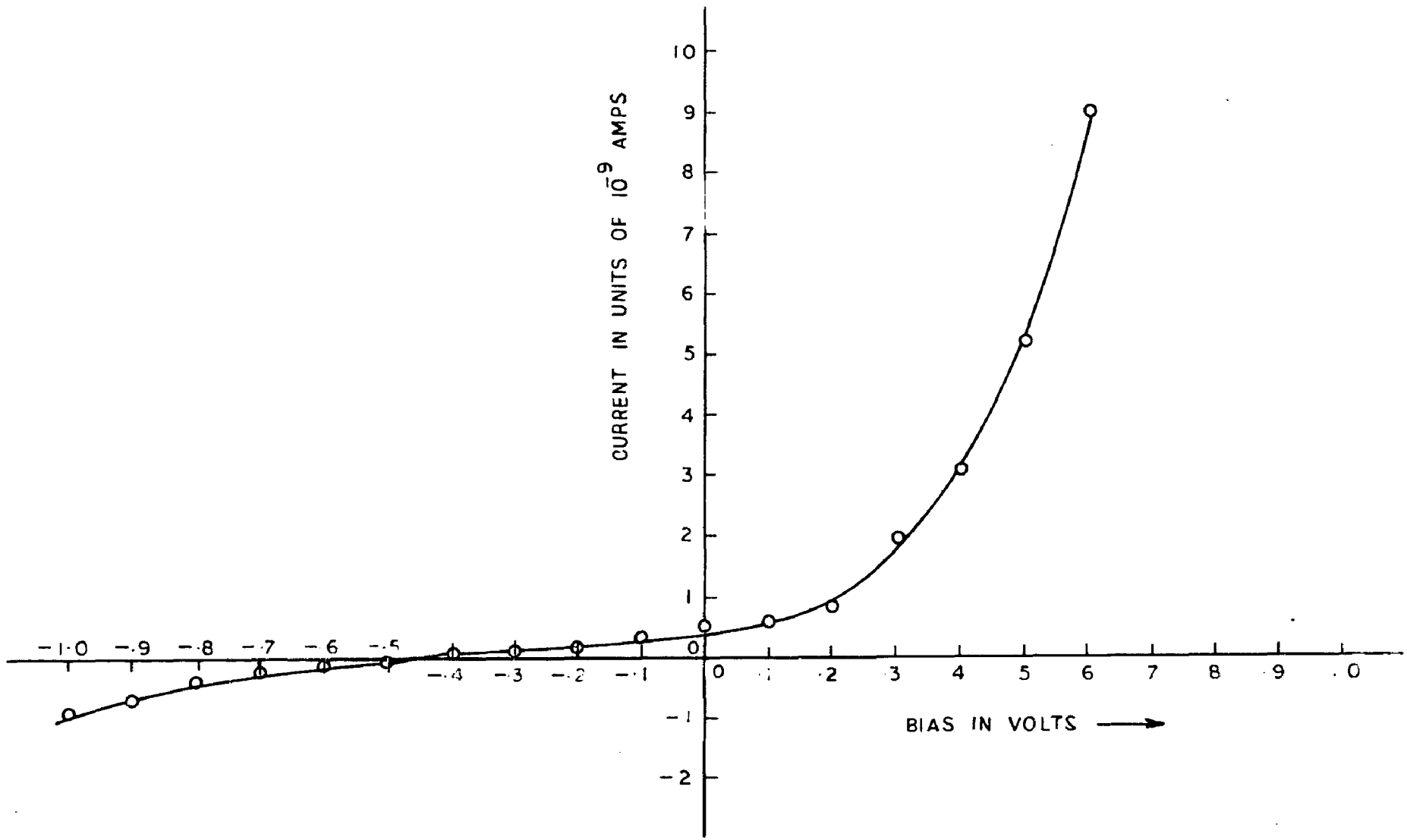

FIG. 7·31 DIODE CHARACTERISTICS OF Al-BARIUM MARGARATE (4 LAYER)-Sn STRUCTURE

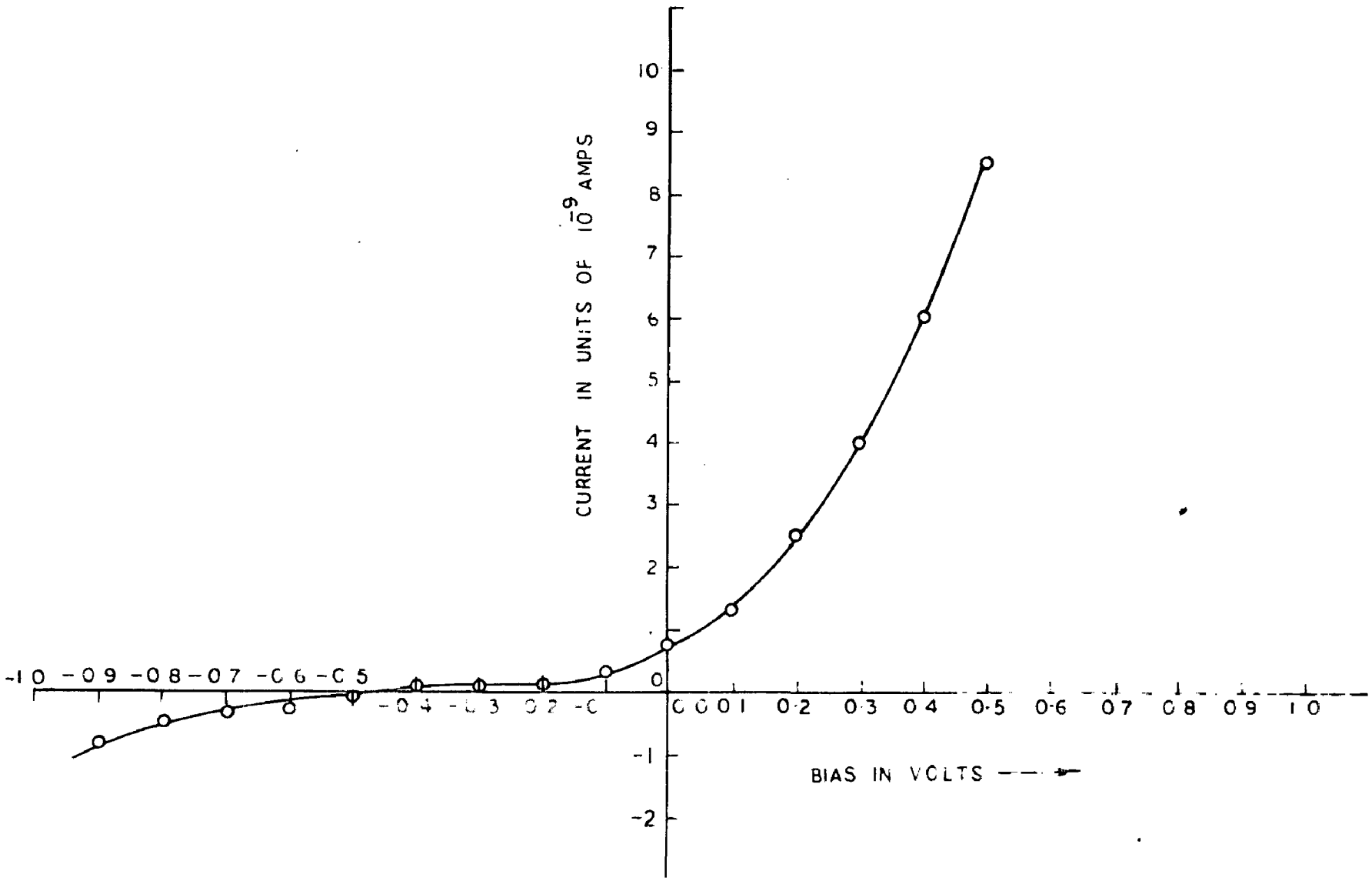

FIG. 7·32 DIODE CHARACTERISTICS OF Al-STEARIC ACID (4 LAYER)-Sn STRUCTURE

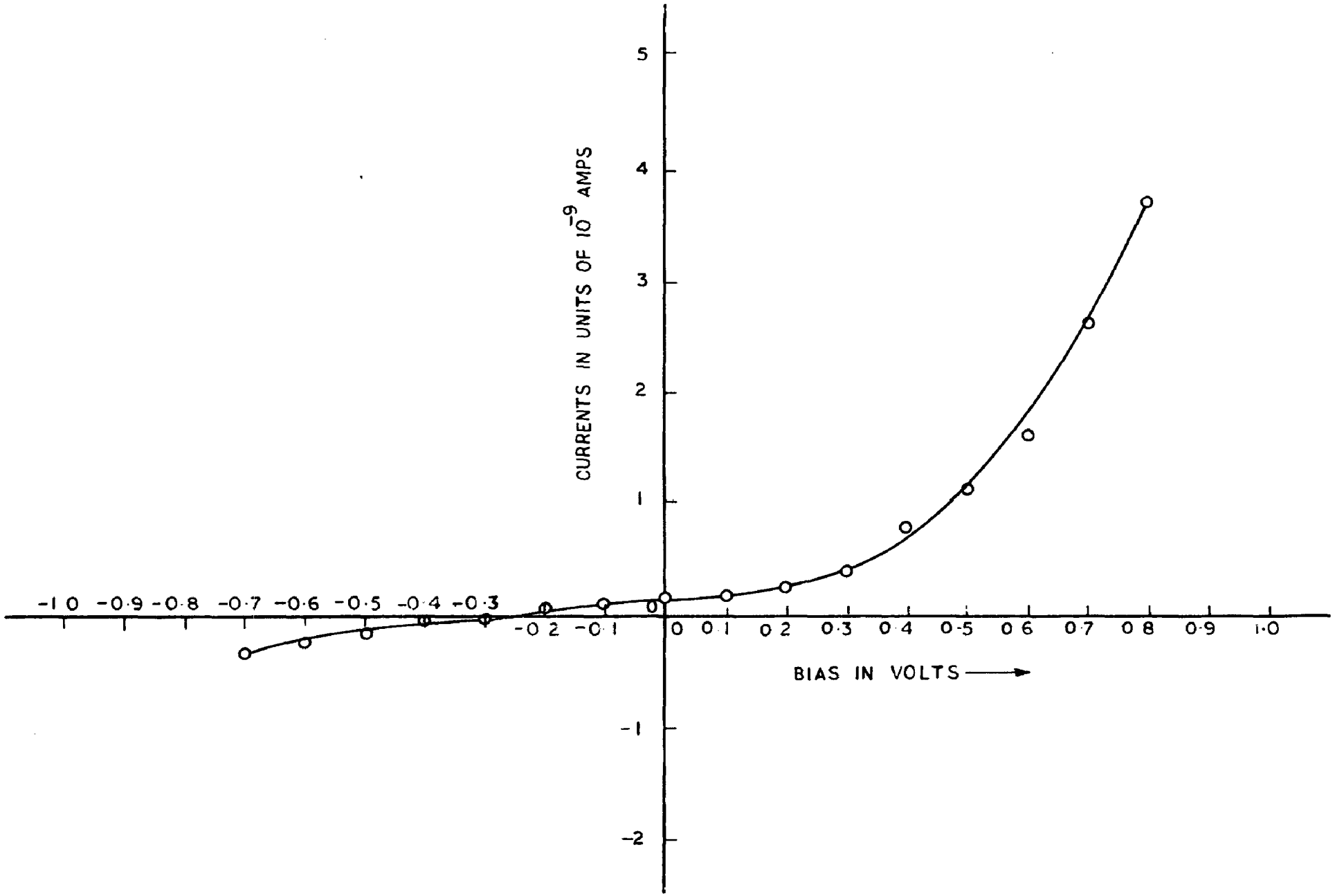

FIG. 7·33 DIODE CHARACTERISTICS OF Al-BARIUM STEARATE (2 LAYER) - Pb STRUCTURE

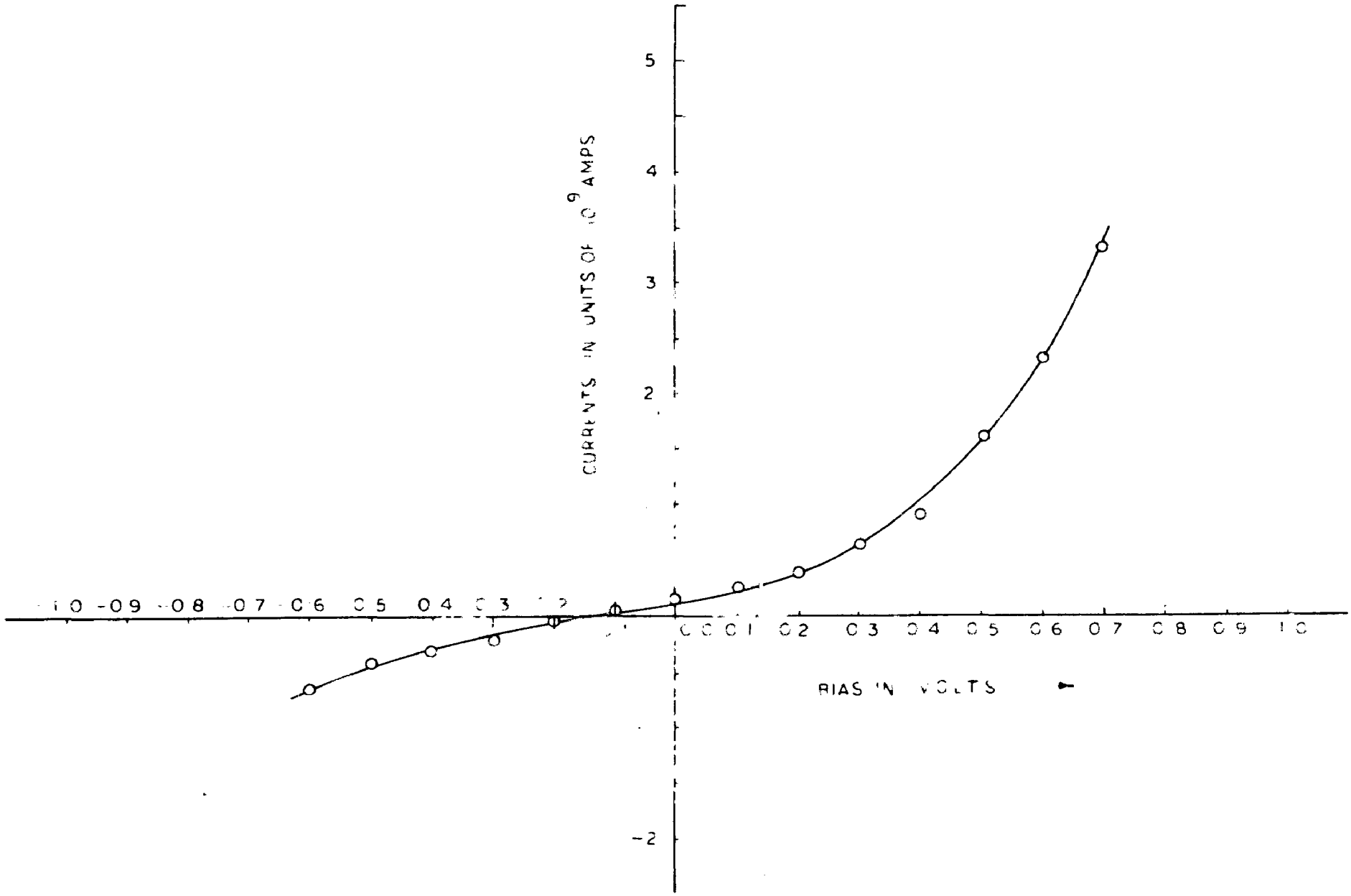

FIG. 7.34 DIODE CHARACTERISTICS OF Al-BARIUM STEARATE (2 LAYER)-Bi STRUCTURE

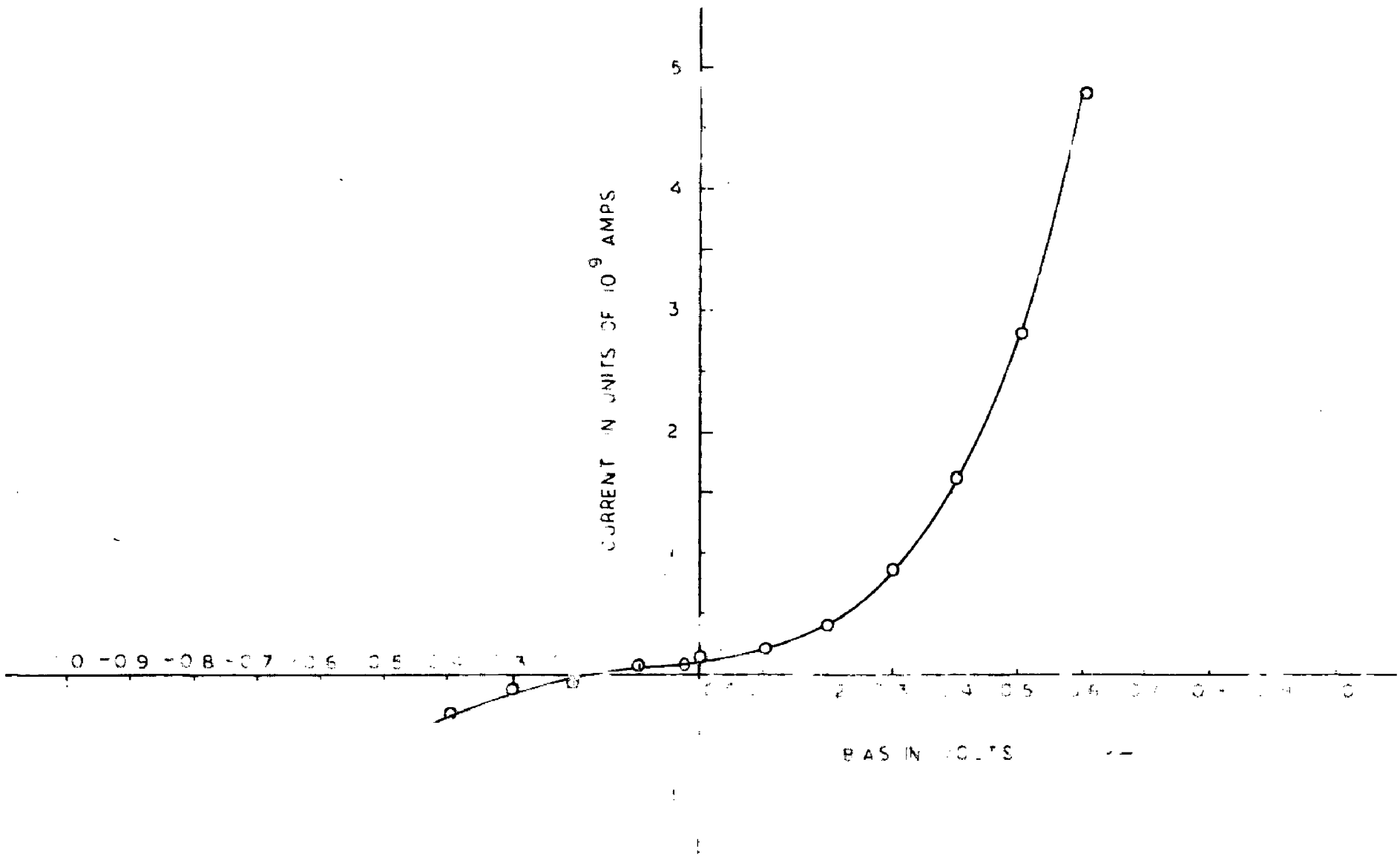

FIG. 7-35 DIODE CHARACTERISTICS OF Al-BARIUM STEARATE (4 LAYER) -To STRUCTURE

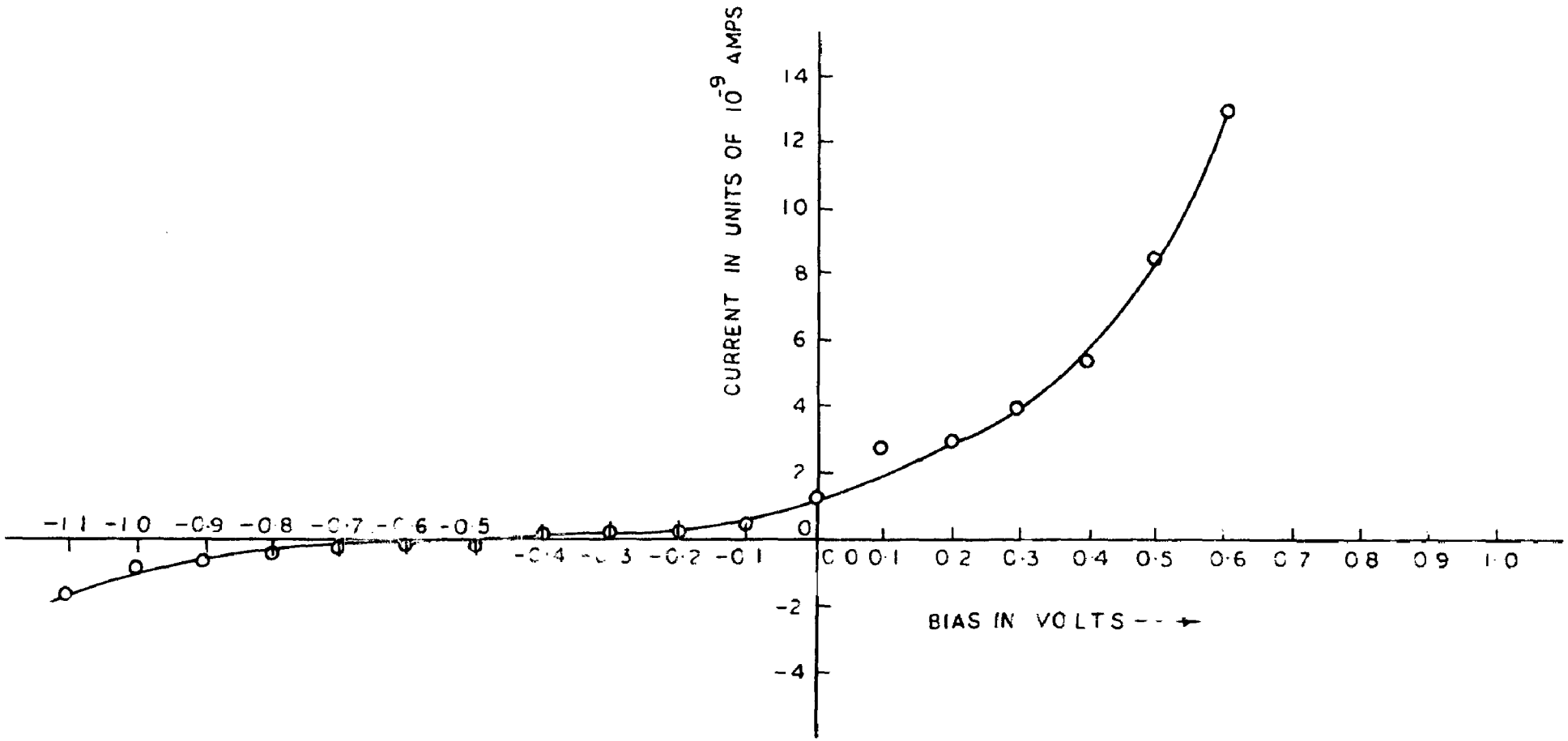

FIG. 7·36 DIODE CHARACTERISTICS OF Al–BARIUM STEARATE (2 LAYER)-Ag STRUCTURE

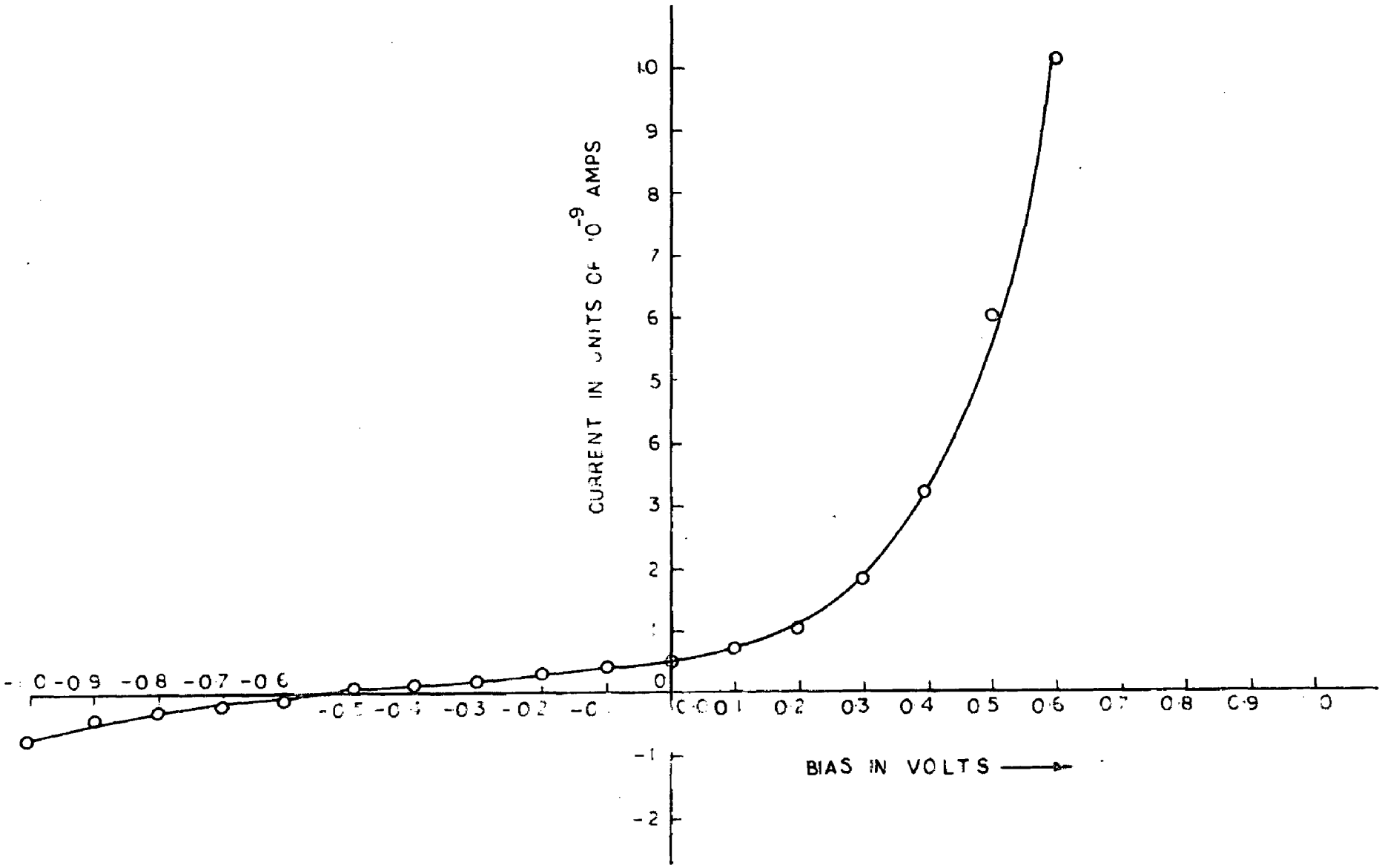

FIG. 7·37 DIODE CHARACTERISTICS OF Sn-BARIUM STEARATE (2 LAYER) - Al STRUCTURE

The difference in the work function of aluminium with other metals has been measured by extrapolating the internal voltage curve to zero thickness. The extrapolated value at zero thickness should give the real difference in work functions of two metals. Taking Al as reference metal and considering its value of work function to be 4.08 eV the work functions of other metals under study viz Sn, Ag, Te, Bi, Pb have been ealculated. The results are summarized in Table 6.

Dependence of the work function of metal film on the thickness on the metal has also been studied. The thickness of the metal film was measured by an electronic Film Thickness Monitor. Experiments were made on tin films in the thickness range 390 Å - 1025 Å. The work function has been found to be independent of the tin film thickness in the thickness range studied.

(e) Time Dependence of Internal Voltage: Decay and Recovery Characteristics.

Observations have also been made on the time dependence of the internal voltage in MIM structure which can also be called a dielectric cell. It has been observed that the internal voltage decreases slowly when discharged in a closed circuit through a very high resistance ($\sim 10^{15}\Omega$). Figure 7.38 shows the discharing of Al-Barium stearate (one layer) - Sn dielectric cell in a closed

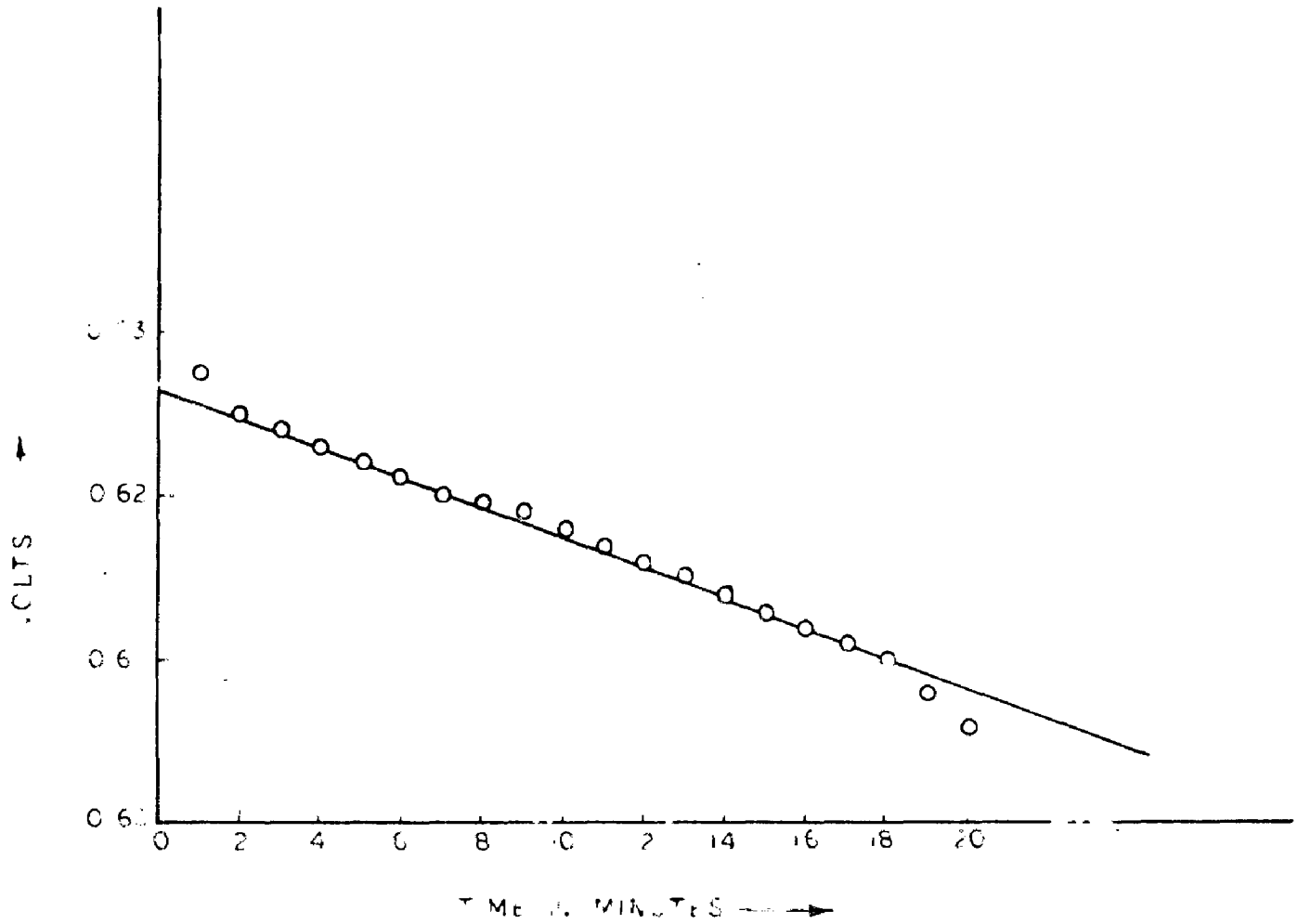

FIG. 7-38 DECAY OF DIELECTRIC CELL (ONE LAYER Al-BARIUM STEARATE-Sn STRUCTURE) IN CLOSED CIRCUIT.

circuit. If the dielectric cell is partially discharged by connecting its terminals to a low resistance and then left in open circuit it shows a subsequent voltage recovery. Figure 7.39 shows the charging of Al - Ba - Stearate (one layer) - Sn dielectric cell in open circuit.

7.2 DISCUSSION: Interpretation of Results.

All the results obtained above in various subsections a,b,c,d and e of section 7.1 will be discussed systematically and in detail below.

Figures 7.1 - 7.14 drawn for tunneling current versus voltage show the existence of internal fields inside the Langmuir-films when sandwiched between dissimilar electrodes. The detailed discussion of all these curves 7.1 - 7.14 has already been given in sec. 7.1a.

Figures 7.15 - 7.23 drawn for internal voltage versus thickness of the dielectric film show that the internal voltage decreases linearly with increasing number of monolayers. In all the structures taken under investigation the lower aluminium electrode always has a tendency to form a very thin oxide layer on it. Therefore the actual structure is Al - Al_2O_3 - O - M. The aluminium oxide layer could have given some contribution to the internal voltage but since the same values of internal voltage (with reverse signs) have been found in the

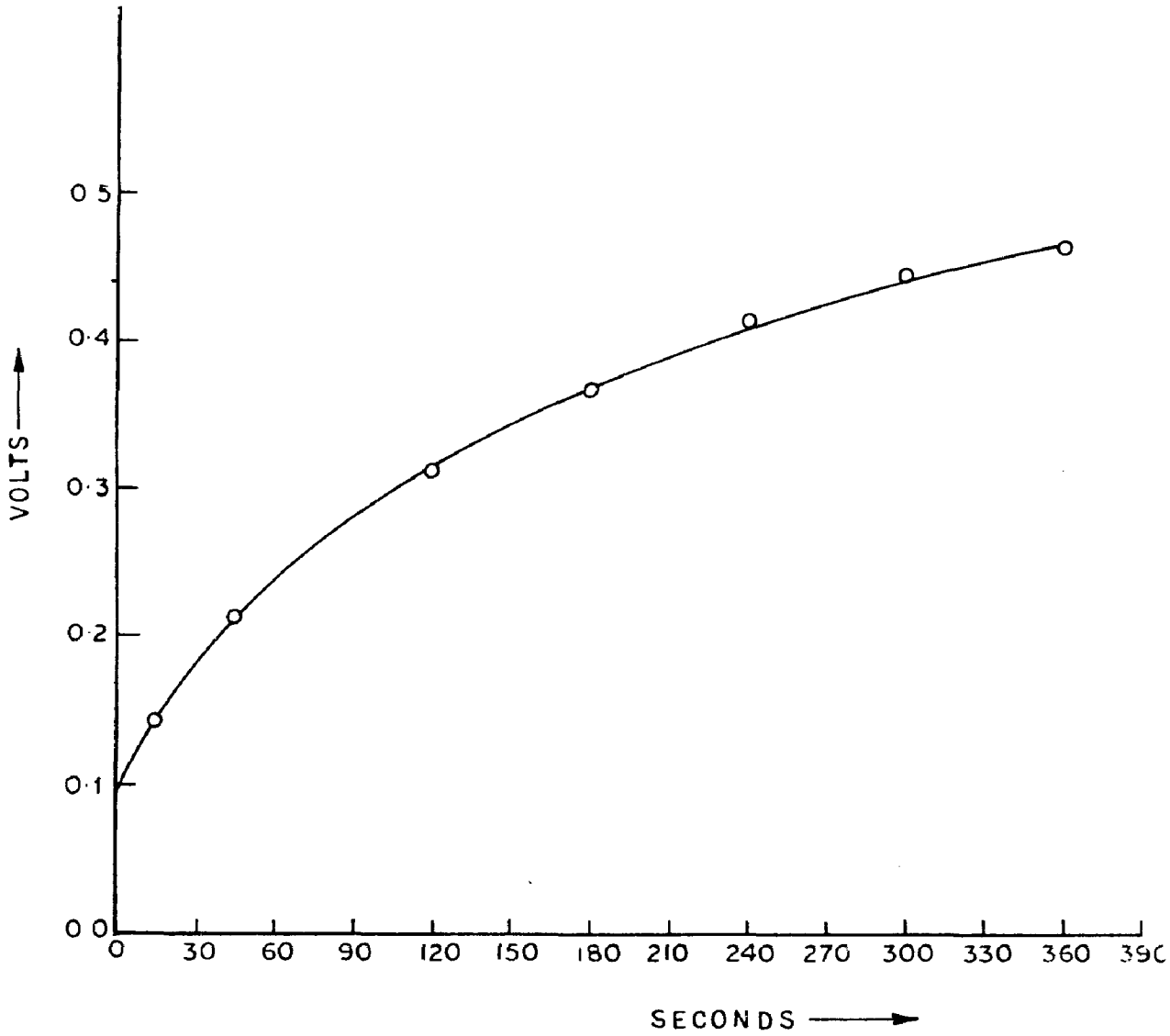

FIG. 7·39 RECOVERY OF DIELECTRIC CELL IN OPEN CIRCUIT

two different configurations Al - O - Sn and Sn - O - Al as shown in figures 7.16 and 7.23, it can be concluded that the oxide layer does not give any contribution to the internal voltage. A further discussion on these naturally grown Al_2O_3 films will be given in the next chapter. However, gold was also tried as the electrode material in order to minimize this oxide formation but the samples were found shorted. This is in agreement with Handy and Scala's work (110).

From figures 7.15 and 7.16, which have been drawn for the structures Al - Ba stearate - Ag and Al - Ba stearate-Sn and which have two curves each one for the odd number of monolayers and the other for the even number of monolayers, it is evident that the odd and even number of layers behave in different fashion. The curves for odd and even number of layers for the figures 7.15 and 7.16 can be empirically represented by the following equations:

For fig. 7.15 (a)

$$V_o = 0.025\, n_o - 0.60 \qquad .. (7.1)$$

and for Fig. 7.15 (b)

$$V_e = 0.02\, n_e - 0.54 \qquad .. (7.2)$$

For fig. 7.16 (a)

$$V_o' = 0.026\, n_o' - 0.67 \qquad .. (7.3)$$

and for Fig. 7.16 (b)

$$V_e' = 0.020n_e' - 0.60 \qquad \text{.. (7.4)}$$

where V_o and V_o' refers to internal voltage for odd number of monolayers.

V_e and V_e' refer to the internal voltage for even number of monolayers.

n_o and n_o' represent the odd number of barium stearate monolayers.

n_e and n_e' represent the even number of barium stearate monolayers.

From figures 7.15 and 7.16 as well as from equations 7.1, 7.2 and 7.3,7.4, the larger voltage observed for the case of odd monolayers is very significant. Figures 7.40(a and b) show the structure of Y type film containing odd and even number of monolayers. From the figure 7.40(a)it is clear that odd number of layer films have one unpaired molecular layer of the dipolar molecules. From figure 7.40(b)it is evident that for a film having even number of layers there are no unpaired dipolar layers and therefore in such a film the molecules of the insulating barrier do not contribute to the polarization effects and therefore to the internal voltage. The curves 7.15 and 7.16, therefore, directly indicate that the internal voltage is related to unpaired layers in the case of odd number of layers. Therefore this addi-

tional voltage is expected to come from the polarization existing in the unpaired layer in the dielectric. However, the voltage in the case of even number of layers results wholly from the difference in the work functions of the two metals due to the absence of the molecular polarization effects (difference in the work functions of aluminium and silver for figure 7.15 b and of aluminium and tin for figure 7.16 b). As deduced in earlier chapter II sec. 2.1, the internal voltage can be expressed in terms of work functions of the electrode as

$$\frac{\Delta V}{2} = \frac{\psi_{m_2} - \psi_{m_1}}{e} \qquad \ldots (7.5)$$

i.e. the internal voltage should be independent of the thickness of dielectric.

This analysis holds good if there are no trapped charges at one or the other of the metal insulator interfaces. If the number of such charges at this interface is m per unit area, then the field due to it is $\frac{em}{\epsilon_o k}$ where k and ϵ_o are dielectric constant of Barium stearate and permittivity of free space, and the potential difference between the electrodes due to this field is $\frac{emn\tau}{\epsilon_o k}$, where n refers to the number of monolayers and τ refers to thickness of a single barium stearate monolayer. Since the trapped charges are also somewhat mobile in the presence of the internal field, they

move in a direction so as to neutralize the internal field. This results in a decrease of the internal voltage inside the dielectric. Hence the observed voltage becomes

$$\frac{\Delta V}{2} = \frac{\Psi_{m_2} - \Psi_{m_1}}{e} - \frac{e\, mn\tau}{\epsilon_o k} \qquad .. (7.6)$$

This equation agrees with the observed behaviour as given in equation (7.2) and (7.4). Equation 7.6 does not agree with the observed behaviour as given in equation (7.1) and (7.3) for odd number of monolayers because an additional voltage term because of the polarization existing in unpaired layers has not been included.

The extrapolated values of voltages for zero dielectric thickness in figures 7.15b and 7.16b should give the difference of work functions of aluminium and silver and of aluminium and tin respectively. The observed polarities of aluminium-barium stearate - silver and aluminium-barium stearate - tin have been found to have aluminium as negative and silver and tin as positive electrodes. Therefore, the work function of silver is 0.53 volts higher than that of aluminium. Similarly the work function of tin is 0.60 volts higher than that of aluminium. By studying the polarity dependent breakdown voltage in a MIM structure with aluminium - aluminium oxide - tin, Simmons found the work function difference between aluminium and tin to be 0.34 volts (Simmons did not use silver). The present result is somewhat

different from that of Simmons', but as has already been seen, the observed internal voltage in our case is a function of the thickness of the insulator film. As can be seen from figures 7.15 and 7.16 as well as from equation (7.6), any increase in the value of the insulator thickness always gives a smaller value of the internal voltage The observed value of internal voltage in figures 7.15b and 7.16b is maximum for a two layer film. But this two layer film also contains some trapped charges and gives a smaller value of internal voltage than what is expected from the true difference of work functions of metals.

Therefore the observed thickness dependence internal voltage in our case, when extrapolated to zero thickness neutralizes the effect of any trapped charges and gives true difference of work functions of the two metals. Simmons' work was done at a fixed thickness and, therefore, the observed internal voltage may not be the true work function difference of aluminium and tin. The present method can be more useful for determination of the work function of metals as it does not involve any breakdown conditions and gives the required results directly. Also the method can be used for studies of any variation of the barrier heights with temperature at the metal-insulator interfaces. The interpretation of the remaining curves in the figures 7.15 - 7.23 with structures Al - Ba Palmitate - Sn, Al - Ba Margarate - Sn, Al - stearic acid - Sn, Al-B stearate - Pb, Al - Ba stearate - Bi, Al - Ba-

stearate - Te and Sn- Ba stearate - Al is essentially the same as described above for Al-Ba Stearate-Ag and Al-Ba Stearate-Sn. The results of internal voltage and intrinsic fields for all these structures have been summarized in Table 4.

Discussion of diode characteristics

Figures 7.24 - 7.37 show the plots of current versus voltage on some Al - O - M structures on a linear scale. It can be seen from several curves that each sandwich behaves like a diode structure. The fact that large intrinsic field exists inside a thin insulator film when sandwiched between dissimilar electrodes has been utilized here to make the metal-insulator-metal structure work as a diode. The working inverse voltage range for a particular Al - Ba stearate (1 layer) - Sn diode structure is about -0.6 volts (see fig. 7.24). The maximum dc forward current is of the order of few nanoamperes. The characteristics of the present diode structures can be understood by the following arguments (180) consider the case of Al - Ba stearate (1 layer) - Sn structure (fig.7.24). The dielectric is sandwiched between dissimilar electrodes, so there exists an intrinsic field because of the work function differences of two metals. The work function of tin is higher than that of the aluminium (170), giving an intrinsic field in the insulating film directed from aluminium to tin. So when tin (i.e. the electrode of higher work function) is negatively

biased the current increases and then becomes unstable. If the tin electrode is positively biased, the applied voltage neutralizes the internal voltage and the current decreases and becomes zero for a voltage which is nearly equal to the internal voltage. If the tin electrode is made more positive, the current starts flowing in the backward direction. Thus it is seen that the operation voltage (working inverse voltage) for this particular diode is -0.6 volt which is nearly equal to the internal voltage of the structure, since at a reverse applied bias voltage greater than this voltage, current will start flowing in reverse direction.

The maximum dc forward current of this diode is very small (of the order of few nanoamperes) but it is suggested that the value of this current may be increased by utilizing a suitably doped dielectric. It is also evident from various curves that for a particular combination of electrodes (say Al and Sn) the working inverse voltage as well as the maximum dc forward currents are maximum for thinnest dielectric layer. Therefore the working inverse voltage as well as the maximum dc forward current of such diodes may be increased by choosing (i) suitable metals for upper and lower electrodes which have larger work function differences (ii) thinner dielectric films.

Work function determination

As has already been discussed the extrapolated value

of internal voltage at zero thickness is the true difference of work functions of two metals. The difference of work functions of the metals Ag, Sn, Bi, Pb and Te has been measured with respect to Al. Taking Al as the reference metal and considering its work function as 4.08 eV (171) the work functions of all other metals under study were calculated. Therefore the study provides a method of determination of work function of metals.

The study of work function was also made for different thicknesses of the metal film(181). The work function has been found to be independent of the metal film thickness in the thickness range (390 - 1025 Å). It is expected since the work function of metal is a property of its band structure and the band structure in thin film form has the same gross structure as in the case of the bulk material. Theoretically this thickness dependence of the work function is expected only for a few atomic layers.

Time dependence of internal Voltage

To understand the behaviour of dielectric cell more precisely , a time dependent study of internal voltage in charging and discharing conditions has been made. Figures 7.38 and 7.39 show the time dependence of internal voltage taken under different conditions. Fig. 7.38 has been plotted for a Al - Ba stearate (1 layer) - Sn structure when the circuit is closed through a very high resistance ($\sim 10^{15}\Omega$). The sandwich shows a slow discharging

behaviour. The initial rate of discharging is 1.5×10^{-5} V/sec, giving a life time value of 4.2×10^{4} sec.

Figure 7.39 has been plotted when the dielectric cell is partially discharged through low resistance and then left for subsequent recovery in open circuit. The voltage rise is nearly exponential in nature with a time constant of about 5 minutes. This recovery process results since after discharging, the double-charge layer has to rebuild itself by diffusion of charges through the dielectric-film. Since the transfer of charges from one face of the dielectric to the other depends upon the resistivity of the dielectric, the time required for the space charge layer to rebuild itself is given by the resistance of the MIM structure multiplied by the capacitance of the same.

Next chapter describes in detail the interesting behaviour of internal voltage in the Langmuir films of barium stearate in the MIM structure with similar electrodes.

TABLE I

MOLECULAR PARAMETERS OF FATTY ACID SOAP MULTILAYERS

Substance	Molecular Formula	Number of carbon atoms in hydrocarbon chain	Value of monolayer Thickness (Å)	Melting point*** °C	Type of Film	Type of solution used	pH of solution
Barium Palmitate	$\lvert C_{15}H_{31}COO\rvert_2Ba$	16	23.25*	63	Y	3×10^{-5}M $BaCl_2$ + 4×10^{-4}M $KHCO_3$	7-7.2
Barium Margarate	$\lvert C_{16}H_{33}COO\rvert_2Ba$	17	24.05*	60	Y	''	7-7.2
Barium Stearate	$\lvert C_{17}H_{35}COO\rvert_2Ba$	18	25.75*	70	Y	''	7-7.2
Stearic Acid	$C_{17}H_{35}COOH$	18	26.00**	70	Y	Only deionized water**	>6**

* Reference 78

** Reference 51

*** Reference 26

TABLE II

TECHNICAL DETAILS OF PREPARATION OF VARIOUS METAL FILMS.

Metal	mp °C *	Evaporation Source	
		Filament	Boat
Ag	961	-	Mo
Al	660	W	-
Au	1063	-	W
Be	1284	-	Mo
Bi	271	-	Ta
Cu	1083	W	-
Pb	328	-	Mo
Sn	232	-	Mo
Te	452	W	-

* Reference 167, p.69

TABLE III

COMPARISON OF VALUES OF INTERNAL VOLTAGE FROM DIFFERENT METHODS

Figure reference	Structure under study	No. of organic film monolayers.	Thickness of Dielectric films Å	INTERNAL VOLTAGE IN VOLTS			
				Breakdown voltage method	Zero Current method	Equal Magnitude Current Method.	Direct Voltage Measurement,
7.1	Al-Ba-Stearate-Sn	1	25.75	0.65	0.64	0.64	0.65
7.2	Al-Ba-Stearate-Sn	3	77.25	0.65	0.65	0.62	0.62
7.3	Al-Ba-Stearate-Sn	2	51.50	0.55	0.57	0.52	0.57
7.4	Al-Ba-Stearate-Sn	4	103.00	0.50	0.47	0.43	0.50
7.5	Al-Ba-Stearate-Sn	6	153.50	0.45	0.46	0.42	0.48
7.6	Al-Ba-Stearate-Sn	8	206.00	0.45	0.46	0.45	0.45
7.7	Al-Ba-Palmitate-Sn	4	93.00	0.45	0.48	0.45	0.48
7.8	Al-Ba-Margarate-Sn	4	96.20	0.50	0.49	0.44	0.47
7.9	Al-Stearic-Acid-Sn	4	104.00	0.45	0.48	0.45	0.48
7.10	Al-Ba-Stearate-Pb	2	51.50	0.25	0.26	0.21	0.20
7.11	Al-Ba-Stearate-Bi	2	51.50	0.15	0.14	0.12	0.16
7.12	Al-Ba-Stearate-Te	4	102.00	0.15	0.16	0.14	0.14
7.13	Al-Ba-Stearate-Ag	2	51.50	0.50	0.47	0.51	0.50
7.14	Sn-Ba-Stearate-Al	2	51.50	0.60	0.58	0.54	0.55

TABLE IV

THICKNESS DEPENDENCE OF INTERNAL VOLTAGE DATA

Figure reference	Structure under study	Internal Voltage in volts for different dielectric film thickness				Internal Fields in MV/Cm for different dielectric film thickness			
		2 layer	4 layer	6 layer	8 layer	2 layer	4 layer	6 layer	8 layer
7.15	Al-Ba-Stearate-Ag	0.50	0.44	0.41	0.38	0.97	0.43	0.26	0.18
7.16	Al-Ba-Stearate-Sn	0.57	0.50	0.48	0.45	1.10	0.49	0.31	0.22
7.17	Al-Ba-Palmitate-Sn	0.56	0.48	0.47	0.42	1.20	0.52	0.33	0.22
7.18	Al-Ba-Margarate-Sn	0.56	0.48	0.44	0.43	1.16	0.50	0.30	0.22
7.19	Al-Stearic-Acid-Sn	0.56	0.48	0.46	0.44	1.07	0.46	0.29	0.21
7.20	Al-Ba-Stearate-Pb	0.20	0.14	0.11	0.10	0.39	0.13	0.07	0.05
7.21	Al-Ba-Stearate-Bi	0.16	0.11	0.08	0.07	0.31	0.10	0.05	0.03
7.22	Al-Ba-Stearate-Te	0.22	0.14	0.12	0.07	0.43	0.13	0.07	0.03
7.23	Sn-Ba-Stearate-Al	0.55	0.52	0.46	0.45	1.06	0.50	0.30	0.22

TABLE V

COMPARISON OF INTERNAL VOLTAGE WITH WORKING INVERSE VOLTAGE (WIV)

Figure reference	Structure	Number of dielectric layers.	Internal voltage* in volts	Working inverse voltage** (WIV) in volt
7.24	Al-Ba-Stearate-Sn	1	0.65	0.60
7.25	Al-Ba-Stearate-Sn	3	0.62	0.60
7.26	Al-Ba-Stearate-Sn	2	0.57	0.55
7.27	Al-Ba-Stearate-Sn	4	0.50	0.50
7.28	Al-Ba-Stearate-Sn	6	0.48	0.45
7.29	Al-Ba-Stearate-Sn	8	0.45	0.40
7.30	Al-Ba-Palmitate-Sn	4	0.48	0.45
7.31	Al-Ba-Margarate-Sn	4	0.47	0.45
7.32	Al-Stearic Acid-Sm	4	0.48	0.45
7.33	Al-Ba-Stearate-Pb	2	0.20	0.23
7.34	Al-Ba-Stearate-Bi	2	0.16	0.15
7.35	Al-Ba-Stearate-Te	4	0.14	0.17
7.36	Al-Ba-Stearate-Ag	2	0.50	0.50
7.37	Sn-Ba Stearate-Al	2	0.55	0.55

** Approximate value derived from various curves 7.24 -7.37

* Mean value of internal voltage derived from various curves 7.15 - 7.23

TABLE VI

WORK FUNCTION DETERMINATION

Fig. No.	Structure under study	Extrapolated value of internal voltage at zero thickness	$\Delta\psi = \psi_{m_2} - \psi_{Al}$	ψ_{Al}^{*}	ψ_{m_2}
7.15	Al-Ba Stearate-Ag	0.53 Volts	0.53 eV	4.08 eV	4.61 eV
7.16	Al-Ba Stearate-Sn	0.60 Volts	0.60 eV	4.08 eV	4.68 eV
7.20	Al-Ba-Stearate-Pb	0.21 Volts	0.21 eV	4.08 eV	4.29 eV
7.21	Al-Ba-Stearate-Bi	0.17 Volts	0.17 eV	4.08 eV	4.25 eV
7.22	Al-Ba-Stearate-Te	0.27 Volts	0.27 eV	4.08 eV	4.35 eV

* Preferred Value of work function from reference (171), E.77.

CHAPTER VIII

RESULTS AND DISCUSSION OF INTERNAL VOLTAGE IN LANGMUIR FILMS WITH SIMILAR ELECTRODES.

Simmons (10) in his pioneering work obtained no internal voltage in capacitor structure with similar electrodes. The justification for this absence of internal voltage as given by Simmons is that there is no work function difference of the two metal electrodes to develop any internal field. A new effect has been found in the present work when an odd number of Langmuir monolayers are sandwiched between similar electrodes (172). A voltage is found to develop in the capacitor system even in this situation of symmetric electrodes. Since this voltage also develops within the system, we have called this voltage also an internal voltage. But it must be emphasized that this voltage has nothing to do with the Simmons' effect arising because of the difference in the electrode work function. The basic reason for the development of this voltage is the fact that the film containing odd number of layers has one unpaired molecular dipolar layer as explained earlier in chapter VII Sec. 7.2. This unpaired layer results in the net polarization effects leading to the observed voltage. As expected, the system with a Langmuir film containing even number of layers between similar electrodes does not show any internal voltage because there is no unpaired layer in such a film and therefore no net polarization effects. Systematic studies have been done on the Langmuir films of barium

stearate. The detailed theory of the development of this voltage has also been given in this chapter (sec.8.2). A detailed quantitative correlation of the experimentally measured voltage with the theoretical results has also been given. This analysis has led to an interesting new method of determining the dipole moment of the molecules which can be suitably oriented in the form of Langmuir films and the dipole moment of barium stearate molecule thus determined. This newly developed method of determining the dipole moment has also been utilized for determination of dipole moment of stearic acid molecule in the Al-stearic acid - Al structure where stearic acid films have been deposited by Langmuir technique. The experimentally observed results have been matched with the known value of dipole moment for free stearic acid molecule and the correlation has been found to be satisfactory.

8.1 RESULTS

The preparation of the sample and the measurement procedures are the same as discussed in the previous chapters VI and VII for the case of dissimilar electrodes. The results obtained for various types of studies have been categorized below.

8.1 a. Study of Current-Voltage Characteristics: Existence of Internal Voltage.

In Fig. 8.1, the tunneling current in the Al - Ba

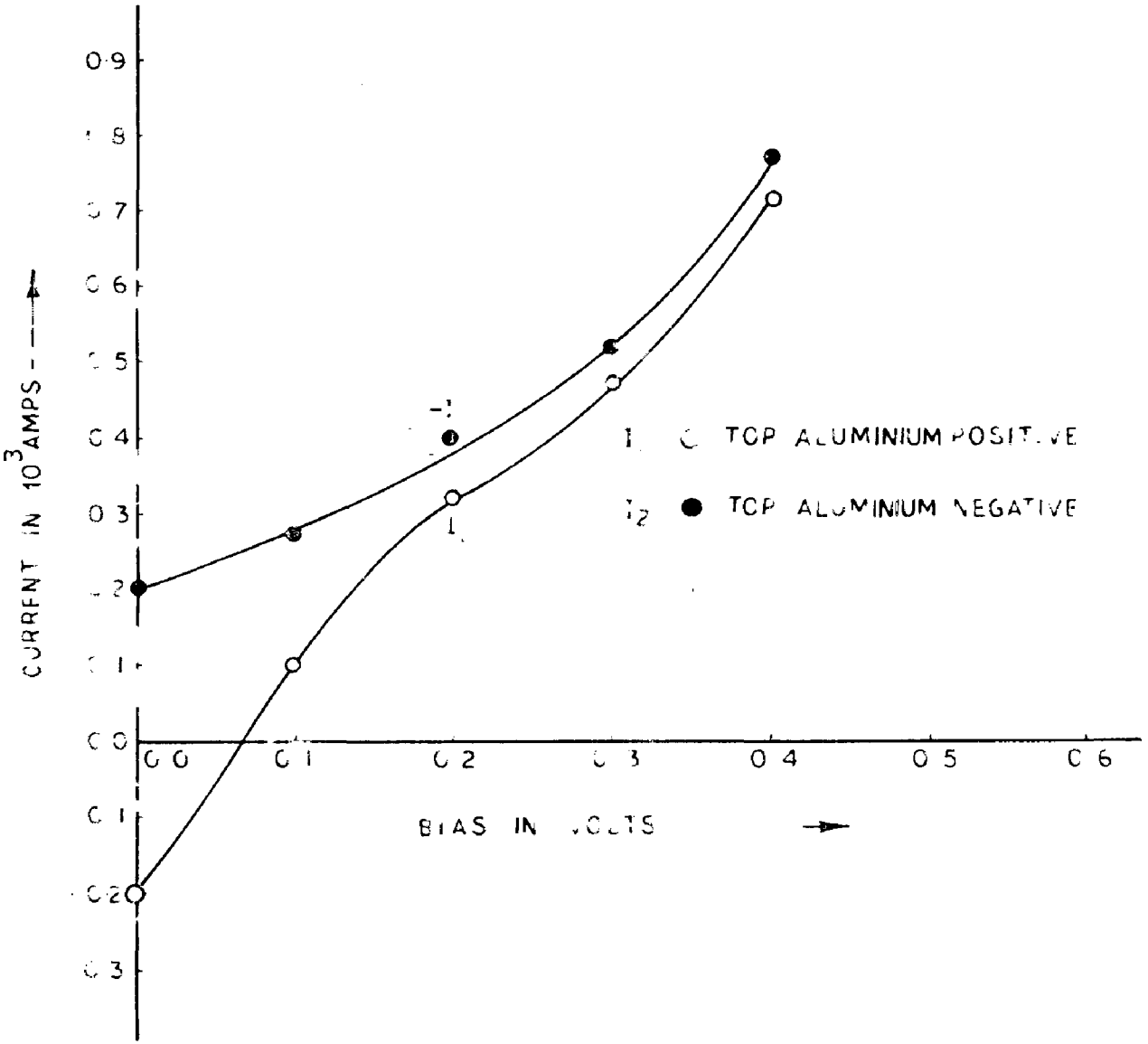

FIG. 8·1 CURRENT–VOLTAGE CHARACTERISTICS OF A ONE LAYER Al–BARIUM STEARATE–Al STRUCTURE IN FORWARD AND BACKWARD DIRECTIONS

stearate (1 layer) - Al structure is shown with the base aluminium electrode biased positive or negative. It is seen from the figure, that when the top aluminium electrode is negatively biased, the current is always negative, but when this electrode is positively biased, the current is negative at low bias voltages but becomes positive at higher bias voltages. These measurements clearly show that there is an internal field in the capacitor structure and its direction is such as to oppose the current flow due to a positive applied bias to the top electrode.

8.1 b. Direct measurement of internal Voltage:
Thickness dependence of internal Voltage.

The above interesting phenomenon of internal voltage has also been studied directly and in systematic details. These voltages have also been measured by the direct voltage measurement method with a high input impedance ($\sim 10^{15}$ ohms) electrometer amplifier used as a voltage measuring device. Figure 8.2(a and b) shows the plots of internal voltage versus number of monolayers in Langmuir films of Barium Stearate. Curve 'a' in fig. 8.2 represents the behaviour for odd number of monolayers whereas the curve 'b' corresponds to the even number of monolayers. It is evident from curve 'a' that there exists an internal voltage in the odd monolayers case and this internal voltage decreases linearly with thickness of the dielectric. Curve 'b' demonstrates the absence of any internal voltage in the

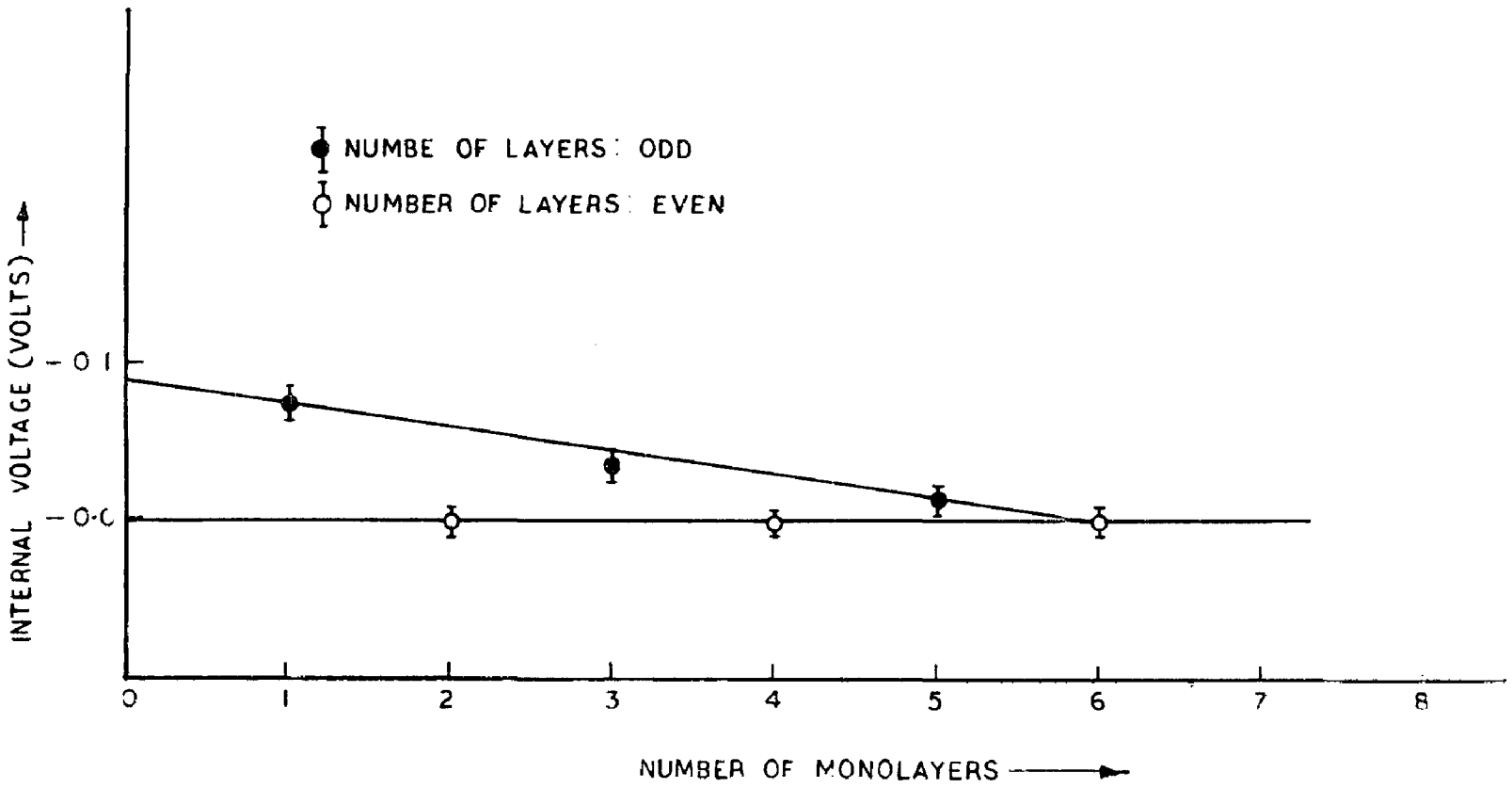

FIG. 8·2 INTERNAL VOLTAGE VERSUS NUMBER OF BARIUM-STEARTE MONOLAYERS IN Al-BARIUM STEARATE Al-STRUCTURE

(Polarity of top Al: positive)

case of even number of monolayers. The scatter in the values of internal voltage has been shown by vertical bars. The dots in the bars show the mean value of internal voltage. This value has been calculated after taking measurements over a number of samples of the same thickness. The curves shown are again the best fit curves about the mean points. The discussion of the results will be given in a later section (sec.8.2)

(c) Determination of dipole moment of barium stearate molecule.

With the knowledge of the internal voltage, in the Al-Barium stearate - Al structure having odd number of monolayers, the dipole moment of barium stearate molecules has been determined. It has been found found to be -0.23 debye in the direction perpendicular to the surface of the film with the negative end of the dipole closer to the bottom aluminium electrode.

8.2 DISCUSSION: INTERPRETATION OF RESULTS

A systematic detailed discussion of the results obtained in the above section is as follows:

As is expected the current at zero applied bias voltage of the above capacitor with odd number of layers should be transient in nature. Therefore this transient behaviour of the current was also studied.

Figure 8.3 represents the zero applied bias current as a function of time. It is noticed that the

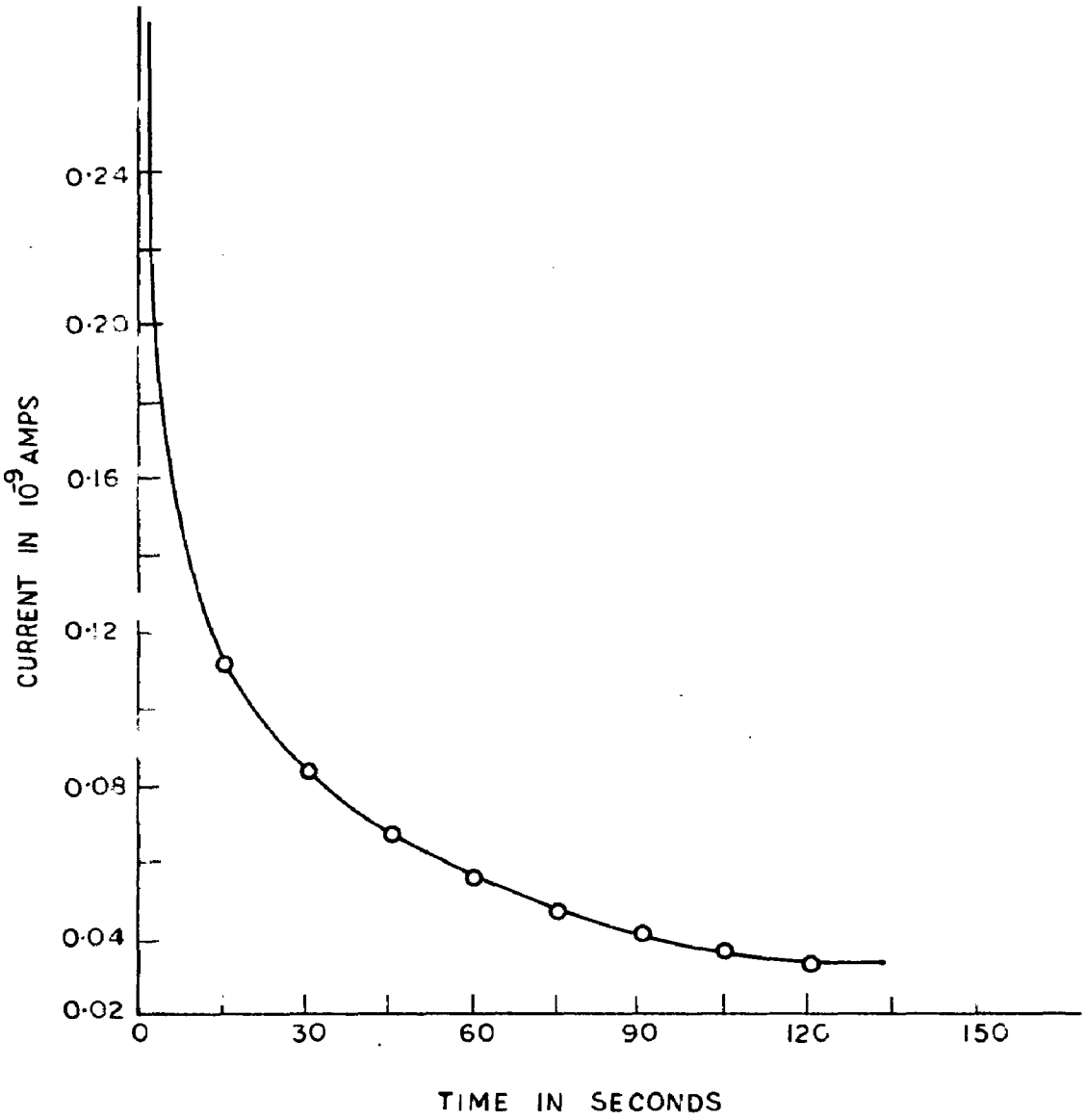

FIG. 8·3 DECAY OF CURRENT WITH TIME IN A ONE LAYER Al BARIUM STEARATE Al STRUCTURE

behaviour of zero bias current is transient and it decreases as a function of time. The current decay characteristics, as evident from figure, consist of two regions. First, an initial rapid decay of the current governed by the time constant of the circuit consisting of capacitor and the resistance of the electrometer amplifier used in series with the capacitor. This decay time is observed to be about one second. After this initial rapid decay the current decrease becomes slow presumably because of a continuous thermal generation of carriers in the space charge region as well as a slow release of trapped charges at these interfaces. The thermal generation phenomenon is somewhat similar to the diode current generation in p-n junctions. The non zero current at zero applied bias indicates the existence of an internal field in this capacitor structure.

Figure 8.2 shows the tunneling currents in the forward and backward bias voltage conditions. When the top aluminium electrode is positively biased, the current is negative at low bias voltage and its value becomes zero at a certain value of applied voltage. Also the current becomes positive at higher bias voltages. This indicates that there is an internal field and hence the internal voltage in the capacitor structure.

The existance of the above mentioned internal voltage can be more systematically understood from figure 8.2 (curves a and b). From curve 'a' it is found that the value of internal voltage for one monolayer capacitor is -0.07 V with the bottom electrode showing negative polarity and this compares well with figure 8.1 where at +0.07V the current is found to be zero.

Again referring to figure 8.2 the internal voltage is always zero for even number of monolayers (Fig.8.2 b) whereas it decreases linearly with increasing number of monolayers for odd layers case (Fig. 8.2 a). The difference in the behaviour for odd and even layers is very interesting and significant since it directly indicates that the internal field is related to unpaired layers in the case of odd number of layers. This type of difference in the behaviour has also been observed in the case of dissimilar electrodes in the previous chapter VII (See Fig. 7.15 and 7.16) and the reason for the occurrence of the internal voltage in the present structure appears to be the same as those discussed for the additional voltage for odd number of layers in the case of dissimilar electrodes. Therefore referring to (i) the figure 7.40 for the orientation of barium stearate molecule in the case of odd and even number of layers, and (ii) the discussion of chapter VII for additional voltage in the odd monolayers case, one expects the internal field and hence the internal voltage in the present case to come

from the polarization existing in the unpaired layer of polar barium stearate molecule. The aluminium electrodes always have a very thin oxide layer on them. This oxide on the lower aluminium electrode forms a double dielectric layer structure (Al - Al_2O_3 - Barium stearate - Al) but since no voltage is observed in the case of even number of monolayers one can conclude that the oxide layer is not giving any observable contribution to the internal voltage. Gold and silver were tried in order to minimize the oxide formation but it was found that these materials when used as first electrode do not make good contacts with barium stearate film because of diffusion. Handy and Scala (110) also drew similar conclusions from their studies.

Possible contribution of light to the internal voltage and tunneling was avoided by making the measurements keeping the capacitor in a dark enclosure.

Theoretical Formulation : This section gives a quantitative formulation of the theory of the development of the above described voltage in the symmetric structure.

The internal voltage in the figure 8.2a can be approximated by the following empirical formula

$$V(n) = V_o + vn \qquad .. (8.1)$$

where V(n) is the voltage for any film of n number of monolayers. V_o =-0.08V is the extrapolated value of

internal voltage at zero thickness and v = + 0.014V is a constant.

To understand this behaviour of the internal voltage consider a thin dielectric slab of thickness 't' and a unit surface area with a uniform polarization P perpendicular to the plane of the film. Then the surface charge density 'σ' is equal to P. Following the rationalized MKS system of units, the field inside the dielectric due to this polarization is E, where

$$E = \frac{P}{\epsilon_0 k} \qquad .. (8.2)$$

where ϵ_0 is the permittivity of free space and k is the dielectric constant of barium stearate (= 2.5). Due to this field the voltage difference between the two faces of the dielectric is

$$V = \frac{Pt}{\epsilon_0 k} \qquad .. (8.3)$$

For the case of the uniform polarization, therefore, the internal voltage will increase with the thickness of the dielectric. In the present system under investigation , however, only one unpaired layer is polarized and other unpaired layers have zero polarization to begin with. It may be assumed that the polarization of unpaired layer gets eually shared among all the 'n' layers thereby making the effective uniform polarization as 1/n times

that of the unpaired monolayer. Thus equation (3) gets modified to

$$V = \frac{Pt}{\epsilon_o km} = \frac{P\tau}{\epsilon_o k} \qquad ..(8.4)$$

(τ being the thickness of one monolayer) thus making the voltage independent of the number of monolayers. The polarization of the monolayer is due to the two carboxylic groups and the barium atom in $(C_{17}H_{35}COO)_2Ba$ complex. If the number of these barium stearate molecules per unit surface area of the dielectric is N and the component of the dipole moment perpendicular to the face of the dielectric is P, then the internal voltage is given by

$$V = \frac{Np}{\tau} \frac{\tau}{\epsilon_o k} = \frac{NP}{\epsilon_o k} \qquad ..(8.5)$$

Thus knowing the dipole moment of barium stearate molecule, the internal voltage can be calculated and vice-versa.

The above analysis holds good if there are no trapped charges at one or the other of the metal insulator interfaces. If the number of such charges at this interface is m per unit area, then the field due to it is $\frac{em}{\epsilon_o k}$ and the potential difference between the electrodes due to this field is $\frac{emn\tau}{\epsilon_o k}$ (where n is number of barium stearate monolayers). Since the trapped charges are also somewhat mobile in the presence of the internal field,

they move in a direction so as to neutralize the internal field. Hence the expected voltage becomes.

$$V = \frac{NP}{\epsilon_o k} - \frac{emn\tau}{\epsilon_o k} \qquad ..(8.6)$$

This equation agrees with the observed behaviour as given in equation (8.1). The first term on the right is responsible for the development of internal voltage as it contains the polarization term whereas the second term shows the decrease of the voltage with thickness. By comparing equations (8.1) and (8.6)

$$V_o = \frac{Np}{\epsilon_o k} \qquad ..(8.7)$$

$$v = \frac{emn\tau}{\epsilon_o k} \qquad ..(8.8)$$

To estimate the value of dipole moment 'p' we consider the following:

The inter hydrocarbon chain distance for barium stearate molecule has been found to be 4.85 Å and the chains are arranged in hexagonal arrays (60). The number of chains per square meter will be $4,88 \times 10^{18}$, and thus the number of barium stearate molecules per square meter of the surface would be $N = 2.44 \times 10^{18}$. Substituting this value of N in the above equation (8.7) the component of the dipole moment of barium stearate molecule is obtained

and is -0.23 debye in the direction perpendicular to the surface of the film with the negative end of the dipole closer to the bottom aluminium electrode. The vertical component of dipole moment in stearic acid chain is -0.93 debye with the negative end nearer to the bottom, when the hydrogen atom is in cis position (173,p.304) with respect to carbonyl oxygen. Figure 8.4 (a and b) show geometries of stearic acid and barium stearate molecules. The vertical component for two of these stearic acid chains would be -1.86 debye. If two hydrogen atoms are now replaced by a barium atom, the dipole moment of the barium-oxygen bond becomes more positive than that of the hydrogen oxygen bond. Barium oxide dipole moment is known to be 7.95 debye (174). Using 3.97 debye for each of barium oxygen bonds in place of the 1.51 debye for the hydroxyl bond we obtain, from Fig. 8.4 b an estimate for the vertical component of the dipole moment of barium stearate, with barium in cis position as 2.76 debye. The present observed value of -0.23 debye lies between the -1.86 debye for the two stearic acid chains and 2.76 debye for the barium stearate molecule. The experimentally observed negative value shows near cancellations of the positive moments of the barium oxide (Ba-O) bond with the negative moments in the carbonyl bonds. The position of the barium atom could be off from the O=C-O

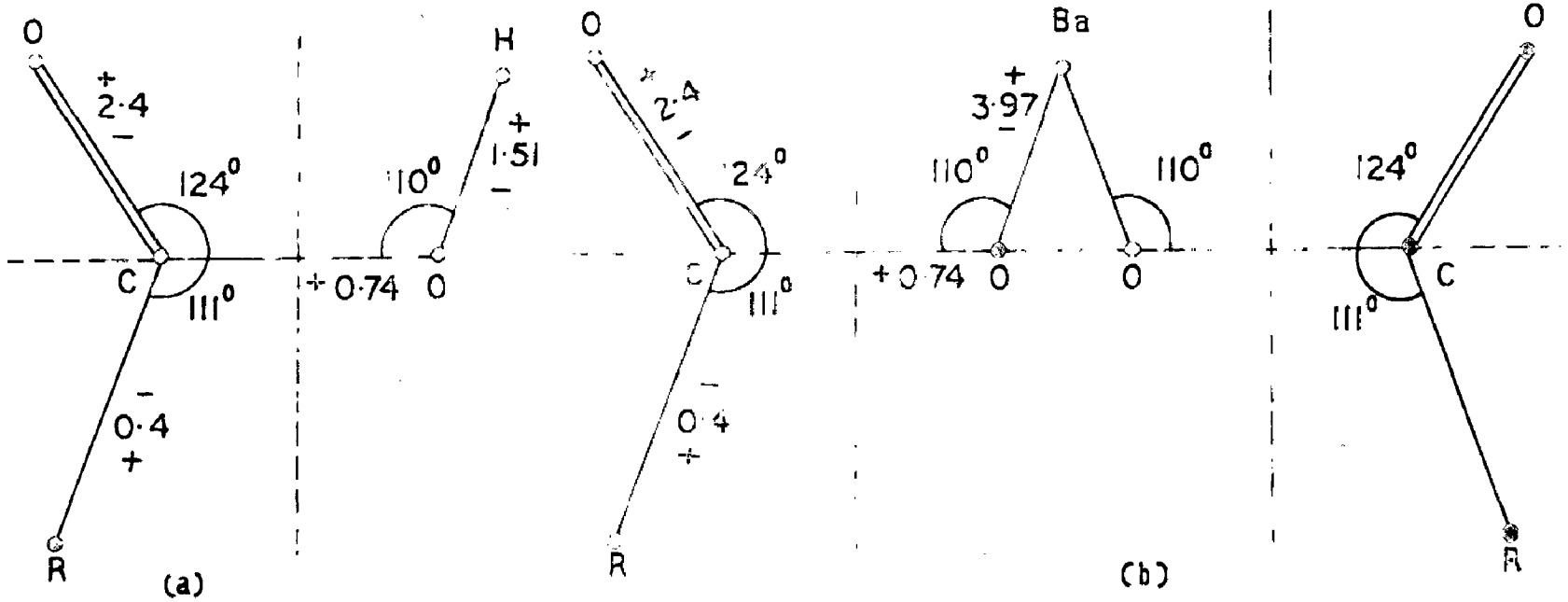

FIG 8·4 MOLECULAR GEOMETRY USED FOR CALCULATING DIPOLE MOMENTS

(a) FOR STEARIC ACID MOLECULE

(b) FOR BARIUM STEARATE MOLECULE

plane which may reduce the component of the bond moment in the O=C-O plane. If we take Ba - O bond about $53^{0}16'$ above the O=C-O plane then the net moment of the barium stearate will agree with the observed value of -0.23 debye.

The number of trapped charges 'm' is obtained from equation 8.8. Putting the values of e, ϵ_0 and k and v the value of these trapped charges per unit area is found to be nearly $0.7 \times 10^{11}/cm^2$. For thin films this seem to be a reasonable number for a metal insulator interface.

The above developed method has been successfully applied for determination of dipole moment of stearic acid molecule. The details are as follows:

Samples of Al - Stearic acid - Al were prepared by the usual technique. Stearic acid films were deposited by the technique (51) described earlier in chapter IV. The internal voltage was measured by the usual technique as used in the previous studies. Fig. 8.5 shows the values of internal voltage at various odd number of stearic acid layers. The extrapolated value of internal voltage at zero thickness (V_0) is -0.17 volts with bottom electrode showing negative polarity. The number of stearic acid chains per square meter as derived earlier is 4.88×10^{18} and hence the number of hydrogen atoms (N) in -COOH group

per square meter is also 4.88×10^{18}. Keeping the values of V_0, N, ϵ_0 (= 8.854×10^{-12}) k (= 2.5 for stearic acid) in equation 8.7, the dipole moment of stearic acid has been found to be -0.24 debye in the direction perpendicular to the surface of the film with the negative end of the dipole closer to the bottom aluminium electrode.

The known dipole moment of a free stearic acid molecule is 1.8 debye (173 p.304) which can be obtained from figure 8.4 a if the O-H bond is assumed to be rotated from the cis planar configuration by an angle about $37^{o}12'$. The vertical component of dipole moment of stearic acid in this position will be -1.21 debye. The measured vertical component the moment comes out to be somewhat less than the expected dipole moment calculated on the basis of an isolated stearic acid molecule. The difference is partly due to the approximate nature of the total number of stearic acid molecules per square meter of the surface since the stearic acid Langmuir films prepared experimentally were not tightly packed (chapt. IX p.143). Further the close proximity of stearic acid all alligned with the dipole moment parallel to one another can cause mutual depolarization effects by bond distortion and thereby reduce the effective dipole moment of each molecule. This may be the mechanism causing a sizable reduction of dipole moment in our experiments.

The results obtained in the present chapter yield a new method for the determination of dipole moment of the

suitably orientable molecules. The results are also helpful in understanding the behaviour of internal voltages in thin dielectric films with similar electrodes and its thickness dependence at low thicknesses. The studies are also helpful in finding out the trapped charges in thin films.

Next chapter describes the detailed and systematic studies of thickness dependence of dielectric loss in the ultra thin Langmuir films.

CHAPTER IX

STUDIES OF THICKNESS DEPENDENCE OF DIELECTRIC LOSS IN ULTRA THIN LANGMUIR FILMS.

INTRODUCTION

As has been described in detail in chapter VII Sec. 7.1 c, the phenomenon of internal fields in asymmetric structures has been utilized to develop a thin film dielectric diode system. Since in the context of this device the dynamic dielectric characteristics (dielectric loss tan δ) of Langmuir films also become important, a detailed and systematic study of this dielectric phenomenon has been carried out and is being presented in this chapter. Frequency and temperature dependence of the dynamic characteristics (tan δ) of these films have already been studied by several workers (51, 105, 108, 110, 113) but the studies of thickness dependence of dielectric loss (tan δ) are very scarce. A detailed review of the above work has already been given in chapter V Sec. 5.3b.

The dielectric loss is a bulk property and should not depend on thickness of the insulator film. However if the film has a defect structure which varies with thickness and takes part in a particular relaxation process, the dielectric loss is expected to become thickness dependent. To the author's knowledge no detailed and systematic study of thickness influence on dielectric loss in Langmuir films has been reported so far.

The present chapter describes a systematic and detailed study of thickness dependence of dielectric loss in Langmuir films in the ultra thin range of 25 - 250 Å (1-10 monolayers).

9.1 Experimental measurements

The samples Al - O - Al were prepared by the usual technique as described in chapter VI. The different dielectric materials chosen for the present investigations are barium plamitate, barium margarate and barium stearate. These are the three consecutive members of the same homologous series and form very good films. The value of tan δ was measured by a Marconi's Universal bridge energized by a 9V dc supply. All the measurements for thickness dependence have been carried out at a fixed frequency of 1000 Hz. which is the oscillator frequency of the bridge. All the measurements were taken at room remperature. Pressure leads were used for contact with aluminium electrodes.

9.2 Results and Discussion

Figures 9.1 - 9.3 give the plots of tan δ_f versus thickness in Al - O - Al structures for different films having 1 - 10 monolayers (thickness $\sim$ 25 - 250 Å). The value of dielectric loss has been plotted after taking loss due to series electrode resistance into account. It is evident from all these figures that the dielectric

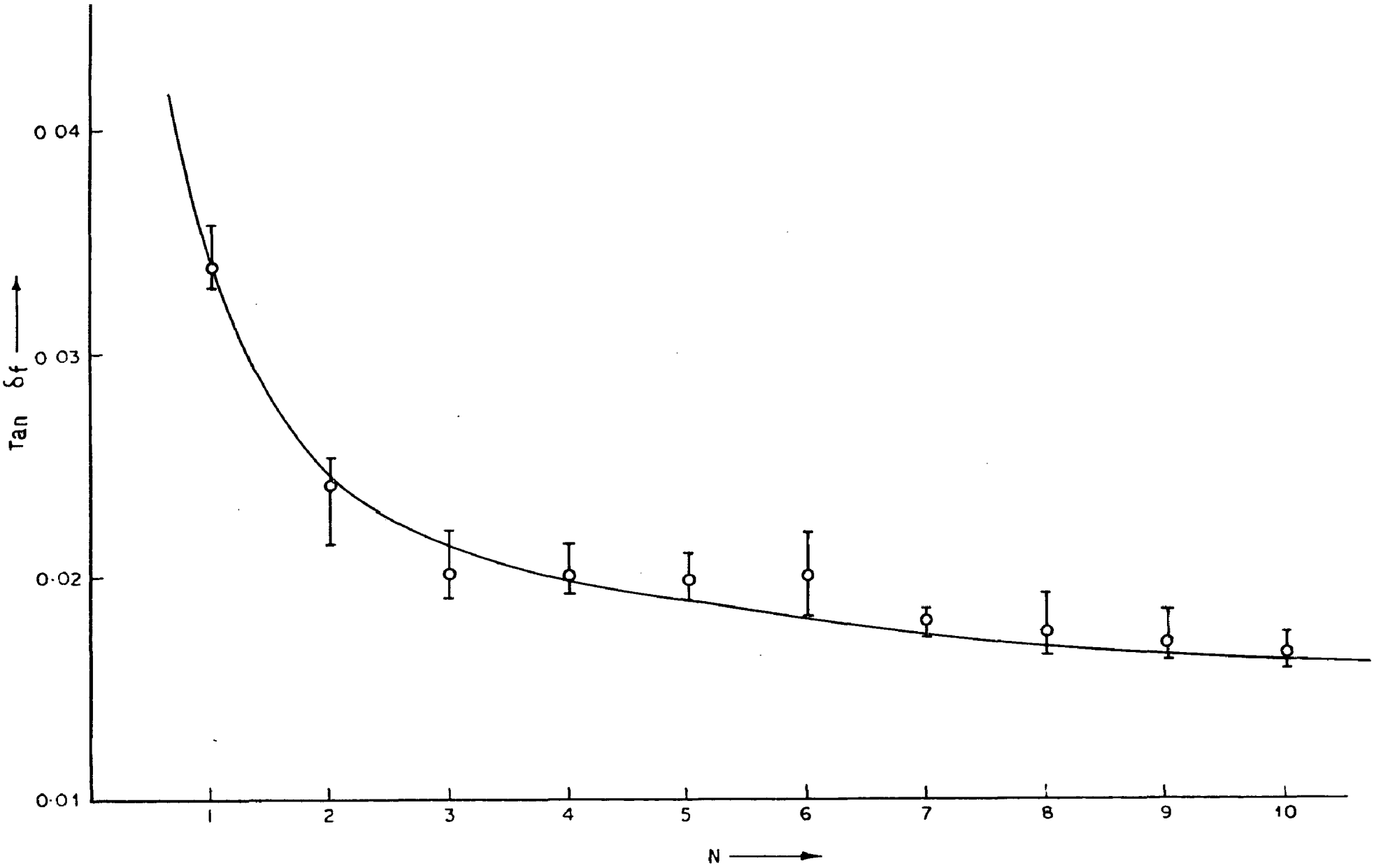

FIG. 9·1 DIELECTIRIC LOSS (Tan δ_f) AS A FUNCTION OF NUMBER OF LAYERS IN LANGMUIR FILMS OF BARIUM PALMITATE

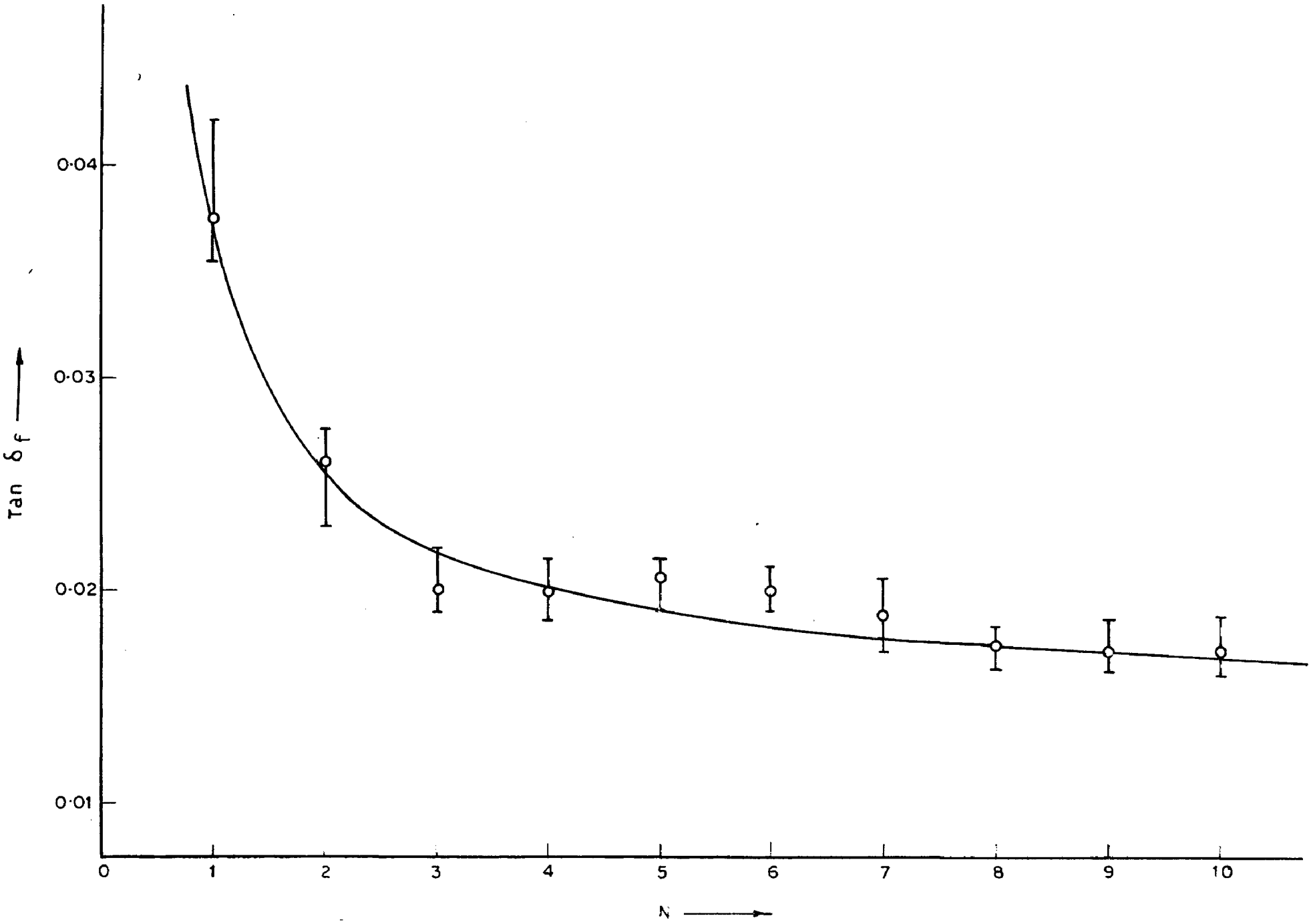

FIG. 9·2 DIELECTIRIC LOSS (Tan δf) AS A FUNCTION OF NUMBER OF LAYERS (N) IN LANGMUIR FILMS OF BARIUM ARACHIDATE

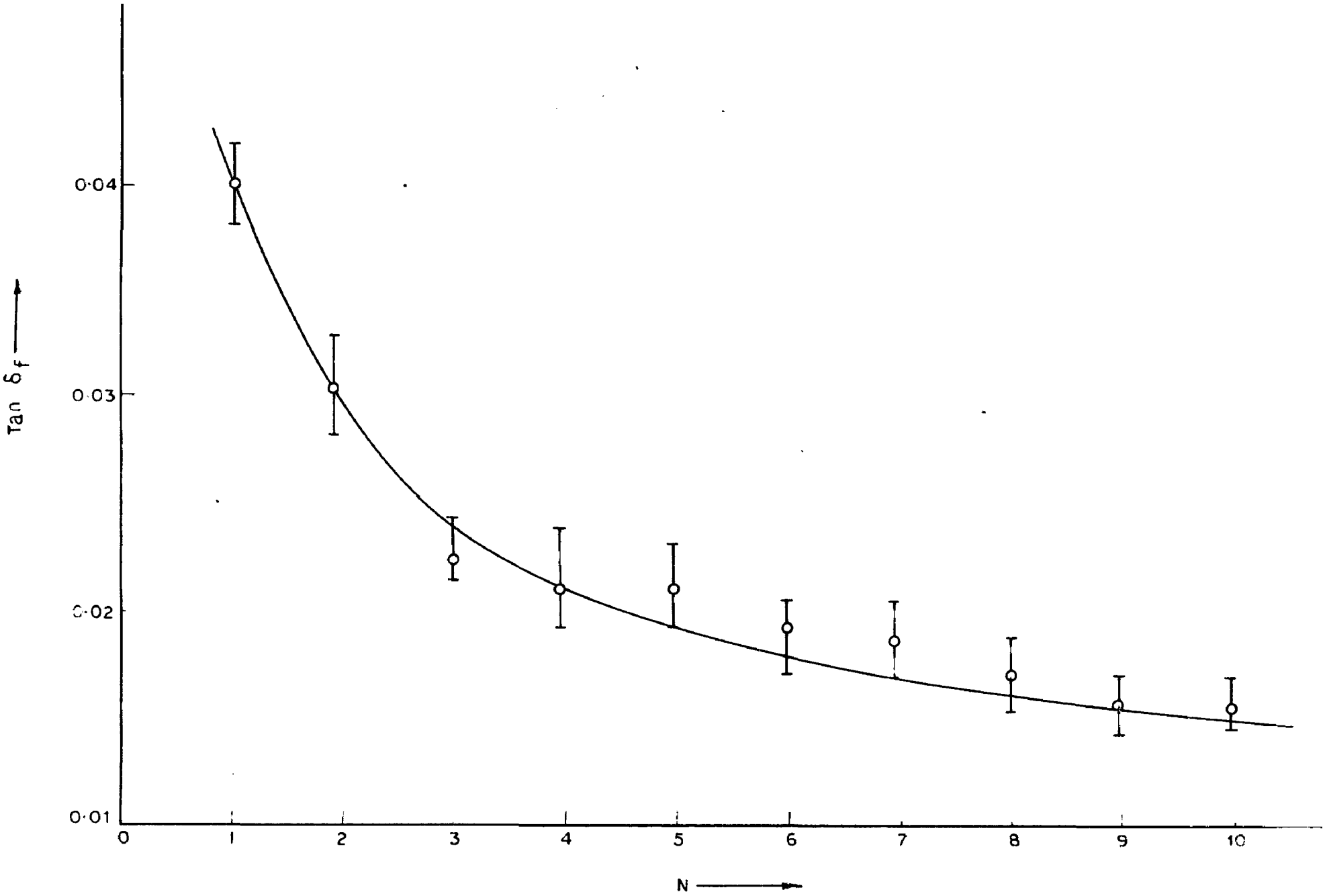

FIG. 9·3 DIELECTRIC LOSS (Tan δ_f) AS A FUNCTION OF NUMBER OF LAYERS (N) IN LANGMUIR FILMS OF BARIUM STEARATE

loss has a dependence on thickness in the very low thickness range. The dots in the graphs show the mean value of five or more observations for the same thickness of the sample and the scatter observed in the experimental data has been shown by vertical bars. The plots shown are the best fit curves about the mean points. The values of thickness for single monolayer of Barium Palmitate, Barium margarate and Barium Stearates are 23.25 Å 24.05 Å and 25.75 Å respectively (78).

The various graphs shown in the figures 9.1 - 9.3 were actually obtained after applying correction due to the influence of the electrode resistance on the loss angle. The measured loss angle is given (178) as

$$\tan \delta_m = \tan \delta_f + \omega R_e C \qquad ..(9.1)$$

where ω is the applied frequency, R_e the electrode resistance and C the film capacitance.

The first term on the right represents loss due to the dielectric film ($\tan \delta_f$) and the second term refers to the loss caused by the series resistance of the measuring electrodes. At higher thicknesses of the dielectric the capacitance will be very low and the loss due to series resistance of the measuring electrodes will be very small. Hence the second term may be neglected for the dielectrics of higher thickness. If the film thickness is low the capacitance will be

high and the loss due to series resistance of measuring electrodes should become significant. Knowing the values of ω , R_e, C and $\tan\delta_m$ from experiments, $\tan\delta_f$ was calculated and plotted in various figures for different substances.

As is evident from the plots 9.1 - 9.3, there is a sharp decrease in the $\tan\delta_f$ values as one goes from 1 to 2 monolayers. But as the thickness of these films is further increased, the decrease in the $\tan\delta_f$ values becomes slow. There is little change in $\tan\delta_f$ values for 8 to 10 monolayers films. Also, it is evident from the curves that after a certain thickness each curve tends to become parallel to the thickness axis. Thus the interesting feature to be noted is that the dielectric loss depends on the film thickness when the thickness is very small.

Weaver (124) made a detailed study of dielectric loss in the ionic films of alkali halide. He suggested the basic loss mechahism in these films to be excess vacancy concentration and pin holes in the dielectric. This latter mechanism which is based on the existance of pin holes seems to operate in the dielectric loss of the ionic films (ref.26,p.193)of barium palmitate, barium margarate and barium stearate studied here. The presence of voids or pin holes in Langmuir films has been confirmed through several studies of other workers. Ries et al. (175,176) have

carried out electron micrograph studies of stearic acid films. From their studies he concluded that voids in stearic acid films are inevitable if the transfer is accomplished at a surface pressure significantly below the collapse pressure of the film. The variability of electrical measurements made on Langmuir films by Handy and Scala (110) also shows indirectly the presence of voids in the film if the transfer is accomplished at low compression. They found that even in the best samples, 2 or 3 monolayers were needed to bridge voids penetrating through the films. In this layer by layer deposition process it has been shown that with increasing number of monolayers the voids in the previous layers are rapidly covered up by succeeding layers thus making the film progressively more and more uniform. This fact is confirmed by d.c. resistivity measurements of Handy and Scala (110) on barium stearate films (1-10 monolayers). The resistivity indeed increase steeply with increasing thickness or decreasing concentration of voids. The author has also studied the d.c. resistivity of the Langmuir films as a function of thickness through measurements of the current at fixed voltages. Figure 8.5 shows the measurements on barium stearate films. The nature of the curve clearly shows that there is a steep increase in the resistivity of the films with increasing thickness as observed by Handy and Scala (110). Holt (113) has also drawn similar conclusions from his

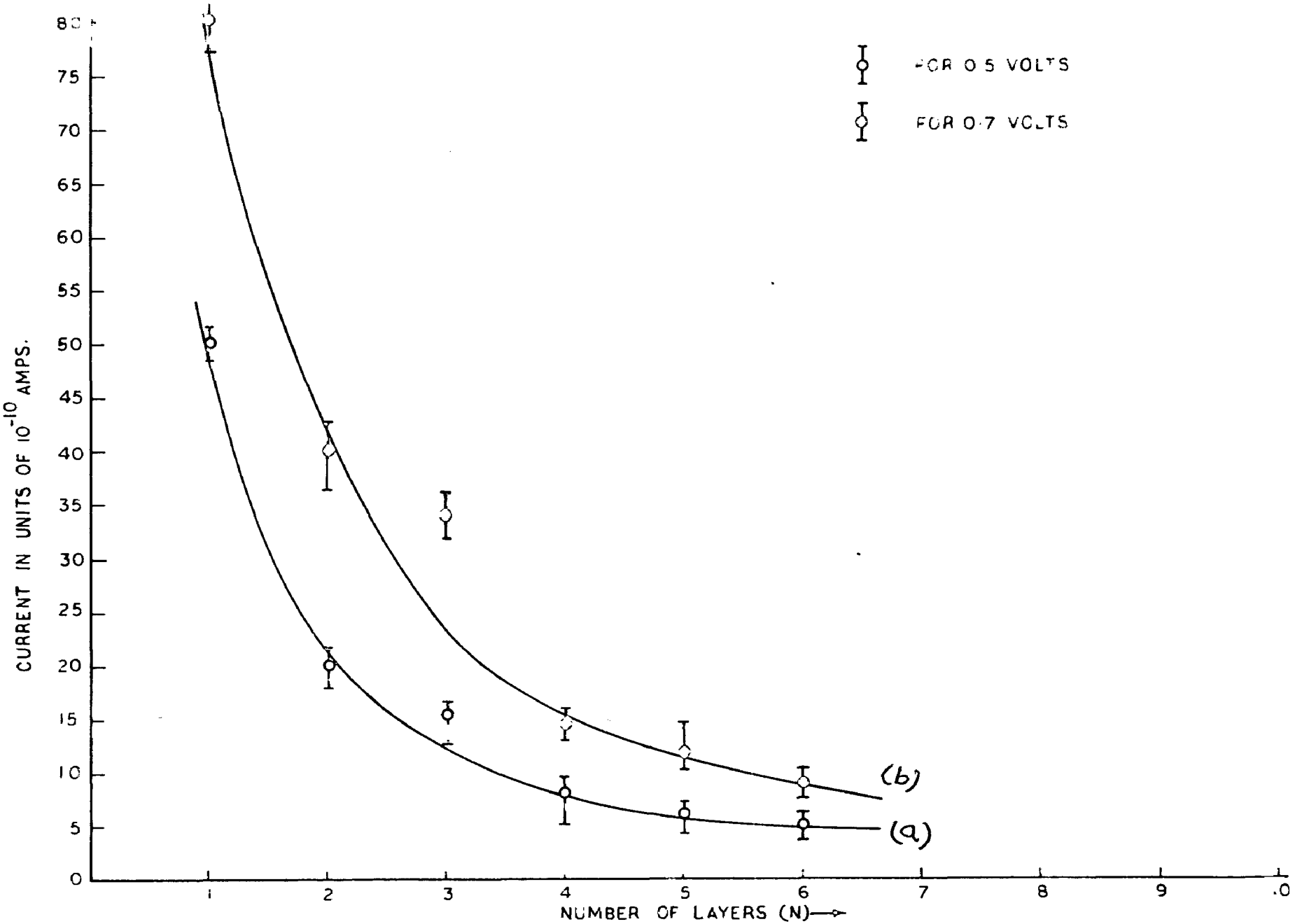

FIG. 9·4 PLOT OF CURRENT AS A FUNCTION OF THICKNESS OF BARIUM STEARATE IN Al-BARIUM STEARATE-Al STRUCTURE

(a) FOR APPLIED BIAS OF 0·5 VOLT

(b) FOR APPLIED BIAS OF 0·7 VOLT

studies of Langmuir films. He also concluded that each deposited monolayer tends to bridge discontinuities and gaps left over by the previous layer. Because of this the multilayers have the interesting property of becoming more uniform as they get thicker.

In the present investigations films were deposited using oleic acid as the '' piston oil''. The surface pressure of oleic acid is about 29 dynes/cm. This is significatly below the collapse pressure of the mono-molecular films (palmitate, margarate and stearate) , which is about 42 dynes/cm. Therefore, a large number of voids can be expected in the films studied here. The observed thickness dependence of the dielectric loss in the films of barium salts of the fatty acids can now be qualitatively explained in terms of the defect structure or voids of the films. Dielectric loss is observed to be very high for a monolayer because large number of voids or pin holes are expected in the single layer film. The loss value drops rapidly for a two layer film because voids will be rapidly bridged when the second layer is deposited on the first. After this the drop in the loss value becomes slower because the voids will now be covered up gradually with increasing number of monolayers. Obviously after certain number of layers the loss should not depend on the thickness of the film. This tendency of the near constancy of the dissipation factor can be seen in the figures for 8-10 layers.

From the above discussion it is clear that if the monolayer molecules are brought nearer by using higher piston force (mechanically or otherwise), the dielectric losses should reduce. This is exactly what has been observed by Marc and Massier in his studies on Langmuir films of calcium stearate (177).

The results obtained in the above studies have been summarised in Table 7.

The above discussion is purely qualitative. A quantitative explanation of the above results is not possible at present because the actual distribution of voids and their thickness dependence in Langmuir films are not known.

TABLE VII

THICKNESS DEPENDENCE OF DIELECTRIC LOSS

Figure reference	Dielectric substance in the sample Al-F-Al	Thickness of a monolayer (Å)	Mean value of Dielectric loss ($\tan \delta_f$) for different thickness									
			1L	2L	3L	4L	5L	6L	7L	8L	9L	10L
9.1	Ba-Palmitate $(C_{15}H_{31}COO)_2Ba$	23.25	0.034	0.024	0,020	0.020	0.020	0.020	0.018	0.018	0.017	0.0
9.2	Ba-Margarate $(C_{16}H_{33}COO)_2Ba$	24.05	0.038	0.026	0.020	0.020	0.020	0.020	0.019	0.018	0.018	0.0
9.3	Ba-Stearate $(C_{17}H_{35}COO)_2Ba$	25.75	0.040	0.030	0.022	0.021	0.021	0.019	0.019	0.017	0.016	0.0

CONCLUDING REMARKS

Summary of the work done

(a) Basic Nature of The Present Investigations.

The purpose of the present study was to show the suitability of the 'built-up' thin films of some long chain fatty acid compounds for the thickness dependent studies of the internal voltages and hence of the internal fields. The advantages of these films are that their thicknesses are closely controllable (down to one monolayer of $\sim$ 25 Å), extremely uniform and accurately known (77-78). An optical device (56) namely ' Thin Film Thickness Step Gauge' has been developed using these Langmuir films. The observance of homogeneity of colours on this step gauge provides sufficient evidence for the uniformity of thicknesses of these films. It is also practicable to get these films almost free from gross defects and conducting imperfections (112). These features constitute a sound basis for studying these films and therefore particularly these films are eminently suited for the thickness dependent studies. Even with the evaporated film systems, for example, it is not easy to carry out such a systematic thickness dependent studies because the very small and uniform thickness of such films are very difficult to obtain. Moreover their thicknesses will have to be measured and they will not be closely controllable. The influence of film thickness on the dielectric loss has also been studied.

(b) Basic Techniques Used

The capacitor structure of the type metal-insulator

metal (MIM) were fabricated using 'built-up' Langmuir films of stearic acid and metallic compounds of some long-chain fatty acids (e.g. barium palmitate, margarate and stearate) as the insulating media between two thermally deposited metal films of nearly constant thickness under high vacuum with the help of a coating unit suitable for this purpose. Insulating films were built-up by a delicate but easy technique of Blodgett and Langmuir (17,18) by which even the films of monomolecular thickness can be built-up by transferring them from the highly cleaned water surface under a constant surface pressure. These films are suitable for use as a dielectric as they offer high dielectric strength $\sim 10^7$ V/cm.(136-147). The reproducibility of these films was quite satisfactory which, of course, was very necessary for the present investigations. The films are also stable under vacuum and metal electrodes could easily be deposited without any damage to them.

The measurement of internal voltage was carried our from the current voltage characteristics in the two polarities (breakdown voltage) as well as by directly using a high impedance voltage measuring device. The details of the measurement technique are given in chapter VI.

Summary of the Results.

It has been shown through the study of tunneling current characteristics in two polarities and direct voltage

measurements that when the insulating film is sandwiched between two asymmetric metal electrodes, a high internal field develops. The internal voltage because of this field has also been measured. A detailed and systematic study of thickness dependence of this internal voltage has been carried out in the thickness range from 1-8 monolayers ($\sim$ 25 - 200 Å). Different behaviour has been observed for the case of odd and even number of monolayers. The internal voltage has been found to decrease linearly with thickness. The I-V characteristics for the two polarities have also been plotted on a linear scale and it has been found that the sandwich behaves like a diode junction. Work functions of the different metals have been measured using aluminium as the reference metal. The study of work function for various thicknesses of the metal film electrode has also been made. The work function has been found to be independent of the electrode thickness. Discharging of the internal voltage in closed circuit and its subsequent recovery in open circuit has also been studied, thereby calculating the life time and time constant of the structure.

The above interesting study of internal voltage has also been extended in the 'built-up' films of barium stearate with symmetric electrodes. The sandwich with even number of monolayers showed no internal voltage. However, with the odd number of monolayers, the sandwich (Al - O - Al) showed an internal voltage. This is a

new and very interesting feature of Langmuir films. This internal voltage developed in the case of an odd number of monolayers has been confirmed through tunneling currents at low voltages in the two polarities and through direct voltage measurement procedure. A thickness dependent study of this internal voltage has also been carried out and the internal voltage has been found to vary with thickness showing a linear decrease. The dipole moment of the organic monolayer molecule has been determined from the knowledge of this internal voltage. This measured dipole moment has been correlated with the theoretically calculated value. Thus a new method for determining the dipole moment of suitably orientable molecules in the form of a Langmuir film has been developed. The method has successfully been applied for determining the dipole-moment of stearic acid molecule when it is in the form of a Langmuir film. The measured value of dipole moment has been correlated with the known value of dipole moment for a free stearic acid molecule. The correlation has been found to be satisfactory. The transient behaviour of current with time or the decay characteristics has also been studied. The trapped impurities per unit area have been estimated from a knowledge of internal voltage.

The phenomenon of internal fields in the asymmetric structures has been utilized to develope a thin film dielectric diode system. In the context of this device the dynamic dielectric characteristics (dielectric loss,

tanδ) of the Langmuir films also become important, a detailed study of thickness dependence of 'tanδ' in the ultra thin range of Langmuir films has been made. It has been observed that dielectric loss has a dependence on thickness at very low thicknesses.

Summary of The Basic Interpretation of Results.

In the case of asymmetric electrodes the difference in the work functions of two metal electrodes occur. This work function difference, in turn develops an intrinsic field in the system. The behaviour of this intrinsic field is such as to enhance the current flow when electrode of lower work function is positively biased and oppose it when the electrode of lower work function is negatively biased. The internal voltage, at the two interfaces, because of this intrinsic field has been found to decrease with increasing thickness of the dielectric film. This is because of the presence of the trapped charges in the dielectric film which, in the presence of intrinsic fields, move in a direction so as to neutralize the double charged layer thereby reducing the internal voltage. Therefore, the internal voltage measured at any thickness will be the reduced value of the actual internal voltage developed because of the work function difference in the two metal electrodes. An extrapolated value of this voltage at zero thickness

will give the actual value of the difference in the work functions of two electrodes. This analysis has been found proper for the $M_1 - O - M_2$ structures with organic film having even number of monolayers.

In the case of odd number of layers, apart from the above reason for the development of internal voltage, an additional voltage has also been found. It is because of the polarization existing in the unpaired dipolar layer in the case of an odd number of monolayers. Thickness dependence of the internal voltage showed the same behaviour as in the case of even number of monolayers.

The samples $M_1 - O - M_2$, for the case of both odd and even number of monolayers, haye been found to work as diode junctions. The maximum forward bias current is of the order of a few nanoamperes. For a particular structure the working inverse voltage (WIV) for this type of diode is comparable with that of the internal voltage. From the knowledge of thickness dependence of internal voltage (Fig. 7.15 - 7.23) and from various curves for diode characteristics (7.24 - 7,37), it is evident that for a particular combination of electrode materials a diode structure of this type will have the maximum working inverse voltage for a single monolayer because the internal voltage for a particular combination is maximum for a single monolayer. The forward current is also maximum for a single monolayer. The working inverse voltage (WIV)for such a type of diode

can be increased by choosing proper metals as the electrode material which have larger work function difference. Furthermore, the maximum dc forward current could be increased by choosing a suitably doped dielectric.

The decay characteristics of internal voltage through a resitance of $\sim 10^{15}$ ohms show that the rate of decay is slow. The subsequent voltage recovery is also an interesting feature of the dielectric cell.

The above study of internal voltage provides a method of determination of work function difference between two metals. If the work function of one of the metals is known the work function of another can be determined.

The independence of work function of metal film of its thickness in the range studied (390 - 1025 Å) is expected. It is because the work function is a property of band structure of the metal and the band structure in thin film form has the same gross structure as in the case of the bulk material. Theoretically this thickness dependence of the work function is expected only for a few atomic layers.

The study of internal voltage in the dielectric film with symmetric electrodes is also very interesting. The structure Al - O - Al with even number of monolayers show the usual behaviour and no internal voltage has been observed in this case. In the case of odd number of mono-

layers, i.e. in the case when the insulating film has a net dipole moment, an internal voltage has been found to exist. This is because the polarization existing in the unpaired polar layer produces an intrinsic field in the insulator film thereby developing an internal voltage at the two interfaces. This is a new and unique feature of the Langmuir films.

The theoretical formulation developed gives a new method of determination of dipole moments of the suitably orientable molecules in the form of Langmuir films.

The studies of dynamic characteristics carried out in the present investigations are also quite interesting. It shows that although dielectric loss is essentially a macroscopic property valid for sufficiently thick samples, however, if the sample has a defect structure which varies with thickness and takes part in a particular relaxation process, the dielectric loss is expected to become thickness dependent. In the present investigations, the dielectric loss has larger values at low thickness but at higher thickness it tends to become thickness independent. The observed thickness dependence of the dielectric loss of Langmuir films has been explained in terms of defect structure or voids present in the films. Dielectric loss is observed to be very high for a monolayer because large number

of voids or pin holes are expected in the single layer film. The loss value drops rapidly for the 2-layer film because voids will be rapidly briedged when the second layer is deposited on the first. After this the drop in the loss value becomes slower because the voids will now be covered up gradually with increasing number of layers. Obviously after certain number of layers the loss should not depend on the thickness of the film. This tendency of the near constancy of the dissipation factor can be seen in various figures 9.1 - 9.3 for 8-10 layers. A quantitative explanation of the results obtained is not possible because the actual distribution of voids and their thickness variation in Langmuir films is not known.

REFERENCES

1. Mott, N.F., and Gurney, R.W., '' Electronic Processes in Ionic Crystals'', 2nd ed., Chap.V, Oxford University Press, Fair Lawn, N.J., 1948.

2. Rose, A., Phys. Rev., 97, 1538 (1955).

3. Lampert, M.A., Rept. Progr. Phys., 27, 329 (1964).

4. Bujatti, M., and Muller, R.S., J. Electrochem. Soc., 112, 702 (1965).

5. Hass, G., J. Am. Ceram. Soc., 33, 353 (1958).

6. Ritter, E., Opt. Acta, 9, 197 (1962).

7. Brady, G.W., J. Phys. Chem., 63, 1119 (1959).

8. Faessler, Von A. and Kramer, H., Ann. Physik, 7, 263 (1959).

9. Dresner, J. and Shallcross, F.V., Solid State Electron, 5, 205 (1962).

10. Simmons, J.G., Phys. Rev. Letters, 10, 10 (1963).

11. Spratt, J.P., Schwarz, R.F. and Kane, B.M., Phys. Rev. Letters 6, 341 (1961).

12. Mead, C.A., J. Appl. Phys. 32, 646 (1961). and Phys.Rev. Letts. 6, 545 (1961).

13. Kanter, H. and Feibelman, W.A. Twenty Second Conference on Physical Electronics, Massachusetts Institute of Technology, March, 1962.

14. Lewicki, G.W. and Mead, C.A., Appl.Phys.Letts.8,98 (1966).

15. Simmons,J.G.,Phys.Rev.Letts.,23,297 (1969).

16. Mead, C.A., Proc. I.R.E. 48, 359 (1960)

17. Blodgett, K.B., J. Amer. Chem. Soc. 57, 1007 (1935); 56, 495 (1934).

18. Blodgett, K.B., and Langmuir, I., Phys. Rev. 51 964 (1937).

19. Srivastava, V.K. in Physics of Thin Films (Edited by G.Hass and R.E. Thun), Vol.7, p.311, Academic Press, New York (1973).

20. Lord Rayleigh, Phil. Mag. 48, 321 (1899).

21. Pockels, A., Nature (London), 43, 437 (1891).

22. Adam, N.K., '' The Physics and Chemistry of Surfaces'', 3rd ed. Chapter II, Oxford Univ. Press. (Clarendon), London and New York 1941.

23. Lord Rayleigh, Proc. Roy.Soc. Ser. A 47, 364 (1890)

24. Lord Rayleigh, Phil. Mag. 30, 386 (1890).

25. Harkins, W.D., Physical Chemistry of Surface films, Rainhold Publishing Corp. New York (1954).

26. Gains Jr. G.L., Insoluble Monolayers at Liquid Gas interfaces, Interscience, New York (1966).

27. Rideal, E.K., Surface Chemistry, 2nd Ed. (1930).

28. Alexander, A.E. Rep. Prog. Phys. 9, 158 (1942).

29. Devaux, H. Smithsonian Inst. Ann. Rept., p.261 (1913).

30. Hardy, W.B., Proc. Roy. Soc. (London), A86,610 (1912).

31. Langmuir, I., Met and Chem. Engg., 18, 468 (1916). Proc. Nat. Acad. Sci., 3, 25 (1917)

32. Bragg, W.L., The Crystalline State, G.Bell and Son Ltd., (London), 1, 169 (1949).

33. Robertson, J.M., Organic Crystals and Molecules, Cornwell Univ. Press, New York, p. 1966 (1953).

34. Muller, Proc. R y. Soc. (London), A114, 546 (1927).

35. Langmuir, I.J. Am. Chem. Soc., 39, 1348 (1917).

36. Harkins, W.D., J. Am. Chem. Soc., 39, 541 (1917).

37. Hardy, W.B., Proc. Roy. Soc. (London), A86, 634 (1912).

38. Rothen, A., Science, 102, 446 (1945).

39. Ellison, A.E.. J. Phys., Chem. 66, 1867 (1962) :

40. Ries, Jr., H.E. Scientific American, 204, 152 (1961).

41. Zocher, H. and Stiebel, F.,Z. Physik, Chem. (Leipzieg) A147, 401 (1930)

42. Adam. N.K., Trans. Farad. Soc. 29, 90 (1933).

43. Bruum, H., Arkiv. Kemi 8, 411 (1955).

44. Tronstad, L. and Feachem, C.G.P., Proc. Roy. Soc. (London), A145, 115, 127 (1934).

45. Bouchat, C., Ann. de Physique, 15, 5 (1931).

46. Tronstad, L.,J. Sci. Instr., 11, 144 (1934).

47. Schulman, J.H. and Rideal, E.K., Proc. Roy, Soc. A130 , 259 (1931).

48. Epstein, H.T., J.Phys. Colloid, Chem. 54, 1053 (1950).

49. Langmuir, I., J. Franklin Inst. 218, 143 (1934).

50. Langmuir, I., Proc. Roy.Soc., Ser. A170 , 1 (1939).

51. Nathoo, M.H., Thin Solid Films 16, 215 (1973).

52. Schulman, J.H., Ann. Rep. Chem.Soc., 36: 94 (1939).

53. Bikerman, J.J., Proc. Roy. Soc., A170, 130 (1939).

54. Bikerman, J.J. Trans. Farad. Soc. 36, 412 (1940).

55. Dénard, L., J. Chim. Phys. Physicochim. Biol.36, 210 (1939).

56. Gupta, S.K., Kapil, A.K., Singal,C.M. and Srivastava, V.K., Pramana, 7, 397 (1976).

57. Blodgett, K.B., J.Phys.Chem., 41, 975 (1937).

58. Havinga, E., and de Wael, J.,Rec. Trav. Chim. 56, 375 (1937).

59. de Wael, J. and Havinga, E., Rec.Trav. Chim. 59, 770 (1940).

60. Germer, L.H. and Storks, K.H., J. Chem. Phys., 6, 280 (1938).

61. Holley, C., Phys. Rev., 51, 1000 (1937).

62. Fankuchen, I., Phys.Rev., 53, 909 (1938).

63. Langmuir, I., Science, 87, 493 (1938).

64. Jankins, G.I., and Norris, A., Nature (London), 144, 441 (1939).

65. Rothen, A., Rev. Sci. Inst., 16, 26 (1945).

66. Rothen, A. and Hanson, M., Rev. Sci. Inst., 19, 839 (1948).

67. Rothen, A. and Hanson, M., Rev. Sci. Inst. 20, 66, (1949).

68. Mattuck, R.D., J. Opt. Soc. Amer. 46, 615, 621, (1956).

69. Mattuck, R.D., Petti, R.D. and Beteman, J.B., J. Opt. Soc. Amer. 46, 782 (1956).

70. Hartman, R.E., J. Opt. Soc. Amer. 44, 192 (1954).

71. Tolansky, S. '' Multiple Beam Interferometry of Surfaces and Films''. Oxford Univ. Press (Clarendon), London and New York, 1948.

72. Tolansky, S., '' An Introduction to Interferometry'' , Longmans, Green, New York, 1955

73. Courtney - Pratt, J.S., Nature (London), 165, 346 (1950).

74. Courtney - Pratt, J.S., Proc. Roy, Soc. (London), A212, 505 (1952).

75. Bailey, A.I. and Courtney - Pratt, J.S., Proc. Roy. Soc., Ser. A227, 500 (1955).

76. Gaines, G.L. Jr., Nature (London) 183, 1110 (1959).

77. Srivastava, V.K. and Verma, A.R., Proc. Roy. Soc., London 80, 222 (1962).

78. Srivastava, V.K. and Verma, A.R., Solid State Commun. 4, 367 (1966).

79. Bateman, J.B., and Covington, E.J., J.Colloid Soci. 16, 531 (1961).

80. Alexander, A.E., J. Chem. Soc., London, 777 (1939).

81. Knott, G., Schulman, J.H. and Wells, A.F., Proc. Roy. Soc., Ser. A176, 534 (1940).

82. Bernstein, S., J. Amer. Chem. Soc. 62, 374 (1940).

83. Clark, G.L., Sterret, R.R. and Leppla, P.W., J. Amer. Chem. Soc. 52, 330 (1935).

84. Holley, C. and Bernstein, S., Phys.Rev. 49, 403 (1936).

85. Holley, C. and Bernstein, S., Phys. Rev. 52, 525, (1937).

86. Stenhagen, E., Trans. Faraday. Soc. 34, 1328 (1938).

87. Bernstein, S., J. Amer. Chem. Soc., 60, 1511 (1938).

88. Bisset, D.C. and Iball, J., Proc. Phys. Soc. London, Sect. A67, 315 (1954).

89. Ehlert, R.C., J. Colloid Sci. 20, 387 (1965).

90. Kapp, D.S. and Wainfan, N., Phys. Rev. 138, 1490 (1965).

91. Clark, G.L., Applied X-ray McGraw Hill Book Co., New York, p. 621 (1955).

92. Stephens, J.F. and Turck-lee, C., J. Appl. Cryst., 2, 1 (1969).

93. Ehrenberg, W. and Spear, W.E., Proc. Phys. Soc. B64, 67 (1951).

94. Lucy, F.A., J. Chem. Phys., 16, 167 (1948).

95. Faucher, J.A., McManus, G.M. and Trurnit, H.J., J. Opt. Soc. Am., 48, 51 (1958).

96. Tomar, M.S. and Srivastava, V.K., Thin Solid Films, 12, S29 (1972).

97. Tomar, M.S. and Srivastava, V.K., Indian J. Pure Appl. Phys. 10, 573 (1972).

98. Tomar, M.S. and Srivastava, V.K., Thin Solid Films, 15, 207 (1973).

99. Tomar, M.S. and Srivastava, V.K., J. Appl. Phys., 45, 1849 (1974).

100. Schopper, H., Z. Phys., 132, 146 (1952).

101. Khanna, U. and Srivastava, V.K., Thin Films, 2, 153 (1972).

102. Porter, E.F. and Wyman, J. Jr., J. Amer. Chem. Soc. 60, 1083 (1938).

103. Porter, E.F. and Wyman, J. Jr., J. Amer. Chem.Soc. 59, 2746 (1937).

104. Porter, E.F. and Wyman, J.Jr., J. Amer. Chem. Soc. 60, 2855 (1938).

105. Race, H.H. and Reynolds, S.I., J. Am. Chem. Soc. 61, 1425 (1939).

106. Race, H.H. and Reynolds, S.I., G.E. Rev., 41, 492, (1938).

107. Race, H.H. and Leonard, S.C., Elect. Engg., 55, 1347 (1936).

108. Buchwald, C.E., Gallagher, D.M., Haskins, C.P., Thatcher, E.M. and Zahl, P.A., Proc. Nat. Acad. Sci. U.S. 24, 204 (1938).

109. Zahl, P.A., Haskins, C.P., Gallagher, D.M. and Buchwald, C.E., Trans. Faraday. Soc. 35, 308 (1939).

110. Handy, R.M. and Scala, L.C., J. Electrochem. Soc. 113, 109 (1966).

111. Drexhage, K.H. and Kuhn, H., Basic Problems in Thin Film Physics, Ed. Niedermayer, R. and Mayer, H., Gottinger Vandenhoech and Ruprecht, p. 339 (1966).

112 Mann, B. and Kuhn, H., J. Appl. Phys., 42, 4398 (1971).

113. Holt, L., Nature (London), 214, 1105 (1967).

114. Horiuchi, S., Yamaguchi, J. and Naito, K., J. Electrochem. Soc., 115, 634 (1968).

115. Khanna, U. and Srivastava, V.K. and Agarwal, V.K., Thin Films 2, 83 (1971).

116. Khanna, U. and Srivastava, V.K., Thin Films 2, 167 (1972).

117. Khanna, U. and Srivastava, V.K., Thin Solid Films, 12, 1 (1972).

118. Khanna, U. and Srivastava, V.K., Phys. Stat. Solidi, A38 , 1 (1976).

119. Chopra, K.L., J. Appl. Phys. 36, 655 (1963).

120. Young, L., Anodic Oxide Films, Academic Press, N.Y. (1967).

121. Feldman, C. and Hacskaylo, M., Rev. Sci. Instr., 33, 1459 (1962).

122. Feldman, C., Rev. Sci. Instr., 26, 463 (1955).

123. Maddocks, F.S. and Thun, R.E., J. Electrochem. Soc., 109, 99 (1962).

124. Weaver, C., Adv. Phys., 11, 85 (1962).

125. Weaver, C., in ' The Use of Thin Films in Physical Investigations', (J.C. Anderson Ed.), Academic Press, New York, p. 283 (1966).

126. Weaver, C. and MacLeod, J.E.S., Br. J. Appl. Phys., 16, 441 (1965).

127. Weaver, C., Vacuum (London), 15, 171 (1965).

128. Hacskaylo, M. and Feldman, C., J. Appl. Phys., 33, 3042 (1962).

129. Hirose, H. and Wada, Y., Japan J. Appl. Phys. 3, 179 (1964).

130. Budenstein, P.P. and Hayes, P.J., J. Appl. Phys. 38, 28 37 (1967).

131. Budenstein, P.P., Hayes, P.J., Smith, J.L. and Smith, W.B., J. Vac. Sci. Tech., 6, 289 (1968).

132. Forlani, F. and Minnaja, N., J. Vac. Sci. Technol. 6, 518 (1969).

133. Klein, N., Thin Solid Films 7, 149 (1971).

134. Klein, N., Advan. Electron.Phys. 26, 309 (1969).

135. Thiessen, P.A., Beischer, D. and Gillhausen, H., Frhr. V. Naturwiss 28, 265 (1940).

136. Agarwal, V.K. and Srivastava, V.K., Thin Solid Films, 8, 377 (1971).

137. Agarwal, V.K. and Srivastava, V.K., Thin Solid Films, 13, S23 (1972).

138. Agarwal, V.K. and Srivastava V.K., Solid State Commn. 12, 829 (1973).

139. Agarwal V.K. and Srivastava,V.K. , J. Electrocomp. Sci. and Technol., 1, 87 (1974).

140. Agarwal, V.K. and Srivastava, V.K., J. Appl. Phys., 44, 2900 (1973).

141. Agarwal, D.K. and Srivastava, V.K.,, Thin Solid Films 14, 367 (1972).

142. Agarwal, D.K. and Srivastava, V.K., Solid State Commun. 11, 1461 (1972).

143. Agarwal, D.K. and Srivastava V.K., Thin Solid Films, 27, 49 (1975).

144. Forlani, F. and Minnaja, N., Phys. Status Solidi, 4, 311 (1964).

145. Srivastava, V.K., Phys. Rev. Letters 30, 1046 (1973).

146. Schottky, W., Z. Phys. 113, 367 (1939).

147. Miles, J.L. and McMahon, H.O., J. Appl. Phys. 32, 1126 (1961).

148. Mann, B., Kuhn, H. and Szentpaly, L.V., Chem.Phys. Lett. 8, 82, (1971).

149. Drexhage, K., Schafer, F. and Kuhn, H., J. Phys. Chem. Solids, 27, 1189 (1966).

150. Szentpaly, L.V., Mobius, D. and Kuhn, H., J. Chem. Phys. 52, 4618 (1970).

151. Kreynina, G.S., Selivanov, L.N. and Shumskaia, T.I., Radio Engg. Elect. Phys., 5, 8 (1960).

152. Kreynina, G.S., Selivanov, L.N. and Shumskaia, T.I., Radio Engg. Elect. Phys. 5, 219 (1960).

153. Kreynina, G.S., Radio Engg. Elect. Phys. 7, 166 (1962).

154. Kreynina, G.S., Radio Engg. Elect. Phys. 7, 1949 (1962).

155. Hickmott, T.W., J. Appl. Phys., 33, 2669 (1962).

156. Hickmott, T.W., J. Appl. Phys., 34, 1569 (1963).

157. Hickmott, T.W., J. Appl. Phys. 35, 2118 (1964).

158. Cola, R.A., Simmons, J.G. and Verderber, R.R., Proc. Natl. Aerospace Electron Conf., 1964, p.118.

159. Hickmott, T.W., J. Appl. Phys., 36, 1885 (1965).

160. Lewowski, T., Sendecki, S. and Sujak, B., Acta Phys. Polon., Vol. 28, (1965).

161. Uzan, R. Roger, A. and Cochard, A., Vide 137, 38 (1967).

162. Simmons, J.G. and Verderber, R.R., Proc. Roy. Soc. London, 301, 77 (1967) and Radio Elect. Engg. 34,81 (1966)

163. Verderber, R.R., Simmons, J.G. and Eales, B., Phil. Mag.,16, 1049 (1967).

164. Gundlach, K.H. and Kadlec, J., Phys. Stat. Solidi (a), 10, 371 (1972).

165. Gundlach, K.H. and Kadlec, J., Thin Solid Fims, 13, 225 (1972).

166. Dearnley, G., Stonehame, A.M. and Morgan, D.V., Rep. Progr. Phys., 33, 1129 (1970).

167. Chopra, K.L., Thin Film Phenomena, McGraw Hill Book Co., p.466 (1969).

168. Strong, J., Modern Physical Laboratory Practice (Blackie, London 1940).

169. Ghosh, K., Amal and Fleng Tom, J. Appl. Phys., 44, 2781 (1973).

170. Gupta, S.K., Singal, C.M. and Srivastava, V.K., J. Appl. Phys. (1977) 48, 2583

171. Robert, C.W. ed. ' Handbook of Chemistry and Physics' (The Chem. Rubber Co., Cleaveland Ohio, 1968-69), E,77.

172. Singal, C.M., Gupta, S.K., Kapil, A.K. and Srivastava, V.K., J. Appl. Phys. (Accepted for publication).

173. Smyth, C.P. in ' Dielectric Constant and Molecular Structure' McGraw-Hill Book Co. Inc. New York (1955). p. 306-307.

174. Robert, C.W. ed. ' Handbook of Chemistry and Physics' (The Chemical Rubber Co. Cleaveland Ohio, 1968-69) E-66.

175. Ries, H.E., Jr. and Walker D.C., J. Colloid Sci. 16, 361 (1961).

176. Ries, H.E., Jr. and Kimball W.A., Nature 181, 901 (1958).

177. Marc, G., and Messier, J., J. Appl. Phys. (1975).

178. Gupta, S.K. and Srivastava, V.K. J. Phys. Chem. Solids, 37, 975 (1976).

179. Gupta, S.K. and Srivastava, V.K., J. Phys. Chem. Solids, 38, 1111 (1977).

180. Gupta, S.K., Singal, C.M. and Srivastava, V.K. J. Electrocomp. Sci. and Technol, 3, 119 (1976).

181. Gupta, S.K., Singal, C.M. and Srivastava, V.K. (To be communicated).

182. Gupta, S.K., Singal, C.M. and Srivastava, V.K. (To be communicated).

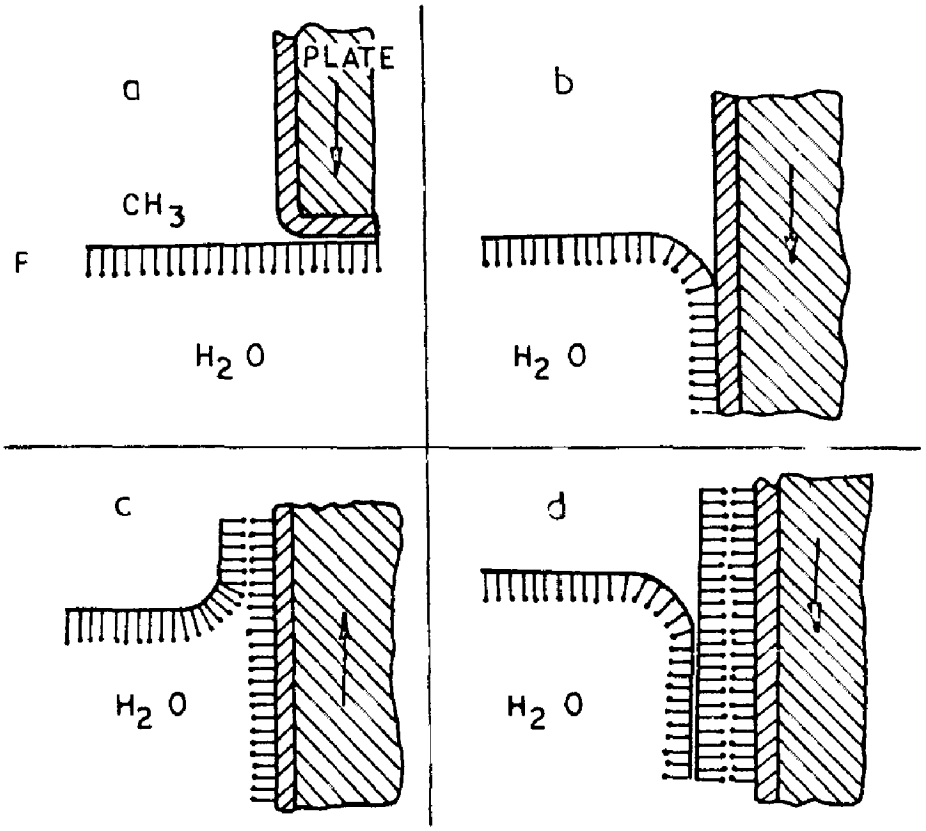

AFTER LANGMUIR PROC ROY SOC. A, 170, (1939)

FIG 4·4 DIAGRAMS SHOWING THE BUILDING UP PROCESS OF Y TYPE FILMS.

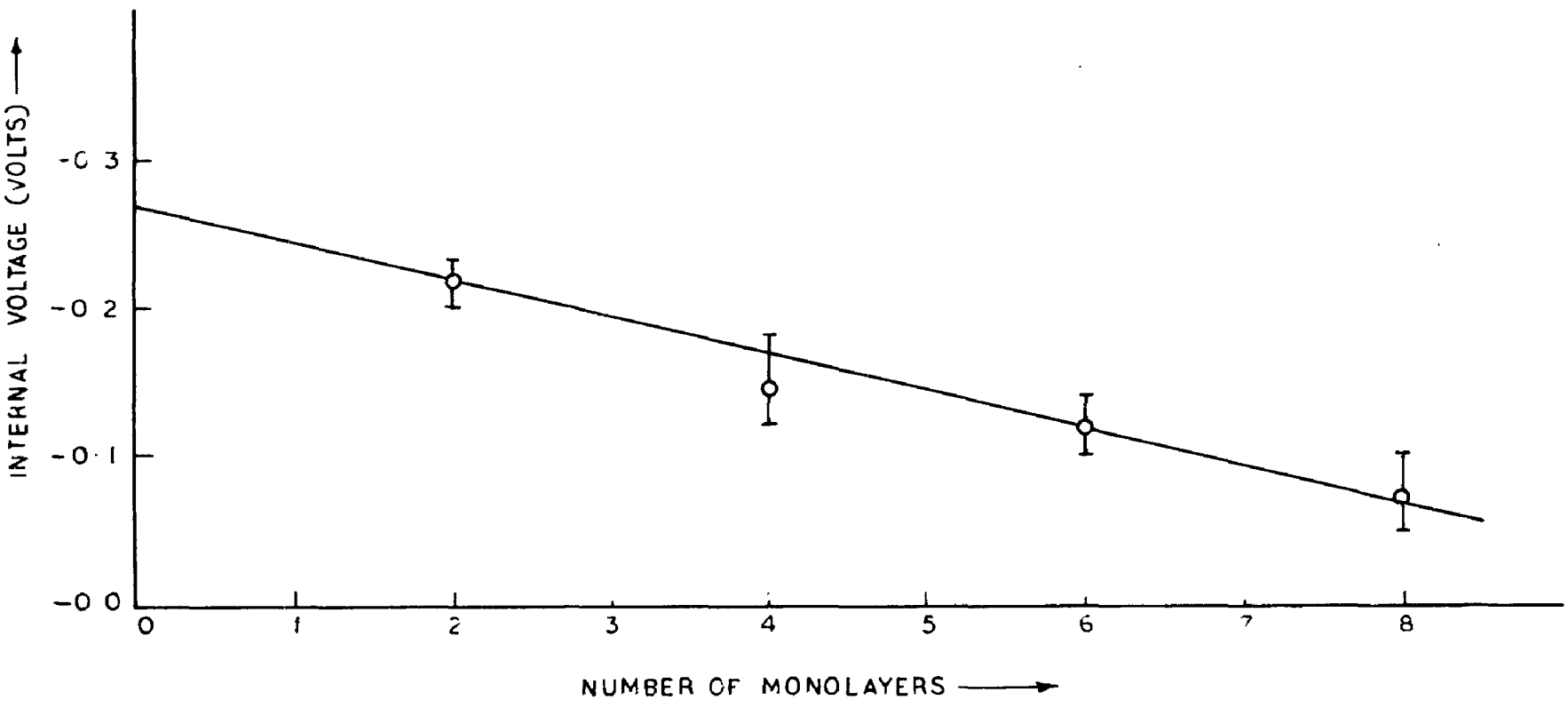

FIG. 7·22 INTERNAL VOLTAGE Vs NUMBER OF MONOLAYERS FOR Al-BARIUM STEARATE-*Te* STRUCTURE

(Polarity of Te: positive)

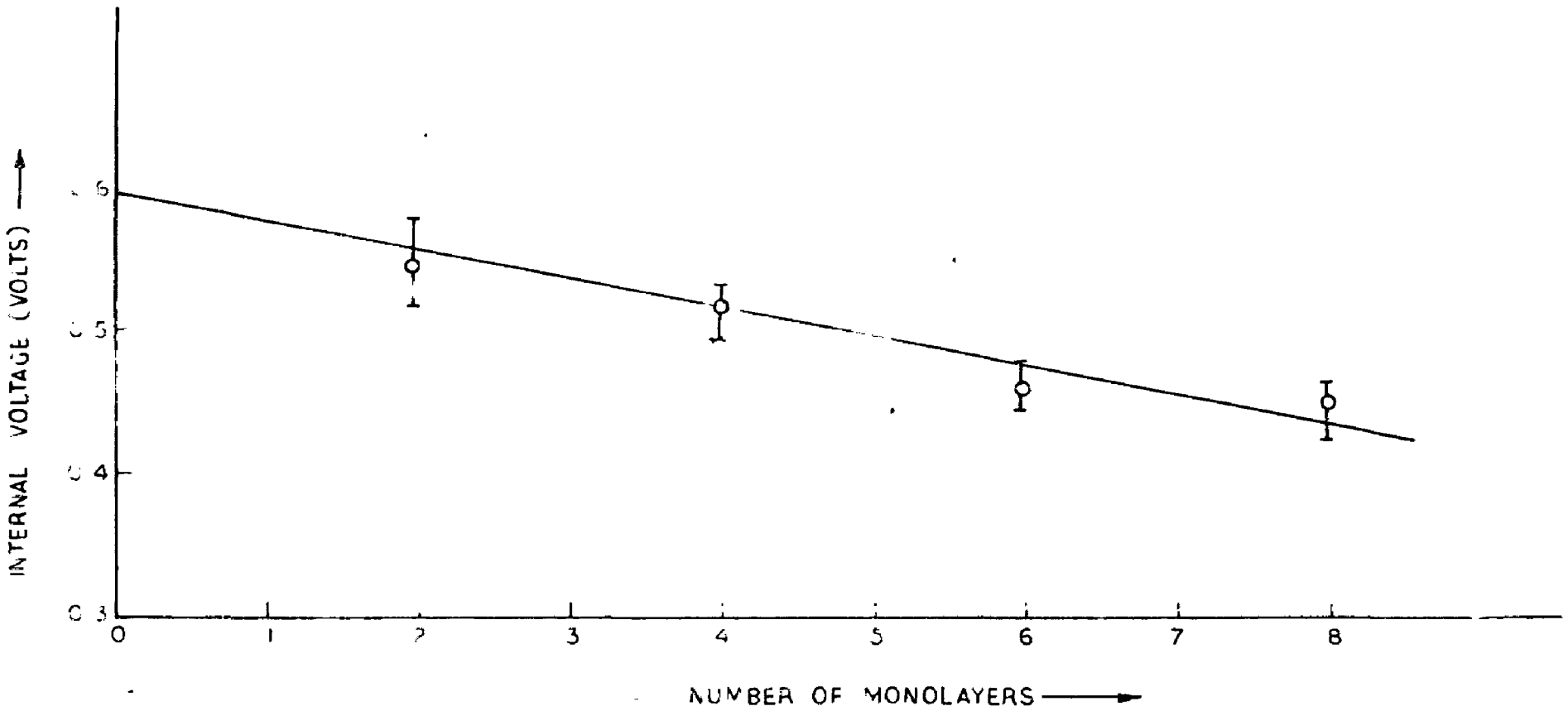

FIG. 7·23 INTERNAL-VOLTAGE Vs NUMBER OF MONOLAYERS FOR Sn-BARIUM STEARATE-Al STRUCTURE

(Polarity of Sn: positive)

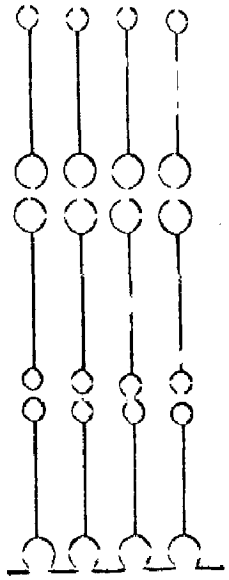

(a)

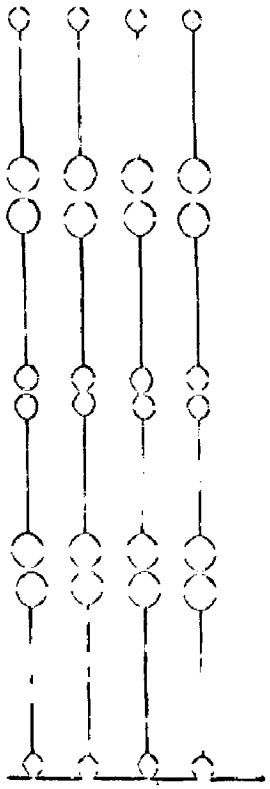

(b)

(a) THREE LAYER FILM

(b) FOUR LAYER FILM

○ CARBOXYLIC GROUP

○ METHYL GROUP

FIG. 7.40 - DIAGRAMMATIC REPRESENTATION OF ODD AND EVEN LAYER FILMS

(IN FIGURE (a) THERE IS ONE UNPAIRED LAYER WHERE AS IN FIGURE (b) ALL LAYERS ARE PAIRED)